frontiers | Research Topics

Therapeutic drug monitoring and clinical toxicology of anti-cancer drugs, volume II

Edited by
Miao Yan, Yao Liu and Jennifer Martin

Published in
Frontiers in Oncology
Frontiers in Pharmacology

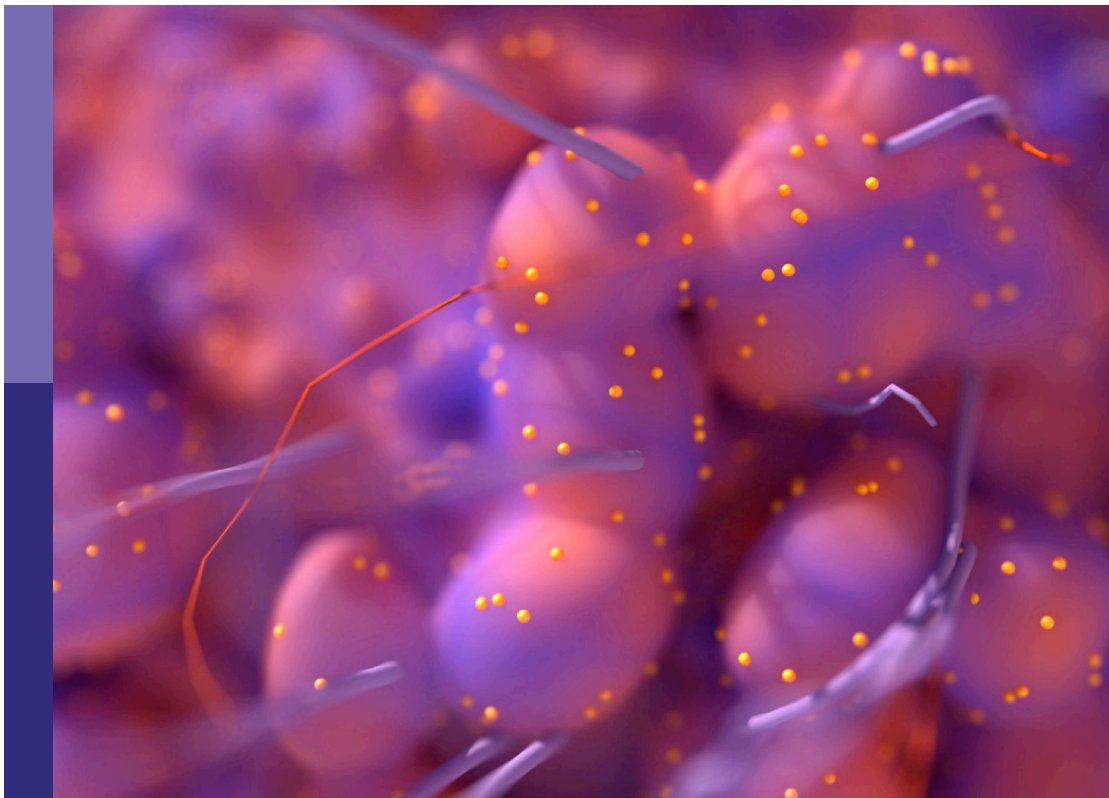

ISSN 1664-8714
ISBN 978-2-83251-975-2
DOI 10.3389/978-2-83251-975-2

About Frontiers

Frontiers is more than just an open access publisher of scholarly articles: it is a pioneering approach to the world of academia, radically improving the way scholarly research is managed. The grand vision of Frontiers is a world where all people have an equal opportunity to seek, share and generate knowledge. Frontiers provides immediate and permanent online open access to all its publications, but this alone is not enough to realize our grand goals.

Frontiers journal series

The Frontiers journal series is a multi-tier and interdisciplinary set of open-access, online journals, promising a paradigm shift from the current review, selection and dissemination processes in academic publishing. All Frontiers journals are driven by researchers for researchers; therefore, they constitute a service to the scholarly community. At the same time, the *Frontiers journal series* operates on a revolutionary invention, the tiered publishing system, initially addressing specific communities of scholars, and gradually climbing up to broader public understanding, thus serving the interests of the lay society, too.

Dedication to quality

Each Frontiers article is a landmark of the highest quality, thanks to genuinely collaborative interactions between authors and review editors, who include some of the world's best academicians. Research must be certified by peers before entering a stream of knowledge that may eventually reach the public - and shape society; therefore, Frontiers only applies the most rigorous and unbiased reviews. Frontiers revolutionizes research publishing by freely delivering the most outstanding research, evaluated with no bias from both the academic and social point of view. By applying the most advanced information technologies, Frontiers is catapulting scholarly publishing into a new generation.

What are Frontiers Research Topics?

Frontiers Research Topics are very popular trademarks of the *Frontiers journals series*: they are collections of at least ten articles, all centered on a particular subject. With their unique mix of varied contributions from Original Research to Review Articles, Frontiers Research Topics unify the most influential researchers, the latest key findings and historical advances in a hot research area.

Find out more on how to host your own Frontiers Research Topic or contribute to one as an author by contacting the Frontiers editorial office: frontiersin.org/about/contact

Therapeutic drug monitoring and clinical toxicology of anti-cancer drugs, volume II

Topic editors

Miao Yan — Central South University, China

Yao Liu — Daping Hospital, China

Jennifer Martin — The University of Newcastle, Australia

Citation

Yan, M., Liu, Y., Martin, J., eds. (2023). *Therapeutic drug monitoring and clinical toxicology of anti-cancer drugs, volume II.* Lausanne: Frontiers Media SA.

doi: 10.3389/978-2-83251-975-2

Table of contents

frontiers | Frontiers in Oncology

TYPE Editorial
PUBLISHED 07 March 2023
DOI 10.3389/fonc.2023.1153714

OPEN ACCESS

EDITED AND REVIEWED BY
Olivier Feron,
Université catholique de Louvain, Belgium

*CORRESPONDENCE
Jennifer H. Martin
jen.martin@newcastle.edu.au

SPECIALTY SECTION
This article was submitted to Pharmacology of Anti-Cancer Drugs, a section of the journal Frontiers in Oncology

RECEIVED 30 January 2023
ACCEPTED 13 February 2023
PUBLISHED 07 March 2023

CITATION
Yan M, Liu Y and Martin JH (2023) Editorial: Therapeutic drug monitoring and clinical toxicology of anti-cancer drugs, volume II.
Front. Oncol. 13:1153714.
doi: 10.3389/fonc.2023.1153714

Editorial: Therapeutic drug monitoring and clinical toxicology of anti-cancer drugs, volume II

Miao Yan[1], Yao Liu[2] and Jennifer H. Martin[3]*

[1]Department of Pharmacy, the Second Xiangya Hospital of Central South University, Changsha, Hunan, China, [2]Department of Pharmacy, Daping Hospital of Army Medical University, Chongqing, China, [3]School of Medicine and Public Health, University of Newcastle, Newcastle, NSW, Australia

KEYWORDS

therapeutic drug monitoring, clinical toxicology, anti-cancer drugs, editorial, precision medicine

Editorial on the Research Topic
Therapeutic drug monitoring and clinical toxicology of anti-cancer drugs, volume II

This is the second editorial in this series examining new oncology therapeutics and applications for which therapeutic drug monitoring (TDM)– adjusting dosages to improve outcomes to individualise patient care – can help individualise drug dosage. In general, TDM has been known to be helpful for over 50 years in most of the chemotherapy dosing of the older but still mainstream oncology therapeutics e.g. the taxanes, 5FU, methotrexate, etc. It has also shown significant utility with TKIs as discussed in the first series as these drugs also have a narrow therapeutic window, display significant inter- and intra-individual pharmacokinetic variability, and have a known concentration-effect relationship which can be utilised by the treating doctor. TDM is now finding additional uses as new drugs are being developed, and because patient physiology is increasingly variable compared to the previous generation. Older and more medically vulnerable patients are also now able to tolerate such chemotherapies now - due to the fact inter alia that supportive therapies e.g. ICU and transplant technologies are available to patients who previously would not have been offered chemotherapy due to comorbidity e.g. reduced organ function, age or concomitant medication. The other new development in this area is the development of an increasing number of oral agents and their combinations, including different families of tyrosine kinase inhibitors, many of which have significant activity in the P450 system and are often substrates for this system also, leading to widely variable dose-exposure relationships.

Stojavana et al. stated in a short report using a rapid snapshot of the literature, new biologics are also entering clinical practice, some based on minimally measured patient pharmacokinetic data, many of which are marketed at a single, maximally tolerated fixed dose, the same dose for each patient regardless of their physiology, comorbidity, diet, and concomitant medications. They note that for the most part, research initiatives are academic, and the evidence base has unfolded according to the clinical need and

specialist areas of research groups. This report and the in-depth review of TDM of three commonly used chemotherapies (busulfan, 5-FU, and methotrexate) by Smita et al. in this context did set the scene for 10 other research reports.

Lin et al. used a SEER population-based analysis and examined the risk of heart disease-related death (HDRD) among anaplastic astrocytoma patients after chemotherapy. In this registry, 7129 anaplastic astrocytoma patients were studied, counterintuitively showing that those treated with chemotherapy compared to those not treated with chemotherapy were associated with a lower risk of HDRD. However, it is noted that the data are registry-based and thus open to large confounding. One likely confounder is that older and more frail patients are not offered some or any chemotherapy due to the risk-benefit ratio being higher than the less frail and younger cohort. And as HDRD is age-related, this could explain such a finding.

Yu et al. used data from 149 breast cancer patients receiving lapatinib to predict a personalised dose regimen using twelve machine learning and deep learning techniques. They chose TabNet to construct the prediction model with the best performance and then ranked four variables that strongly correlated with lapatinib dose: treatment protocols, weight, number of chemotherapy treatments, and number of metastases. Finally, the confusion matrix was used to validate the model for a dosing regimen of 1,250 mg lapatinib (precision = 81% and recall = 95%) and a dosing regimen of 1,000 mg lapatinib (precision = 87% and recall = 64%). A confusion matrix (also known as an error matrix) is a specific table layout that allows visualization of the performance of an algorithm in machine learning. However, although this model shows good predictive performance in a retrospective audit, validation in a new population and comparison to existing algorithms have not been undertaken.

Tan et al. studied genetic polymorphisms in CYP2C19 in 139 Chinese patients with lung cancer and studied the effect of these on exposure and adverse events of anlotinib, a small molecular multi-targeting tyrosine kinase inhibitor (TKI). As seen with other TKIs, there were significant variances (nearly 20-fold) in plasma trough concentration (3.95–52.88 ng/ml) and peak plasma concentration (11.53–42.8 ng/ml) following administration of 8 mg anlotinib; similar variances were seen with the 12mg dose tablet. Specific genetic mutations in CYP 2C19 accounted for much of this. Importantly, the mutations in CYP2C19 and corresponding higher exposures were correlated with higher incidences of hypertension and hemoptysis.

TDM requires timely access to a validated drug measurement system. This can be expensive when only a few patients are using a wide variety of oncology drugs. In order to make this more efficient, Jiang et al. developed a rapid determination of nine Tyrosine Kinase Inhibitors for the treatment of hepatocellular carcinoma in human plasma by QuEChERS-UPLC-MS/MS using the QuEChERS (Quick, Easy, Cheap, Effective, Rugged, and Safe) method. Lenvatinib, sorafenib, cabozantinib, apatinib, gefitinib, regorafenib, and anlotinib showed reasonable linearity over the range of 0.1–10 ng/ml, with the range 1–100 ng/ml showing linearity for tivantinib and galunisertib. All the linear correlation coefficients for all standard curves were ≥ 0.9966. The limits of detection and the limits of quantitation range were reasonable. The method was deemed satisfactory with an accuracy of -7.34–6.64%, selectivity, matrix effect (ME) of 90.48–107.77%, recovery, and stability. The proposed method is simple, efficient, reliable, and applicable for the detection of multiple commonly used TKIs in human plasma samples.

Lenalidomide (LEN) therapy is important in multiple myeloma (MM) and non-Hodgkin lymphoma (NHL), but requires dose adjustment in renal impairment. However, the optimal concentration range has not been clearly defined. Song et al. undertook a prospective observational study of the exposure-safety relationship of LEN to determine the target concentration for toxicity. Out of the 61 patients enrolled in this study, hematological toxicity was reported in 15 (24.59%) patients. The LEN C_{min} showed remarkable differences (p = 0.031) among patients with or without hematological toxicity, while no association between C_{1h} values and toxicity was noted. By ROC analysis, a C_{min} threshold of 10.95 ng/mL was associated with the best sensitivity and specificity for toxicity events (AUC = 0.687; sensitivity = 0.40; specificity = 0.935). By multivariate logistic regression, a LEN C_{min} below 10.95 ng/mL was associated with a markedly decreased risk of hematological toxicity (<10.95 ng/mL vs. >10.95 ng/mL: OR = 0.023, 95% CI = 0.002–0.269; p = 0.003).

Chen et al. sought to understand immune-related adverse events in NSCLC patients with concomitant hypertension in patients receiving PD-1/PD-L1 inhibitors using disproportionality analysis in the Food and Drug Administration (FDA) Adverse Event Reporting System (FAERS) database. Among 17,163 NSCLC patients under treatment with a single-agent anti-programmed death-1/programmed death ligand-1 (PD-1/PD-L1) inhibitor (nivolumab, pembrolizumab, cemiplimab, durvalumab, atezolizumab, and avelumab), 497 patients had hypertension, while 16,666 patients had no hypertension. 4,283 pulmonary AEs were reported, including 166 patients with hypertension and 4,117 patients without hypertension. Compared with patients without hypertension, patients with hypertension were positively associated with increased reporting of interstitial lung disease (ROR = 3.62, 95% CI 2.68–4.89, IC = 1.54, IC_{025} = 0.57) among patients receiving anti-PD-1 treatment.

Cardiotoxicity is a well-known pathophysiological consequence in breast cancer patients receiving trastuzumab. Trastuzumab-related cardiotoxicity typically results in an overall decline in cardiac function, primarily characterized by a reduction in left ventricular ejection fraction (LVEF) and the development of symptoms associated with heart failure. Current strategies for the monitoring of cardiac function during trastuzumab therapy include serial echocardiography, which is cost-ineffective as well as offers limited specificity, while offering limited potential in monitoring early onset of cardiotoxicity. However, biomarkers have been shown to be aberrant prior to any detectable functional or clinical deficit in cardiac function. Pillai et al. aims to develop a panel of novel biomarkers and circulating miRNAs for the early screening of trastuzumab-induced cardiotoxicity. Patients with a clinical diagnosis of invasive ductal carcinoma were enrolled in the study,

with blood specimens collected and echocardiography performed prior to trastuzumab therapy initiation at baseline and 3, 6 months after trastuzumab therapy, respectively. Following 6-months of trastuzumab therapy, about 18% of the subjects developed cardiotoxicity, as defined by a reduction in LVEF. The results showed significant upregulation of biomarkers and circulating miRNAs, specific to cardiac injury and remodeling, at 3- and 6-months post-trastuzumab therapy. These biomarkers and circulating miRNAs significantly correlated with the cardiac injury-specific markers, troponin I and T. The findings in this study demonstrate the translational applicability of the proposed biomarker panel in the early preclinical diagnosis of trastuzumab-induced cardiotoxicity, further allowing management of cardiac function decline and improving health outcomes for breast cancer patients.

de Vries et al. have investigated whether high exposure is a reason for the discontinuation of pembrolizumab due to immune-related adverse effects (irAEs). This is important as these drugs are very effective and discontinuing them may aggravate the disease of patients. They note the currently available pharmacokinetic (PK) and pharmacodynamic (PD) data to reassess these dosing strategies are insufficient and based on data that is not directly relevant to clinical practice. They highlight the importance of TDM by using plasma measurements after a single 200 mg pembrolizumab dose in a treatment-naive patient with non-small cell lung cancer (NSCLC). Their work notes the complexity of drug exposure, receptor occupancy, and the T-cell effect, and how simple PK-PD models do not reflect this. A validated ELISA quantified pembrolizumab levels in 15 samples within 123 days after the administration did show some interesting effects on clearance after 15 days, suggesting drug exposure measurements can be helpful if samples are taken at appropriate times. For example, after day 77, accelerated non-linear clearance observed suggested that the pembrolizumab drug targets were fully saturated at concentrations above 0.6 μg/mL, 43 to 61 times lower than the steady-state trough levels of the currently registered fixed-dose regimens.

Cardiac arrhythmias associated with immune checkpoint inhibitors detected by the FDA adverse event reporting system (FAERS) were investigated by Wang et al.. Specifically, the clinical characteristics of patients reported with ICI-related cardiac arrhythmias were compared between fatal and non-fatal groups, and the time to onset following different ICI regimens was further investigated. Nearly 2000 ICI–associated cardiac arrhythmias were reported, greater in men than women, and more were reported in patients with lung, pleura, thymus, and heart cancers (38.02% of 1957 patients). Interestingly, the spectrum of arrhythmias induced by ICIs differed among therapeutic regimens, but there appeared to be no difference in the onset time between monotherapy and a combination regimen. Moreover, reports of ICI-associated arrhythmias were associated with other concurrent cardiotoxicity, much of which can be explained by the types of cancers patients that with heart disease are co-associated with and the fact that ICIs are currently used (e.g., smoking and lung cancer).

Taken together, this Research Topic provides an overview of *Therapeutic Drug Monitoring and Clinical Toxicology of Anti-Cancer Drugs II* to summarize and confirm that TDM for clinical antineoplastic drugs can better serve patients and improve drug safety.

Author contributions

All authors listed have made a substantial, direct, and intellectual contribution to the work, and approved it for publication.

Acknowledgments

We wish to thank all the authors contributing to this Frontiers Research Topic and all the reviewers who have helped to make this a great topic.

Conflict of interest

The authors declare that the research was conducted in the absence of any commercial or financial relationships that could be construed as a potential conflict of interest.

Publisher's note

frontiers | Frontiers in Oncology

ORIGINAL RESEARCH
published: 03 June 2022
doi: 10.3389/fonc.2022.893966

Predicting Lapatinib Dose Regimen Using Machine Learning and Deep Learning Techniques Based on a Real-World Study

Ze Yu[1†], Xuan Ye[2,3†], Hongyue Liu[2,3], Huan Li[2,3], Xin Hao[4], Jinyuan Zhang[5], Fang Kou[1], Zeyuan Wang[6], Hai Wei[1], Fei Gao[5*] and Qing Zhai[2,3*]*

[1] Institute of Interdisciplinary Integrative Medicine Research, Shanghai University of Traditional Chinese Medicine, Shanghai, China, [2] Department of Pharmacy, Fudan University Shanghai Cancer Center, Shanghai, China, [3] Department of Oncology, Shanghai Medical College of Fudan University, Shanghai, China, [4] Dalian Medicinovo Technology Co., Ltd., Dalian, China, [5] Beijing Medicinovo Technology Co., Ltd., Beijing, China, [6] Faculty of Engineering, School of Computer Science, The University of Sydney, Sydney, NSW, Australia

OPEN ACCESS

Edited by:
Miao Yan,
Central South University, China

Reviewed by:
Haewon Byeon,
Inje University, South Korea
Yang Zhang,
Harbin Institute of Technology, China

***Correspondence:**
Hai Wei
wei_hai@hotmail.com
Fei Gao
gaofei9000@163.com
Qing Zhai
zhaiqing63@126.com

[†]These authors share first authorship

Specialty section:
This article was submitted to Pharmacology of Anti-Cancer Drugs, a section of the journal Frontiers in Oncology

Received: 11 March 2022
Accepted: 05 May 2022
Published: 03 June 2022

Citation:
Yu Z, Ye X, Liu H, Li H, Hao X, Zhang J, Kou F, Wang Z, Wei H, Gao F and Zhai Q (2022) Predicting Lapatinib Dose Regimen Using Machine Learning and Deep Learning Techniques Based on a Real-World Study. Front. Oncol. 12:893966. doi: 10.3389/fonc.2022.893966

Lapatinib is used for the treatment of metastatic HER2(+) breast cancer. We aim to establish a prediction model for lapatinib dose using machine learning and deep learning techniques based on a real-world study. There were 149 breast cancer patients enrolled from July 2016 to June 2017 at Fudan University Shanghai Cancer Center. The sequential forward selection algorithm based on random forest was applied for variable selection. Twelve machine learning and deep learning algorithms were compared in terms of their predictive abilities (logistic regression, SVM, random forest, Adaboost, XGBoost, GBDT, LightGBM, CatBoost, TabNet, ANN, Super TML, and Wide&Deep). As a result, TabNet was chosen to construct the prediction model with the best performance (accuracy = 0.82 and AUC = 0.83). Afterward, four variables that strongly correlated with lapatinib dose were ranked *via* importance score as follows: treatment protocols, weight, number of chemotherapy treatments, and number of metastases. Finally, the confusion matrix was used to validate the model for a dose regimen of 1,250 mg lapatinib (precision = 81% and recall = 95%), and for a dose regimen of 1,000 mg lapatinib (precision = 87% and recall = 64%). To conclude, we established a deep learning model to predict lapatinib dose based on important influencing variables selected from real-world evidence, to achieve an optimal individualized dose regimen with good predictive performance.

Keywords: lapatinib, machine learning, deep learning, TabNet, breast cancer, real-world study, individualized medication model

HIGHLIGHTS

1. What is the current knowledge on the topic?

Lapatinib was approved in China to treat patients with HER2(+) metastatic breast cancer in combination with capecitabine based on a single-arm, open-label study (EGF10949). Two dose regimens are commonly recommended for lapatinib, 1,250 mg of lapatinib in combination with

capecitabine and 1,000 mg of lapatinib in combination with trastuzumab. Under the recommended dose regimen, lapatinib can be well tolerated with minimal avoidance of drug toxicities.

2. What question did this study address?

In this study, we established a deep learning model to predict the lapatinib dose based on important influencing variables from real-world evidence, resulting in getting the optimal individualized dose regimen.

3. What does this study add to our knowledge?

This study provides a new perspective and guidance for lapatinib dose administration where few studies focused on individualized lapatinib dose treatment in breast cancer patients previously.

4. How might this change clinical pharmacology or translational science?

Models based on machine learning and deep learning methods could help clinicians treat breast cancer patients with individualized lapatinib dose regimens to get the optimal effect and reduce adverse events.

INTRODUCTION

Lapatinib is a selective inhibitor of the tyrosine kinase receptor and human epidermal growth factor receptor-2 (HER2) and has activity in HER2-overexpressing breast cancer (1–3). By binding to the ATP-binding site of the receptor's intracellular domain, lapatinib blocks HER2 tyrosine kinase activity leading to inhibition of tumor cell growth (4). After the progress with anthracycline, taxane, and trastuzumab in China, lapatinib has been introduced for the treatment of advanced/metastatic HER2(+) breast cancer (1, 4–6). Two dose regimens are commonly recommended for lapatinib, which can be optimally tolerated (7). For patients with advanced HER2(+) breast cancer progressing with therapy with anthracyclines, taxanes, and trastuzumab, it is recommended to administer 1,250 mg of lapatinib in combination with capecitabine (4). For patients with metastatic HER2(+), hormone receptor(-) breast cancer upon progressing with therapy with trastuzumab and chemotherapy, it is recommended to administer 1,000 mg of lapatinib in combination with trastuzumab (4). Under the recommended dose regimen, lapatinib can be well tolerated with minimal avoidance of drug toxicities, which are skin rash and diarrhea predominantly (6, 8–10). Therefore, a promising model to predict an appropriate individualized dose regimen is important to get a balance of lapatinib efficacy and toxicities to improve the treatment outcome.

With the rapid development of information technology, real-world study has become an important data source for clinical research (11). Most real-world studies use information from electronic medical records, examination data, and follow-up records during diagnosis and treatment. Real-world study is a process of data mining, model building, and clinical feature data extraction. The main advantages of real-world studies include rich evidence resources, good external validity, individualized program application, and being closer to clinical practice (12, 13). Compared with conventional modeling methods, machine learning and deep learning techniques have indubitable advantages in dealing with real-world evidence, such as the following: (1) machine learning and deep learning can deal with more complex, high-dimensional, and interactive variables, which is lacking in traditional models, and (2) machine learning and deep learning models have stronger generalization and better accuracy than traditional models (14–16). Recently, some algorithms with more sophisticated principles have been developed, such as eXtreme Gradient Boosting (XGBoost), light gradient boosting machine (LightGBM), Categorical Boosting (CatBoost), Gradient Boosting Decision Tree (GBDT), and TabNet, which have been highly recognized in algorithm competitions (17–21). Recently, the application of machine learning and deep learning techniques based on real-world study has been a trend, such as a novel prognostic scoring system of intrahepatic cholangiocarcinoma with ensemble machine learning algorithms (XGBoost, random forest, and GBDT), a prediction model of tacrolimus blood concentration in patients with autoimmune diseases using XGBoost, a novel vancomycin dose prediction model through XGBoost, and warfarin maintenance dose prediction through LightGBM (22–25). Many studies have demonstrated the advantages of machine learning algorithms over traditional statistical methods. With the increasing number of input subject data, machine learning and deep learning models can continually optimize parameters to achieve better performance and practicality.

In order to achieve a balance of drug efficacy and toxicities, an appropriate dose regimen is important for patients' treatment outcome. In this study, we aim to establish a model based on machine learning and deep learning techniques to predict the lapatinib dose based on important influencing variables from real-world evidence, resulting in getting the optimal individualized dose regimen.

METHODS

Study Population

This is a retrospective, real-world study. Patients who were diagnosed with breast cancer and treated with lapatinib were included from July 2016 and June 2017 at Fudan University Shanghai Cancer Center (FUSCC). One hundred fifty-four patients were enrolled, including 55 at the initial dose of 1,000 mg, 94 at the initial dose of 1,250 mg, and 5 at the initial dose of 500 mg. This study mainly considered patients with commonly recommended dose regimens, namely, 1,000 mg and 1,250 mg. Therefore, after excluding patients with an initial dose of 500 mg, 149 patients remained. This study was approved by the ethics committee (No. 2016-106-1159-K1), and informed consents were included.

Data Collection and Processing

All data were collected from electronic medical records. Demographic information included continuous variables, such as age, height, and weight, and binary variables, such as age ≥52 years or not. Combination medication information included the

prior use of anthracycline, taxane, platinum, fluorouracil, and trastuzumab. Physiopathological conditions indicated that patients had hypertension, diabetes, heart disease, other underlying diseases (including small samples of epilepsy, hepatitis, hyperthyroidism, chronic enteritis, Hashimoto's thyroiditis, hepatitis B), and postmenopausal or not. Treatment protocol information included number of previous chemotherapy regiments, Ki-67, prior endocrine therapy, estrogen receptors (ER), progesterone receptors (PR), disease stage, operation, Eastern Cooperative Oncology Group (ECOG), number of metastases, lung metastases, liver metastases, bone metastases, brain metastases, protocol_1 (combination regimen of lapatinib + capecitabine), protocol_2 (combination regimen of paclitaxel + carboplatin + herceptin + lapatinib), protocol_3 (combination regimen of vinorelbine + lapatinib), and protocol_4 (other combination regimens).

There were two initial dose regimens of lapatinib, 1,000 and 1,250 mg, which were converted to binary variables, where 1,250 mg corresponds to "1" and 1,000 mg corresponds to "0." According to the National Cancer Institute Common Terminology Criteria for Adverse Events (NCI-CTCAE, version 5.0), patients with adverse drug reactions of grade ≤ 2 were considered to have drug safety. In addition, according to a previous study on lapatinib in breast cancer patients at FUSCC, the median progression-free survival (PFS) was 8.1 months; therefore, patients with PFS >8.1 months were considered to have drug effectiveness herein (1). The safety and effectiveness of the drug regimen were also converted to binary variables, where patients showing both safety and effectiveness correspond to "1," and other situations (either showing safety or effectiveness; not showing safety or effectiveness) correspond to "0." The target variable was the initial dose regimen of lapatinib (1,000 or 1,250 mg). The variables with extremely imbalanced positive and negative sample sizes in the dataset were eliminated. In terms of data with missing values, the variables were interpolated by the random forest algorithm through learning information about similar patients.

Variable Selection and Model Establishment

The modeling process is illustrated in **Figure 1**. After collecting and processing data of all eligible samples, the sequential forward selection (SFS) algorithm based on RF was applied for selecting the minimum size and optimum performance of the feature subset (26). The SFS algorithm added one feature to the feature subset each time, iteratively generated a new model, and calculated the model performance (f1_score). F1_score is a comprehensive evaluation index of precision and recall, and higher f1_score indicates better model robustness. The iteration stopped when f1_score of the feature subset reached the optimal value. The feature subset with the minimum size and optimum f1_score was therefore selected.

The training cohort and test cohort were divided according to 8:2. The dose prediction model was established and compared by 12 algorithms, which were algorithms with good predictive ability in various common algorithm types, including logistic regression, support vector machine (SVM), random forest (RF), Adaboost, XGBoost, gradient-boosted decision tree, LightGBM, CatBoost, TabNet, Artificial Neural Network (ANN), Super TML, and Wide&Deep, respectively. As a novel deep learning architecture, we implemented the TabNet model exactly as described in Arik and Pfister, used a sparsemax attention, and included the sparsification term in the loss function (21). The model-specific hyperparameters were n_d = 8, n_a = 8, n_steps = 3, gamma = 1.3, cat_emb_dim = 1, n_independent = 2, n_shared = 2, epsilon = 1e-15, momentum = 0.02, lambda_sparse = 0.001, seed = 0, clip_value = 1, verbose = 1,

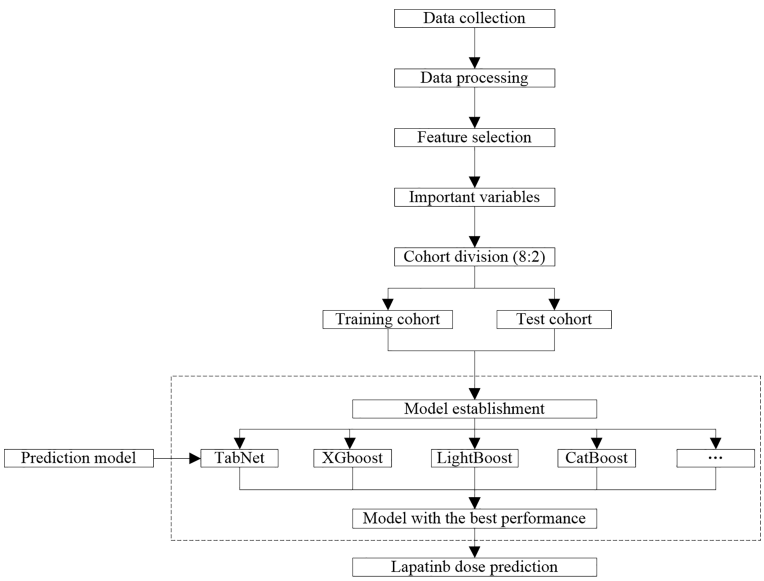

FIGURE 1 | Workflow of data process and model establishment.

max_epochs = 200, virtual_batch_size = 16, batch_size = 64. TabNet architecture and implementation details are illustrated in **Supplementary Figures S1–S4**.

Statistical Analysis

Subsequently, based on the selected important variables, the evaluation metrics for model performance were calculated, including precision, recall, f1_score, accuracy, and area under the curve (AUC). The model with the best predictive performance in the test cohort was selected to predict the lapatinib dose regimen. The specific formula of evaluation metrics are as follows:

Accuracy = (TP + TN)/(TP+FN+FP+TN)

Precision = TP/(TP + FP)

Recall = TP/(TP + FN)

f1_score = 2 × TP/(2 × TP + FP + FN)

TP: true positive, indicating that the positive class is predicted as the number of positive classes; TN: true negative, indicating that the negative class is predicted as the number of negative classes; FP: false positive, indicating that the negative class is predicted as the number of positive classes; FN: false negative, indicating that the positive class is predicted as the number of negative classes.

f1_score is used to measure the merits and defects of the model; higher f1_score indicates better model performance.

The importance of variables refers to the degree to which each variable in the model contributes to improving the predictive power of the whole model. Herein, we used the algorithm with the best model performance to calculate and rank the variable importance scores. In terms of importance score calculation and ranking by TabNet, the Feature Transformer layer realizes the calculation and processing of features selected by the current step. Analogous to a decision tree, for a given set of features, a decision tree constructs a combination of size relations of individual features, namely, a decision manifold. A simple neural network is used to simulate the decision manifold of the decision tree through a fully connected (FC) layer, but the FC layer constructs a set of simple linear relations and does not consider more complicated cases. TabNet performs feature calculation through a more complex Feature Transformer layer. Its decision manifold may not be similar to that of the decision tree, and it may do better than the decision tree in some Feature combinations (21). Univariate analysis was performed through the Mann–Whitney U test on continuous variables and the chi-square test on classified variables.

Eventually, the confusion matrix was used to visualize the performance of the algorithm and further analyze the model performance. The confusion matrix was realized by the Matplotlib package. All experiments of machine learning and deep learning algorithms were run on Windows 10 with Intel(R) Core(TM) i5-10400F CPU @ 2.90GHz 12CPUs and 512GB memory. Data analysis was conducted using python 3.8.8 and IBM SPSS Statistics 22.

We carried out six-fold cross-validation for each model with calculating the mean, standard deviation, and P-value of each indicator. As shown in **Table 1**, the better performance of the TabNet model on stability and robustness was observed compared with other models. As shown in **Table 2**, the importance of "Treatment protocols" has always ranked ahead of other variables.

TABLE 1 | Prediction performance of different algorithms with six-fold cross-validation.

Metrics Algorithms	Dose regimen[a]	Precision (mean ± std, P)	Recall (mean ± std, P)	f1_score (mean ± std, P)	Support	Accuracy (mean ± std, P)	AUC (mean ± std, P)
LR	0	0.47 ± 0.34 (0.317)	0.15 ± 0.11 (0.785)	0.23 ± 0.16 (0.668)	11	0.68 ± 0.06 (0.463)	0.59 ± 0.11 (0.489)
	1	0.65 ± 0.03 (0.482)	0.91 ± 0.05 (0.317)	0.78 ± 0.04 (0.409)	19		
SVM	0	0.92 ± 0.09 (0.317)	0.31 ± 0.10 (0.585)	0.42 ± 0.14 (0.48)	11	0.71 ± 0.07 (0.405)	0.30 ± 0.13 (0.408)
	1	0.71 ± 0.06 (0.429)	0.99 ± 0.02 (0.317)	0.81 ± 0.04 (0.377)	19		
RF	0	0.81 ± 0.15 (0.317)	0.42 ± 0.18 (0.525)	0.56 ± 0.17 (0.484)	11	0.75 ± 0.05 (0.424)	0.79 ± 0.03 (0.397)
	1	0.73 ± 0.05 (0.418)	0.94 ± 0.04 (0.317)	0.83 ± 0.03 (0.388)	19		
AdaBoost	0	0.81 ± 0.07 (0.431)	0.42 ± 0.10 (0.435)	0.58 ± 0.07 (0.305)	11	0.76 ± 0.04 (0.418)	0.77 ± 0.06 (0.363)
	1	0.74 ± 0.06 (0.394)	0.92 ± 0.09 (0.373)	0.82 ± 0.09 (0.381)	19		
XGBoost	0	0.80 ± 0.14 (0.317)	0.44 ± 0.07 (0.585)	0.58 ± 0.09 (0.48)	11	0.76 ± 0.05 (0.405)	0.76 ± 0.04 (0.406)
	1	0.74 ± 0.03 (0.429)	0.93 ± 0.04 (0.317)	0.83 ± 0.04 (0.377)	19		
GBDT	0	0.77 ± 0.17 (0.317)	0.59 ± 0.14 (0.467)	0.67 ± 0.14 (0.4)	11	0.79 ± 0.08 (0.368)	0.81 ± 0.11 (0.357)
	1	0.79 ± 0.06 (0.388)	0.88 ± 0.06 (0.317)	0.84 ± 0.06 (0.354)	19		
LightGBM	0	0.69 ± 0.16 (0.391)	0.44 ± 0.07 (0.585)	0.54 ± 0.11 (0.505)	11	0.72 ± 0.08 (0.424)	0.76 ± 0.06 (0.413)
	1	0.74 ± 0.09 (0.434)	0.87 ± 0.12 (0.343)	0.80 ± 0.07 (0.391)	19		
CatBoost	0	0.84 ± 0.11 (0.317)	0.53 ± 0.11 (0.467)	0.65 ± 0.09 (0.4)	11	0.79 ± 0.09 (0.368)	0.78 ± 0.04 (0.362)
	1	0.77 ± 0.04 (0.388)	0.93 ± 0.05 (0.317)	0.85 ± 0.04 (0.354)	19		
TabNet	0	0.87 ± 0.03 (0.317)	0.64 ± 0.01 (0.525)	0.73 ± 0.01 (0.461)	11	0.82 ± 0.05 (0.405)	0.83 ± 0.01 (0.397)
	1	0.81 ± 0.02 (0.413)	0.95 ± 0.03 (0.317)	0.87 ± 0.02 (0.38)	19		
ANN	0	0.42 ± 0.11 (0.549)	0.45 ± 0.15 (0.585)	0.44 ± 0.13 (0.568)	11	0.55 ± 0.06 (0.484)	0.58 ± 0.07 (0.482)
	1	0.67 ± 0.05 (0.453)	0.54 ± 0.06 (0.43)	0.62 ± 0.04 (0.442)	19		
Super TML	0	0.78 ± 0.11 (0.427)	0.34 ± 0.11 (0.415)	0.48 ± 0.09 (0.361)	11	0.71 ± 0.05 (0.385)	0.56 ± 0.07 (0.354)
	1	0.70 ± 0.04 (0.323)	0.93 ± 0.05 (0.367)	0.80 ± 0.04 (0.381)	19		
Wide&Deep	0	0.69 ± 0.09 (0.549)	0.43 ± 0.12 (0.585)	0.54 ± 0.11 (0.568)	11	0.72 ± 0.07 (0.328)	0.74 ± 0.12 (0.389)
	1	0.72 ± 0.03 (0.355)	0.87 ± 0.04 (0.243)	0.79 ± 0.04 (0.355)	19		

[a]*Regimen of 1,000 mg lapatinib corresponds to "0," and regimen of 1,250 mg lapatinib corresponds to "1."*

TABLE 2 | Feature importance from TabNet with six-fold cross-validation.

Feature	Importance (mean ± std)	P value
Treatment protocols	0.47 ± 0.05	0.612
Weight	0.23 ± 0.07	0.345
Number of chemotherapy treatments	0.16 ± 0.05	0.472
Number of metastases	0.05 ± 0.09	0.247

Treatment protocols including protocol_1 (combination regimen of lapatinib + capecitabine), protocol_2 (combination regimen of paclitaxel + carboplatin + herceptin + lapatinib), protocol_3 (combination regimen of vinorelbine + lapatinib), and protocol_4 (other combination regimens).

RESULTS

Patients and Treatments

A total of 149 breast cancer patients were enrolled from FUSCC in this study; the population characteristics are illustrated in **Table 3**. There were 55 (36.90%) patients administered an initial lapatinib regimen of 1,000 mg, and 94 (63.10%) patients administered an initial lapatinib regimen of 1,250 mg. The median age of the patients was 51 years (interquartile range [IQR] 42~58 years), and 51.78% of patients were aged over 51 years. Patients using anthracycline, taxane, platinum, fluorouracil, and trastuzumab occupied 67.79%, 89.93%, 42.28%, 50.34%, and 91.28%, respectively. Comorbidities including hypertension, diabetes, and heart disease occupied 12.08%, 4.03%, and 3.36%, respectively. A percentage of 59.73% of patients were postmenopausal; 51.68% of patients had ≥3 previous chemotherapy regiments. Patients having ER and PR occupied 55.03% and 68.46%, respectively. A percentage of 75.84% of patients were in stage IV, 19.46% in stage III, and 4.70% in stage II. The most common metastatic site was in the lung (42.28%), bone (31.54%), liver (26.85%), and brain (18.12%). Patients using protocol_1, protocol_2, protocol_3, and protocol_4 were 67.11%, 16.11%, 6.71%, and 10.07%, respectively. There were 46 (30.87%) patients showing both safety and effectiveness of lapatinib treatment.

Variable Selection

After deleting variables with extremely imbalanced positive and negative sample sizes (such as diabetes, heart disease, operation, and ECOG), features were selected based on 26 variables through the SFS method. RF models were established using the selected 1 to 26 variables, and the f1_score of each model was obtained (**Figure 2**). With increasing number of included variables, f1_score rises first and then reaches its maximum value at four variables (f1_score = 0.68). As we pursued a concise and accurate model with minimal variables but high predictive performance, the first four important variables were selected to establish the prediction model, including weight, number of chemotherapy treatments, number of metastases, and treatment protocols.

Model Establishment

In **Table 1**, we presented the predictive performance of 12 models. TabNet had precision = 0.87, recall = 0.64, and f1_score = 0.73 for the 1,000-mg regimen prediction, and precision = 0.81, recall = 0.95, and f1_score = 0.87 for 1,250-mg regimen prediction, which indicate a comprehensive good predictive ability. In addition, accuracy = 0.82 and AUC = 0.83 for the whole TabNet model, which were higher than those for other algorithms. This shows that TabNet has competitiveness to predict the initial dose regimen of lapatinib accurately and establish a robust prediction model. On this basis, the importance scores of four selected variables were calculated and ranked by TabNet (**Table 2**). It can be seen that the most important variables were treatment protocols, weight, number of chemotherapy treatments, and number of metastases, with the importance scores of 0.47, 0.23, 0.16, and 0.05, in descending order. The P-values of treatment protocols, weight, and number of chemotherapy treatments were 0.612, 0.345, 0.472, and 0.247, respectively.

The test cohort consisted of 30 patients, among which 19 patients took lapatinib 1,250 mg and 11 patients took lapatinib 1,000 mg. The dose of lapatinib was recommended for patients by establishing a confusion matrix based on the TabNet prediction model (**Figure 3**). The model recommended a dose regimen of 1,250 mg lapatinib accurately for 18 patients, and four patients were recommended the wrong dose, with a precision of 82% and a recall rate of 95%; the model recommended a dose regimen of 1,000 mg lapatinib accurately for seven patients, and one patient was recommended the wrong dose, with a precision of 88% and a recall rate of 64%.

DISCUSSION

Lapatinib was approved in China to treat patients with HER2(+) metastatic breast cancer in combination with capecitabine based on a single-arm, open-label study (EGF10949), which evaluates the drug efficacy and safety (1, 27). Our study focused on the establishment of a prediction model for lapatinib dose, mainly evaluating two dose regimens (1,000 and 1,250 mg). We used TabNet, a leading-edge deep learning technique, to construct the prediction model with good performance (accuracy = 0.82 and AUC = 0.83). Afterward, important variables that strongly correlated with lapatinib dose were ranked *via* an importance score, including treatment protocols, weight, number of chemotherapy treatments, and number of metastases. Lastly, the confusion matrix was used to validate the model; it can be seen that the dose regimen of 1,000 mg lapatinib had a precision of 88% and a recall rate of 64%, and the dose regimen of 1,250 mg lapatinib had a precision of 82% and a recall rate of 95%.

As a novel deep learning technique, TabNet uses a sequential attention mechanism to choose a subset of meaningful features to process at each decision step, enabling interpretability and

TABLE 3 | Description of demographic and clinical characteristics.

Categories	Variables	Cases (N = 149)	Missing rate
Lapatinib information	Initial dose regimen, n (%)[a]		0
	0	55 (36.90%)	
	1	94 (63.10%)	
Demographic information	Age, year, median (IQR)	51 (42.0–58.0)	0
	Height, cm, median (IQR)	160.2 (158.0–162.0)	0
	Weight, kg, median (IQR)	58.3 (53.0–64.0)	0
	Age ≥ 52 years, n (%)	77 (51.78%)	0
Drug combination	Prior use of anthracycline, n (%)	101 (67.79%)	0
	Prior use of taxane, n (%)	134 (89.93%)	0
	Prior use of platinum, n (%)	63 (42.28%)	0
	Prior use of fluorouracil, n (%)	75 (50.34%)	0
	Prior use of trastuzumab, n (%)	136 (91.28%)	0
Physiopathological condition	Hypertension, n (%)	18 (12.08%)	0
	Diabetes, n (%)	6 (4.03%)	0
	Heart disease, n (%)	5 (3.36%)	0
	Other underlying diseases, n (%)	14 (9.4%)	0
	Postmenopausal, n (%)	89 (59.73%)	2.7%
Treatment information	Number of chemotherapy treatments, n (%)		0
	<3	72 (48.32%)	
	≥3	77 (51.68%)	
	Ki-67, median (IQR)	38.1 (20.0–50.0)	8.7%
	Prior endocrine therapy, n (%)	54 (36.24%)	0
	ER, n (%)		0
	0	67 (44.97%)	
	1	82 (55.03%)	
	PR, n (%)		0
	0	47 (31.54%)	
	1	102 (68.46%)	
	Stage, n (%)		0
	2	7 (4.70%)	
	3	29 (19.46%)	
	4	113 (75.84%)	
	Operation, n (%)		0
	0	13 (8.72%)	
	1	131 (87.92%)	
	2	2 (1.34%)	
	ECOG, n (%)		2.0%
	1	145 (97.32%)	
	2	4 (2.68%)	
	Number of metastases, n (%)		0
	0	36 (24.16%)	
	1	60 (40.27%)	
	2	33 (22.15%)	
	3	14 (9.04%)	
	4	6 (4.03%)	
	Metastases, n (%)		0
	<2	96 (64.43%)	
	≥2	53 (35.57%)	
	Lung metastases, n (%)	63 (42.28%)	0
	Liver metastases, n (%)	40 (26.85%)	0
	Bone metastases, n (%)	47 (31.54%)	0
	Brain metastases, n (%)	27 (18.12%)	0
	Other metastases, n (%)	35 (23.49%)	0
	Treatment protocols, n (%)[b]		0
	Protocol_1	100 (67.11%)	
	Protocol_2	24 (16.11%)	
	Protocol_3	10 (6.71%)	
	Protocol_4	15 (10.07%)	
Safety and effectiveness	Safety and effectiveness, n (%)[c]		0
	1	46 (30.87%)	
	0	103 (69.13%)	

[a]*Regimen of 1250 mg lapatinib corresponds to "1," and regimen of 1,000 mg lapatinib corresponds to "0."*

[b]*Protocol_1 indicates combination regimen of lapatinib + capecitabine, protocol_2 indicates combination regimen of paclitaxel + carboplatin + herceptin + lapatinib, protocol_3 indicates combination regimen of vinorelbine + lapatinib, and protocol_4 indicates other combination regimens.*

[c]*Patient showing both safety and effectiveness corresponds to "1," and other situations (either showing safety or effectiveness; not showing safety nor effectiveness) corresponds to "0." IQR, interquartile range; ER, estrogen receptors; PR, progesterone receptors; ECOG, Eastern Cooperative Oncology Group.*

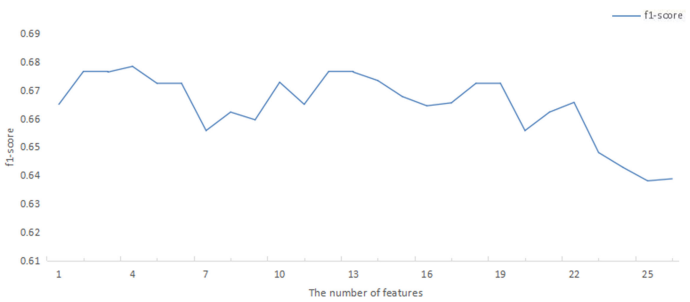

FIGURE 2 | F1_score of RF model corresponding to the number of ranked variables. RF, random forest.

more efficient learning as the learning capacity used for the most salient features (21). Additionally, based on retaining the end-to-end and representation learning characteristics of deep neural networks, TabNet also has the advantages of tree model interpretability and sparse feature selection (28). Other studies based on real-world evidence show that TabNet outperforms ensemble tree-based algorithms, since it can process a highly nonlinear relationship with its depth, without overfitting due to instance-wise feature selection (21). In this study, we applied TabNet, super TML, Wide&Deep, and ANN, which are algorithms with good predictive ability in various network algorithm types. After comparing the different network models, the TabNet model shows the best prediction performance (**Table S1**). Later, we will increase multicenter data. With larger data volume, we will build different network models and explore the optimum one to predict the dose of lapatinib to assist clinical medication.

As one of the most important variables influencing lapatinib dose, protocols of combination therapy accounted for a different proportion in this study as follows: protocol_1, protocol_2, protocol_3, and protocol_4 accounted for 67.11%, 16.11%, 6.71%, and 10.07%, respectively. The combination of lapatinib + cape citabine (protocol_1) was one of the common recommended regimens for patients with HER2(+) breast cancer with prior treatment of taxanes, anthracyclines, and/or trastuzumab (29, 30). Clinicians generally used lapatinib at a dose of 1,250 mg daily continuously plus capecitabine at a dose of 2,000 mg daily, and the combination can achieve superior treatment efficacy than capecitabine monotherapy (29, 31). In addition, a study on Japanese breast cancer patients found a drug–drug interaction and pharmacokinetics interaction between lapatinib and paclitaxel, as the AUC and Cmax of these patients given the combination therapy were affected (32). In Rezai et al.'s study, a pharmacokinetic interaction was found between lapatinib and

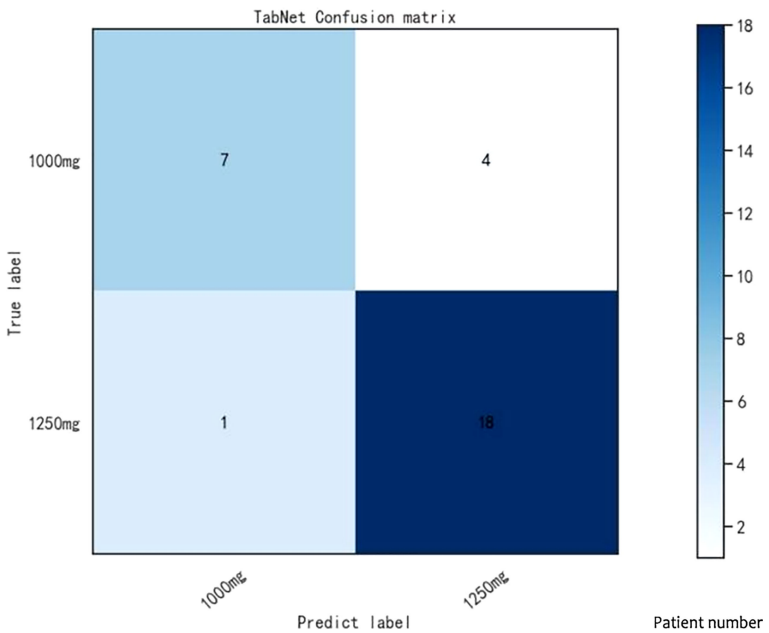

FIGURE 3 | Confusion matrix in TabNet model.

vinorelbine, and the use of lapatinib can remarkably decrease the vinorelbine clearance (33). It has been proven that therapy of lapatinib combined with other drugs can commonly improve the time to progression and/or achieve longer survival time in these patients (29, 34, 35). Normally, previous studies focused on the efficacy and safety of combination therapy; few investigated the effect on dose regimen. Further research is needed to confirm the relationships between combination therapy and drug doses.

For the physiological features, previous studies found that patients with lower weight were more likely to have higher lapatinib plasma levels (P = 0.055) (36). The researchers believed that patients without fasting and lapatinib dose were not adjusted to low body weight during drug intake, which would lead to increased lapatinib body levels (36). The number of chemotherapy treatments was identified as an important influencing variable for lapatinib dose, and a previous study showed that three or more prior treatments strongly correlated with worse survival (1). Additionally, some studies found that organ metastases (such as liver and brain metastases) show a strong relationship with morbidity, mortality, and survival rate in breast cancer patients, which may affect the lapatinib dose regimen (37–39). In this study, the number of metastases has a remarkable effect on lapatinib dose whose correlation was previously investigated by few studies, which warranted further research.

According to the confusion matrix results, the classifier correctly identified 82% of patients using the 1,250-mg lapatinib regimen and 88% of patients using the 1,000-mg lapatinib regimen, indicating a remarkable prediction performance. Nevertheless, the sample size in the training and test cohorts was small. Large samples are required to verify this result.

CONCLUSION

Our study endeavored to build a dose prediction model *via* machine learning and deep learning methods, which could mine deep data based on real-world evidence. Through a comparison of different algorithms, TabNet was selected to establish the model based on the strength of its predictive ability. To our knowledge, few studies focused on lapatinib dose prediction previously, and this study provides a new perspective and guidance for lapatinib dose administration with a more concise and accurate model. Compared with conventional models, machine learning and deep learning models mine and use unexploited variables to cover the shortage of clinical experience from the real world. One limitation in this study was the limited sample size that affected the model to further optimize the performance. In future, more real-world evidence should be added in the model to optimize its performance, and larger prospective clinical studies will be needed to investigate the further interactions between different variables and lapatinib dose.

DATA AVAILABILITY STATEMENT

The raw data supporting the conclusions of this article will be made available by the authors, without undue reservation.

ETHICS STATEMENT

The studies involving human participants were reviewed and approved by the Ethics Committee at Fudan University Shanghai Cancer Center (FUSCC) (No. 2016-106-1159-K1). The patients/participants provided their written informed consent to participate in this study.

AUTHOR CONTRIBUTIONS

ZY and XY led the research and provided medical support. FK analyzed and interpreted the data. HYL, JZ, and ZW analyzed the data and provided technical support. HL and XH wrote the manuscript. HW and FG provided methodological guidance. QZ provided technical and medical guidance. All authors contributed to the article and approved the submitted version.

FUNDING

FG was supported by the National Key Research and Development Program (2020YFC2005502, 2020YFC2005503). QZ was supported by the Clinical Research Plan of SHDC [SHDC2020CR3085B].

SUPPLEMENTARY MATERIAL

The Supplementary Material for this article can be found online at: https://www.frontiersin.org/articles/10.3389/fonc.2022.893966/full#supplementary-material

REFERENCES

1. Ye X, Luo X, Du Q, Li H, Liu HY, Yu B, et al. Efficacy and Safety of Lapatinib in Chinese Breast Cancer Patients: A Real-World Study. *Ann Transl Med* (2020) 8(5):240. doi: 10.21037/atm.2020.03.21
2. Bonde GV, Yadav SK, Chauhan S, Mittal P, Ajmal G, Thokala S, et al. Lapatinib Nano-Delivery Systems: A Promising Future for Breast Cancer Treatment. *Expert Opin Drug Deliv* (2018) 15(5):495–507. doi: 10.1080/17425247.2018.1449832
3. Opdam FL, Guchelaar HJ, Beijnen JH, Schellens JH. Lapatinib for Advanced or Metastatic Breast Cancer. *Oncologist* (2012) 17(4):536–42. doi: 10.1634/theoncologist.2011-0461
4. Voigtlaender M, Schneider-Merck T, Trepel M. Lapatinib. *Recent Results Cancer Res* (2018) 211:19–44. doi: 10.1007/978-3-319-91442-8_2
5. Giampaglia M, Chiuri VE, Tinelli A, De Laurentiis M, Silvestris N, Lorusso V. Lapatinib in Breast Cancer: Clinical Experiences and Future Perspectives. *Cancer Treat Rev* (2010) 36 Suppl 3:S72–9. doi: 10.1016/S0305-7372(10)70024-4

6. Estévez LG, Suarez-Gauthier A, García E, Miró C, Calvo I, Fernández-Abad M, et al. Molecular Effects of Lapatinib in Patients With HER2 Positive Ductal Carcinoma *In Situ*. *Breast Cancer Res* (2014) 16(4):R76. doi: 10.1186/bcr3695
7. Crown J, Kennedy MJ, Tresca P, Marty M, Espie M, Burris HA, et al. Optimally Tolerated Dose of Lapatinib in Combination With Docetaxel Plus Trastuzumab in First-Line Treatment of HER2-Positive Metastatic Breast Cancer. *Ann Oncol* (2013) 24(8):2005–11. doi: 10.1093/annonc/mdt222
8. Frankel C, Palmieri FM. Lapatinib Side-Effect Management. *Clin J Oncol Nurs* (2010) 14(2):223–33. doi: 10.1188/10.CJON.223-233
9. Fontanella C, Lederer B, Nekljudova V, Untch M, von Minckwitz G, Loibl S. Does Toxicity Predict Efficacy? Insight Into the Mechanism of Action of Lapatinib. *J Clin Oncol* (2014) 32(30):3458–9. doi: 10.1200/JCO.2014.57.0499
10. Tao G, Chityala PK. Epidermal Growth Factor Receptor Inhibitor-Induced Diarrhea: Clinical Incidence, Toxicological Mechanism, and Management. *Toxicol Res (Camb)* (2021) 10(3):476–86. doi: 10.1093/toxres/tfab026
11. Blonde L, Khunti K, Harris SB, Meizinger C, Skolnik NS. Interpretation and Impact of Real-World Clinical Data for the Practicing Clinician. *Adv Ther* (2018) 35(11):1763–74. doi: 10.1007/s12325-018-0805-y
12. Palacios M. The Quality of Research With Real-World Evidence. *Colomb Med (Cali)* (2019) 50(3):140–1. doi: 10.25100/cm.v50i3.4259
13. Robson C. *Real World Research. 3rd Edn*. United Kingdom: John Wiley & Sons Ltd (2011).
14. Mo X, Chen X, Li H, Li J, Zeng F, Chen Y, et al. Early and Accurate Prediction of Clinical Response to Methotrexate Treatment in Juvenile Idiopathic Arthritis Using Machine Learning. *Front Pharmacol* (2019) 10:1155. doi: 10.3389/fphar.2019.01155
15. Lee HC, Yoon SB, Yang SM, Kim WH, Ryu HG, Jung CW, et al. Prediction of Acute Kidney Injury After Liver Transplantation: Machine Learning Approaches vs. Logistic Regression Model. *J Clin Med* (2018) 7(11):428. doi: 10.3390/jcm7110428
16. Kruppa J, Ziegler A, König IR. Risk Estimation and Risk Prediction Using Machine-Learning Methods. *Hum Genet* (2012) 131(10):1639–54. doi: 10.1007/s00439-012-1194-y
17. Chen T, Guestrin C. XGBoost: A Scalable Tree Boosting System. In: *Proceedings of the 22nd ACM SIGKDD International Conference on Knowledge Discovery and Data Mining*. San Francisco, CA: ACM (2016). p. 785–94.
18. Ke G, Meng Q, Finley T, Wang T, Chen W, Ma W, et al. A Highly Efficient Gradient Boosting Decision Tree. In: *Proceedings of the Advances in Neural Information Processing Systems*. Long Beach, CA, USA: Curran Associates, Inc (2017). p. 3146–54.
19. Prokhorenkova L, Gusev G, Vorobev A, Dorogush AV, Gulin A. *Catboost: Unbiased Boosting With Categorical Features*. (2017).
20. Zhang J, Mucs D, Norinder U, Svensson F. LightGBM: An Effective and Scalable Algorithm for Prediction of Chemical Toxicity-Application to the Tox21 and Mutagenicity Data Sets. *J Chem Inf Model* (2019) 59(10):4150–8. doi: 10.1021/acs.jcim.9b00633
21. Arik SO, Pfister T. *TabNet: Attentive Interpretable Tabular Learning*. (2019). p. 07442.
22. Huang X, Yu Z, Wei X, Shi J, Wang Y, Wang Z, et al. Prediction of Vancomycin Dose on High-Dimensional Data Using Machine Learning Techniques. *Expert Rev Clin Pharmacol* (2021) 14(6):761–71. doi: 10.1080/17512433.2021.1911642
23. Liu Y, Chen J, You Y, Xu A, Li P, Wang Y, et al. An Ensemble Learning Based Framework to Estimate Warfarin Maintenance Dose With Cross-Over Variables Exploration on Incomplete Data Set. *Comput Biol Med* (2021) 131:104242. doi: 10.1016/j.compbiomed.2021.104242
24. Li Z, Yuan L, Zhang C, Sun J, Wang Z, Wang Y, et al. A Novel Prognostic Scoring System of Intrahepatic Cholangiocarcinoma With Machine Learning Basing on Real-World Data. *Front Oncol* (2021) 10:576901. doi: 10.3389/fonc.2020.576901
25. Zheng P, Yu Z, Li L, Liu S, Lou Y, Hao X, et al. Predicting Blood Concentration of Tacrolimus in Patients With Autoimmune Diseases Using Machine Learning Techniques Based on Real-World Evidence. *Front Pharmacol* (2021) 12:727245. doi: 10.3389/fphar.2021.727245
26. Hatamikia S, Maghooli K, Nasrabadi AM. The Emotion Recognition System Based on Autoregressive Model and Sequential Forward Feature Selection of Electroencephalogram Signals. *J Med Signals Sens* (2014) 4(3):194–201. doi: 10.4103/2228-7477.137777
27. Xu BH, Jiang ZF, Chua D, Shao ZM, Luo RC, Wang XJ, et al. Lapatinib Plus Capecitabine in Treating HER2-Positive Advanced Breast Cancer: Efficacy, Safety, and Biomarker Results From Chinese Patients. *Chin J Cancer* (2011) 30(5):327–35. doi: 10.5732/cjc.010.10507
28. Yan J, Xu T, Yu Y, Xu HX. Rainfall Forecast Model Based on the TabNet Model. *Water* (2021) 13(9):1272. doi: 10.3390/w13091272
29. Cameron D, Casey M, Press M, Lindquist D, Pienkowski T, Romieu CG, et al. A Phase III Randomized Comparison of Lapatinib Plus Capecitabine Versus Capecitabine Alone in Women With Advanced Breast Cancer That has Progressed on Trastuzumab: Updated Efficacy and Biomarker Analyses. *Breast Cancer Res Treat* (2008) 112(3):533–43. doi: 10.1007/s10549-007-9885-0
30. Ma F, Ouyang Q, Li W, Jiang Z, Tong Z, Liu Y, et al. Pyrotinib or Lapatinib Combined With Capecitabine in HER2-Positive Metastatic Breast Cancer With Prior Taxanes, Anthracyclines, and/or Trastuzumab: A Randomized, Phase II Study. *J Clin Oncol* (2019) 37(29):2610–9. doi: 10.1200/JCO.19.00108
31. Geyer CE, Forster J, Lindquist D, Chan S, Romieu CG, Pienkowski T, et al. Lapatinib Plus Capecitabine for HER2-Positive Advanced Breast Cancer. *N Engl J Med* (2006) 355(26):2733–43. doi: 10.1056/NEJMoa064320
32. Inoue K, Kuroi K, Shimizu S, Rai Y, Aogi K, Masuda N, et al. Safety, Pharmacokinetics and Efficacy Findings in an Open-Label, Single-Arm Study of Weekly Paclitaxel Plus Lapatinib as First-Line Therapy for Japanese Women With HER2-Positive Metastatic Breast Cancer. *Int J Clin Oncol* (2015) 20(6):1102–9. doi: 10.1007/s10147-015-0832-5
33. Rezai K, Urien S, Isambert N, Roche H, Dieras V, Berille J, et al. Pharmacokinetic Evaluation of the Vinorelbine-Lapatinib Combination in the Treatment of Breast Cancer Patients. *Cancer Chemother Pharmacol* (2011) 68(6):1529–36. doi: 10.1007/s00280-011-1650-8
34. Patel TA, Ensor JE, Creamer SL, Boone T, Rodriguez AA, Niravath PA, et al. A Randomized, Controlled Phase II Trial of Neoadjuvant Ado-Trastuzumab Emtansine, Lapatinib, and Nab-Paclitaxel Versus Trastuzumab, Pertuzumab, and Paclitaxel in HER2-Positive Breast Cancer (TEAL Study). *Breast Cancer Res* (2019) 21(1):100. doi: 10.1186/s13058-019-1186-0
35. Cameron D, Casey M, Oliva C, Newstat B, Imwalle B, Geyer CE. Lapatinib Plus Capecitabine in Women With HER-2-Positive Advanced Breast Cancer: Final Survival Analysis of a Phase III Randomized Trial. *Oncologist* (2010) 15(9):924–34. doi: 10.1634/theoncologist.2009-0181
36. Cizkova M, Bouchalova K, Friedecky D, Polynkova A, Janostakova A, Radova L, et al. High Lapatinib Plasma Levels in Breast Cancer Patients: Risk or Benefit? *Tumori* (2012) 98(1):162–5. doi: 10.1177/030089161209800123
37. Cameron D, Casey M, Oliva C, Newstat B, Imwalle B, Geyer CE. Lapatinib Plus Capecitabine in Women With HER-2-Positive Advanced Breast Cancer: Final Survival Analysis of a Phase III Randomized Trial. *Oncologist* (2010) 15(9):924–34. doi: 10.1634/theoncologist.2009-0181
38. Göksu SS, Bozcuk H, Koral L, Çakar B, Gündüz S, Tatlı AM, et al. Factors Predicting Lapatinib Efficacy in HER-2+ Metastatic Breast Carcinoma: Does it Work Better in Different Histologic Subtypes? *Indian J Cancer* (2015) 52(4):517–9. doi: 10.4103/0019-509X.178382
39. Tomasello G, Bedard PL, de Azambuja E, Lossignol D, Devriendt D, Piccart-Gebhart MJ. Brain Metastases in HER2-Positive Breast Cancer: The Evolving Role of Lapatinib. *Crit Rev Oncol Hematol* (2010) 75(2):110–21. doi: 10.1016/j.critrevonc.2009.11.003

Conflict of Interest: Author JZ and FG are employed by Beijing Medicinovo Technology Co. Ltd., China. Author XH is employed by Dalian Medicinovo Technology Co., Ltd., China.

The remaining authors declare that the research was conducted in the absence of any commercial or financial relationships that could be construed as a potential conflict of interest.

this article, or claim that may be made by its manufacturer, is not guaranteed or endorsed by the publisher.

frontiers | Frontiers in Oncology

ORIGINAL RESEARCH
published: 20 June 2022
doi: 10.3389/fonc.2022.870843

The Risk of Heart Disease-Related Death Among Anaplastic Astrocytoma Patients After Chemotherapy: A SEER Population-Based Analysis

Qi Lin[1†], Jia-Hao Bao[2†], Fei Xue[1], Jia-Jun Qin[1], Zhen Chen[1], Zhong-Rong Chen[1], Chao Li[1], Yi-Xuan Yan[2], Jin Fu[1‡], Zhao-Li Shen[1*‡] and Xian-Zhen Chen[1*‡]*

[1] Department of Neurosurgery, Shanghai Tenth People's Hospital, Tongji University School of Medicine, Shanghai, China, [2] Hospital of Stomatology, Guanghua School of Stomatology, Sun Yat-sen University, Guangdong Provincial Key Laboratory of Stomatology, Guangzhou, China

OPEN ACCESS

Edited by:
Yao Liu,
Daping Hospital, China

Reviewed by:
Ajay Chatrath,
University of Virginia, United States
Mingwei Zhang,
First Affiliated Hospital of Fujian Medical University, China
Hualin Song,
Tianjin Medical University Cancer Institute and Hospital, China

***Correspondence:**
Xian-Zhen Chen
chenxianzheny@126.com
Zhao-Li Shen
leelies@sina.com
Jin Fu
fujin@tongji.edu.cn

[†]These authors have contributed equally to this work and share first authorship

[‡]These authors have contributed equally to this work

Specialty section:
This article was submitted to Pharmacology of Anti-Cancer Drugs, a section of the journal Frontiers in Oncology

Received: 07 February 2022
Accepted: 12 May 2022
Published: 20 June 2022

Citation:
Lin Q, Bao J-H, Xue F, Qin J-J, Chen Z, Chen Z-R, Li C, Yan Y-X, Fu J, Shen Z-L and Chen X-Z (2022) The Risk of Heart Disease-Related Death Among Anaplastic Astrocytoma Patients After Chemotherapy: A SEER Population-Based Analysis. Front. Oncol. 12:870843. doi: 10.3389/fonc.2022.870843

Background: Despite improved overall survival outcomes, chemotherapy has brought concerns for heart disease–related death (HDRD) among cancer patients. The effect of chemotherapy on the risk of HDRD in anaplastic astrocytoma (AA) patients remains unclear.

Methods: We obtained 7,129 AA patients from the Surveillance, Epidemiology, and End Results (SEER) database from 1975 to 2016. Kaplan–Meier and Cox regression analysis were conducted to evaluate the effect of chemotherapy on the HDRD risk. Based on the competing risk model, we calculated the cumulative incidences of HDRD and non-HDRD and performed univariate and multivariate regression analyses. Then, a 1:1 propensity score matching (PSM) was used to improve the comparability between AA patients with and without chemotherapy. Landmark analysis at 216 and 314 months was employed to minimize immortal time bias.

Results: AA patients with chemotherapy were at a lower HDRD risk compared to those patients without chemotherapy (adjusted HR=0.782, 95%CI=0.736–0.83, $P<0.001$). For competing risk regression analysis, the cumulative incidence of HDRD in non-chemotherapy exceeded HDRD in the chemotherapy group ($P<0.001$) and multivariable analysis showed a lower HDRD risk in AA patients with chemotherapy (adjusted SHR=0.574, 95%CI=0.331–0.991, $P=0.046$). In the PSM-after cohort, there were no significant association between chemotherapy and the increased HDRD risk (adjusted SHR=0.595, 95%CI=0.316–1.122, $P=0.11$). Landmark analysis showed that AA patients who received chemotherapy had better heart disease–specific survival than those in the non-chemotherapy group ($P=0.007$) at the follow-up time points of 216 months. No difference was found when the follow-up time was more than 216 months.

Conclusion: AA patients with chemotherapy are associated with a lower risk of HDRD compared with those without chemotherapy. Our findings may help clinicians make a decision about the management of AA patients and provide new and important evidence for applying chemotherapy in AA patients as the first-line treatment. However, more research is needed to confirm these findings and investigate the correlation of the risk of HDRD with different chemotherapy drugs and doses.

Keywords: anaplastic astrocytoma, chemotherapy, SEER, heart disease-related death, cardio-oncology

INTRODUCTION

Gliomas are the most common primary malignant neoplasms of the central nervous system with an incidence of five-to-six cases per 100,000 persons per year. Anaplastic astrocytoma (AA), a WHO grade III glioma, is a diffusely infiltrating, malignant, astrocytic, primary brain tumor (1). It constitutes approximately 6.1% of all gliomas with a median age of onset of 41 years (2, 3). Approximately 7,175 patients were newly diagnosed from 2014 to 2018 in the United States according to the Central Brain Tumor Registry of the United States (4). Patients with AA have traditionally been thought to have a terrible prognosis. The 5-year relative survival rate for AA patients has been poor at 30.5% (95%CI=29.7–31.2), and the 10-year relative survival rate has dropped to 22.2% (95%CI=21.4–23.0) (4). Although the bulk of the tumor can often be resected, the tumor almost always reoccurs due to the rapid proliferation of infiltrative residual tumor cells (5). The standardized treatment for AA is surgical removal, radiotherapy, and chemotherapy according to the National Comprehensive Cancer Network Guidelines.

Temozolomide (TMZ), an oral monofunctional alkylating agent, which has been approved by the U.S. Food and Drug Administration (FDA) for use in the treatment of anaplastic astrocytoma for the first line, is the world-recognized standardized chemotherapy method for AA (6). Previous studies have shown that TMZ can bring overall survival benefits in AA patients and TMZ is generally better tolerated compared with the primary treatment regimen PCV (procarbazine, lomustine, and vincristine). While chemotherapy can improve overall survival outcomes, its toxicity has aroused clinicians' and researchers' attention. Many chemotherapy drugs such as anthracycline agents and cyclophosphamide increase the risk of cardiovascular disease, including heart failure and myocardial infarction (7). The most common toxicities of TMZ including gastrointestinal side effects and myelosuppression have been reported (8–10). Recently, TMZ has been found to be associated with liver toxicity. As for heart toxicity, the accumulation of TMZ can cause an unusual cardiomyopathy, which restricts its use in clinics (10).

However, most of the previous studies were aimed to figure out the efficacy of chemotherapy on AA patients' overall survival, and long-term follow-up studies on the association between chemotherapy and heart disease-related death (HDRD) have been limited (8, 11–14). Thus, there is a need for clinicians and oncologists to explore whether chemotherapy increases the risk of HDRD in AA patients. The Surveillance, Epidemiology, and End Results (SEER) database provides the clinical information of cancer patients to investigate the prognostic factors of survival (15). Based on the SEER database, Guan et al. found that chemotherapy was associated with a lower cardiovascular death risk in primary central nervous system lymphoma patients than those without chemotherapy (16). Janick Weberpals found that a long-term heart-specific mortality among breast cancer survivors treated with chemotherapy or radiotherapy is not increased compared with the general population (17). However, no similar articles in AA have been published yet. Our study innovatively intends to investigate whether chemotherapy increases the risk of HDRD in AA patients on the basis of the SEER database, using competing risk regression analysis, PSM, and landmark analysis.

Abbreviations: AA, anaplastic astrocytoma; CI, confidence interval; CIF, cumulative incidence function; HDRD, heart disease–related death; HDSS, heart disease–specific survival; HR, hazard ratio; SEER, Surveillance, Epidemiology, and End Results; PSM, propensity score matching; SHR, subdistribution hazard ratio; TMZ, temozolomide.

METHODS

Data Source

Data were extracted from the SEER database (https://seer.cancer.gov/), which were downloaded using the SEER Stat 8.3.8 software. The SEER program is an authoritative population-based cancer registry, which covers approximately 34.6% of the U.S. population. Patients have been de-identified in the database, and no ethical approval was needed. The ethical approval of this publicly available information was not required (18).

Study Population and Variables

Patients diagnosed with AA as a primary tumor were obtained from the SEER database. According to the International Classification of Diseases for Oncology, the Third Edition (ICD-O-3), the code of AA was 9401. We identified 7,560 patients with a diagnosis of AA between the years 1975 and 2016. Cases without a definite survival time were excluded. We also excluded patients with an unknown information of chemotherapy, and finally, 7,129 eligible patients were included for subsequent analysis.

Patients were classified into two groups depending on the chemotherapy status (yes versus no). However, the type of chemotherapy treatment and doses were unclear. Covariates

included the age at diagnosis (≤34 years old, 35–50 years old, 51–65 years old, >66 years old), sex (male, female), race (white, black, others), marital status (single/unmarried, married, divorced/separated, widowed/others), year of diagnosis (~1998, 1999–2005, 2006–2012, 2013–2016), surgery (yes, no), previous history of malignant tumor (sequence number: yes, no), tumor size (≤4 cm, >4 cm, unknown), surgery method (gross total resection, subtotal resection, biopsy and local excision, no surgery, others), primary site (supratentorial tumor, infratentorial tumor, others), and radiation (yes, no). The HDRD information was extracted from the reason-of-death data from the SEER database. According to ICD-10 codes, HDRD was defined as death from heart diseases (I00–I09, I11, I13, I20–I51) including acute rheumatic fever (I00–I02), chronic rheumatic heart diseases (I05–I09), hypertensive heart disease (I11), hypertensive heart and renal disease (I13), ischemic heart diseases (I20–I25), pulmonary heart disease, the diseases of pulmonary circulation (I26–I28), and other forms of heart disease (I30–I51).

Statistical Analysis

The different clinicopathologic characteristics between chemotherapy and non-chemotherapy groups were analyzed and evaluated using Pearson's chi-square test. The Kaplan–Meier method was conducted to estimate heart disease-specific survival (HDSS) in different groups, and the differences between the curves were analyzed by the log-rank test. Only death from heart disease was considered as an event in the Kaplan–Meier method. For univariate and multivariate analyses, the Cox regression model was used to access the hazard ratio (HR) and 95% confidence intervals (95% CIs) to analyze the effect of chemotherapy on HDRD in AA patients. Kaplan–Meier curves and the Cox regression model were conducted using the R package "survival."

For competing risk analysis, HDRD and other cause-related deaths were two competing endpoint events (19). HDRD was considered as the primary event of interest, whereas death due to other causes was defined as a competing risk event, and an alive patient was considered as a censored event. The probability of developing primary and competing events were shown by the calculating crude cumulative incidence function (CIF) using the Fine–Gray competing risk model, which was grouped by age, chemotherapy, diagnosis time, marital status, race, radiation, sequence number, sex, surgery, surgery method, and tumor size (20, 21). The differences in CIF among subgroups were estimated with the Gray's test (22). The CIF curves for each variable were plotted using the R package "cmprsk". Then, univariate and multivariate competing risk regression analyses were employed to calculate the subdistribution hazard ratio (SHR) and 95%CI to evaluate the independent effect of chemotherapy on HDRD in AA (23).

Regarding the effect of the confounding factors between the chemotherapy and non-chemotherapy groups in the SEER cohort, we employed the PSM method to improve the comparability between groups with the R package "MatchIt". We applied age, sex, race, marital status, the year of diagnosis, primary site, tumor size, surgery, radiation, and sequence number as covariates to calculate propensity scores with a logistic regression model. The caliper value was set as 0.1. The nearest-neighbor matching method was employed, and patients were matched between 2 groups at a ratio of 1:1 (24, 25). Then, landmark analysis was conducted to avoid immortal time bias that might exist in the chemotherapy group. We chose 216 and 340 months as timepoints. The HDSS between chemotherapy and non-chemotherapy groups was estimated using the Kaplan–Meier approach. Univariate and multivariate analyses, stratified analysis, and interaction tests were also conducted in the PSM-after cohort. The landmark analysis was employed to minimize immortal time bias. Minimum follow-up times of 216 and 340 months were selected for analysis (26).

R software version 4.1.1 (https://www.r-project.org/) was used for statistical analysis and visualization (27). The following R packages were also utilized: rms, survminer, ggplot2, glmnet, pec, cobalt, and DescTools. Two-tailed *P*-values <0.05 were considered as statistically significant.

RESULTS

Demographics and Clinicopathological Findings

In all, 7,129 patients diagnosed with AA were enrolled in this study. **Table 1** summarized the demographic characteristics of patients with a chemotherapy status. Of the cohort, 4,196 patients (58.9%) were stratified into the chemotherapy group, and 2,933 patients (41.1%) were stratified into the non-chemotherapy group. Statistically significant differences ($P<0.001$) were noted, between the chemotherapy group and the non-chemotherapy group, in age (42.99% vs. 57.14% age > 50 years old), marital status (26.76% vs. 24.55% single, 6.2% vs. 14.05% widowed), the year of diagnosis(61.99% vs. 32.42% after 2006), primary site (5.93% vs. 7.47% infratentorial, 75.83% vs. 70.99% supratentorial), tumor size (23.52% vs. 13.19% less than 4 cm, 21.02% vs. 9.85% more than 4 cm), surgery (59.96% vs. 34.3% yes), radiation (66.8% vs. 34.67% yes), and surgery method (16.87% vs. 10.47% biopsy and local excision, 20.97% vs. 10.64% gross total resection, 21.07% vs. 12.21% subtotal resection, 15.87% vs. 38.6% others). After a median follow-up of 75 months, there were a total of 5,257 deaths; 71 of them were related to heart disease.

Survival Analysis and Cox Regression Analysis in AA Patients

Survival analysis was conducted in AA patients grouped by the chemotherapy status and covariates with a certain HDSS status and time. In the Kaplan–Meier curves and log-rank test, as shown in **Figures 1** and **S1**, patients who received chemotherapy enjoyed longer HDSS ($P<0.001$). Covariates including age at diagnosis, marital status, year of diagnosis, primary site, surgery and surgery method, and radiation were associated with HDSS. Similarly, in terms of HDSS, univariate Cox regression analysis also displayed an association between the improvement with HDSS and the patients' chemotherapy status (unadjusted

TABLE 1 | The demographic characteristics of anaplastic astrocytoma patients before PSM.

Characteristic	Total	Non-Chemotherapy	Chemotherapy	P	Statistic Value
	n = 7,129	n = 2,933	n = 4,196		
Age.cat, n (%)				<0.001	331.969
~34	1,805 (25.32)	646 (22.03)	1,159 (27.62)		
35~50	1,844 (25.87)	611 (20.83)	1,233 (29.39)		
51~65	1,795 (25.18)	664 (22.64)	1,131 (26.95)		
66~	1,685 (23.64)	1,012 (34.5)	673 (16.04)		
Sex, n (%)				0.039	4.265
Female	3,191 (44.76)	1,356 (46.23)	1,835 (43.73)		
Male	3,938 (55.24)	1,577 (53.77)	2,361 (56.27)		
Race, n (%)				0.2	3.22
Black	426 (5.98)	192 (6.55)	234 (5.58)		
Others	448 (6.28)	189 (6.44)	259 (6.17)		
White	6,255 (87.74)	2,552 (87.01)	3,703 (88.25)		
Marital Status, n (%)				<0.001	125.67
Divorced/Separated	518 (7.27)	213 (7.26)	305 (7.27)		
Married	4,096 (57.46)	1,588 (54.14)	2,508 (59.77)		
Single/Unmarried	1,843 (25.85)	720 (24.55)	1,123 (26.76)		
Widowed/Others	672 (9.43)	412 (14.05)	260 (6.2)		
Diagnosis, n (%)				<0.001	696.04
~1998	1,864 (26.15)	1,173 (39.99)	691 (16.47)		
1999~2005	1,713 (24.03)	809 (27.58)	904 (21.54)		
2006~2012	2,060 (28.9)	570 (19.43)	1,490 (35.51)		
2013~2016	1,492 (20.93)	381 (12.99)	1,111 (26.48)		
Primary Site, n (%)				<0.001	21.361
Infratentorial	468 (6.56)	219 (7.47)	249 (5.93)		
Others	1,397 (19.6)	632 (21.55)	765 (18.23)		
Supratentorial	5,264 (73.84)	2,082 (70.99)	3,182 (75.83)		
Hist. Type, n (%)				1	Fisher
Astrocytoma, anaplastic	7,129 (100)	2,933 (100)	4,196 (100)		
Tumor Size, n (%)				<0.001	350.623
~4	1,374 (19.27)	387 (13.19)	987 (23.52)		
4~	1,171 (16.43)	289 (9.85)	882 (21.02)		
Unknown	4,584 (64.3)	2,257 (76.95)	2,327 (55.46)		
Surgery, n (%)				<0.001	453.793
NO	3,607 (50.6)	1,927 (65.7)	1,680 (40.04)		
YES	3,522 (49.4)	1,006 (34.3)	2,516 (59.96)		
Surgery Method, n (%)				<0.001	596.69
Biopsy and local excision	1,015 (14.24)	307 (10.47)	708 (16.87)		
Gross total resection	1,192 (16.72)	312 (10.64)	880 (20.97)		
No surgery	1,882 (26.4)	824 (28.09)	1,058 (25.21)		
Others	1,798 (25.22)	1,132 (38.6)	666 (15.87)		
Subtotal resection	1,242 (17.42)	358 (12.21)	884 (21.07)		
Radiation, n (%)				<0.001	715.124
NO	3,309 (46.42)	1,916 (65.33)	1,393 (33.2)		
YES	3,820 (53.58)	1,017 (34.67)	2,803 (66.8)		
Sequence Number, n (%)				<0.001	11.381
NO	6,450 (90.48)	2,612 (89.06)	3,838 (91.47)		
YES	679 (9.52)	321 (10.94)	358 (8.53)		
Outcome 1, n (%)				<0.001	17.561
Non HDRD	7,058 (99)	2,886 (98.4)	4,172 (99.43)		
HDRD	71 (1)	47 (1.6)	24 (0.57)		
Outcome 2, n (%)				<0.001	275.38
Survival	1,872 (26.26)	473 (16.13)	1,399 (33.34)		
HDRD	71 (1)	47 (1.6)	24 (0.57)		
Competing event	5,186 (72.75)	2,413 (82.27)	2,773 (66.09)		

HR=0.329, 95%CI=0.2–0.54, *P*<0.001; **Figure 2**). Older age was a significant predictor of an increased HDRD. The year of diagnosis between 2013 and 2016 (unadjusted HR=0.344, 95% CI=0.13–0.909, *P*=0.031), surgery treatment in the primary tumor site (unadjusted HR=0.549, 95%CI=0.329-0.914, *P*=0.001), and radiation treatment (unadjusted HR=0.462, 95% CI=0.288-0.743, *P*=0.001) were associated with a significantly improved HDSS. After adjustment for covariates, the result of multivariate Cox regression analysis showed that the risk of HDRD was decreased in AA patients who received chemotherapy (adjusted HR=0.782, 95%CI=0.736–0.83, *P*<0.001; **Figure 2**).

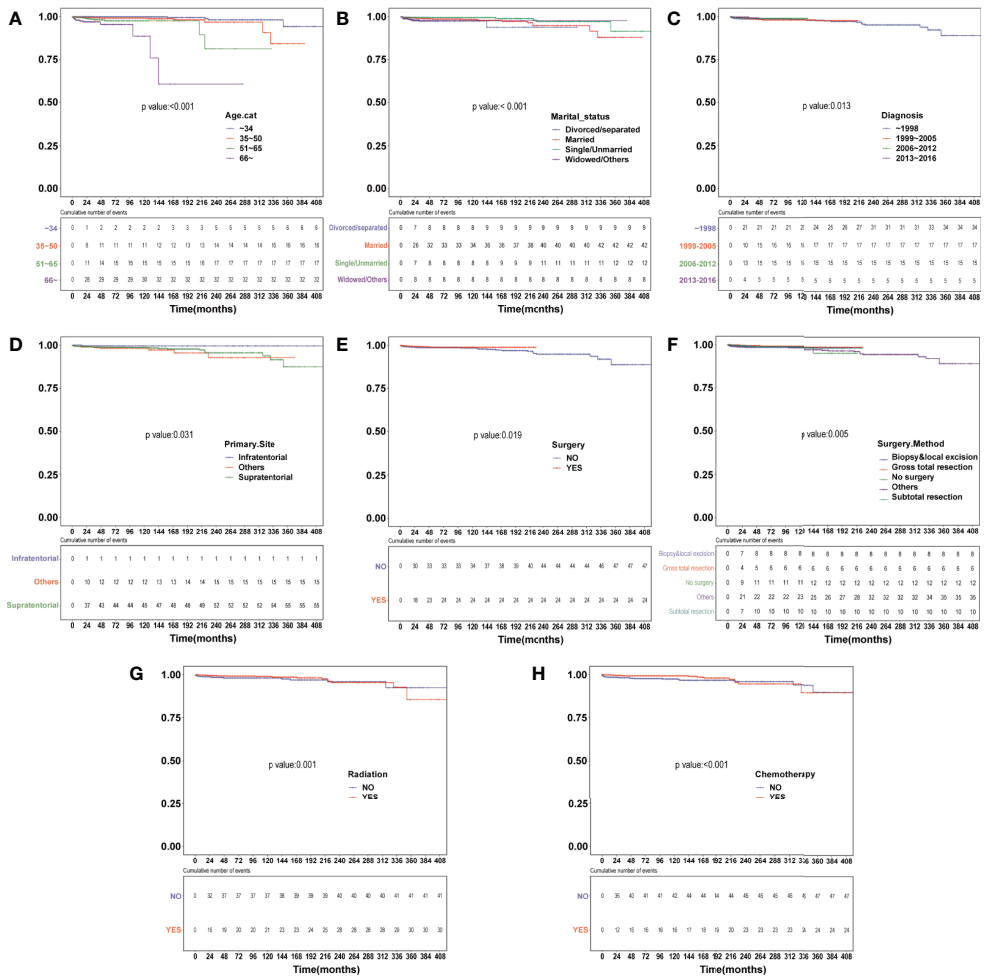

FIGURE 1 | Heart disease–specific survival (HDSS) curves of anaplastic astrocytoma patients stratified according to **(A)** age at diagnosis, **(B)** marital status, **(C)** year of diagnosis, **(D)** primary site, **(E)** surgery, **(F)** surgery method, **(G)** radiation and **(H)** chemotherapy based on Kaplan–Meier method.

Competing Risk Regression Analysis of HDRD in AA Patients

Considering HRRD and other cause-related deaths were two competing endpoint events, we utilized competing risk regression analysis to explore the effect of chemotherapy on the risk of HDRD. The CIF curves for all variables are shown in **Figures 3** and **S2**. Anaplastic astrocytoma patients with chemotherapy were at a lower HDRD risk compared to those patients with no chemotherapy (P<0.001). Meanwhile, older age was associated with higher HDRD cumulative incidences than younger age (P<0.001). However, other covariates including sex, years of diagnosis, marital status, primary site, race, radiation, surgery and surgery method, sequence number, and tumor size showed no statistical significance for the cumulative incidences of HDRD. As shown in **Figure 4A**, in the competing risk regression model, univariate analysis showed the chemotherapy status (unadjusted SHR = 0.378, 95%CI = 0.229–0.622, P<0.001) and age (35–50 y, P = 0.041; 51–65 y, P = 0.023; >66 y, P < 0.001) were correlated with HDRD, which were consistent with CIF. In multivariate analysis, we adjusted covariates and found that age was independently associated with HDRD and AA patients with chemotherapy still showed a decreased probability of HDRD (adjusted SHR=0.574, 95%CI=0.331–0.991, P=0.046, **Figure 4A**), as expected. Additionally, we conducted stratified analysis and interaction tests to control the influence of covariates, based on several clinical factors including age, sex, marital status, year of diagnosis, tumor size, surgery and surgery method, radiation, and sequence number (**Figure 4B**). In the subgroups of age (35–50 y) and age (>60 y), patients with chemotherapy showed the decreasing risk of HDRD (35–50 y, unadjusted SHR=0.355, 95%CI=0.121–0.928, P=0.035; >60 y, unadjusted SHR=0.281, 95%CI=0.108–0.729, P=0.009). In both female and male subgroups, the married subgroup, year of diagnosis between 2006 and 2012 subgroup, tumor size >4 cm and unknown subgroup, surgery treatment in

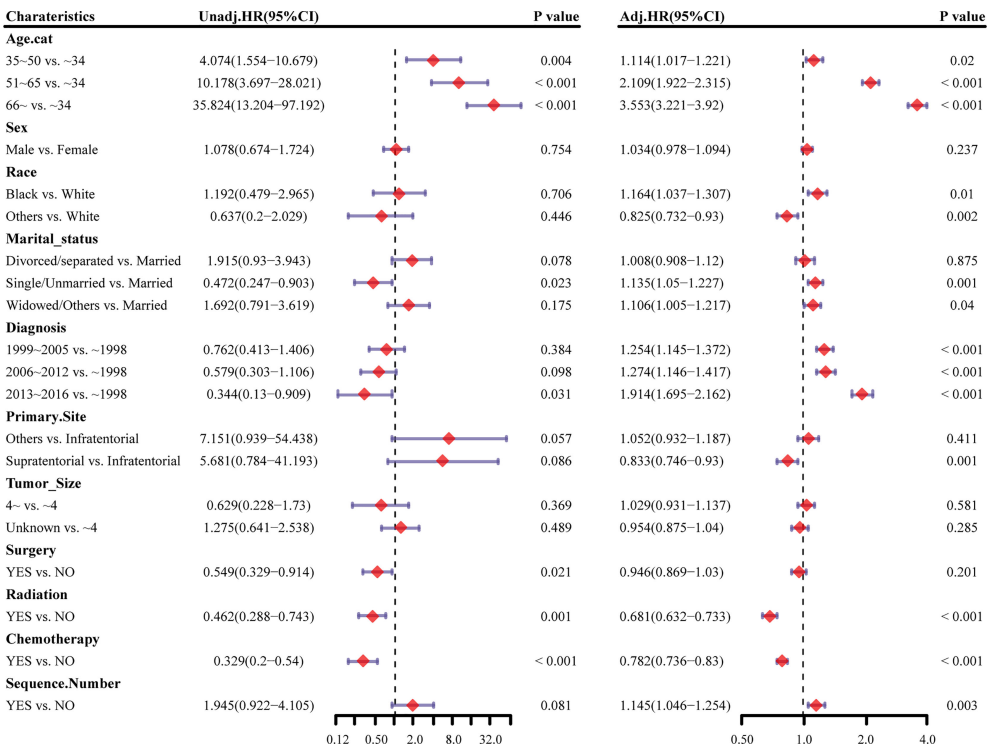

FIGURE 2 | Forest plots showing different results of (left) univariable and (right) multivariable analysis for heart disease–related mortality based on the Cox proportional hazards model. HR, hazard ratio; CI, confidence interval.

the primary site subgroup, received biopsy and local excision subgroup and subtotal resection subgroup, no radiation treatment subgroup, and no sequence number subgroup, chemotherapy was associated with a lower risk of HDRD with statistical significance. Meanwhile, chemotherapy did not increase the risk of HDRD in any of subgroups (**Figure 4B**). The subgroups of age >66 y (SHR for interaction=0.09, 95%CI=0.009–0.93, *P*=0.043) and surgery treatment in the primary site (SHR for interaction=0.353, 95%CI=0.125–0.997, *P*=0.049) displayed that there existed interactions between the effect of age/surgery and chemotherapy on the risk of HDRD (**Figure 4B**), which appeared to be effect modifiers between chemotherapy and HDRD. These results suggest robustness to our overall analysis.

Effect of Chemotherapy on HDRD in AA Patients in PSM-After Cohort

For the sake of minimizing the impact of confounding factors and confirming the role of chemotherapy on the HDRD risk, we performed a 1:1 PSM and obtained a balanced cohort (PSM-after cohort) including the non-chemotherapy group (n=2,085) and

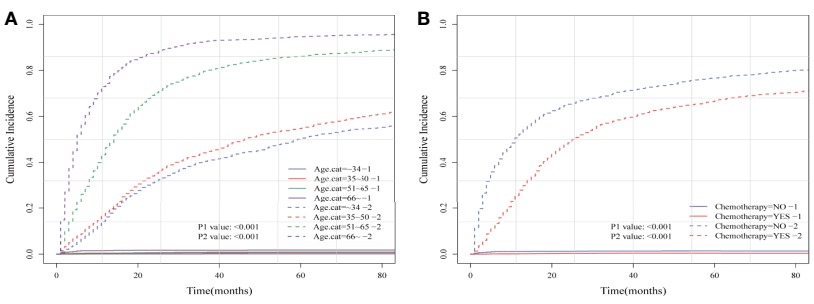

FIGURE 3 | Cumulative incidence plots based on the competing risk regression model of anaplastic astrocytoma patients stratified according to **(A)** age at diagnosis and **(B)** chemotherapy status.

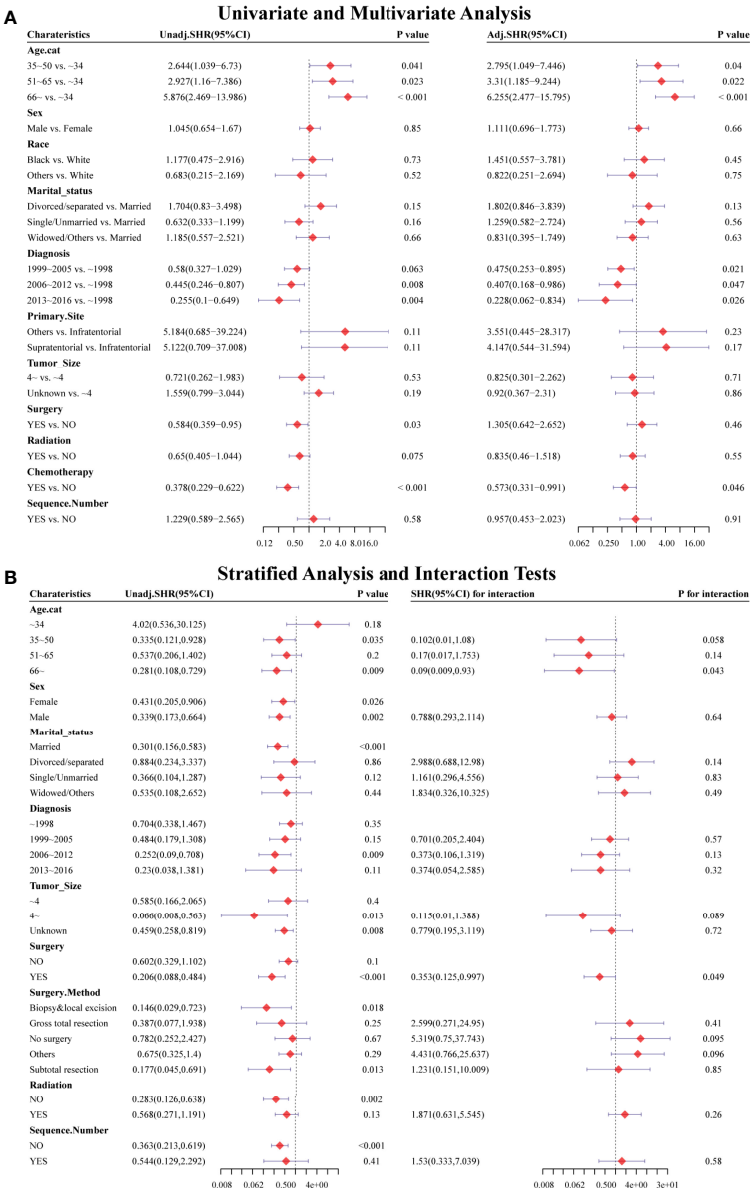

FIGURE 4 | Forest plots showed the results of (**A**, left) univariable and (**A**, right) multivariable analysis based on the competing risk regression model. Forest plots showed the results of (**B**, left) stratified analysis and (**B**, right) interaction tests based on the competing risk regression model. SHR: subdistribution hazard ratio; CI, confidence interval.

chemotherapy group (n=2,085). **Figure 5** showed the assessment methods of the covariate balance: after matching, all SMD values were lower than 0.1 (**Figure 5A**); the kernel density functions of the chemotherapy group and non-chemotherapy group were much closer than the cohort before PSM (**Figures 5B, C**); the histogram of the propensity score distribution of the chemotherapy group was similar to that of the non-chemotherapy group (**Figures 5D, E**). The characteristics of the matched patients were displayed in **Table 2**; apart from the marital status (P = 0.035), surgery and surgery method (P = 0.002), and sequence number (P=0.0036), almost all of the covariates were similarly distributed between the chemotherapy group and non-chemotherapy group.

Univariate and multivariate analyses based on competing risk regression analysis were conducted again in the PSM-after cohort, as shown in **Figure 6A**. The subgroup age 51–65 y (unadjusted SHR=3.14, 95%CI=1.032–9.549, P=0.044; adjusted SHR=4.664, 95%CI=1.588–13.7, P=0.005) and age >66y (unadjusted SHR=3.739, 95%CI= 1.251–11.175, P=0.018; adjusted SHR= 6.867, 95%CI= 2.491–18.931, P<0.001) were still associated with an increased probability of HDRD in both univariate and multivariate analyses. No differences were found (unadjusted

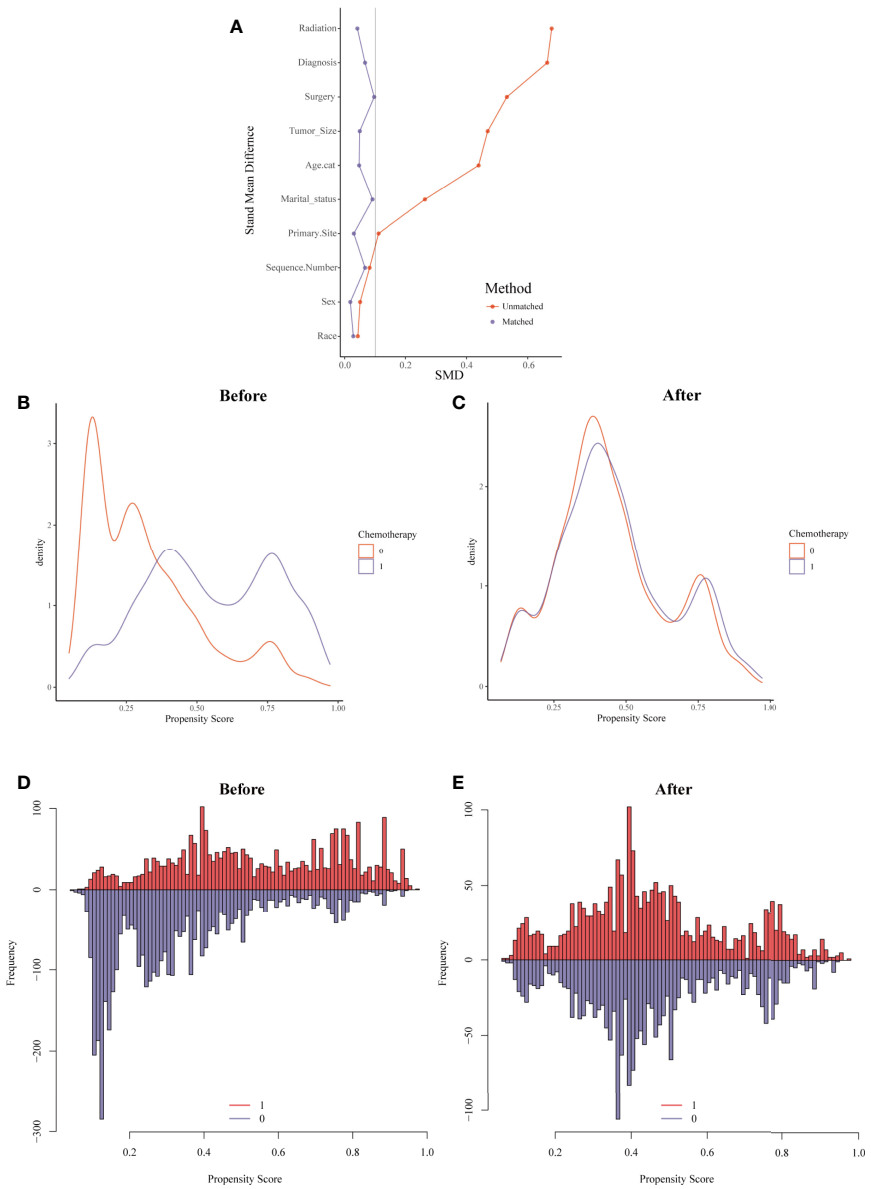

FIGURE 5 | Evaluation of the covariate balance by propensity score matching (PSM). **(A)** The loveplot showed SMD across covariates before and after PSM. **(B, C)** Kernel density showed the distribution balance of chemotherapy and non-chemotherapy groups **(B)** before PSM and **(C)** after PSM. **(D, E)** Histogram showed the balance of the chemotherapy group and non-chemotherapy group **(D)** before PSM and **(E)** after PSM.

SHR= 0.572, 95%CI=0.304–1.077, *P*=0.084; adjusted SHR=0.595, 95%CI=0.316–1.122, *P*=0.11) between the chemotherapy group and the non-chemotherapy group in univariate and multivariate analyses. Furthermore, we also conducted stratified analysis; the PSM-after cohort was stratified into subgroups according to covariates (**Figure 6B**). The *P*-value >0.05 appeared in almost all subgroups so that the interaction test was performed, which showed that no covariates interacted with the chemotherapy status. These results confirmed that chemotherapy for AA patients did not increase the risk of HDRD.

Landmark Analysis of HDSS in PSM-After Cohort

Kaplan–Meier analysis was performed in the PSM-after cohort. The chemotherapy status (*P*=0.04), age (*P*<0.001), and primary site (*P*=0.024) were statistically significant (**Figures 7A–C**). No statistical difference was observed in sex, race, marital status, the year of diagnosis, tumor size, surgery, surgery method, radiation, and sequence number (**Figure S2**). Similar to the previous results, patients who were older or did not receive chemotherapy had a higher risk of HDRD. Subsequently, we

TABLE 2 | The demographic characteristics of anaplastic astrocytoma patients after PSM.

Characteristic	Total	Non-Chemotherapy	Chemotherapy	P
	n = 4,170	n = 2,933	n = 4,196	
Age.cat, n (%)				0.51
~34	1,003 (24.05)	490 (23.5)	513 (24.6)	
35~50	1,054 (25.28)	514 (24.65)	540 (25.9)	
51~65	1,069 (25.64)	548 (26.28)	521 (24.99)	
66~	1,044 (25.04)	533 (25.56)	511 (24.51)	
Sex, n (%)				0.575
Female	1,887 (45.25)	953 (45.71)	934 (44.8)	
Male	2,283 (54.75)	1,132 (54.29)	1,151 (55.2)	
Race, n (%)				0.662
Black	282 (6.76)	144 (6.91)	138 (6.62)	
Others	283 (6.79)	148 (7.1)	135 (6.47)	
White	3,605 (86.45)	1,793 (86)	1,812 (86.91)	
Marital Status, n (%)				0.035
Divorced/Separated	321 (7.7)	175 (8.39)	146 (7)	
Married	2,348 (56.31)	1,129 (54.15)	1,219 (58.47)	
Single/Unmarried	1,080 (25.9)	564 (27.05)	516 (24.75)	
Widowed/Others	421 (10.1)	217 (10.41)	204 (9.78)	
Diagnosis, n (%)				0.203
~1998	1,341 (32.16)	656 (31.46)	685 (32.85)	
1999~2005	1,142 (27.39)	561 (26.91)	581 (27.87)	
2006~2012	1,026 (24.6)	513 (24.6)	513 (24.6)	
2013~2016	661 (15.85)	355 (17.03)	306 (14.68)	
Primary Site, n (%)				0.629
Infratentorial	316 (7.58)	165 (7.91)	151 (7.24)	
Others	880 (21.1)	445 (21.34)	435 (20.86)	
Supratentorial	2,974 (71.32)	1,475 (70.74)	1,499 (71.89)	
Tumor Size, n (%)				0.285
~4	681 (16.33)	347 (16.64)	334 (16.02)	
4~	503 (12.06)	266 (12.76)	237 (11.37)	
Unknown	2,986 (71.61)	1,472 (70.6)	1,514 (72.61)	
Surgery, n (%)				0.002
NO	2,625 (62.95)	1,264 (60.62)	1,361 (65.28)	
YES	1,545 (37.05)	821 (39.38)	724 (34.72)	
Surgery Method, n (%)				0.002
Biopsy and local excision	482 (11.56)	258 (12.37)	224 (10.74)	
Gross total resection	473 (11.34)	254 (12.18)	219 (10.5)	
No surgery	1,371 (32.88)	626 (30.02)	745 (35.73)	
Others	1,292 (30.98)	659 (31.61)	633 (30.36)	
Subtotal resection	552 (13.24)	288 (13.81)	264 (12.66)	
Radiation, n (%)				0.192
NO	2,239 (53.69)	1,141 (54.72)	1,098 (52.66)	
YES	1,931 (46.31)	944 (45.28)	987 (47.34)	
Sequence Number, n (%)				0.036
NO	3,721 (89.23)	1,839 (88.2)	1,882 (90.26)	
YES	449 (10.77)	246 (11.8)	203 (9.74)	

conducted landmark analysis at 216 and 340 months to minimize immortal time bias that might exist in the chemotherapy group. Patients who received chemotherapy had better HDSS than those in the non-chemotherapy group (P=0.007) at the follow-up time point of 216 months. In the group of the follow-up time between 216 months and 340 months (P=0.057) and the group of the follow-up time of more than 340 months (P=0.497), there was no difference between the chemotherapy and non-chemotherapy groups in HDSS. However, information regarding chemotherapy drugs and doses was lacking. More research is needed to reveal the correlation of the risk of HDRD with different chemotherapy drugs and doses.

DISCUSSION

With improving long-term cancer survival, an increasing proportion of these patients are living with long-term adverse effects and complications of cancer therapy (28–30). In a previous study, Omar Abdel-Rahman found that cardiac death is a significant reason of death and there is a difference among variable cancer types (31). It was reported that cardiotoxicity is a potential adverse effect of various cancer treatments, which is responsible for significant mortality in the oncology patients, specifically due to left ventricular dysfunction (32). Many chemotherapy drugs such as anthracycline agents and cyclophosphamide improves overall survival and disease-free

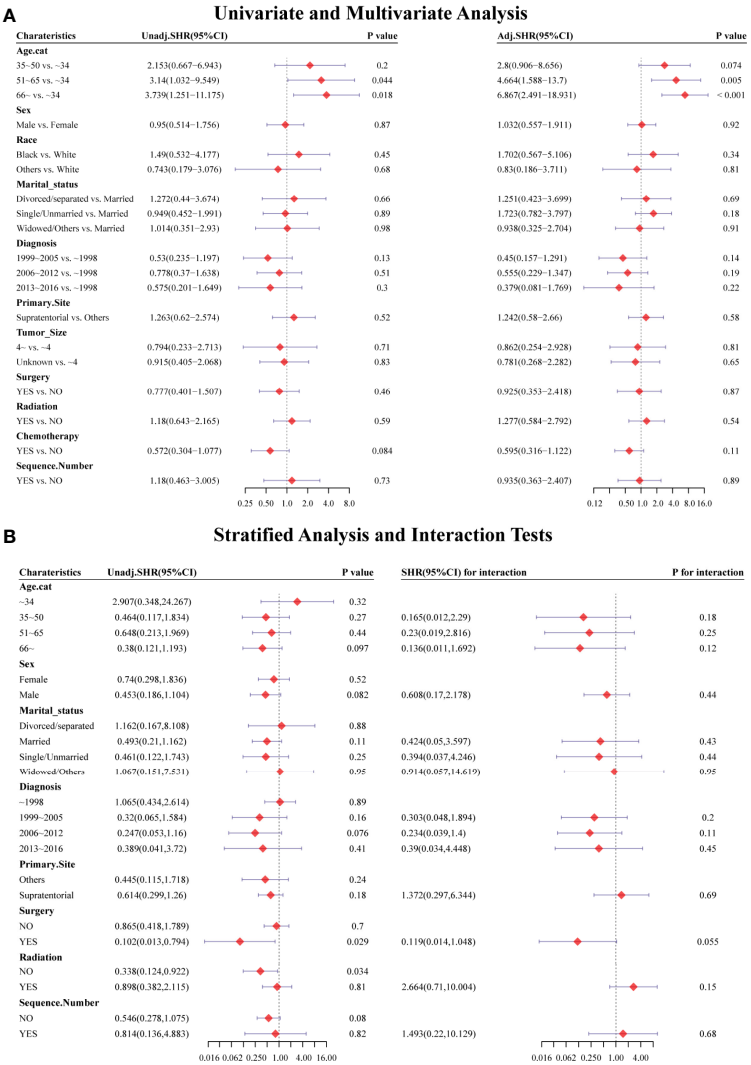

FIGURE 6 | Forest plots showed the results of (**A**, left) univariable and (**A**, right) multivariable analysis in the PSM-after cohort. Forest plots showed the results of (**B**, left) stratified analysis and (**B**, right) interaction tests in the PSM-after cohort. SHR: subdistribution hazard ratio; CI, confidence interval.

survival in patients in many cancer patients, but there has been an increasing concern regarding their cardiotoxicity (33, 34). These did provide an important insight into the mechanisms and principles of whether and how chemotherapy can affect cardiac function (35).

AA is a relatively rare tumor with poor prognosis (36). The optimal treatment for AA is still controversial (37). Surgery resection, radiotherapy, and chemotherapy are recommended as the first line of the treatment regimen (38, 39). Owing to the characteristics of infiltrative tumor growth, it is nearly impossible to achieve a complete surgical resection. After radiotherapy, tumor recurrence or the development of a secondary glioblastoma is usually expected. Thus, chemotherapy treatments are always recommended. Since there are limited trails about the effect of chemotherapy in AA patients, it is more necessary to understand better the risk of HDRD-associated chemotherapy in the AA patients of clinical trials (40, 41).

In this large population-based research, we utilized the SEER database to analyze the effect of chemotherapy on the risk of HDRD in AA patients. In Kaplan–Meier and Cox regression analyses, we clarified the association between clinical characteristics and HDSS and predicted the risk of an individual's clinical outcome through HRs. We found that chemotherapy is associated with a significantly decreased risk of HDRD among AA patients. In view of existing competing events including other cause-related deaths, we conducted competing risk regression analysis to confirm the role of chemotherapy in AA patients. The result of competing risk regression analysis showed that AA patients who underwent chemotherapy were at a lower HDRD risk in comparison with

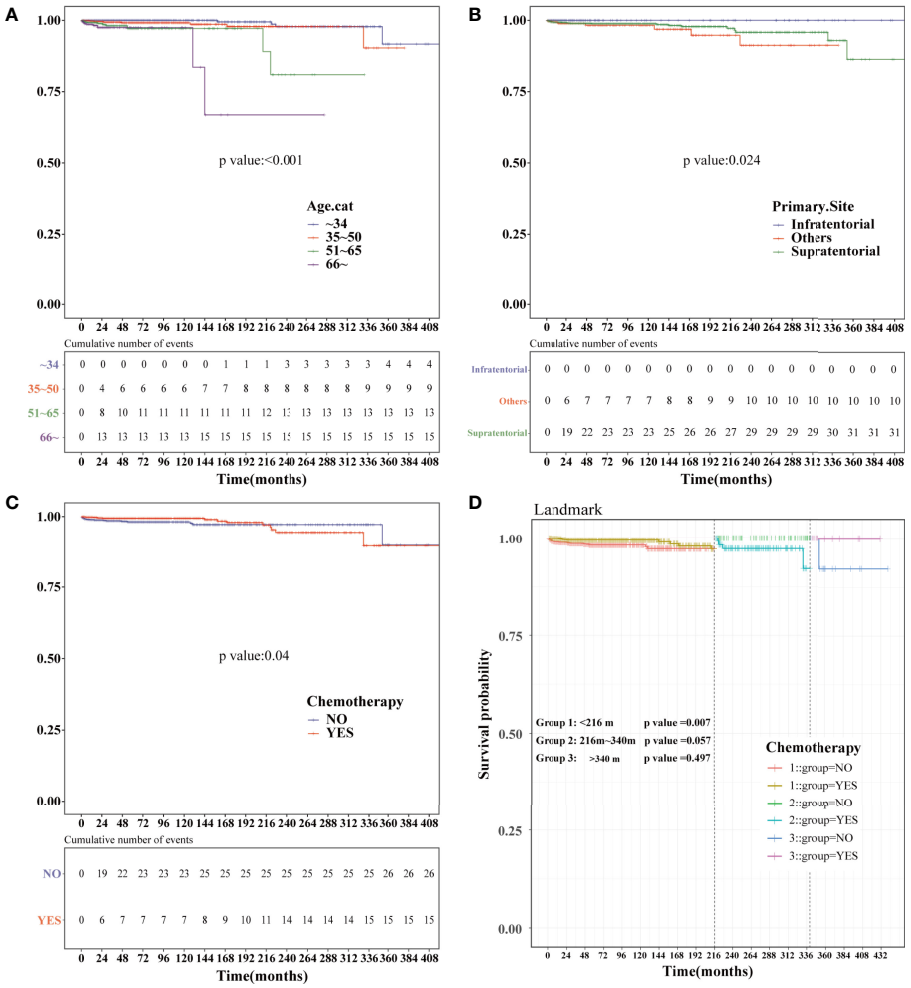

FIGURE 7 | Kaplan–Meier and landmark analysis of HDSS in the PSM-after cohort. HDSS curves of anaplastic astrocytoma patients stratified according to **(A)** age at diagnosis, **(B)** primary site and **(C)** chemotherapy based on the Kaplan–Meier method. **(D)** Landmark analysis of HDSS stratified according to chemotherapy in the PSM-after cohort at 216 and 340 months.

those patients with no chemotherapy treatment (unadjusted SHR=0.378, 95%CI=0.229–0.622, P<0.001). Meanwhile, multivariate analysis confirmed the independent effect of chemotherapy on HDRD in AA (adjusted SHR=0.574, 95% CI=0.331–0.991, P=0.046). In addition, we found that covariates like age significantly impact on HDRD; stratified analysis and interaction tests were performed, which provided robust evidence to our analysis. Furthermore, PSM was employed between the chemotherapy group and the non-chemotherapy group to minimize the effect of covariates, in order to achieve the "post-randomization." In the PSM-after cohort, univariate and multivariate analyses showed no significant difference between the chemotherapy group and the non-chemotherapy group on HDRD (unadjusted SHR= 0.572, 95%CI=0.304–1.077, P=0.084; adjusted SHR=0.595, 95% CI=0.316–1.122, P=0.11). Then, landmark analysis was used to correct immortal time bias in the PSM-after cohort. These results confirmed that chemotherapy did not decrease the HDSS in AA patients.

To the best of our knowledge, it is the first study to explore the effect of chemotherapy on the risk of HDRD and associated risk factors in AA patients. Since AA is a relatively rare tumor and the clinical trials were limited, the treatment regimen of AA was established according to principle of glioblastoma. The role of chemotherapy in AA, particularly TMZ, is currently under experiment (42–44). In this study, the result of our analysis identified a significantly decreased risk of HDRD with chemotherapy on AA patients, even after controlling the impact of competing events. Furthermore, both HDSS and other cause-related survival were significantly higher in AA patients with chemotherapy compared with those without chemotherapy, which may bring new insights into chemotherapy benefits in AA patients. After minimizing the effect of covariates by PSM, we still found that chemotherapy did not increase the risk of HDRD, which

provided a favorable complement to our previous analysis. Moreover, patients who were diagnosed with AA decades ago were treated with no chemotherapy treatment or traditional chemotherapy regimen including the PCV regimen or carmustine, which has severe side effects such as hematologic, hepatic, and cardiac toxicity (44–46). Recently, TMZ has been widely used in AA patients with the advantages of convenience to administer, less toxicity, and similar efficacy compared to PCV (47–49). A recent randomized phase III CATION trial on concurrent and adjuvant TMZ without 1p/19q co-deletion in anaplastic glioma patients revealed an HR reduction for the overall survival of 0.645 after adjuvant TMZ (95% CI=0.450–0.926, P= 0.0014). Since we did not identify the impact of a specific chemotherapy treatment regimen on the risk of HDRD in AA patients, we took the year of diagnosis into consideration (50). In univariable and multivariable analyses based on the competing risk regression model, the diagnosis years between 2013 and 2016 are associated with a lower risk of HDRD compared with patients diagnosed before 1998. We supposed that it implied the impact of changes in the treatment plan, nursing treatment, and the advance of cardiovascular treatment. Nevertheless, more future clinical trials should be conducted to investigate the positive and negative roles of chemotherapy (especially TMZ) in AA patients.

In our study, we also found that age at diagnosis is one of the most important prognostic factors of HDSS and OS in AA patients, and age at diagnosis is also one of the most important covariates in our study. We employed multiple methods to minimize its impact on our main issue. Even after PSM, the older age was still associated with a high risk of HDRD in univariate and multivariate analysis, particularly in those patients who were older than 51 years old. The numbers of studies have identified the different characteristics and clinical outcomes in the malignant glioma patients of different ages (51–53). Older age is widely recognized as a risk factor and poor prognostic factor for both heart disease and cancer. In addition, the probability of receiving surgery, radiotherapy, and chemotherapy was found to be influenced by age (54–56). Elderly patients are less tolerant of the toxicity of chemotherapy drugs and more likely to suffer adverse effects and complications. Clinicians should pay more attention to the management of elder patients and should not ignore the probability of rare complications. Elderly AA patients have special needs, and a comprehensive assessment is required to provide the optimal and personalized treatment.

There are some advantages to our study. Firstly, we are the first to investigate the impact of chemotherapy on the risk of HDRD in AA patients. Secondly, due to the relatively low incidence, clinical trials were limited and difficult to perform. Simultaneously, the studies conducted in the single medical center were not applicable to discuss the risk of HDRD in cancer patients because of the small sample size, large selection bias, and low statistical efficiency. We applied the SEER database consisting of the large-scale, population-based data with longitudinal follow-up information, increasing the power to evaluate the heart disease-related outcomes. Thirdly, considering the impact of competing events, we applied the competing risk regression model to avoid false-positive results. We also utilized PSM to correct the covariables and used landmark analysis to minimize immortal time bias.

Although our study provides a robust result about the impact of chemotherapy on HDRD in AA patients, there are still some limitations. Firstly, the SEER database did not allow us to differentiate the chemotherapy information including drug regimens and doses but only "yes" versus "no/unknown" options. We cannot get access to information about specific chemotherapy drugs and regimen. Therefore, we can only assume chemotherapy drugs and give a speculation of PCV or TMZ based on the glioma treatment guidelines from the NCCN and literature reviews. Secondly, all the patients were from the United States, and the cases from Asia and Europe are still needed to verify our studies. Thirdly, as an observational study, there are some limitations in nature. Some baseline difference between groups cannot be balanced very well, compared with prospective studies, even though many methods were applied in our study. In addition, a lot of clinical information including the reason of death was missing. The exact HDRD events for each patient were not provided in the SEER database. It was suggested that if a cancer diagnosis is made very recently, death certifiers and hospital were more likely to record cancer as the cause of death. Even the rigorous quality assurance program in the SEER database (57) cannot guarantee that every medical registrar can record the exact reason of death for every cancer patient, especially those with noncancer causes. All these reasons may lead to the inaccuracy of the number of HDRD and compromise our investigation of the association between the risk of HDRD and chemotherapy in AA patients (31).

CONCLUSION

In conclusion, AA patients with chemotherapy are associated with a lower risk of HDRD compared with those without chemotherapy treatment based on a large-sized population. Our findings may help clinicians make a decision about the management of AA patients and provide new and important evidence for applying chemotherapy in AA patients as the first-line treatment. Additionally, the results of our study need to be further verified in prospective randomized trials.

DATA AVAILABILITY STATEMENT

The analyzed data could be obtained at the SEER database (https://seer.cancer.gov/). Further inquiries can be directed to the corresponding authors.

AUTHOR CONTRIBUTIONS

X-ZC, Z-LS, and JF: study concept and design, funding acquisition, interpretation of results, article review and editing. QL and J-HB: data collection and analysis, interpretation of results, figure design, manuscript writing, article review and editing. FX, J-JQ, and Z-RC: interpretation of results and figure design. Z-RC, CL, and Y-XY: manuscript writing. All authors contributed to the article and approved the final submitted version.

FUNDING

This study was supported by grants from the Project of Shenkang Hospital Development Center of Shanghai (Grant No. 16CR3048A) and the Project of Shanghai Chongming district "sustainable development science and technology" (Grant No. CKY2020-28).

SUPPLEMENTARY MATERIAL

The Supplementary Material for this article can be found online at: https://www.frontiersin.org/articles/10.3389/fonc.2022.870843/full#supplementary-material

Supplementary Figure 1 | Heart disease specific survival curves of anaplastic astrocytoma patients stratified according to **(A)** sex, **(B)** race, **(C)** tumor size, **(D)** sequence number based on Kaplan-Meier method.

Supplementary Figure 2 | Cumulative incidence plots based on competing risk regression model of anaplastic astrocytoma patients stratified according to **(A)** Sex, **(B)** race, **(C)** marital status, **(D)** the year of diagnosis, **(E)** primary site, **(F)** tumor size, **(G)** surgery, **(H)** surgery method, **(I)** radiation and **(J)** sequence number.

Supplementary Figure 3 | Heart disease specific survival curves of anaplastic astrocytoma patients in PSM-after cohort stratified according to **(A)** sex, **(B)** race, **(C)** marital status, **(D)** the year of diagnosis, **(E)** tumor size, **(F)** surgery, **(G)** surgery method, **(H)** radiation and **(I)** sequence number based on Kaplan-Meier method.

REFERENCES

1. Grimm SA, Chamberlain MC. Anaplastic Astrocytoma. *CNS Oncol* (2016) 5 (3):145–57. doi: 10.2217/cns-2016-0002
2. Louis DN, Ohgaki H, Wiestler OD, Cavenee WK, Burger PC, Jouvet A, et al. The 2007 Who Classification of Tumours of the Central Nervous System. *Acta Neuropathol* (2007) 114(2):97–109. doi: 10.1007/s00401-007-0243-4
3. Hong JB, Roh TH, Ahn SS, Kim JY, Kang SG, Chang JH, et al. Predicting Survival Using the 2016 World Health Organization Classification for Anaplastic Glioma. *Clin Neuropathol* (2020) 39(4):188–95. doi: 10.5414/np301228
4. Ostrom QT, Cioffi G, Waite K, Kruchko C, Barnholtz-Sloan JS. Cbtrus Statistical Report: Primary Brain and Other Central Nervous System Tumors Diagnosed in the United States in 2014-2018. *Neuro Oncol* (2021) 23(12 Suppl 2):iii1–iii105. doi: 10.1093/neuonc/noab200
5. Wang S, Yao F, Lu X, Li Q, Su Z, Lee J-H, et al. Temozolomide Promotes Immune Escape of Gbm Cells *Via* Upregulating Pd-L1. *Am J Cancer Res* (2019) 9(6):1161–71.
6. Jiapaer S, Furuta T, Tanaka S, Kitabayashi T, Nakada M. Potential Strategies Overcoming the Temozolomide Resistance for Glioblastoma. *Neurol Med Chir* (2018) 58(10):405–21. doi: 10.2176/nmc.ra.2018-0141
7. Abe J-I, Yusuf SW, Deswal A, Herrmann J. Cardio-Oncology: Learning From the Old, Applying to the New. *Front Cardiovasc Med* (2020) 7:601893. doi: 10.3389/fcvm.2020.601893
8. Trinh VA, Patel SP, Hwu WJ. The Safety of Temozolomide in the Treatment of Malignancies. *Expert Opin Drug Saf* (2009) 8(4):493–9. doi: 10.1517/14740330902918281
9. Parakh S, Hamid A, Cher L, Gan HK. Temozolomide-Associated Liver Fibrosis. *J Clin Pharmacol* (2016) 56(11):1448–9. doi: 10.1002/jcph.753
10. Huang G, Zhang N, Bi X, Dou M. Solid Lipid Nanoparticles of Temozolomide: Potential Reduction of Cardial and Nephric Toxicity. *Int J Pharm* (2008) 355 (1-2):314–20. doi: 10.1016/j.ijpharm.2007.12.013
11. Nagane M. Dose-Dense Temozolomide: Is It Still Promising? *Neurol Med Chir (Tokyo)* (2015) 55(1):38–49. doi: 10.2176/nmc.ra.2014-0277
12. Castro GN, Cayado-Gutiérrez N, Zoppino FCM, Fanelli MA, Cuello-Carrión FD, Sottile M, et al. Effects of Temozolomide (Tmz) on the Expression and Interaction of Heat Shock Proteins (Hsps) and DNA Repair Proteins in Human Malignant Glioma Cells. *Cell Stress Chaperones* (2015) 20(2):253–65. doi: 10.1007/s12192-014-0537-0
13. Tan AC, Ashley DM, López GY, Malinzak M, Friedman HS, Khasraw M. Management of Glioblastoma: State of the Art and Future Directions. *CA Cancer J Clin* (2020) 70(4):299–312. doi: 10.3322/caac.21613
14. Zhang J, Stevens MF, Bradshaw TD. Temozolomide: Mechanisms of Action, Repair and Resistance. *Curr Mol Pharmacol* (2012) 5(1):102–14. doi: 10.2174/1874467211205010102
15. Doll KM, Rademaker A, Sosa JA. Practical Guide to Surgical Data Sets: Surveillance, Epidemiology, and End Results (Seer) Database. *JAMA Surg* (2018) 153(6):588–9. doi: 10.1001/jamasurg.2018.0501
16. Guan T, Qiu Z, Su M, Yang J, Tang Y, Jiang Y, et al. Cardiovascular Death Risk in Primary Central Nervous System Lymphoma Patients Treated With Chemotherapy: A Registry-Based Cohort Study. *Front Oncol* (2021) 11:641955. doi: 10.3389/fonc.2021.641955
17. Weberpals J, Jansen L, Müller OJ, Brenner H. Long-Term Heart-Specific Mortality Among 347 476 Breast Cancer Patients Treated With Radiotherapy or Chemotherapy: A Registry-Based Cohort Study. *Eur Heart J* (2018) 39 (43):3896–903. doi: 10.1093/eurheartj/ehy167
18. Sturgeon KM, Deng L, Bluethmann SM, Zhou S, Trifiletti DM, Jiang C, et al. A Population-Based Study of Cardiovascular Disease Mortality Risk in Us Cancer Patients. *Eur Heart J* (2019) 40(48):3889–97. doi: 10.1093/eurheartj/ehz766
19. Dutz A, Löck S. Competing Risks in Survival Data Analysis. *Radiother Oncol* (2019) 130:185–9. doi: 10.1016/j.radonc.2018.09.007
20. Austin PC, Fine JP. Practical Recommendations for Reporting Fine-Gray Model Analyses for Competing Risk Data. *Stat Med* (2017) 36(27):4391–400. doi: 10.1002/sim.7501
21. Andersen PK, Keiding N. Interpretability and Importance of Functionals in Competing Risks and Multistate Models. *Stat Med* (2012) 31(11-12):1074–88. doi: 10.1002/sim.4385
22. Dignam JJ, Kocherginsky MN. Choice and Interpretation of Statistical Tests Used When Competing Risks Are Present. *J Clin Oncol* (2008) 26(24):4027–34. doi: 10.1200/JCO.2007.12.9866
23. Scrucca L, Santucci A, Aversa F. Regression Modeling of Competing Risk Using R: An in Depth Guide for Clinicians. *Bone Marrow Transplant* (2010) 45(9):1388–95. doi: 10.1038/bmt.2009.359
24. Hwang WL, Tendulkar RD, Niemierko A, Agrawal S, Stephans KL, Spratt DE, et al. Comparison Between Adjuvant and Early-Salvage Postprostatectomy Radiotherapy for Prostate Cancer With Adverse Pathological Features. *JAMA Oncol* (2018) 4(5):e175230. doi: 10.1001/jamaoncol.2017.5230
25. McCaffrey DF, Ridgeway G, Morral AR. Propensity Score Estimation With Boosted Regression for Evaluating Causal Effects in Observational Studies. *Psychol Methods* (2004) 9(4):403–25. doi: 10.1037/1082-989x.9.4.403
26. Suissa S. Immortal Time Bias in Pharmaco-Epidemiology. *Am J Epidemiol* (2008) 167(4):492–9. doi: 10.1093/aje/kwm324
27. Null R, Team R, Null R, Writing TC, Null R, Team R, et al. R: A Language and Environment for Statistical Computing. *Computing* (2011) 1:12–21.
28. Tykocki T, Eltayeb M. Ten-Year Survival in Glioblastoma. A Systematic Review. *J Clin Neurosci* (2018) 54:7–13. doi: 10.1016/j.jocn.2018.05.002
29. Ernst J, Peuker M, Schwarz R, Fischbeck S, Beutel ME. [Long-Term Survival of Adult Cancer Patients From a Psychosomatic Perspective - Literature Review and Consequences for Future Research]. *Z Psychosom Med Psychother* (2009) 55(4):365–81. doi: 10.13109/zptm.2009.55.4.365
30. Stringfield O, Arrington JA, Johnston SK, Rognin NG, Peeri NC, Balagurunathan Y, et al. Multiparameter Mri Predictors of Long-Term Survival in Glioblastoma Multiforme. *Tomography* (2019) 5(1):135–44. doi: 10.18383/j.tom.2018.00052
31. Abdel-Rahman O. Risk of Cardiac Death Among Cancer Survivors in the United States: A Seer Database Analysis. *Expert Rev Anticancer Ther* (2017) 17 (9):873–8. doi: 10.1080/14737140.2017.1344099
32. Yang F, Li C, Guo Y, Yu Y, Mao S, Wang R, et al. Effects of Radical Cystectomy, Radiotherapy, and Chemotherapy on the Risk of Long-Term

Heart-Specific Death in Bladder Cancer Patients. *Transl Androl Urol* (2021) 10(10):3826–36. doi: 10.21037/tau-21-835
33. Sparano JA. Use of Dexrazoxane and Other Strategies to Prevent Cardiomyopathy Associated With Doxorubicin-Taxane Combinations. *Semin Oncol* (1998) 25(4 Suppl 10):66–71.
34. Yang R, Tan C, Najafi M. Cardiac Inflammation and Fibrosis Following Chemo/Radiation Therapy: Mechanisms and Therapeutic Agents. *Inflammopharmacology* (2021) 30(1):73–89. doi: 10.1007/s10787-021-00894-9
35. Ananthan K, Lyon AR. The Role of Biomarkers in Cardio-Oncology. *J Cardiovasc Transl Res* (2020) 13(3):431–50. doi: 10.1007/s12265-020-10042-3
36. Omuro A, DeAngelis LM. Glioblastoma and Other Malignant Gliomas: A Clinical Review. *Jama* (2013) 310(17):1842–50. doi: 10.1001/jama.2013.280319
37. Nayak L, Reardon DA. High-Grade Gliomas. *Continuum (Minneap Minn)* (2017) 23(6, Neuro-oncology):1548–63. doi: 10.1212/con.0000000000000554
38. Rao SAM, Srinivasan S, Patric IRP, Hegde AS, Chandramouli BA, Arimappamagan A, et al. A 16-Gene Signature Distinguishes Anaplastic Astrocytoma From Glioblastoma. *PloS One* (2014) 9(1):e85200. doi: 10.1371/journal.pone.0085200
39. Caccese M, Padovan M, D'Avella D, Chioffi F, Gardiman MP, Berti F, et al. Anaplastic Astrocytoma: State of the Art and Future Directions. *Crit Rev Oncol/Hematol* (2020) 153:7. doi: 10.1016/j.critrevonc.2020.103062
40. Allen JC, Walker R, Luks E, Jennings M, Barfoot S, Tan C. Carboplatin and Recurrent Childhood Brain Tumors. *J Clin Oncol* (1987) 5(3):459–63. doi: 10.1200/jco.1987.5.3.459
41. Wick W, Platten M, Meisner C, Felsberg J, Tabatabai G, Simon M, et al. Temozolomide Chemotherapy Alone Versus Radiotherapy Alone for Malignant Astrocytoma in the Elderly: The Noa-08 Randomised, Phase 3 Trial. *Lancet Oncol* (2012) 13(7):707–15. doi: 10.1016/s1470-2045(12)70164-x
42. van den Bent MJ, Brandes AA, Taphoorn MJ, Kros JM, Kouwenhoven MC, Delattre JY, et al. Adjuvant Procarbazine, Lomustine, and Vincristine Chemotherapy in Newly Diagnosed Anaplastic Oligodendroglioma: Long-Term Follow-Up of Eortc Brain Tumor Group Study 26951. *J Clin Oncol* (2013) 31(3):344–50. doi: 10.1200/jco.2012.43.2229
43. Cairncross G, Wang M, Shaw E, Jenkins R, Brachman D, Buckner J, et al. Phase Iii Trial of Chemoradiotherapy for Anaplastic Oligodendroglioma: Long-Term Results of Rtog 9402. *J Clin Oncol* (2013) 31(3):337–43. doi: 10.1200/JCO.2012.43.2674
44. Geurts M, Snijders TJ, van den Bent MJ. Treatment of Anaplastic Gliomas: Evidences and Controversies. *Curr Opin Oncol* (2021) 33(6):621–5. doi: 10.1097/cco.0000000000000785
45. Kristof RA, Neuloh G, Hans V, Deckert M, Urbach H, Schlegel U, et al. Combined Surgery, Radiation, and Pcv Chemotherapy for Astrocytomas Compared to Oligodendrogliomas and Oligoastrocytomas Who Grade Iii. *J Neurooncol* (2002) 59(3):231–7. doi: 10.1023/a:1019987116596
46. Blondin NA, Becker KP. Anaplastic Gliomas: Radiation, Chemotherapy, or Both? *Hematol Oncol Clin North Am* (2012) 26(4):811–23. doi: 10.1016/j.hoc.2012.04.003
47. Brandes AA, Nicolardi L, Tosoni A, Gardiman M, Iuzzolino P, Ghimenton C, et al. Survival Following Adjuvant Pcv or Temozolomide for Anaplastic Astrocytoma. *Neuro Oncol* (2006) 8(3):253–60. doi: 10.1215/15228517-2006-005
48. Brada M, Stenning S, Gabe R, Thompson LC, Levy D, Rampling R, et al. Temozolomide Versus Procarbazine, Lomustine, and Vincristine in Recurrent High-Grade Glioma. *J Clin Oncol* (2010) 28(30):4601–8. doi: 10.1200/jco.2009.27.1932
49. Hwang K, Kim TM, Park CK, Chang JH, Jung TY, Kim JH, et al. Concurrent and Adjuvant Temozolomide for Newly Diagnosed Grade III Gliomas Without 1p/19q Co-Deletion: A Randomized, Open-Label, Phase 2 Study (Knog-1101 Study). *Cancer Res Treat* (2020) 52(2):505–15. doi: 10.4143/crt.2019.421
50. Van Den Bent MJ, Erridge S, Vogelbaum MA, Nowak AK, Sanson M, Brandes AA, et al. Results of the Interim Analysis of the Eortc Randomized Phase Iii Catnon Trial on Concurrent and Adjuvant Temozolomide in Anaplastic Glioma Without 1p/19q Co-Deletion: An Intergroup Trial. *J Clin Oncol* (2016) 34(18_suppl):LBA2000–LBA. doi: 10.1200/JCO.2016.34.18_suppl.LBA2000
51. Qu H-Q, Jacob K, Fatet S, Ge B, Barnett D, Delattre O, et al. Genome-Wide Profiling Using Single-Nucleotide Polymorphism Arrays Identifies Novel Chromosomal Imbalances in Pediatric Glioblastomas. *Neuro Oncol* (2010) 12(2):153–63. doi: 10.1093/neuonc/nop001
52. Bandopadhayay P, Bergthold G, London WB, Goumnerova LC, Morales La Madrid A, Marcus KJ, et al. Long-Term Outcome of 4,040 Children Diagnosed With Pediatric Low-Grade Gliomas: An Analysis of the Surveillance Epidemiology and End Results (Seer) Database. *Pediatr Blood Cancer* (2014) 61(7):1173–9. doi: 10.1002/pbc.24958
53. Jones C, Perryman L, Hargrave D. Paediatric and Adult Malignant Glioma: Close Relatives or Distant Cousins? *Nat Rev Clin Oncol* (2012) 9(7):400–13. doi: 10.1038/nrclinonc.2012.87
54. Iwamoto FM, Reiner AS, Nayak L, Panageas KS, Elkin EB, Abrey LE. Prognosis and Patterns of Care in Elderly Patients With Glioma. *Cancer* (2009) 115(23):5534–40. doi: 10.1002/cncr.24612
55. Iwamoto FM, Cooper AR, Reiner AS, Nayak L, Abrey LE. Glioblastoma in the Elderly: The Memorial Sloan-Kettering Cancer Center Experience (1997-2007). *Cancer* (2009) 115(16):3758–66. doi: 10.1002/cncr.24413
56. Smoll NR, Hamilton B. Incidence and Relative Survival of Anaplastic Astrocytomas. *Neuro Oncol* (2014) 16(10):1400–7. doi: 10.1093/neuonc/nou053
57. Halanych JH, Shuaib F, Parmar G, Tanikella R, Howard VJ, Roth DL, et al. Agreement on Cause of Death Between Proxies, Death Certificates, and Clinician Adjudicators in the Reasons for Geographic and Racial Differences in Stroke (Regards) Study. *Am J Epidemiol* (2011) 173(11):1319–26. doi: 10.1093/aje/kwr033

Conflict of Interest: The authors declare that the research was conducted in the absence of any commercial or financial relationships that could be construed as a potential conflict of interest.

frontiers | Frontiers in Oncology

TYPE Correction
PUBLISHED 04 August 2022
DOI 10.3389/fonc.2022.995352

OPEN ACCESS

APPROVED BY
Frontiers Editorial Office,
Media SA, Switzerland

*CORRESPONDENCE
Xian-Zhen Chen
Chenchenxianzheny@126.com
Zhao-Li Shen
Shenleelies@sina.com
Jin Fu
fujin@tongji.edu.cn

†These authors have contributed equally to this work and share first authorship

‡These authors have contributed equally to this work

SPECIALTY SECTION
This article was submitted to Pharmacology of Anti-Cancer Drugs, a section of the journal Frontiers in Oncology

RECEIVED 15 July 2022
ACCEPTED 19 July 2022
PUBLISHED 04 August 2022

CITATION
Lin Q, Bao J-H, Xue F, Qin J-J, Chen Z, Chen Z-R, Li C, Yan Y-X, Fu J, Shen Z-L and Chen X-Z (2022) Corrigendum: The risk of heart disease-related death among anaplastic astrocytoma patients after chemotherapy: A SEER population-based analysis. *Front. Oncol.* 12:995352. doi: 10.3389/fonc.2022.995352

Corrigendum: The risk of heart disease-related death among anaplastic astrocytoma patients after chemotherapy: A SEER population-based analysis

Qi Lin[1†], Jia-Hao Bao[2†], Fei Xue[1], Jia-Jun Qin[1], Zhen Chen[1], Zhong-Rong Chen[1], Chao Li[1], Yi-Xuan Yan[2], Jin Fu[1*‡], Zhao-Li Shen[1*‡] and Xian-Zhen Chen[1*‡]

[1]Department of Neurosurgery, Shanghai Tenth People's Hospital, Tongji University School of Medicine, Shanghai, China, [2]Hospital of Stomatology, Guanghua School of Stomatology, Sun Yat-sen University, Guangdong Provincial Key Laboratory of Stomatology, Guangzhou, China

KEYWORDS

anaplastic astrocytoma, chemotherapy, SEER, heart disease-related death, cardio-oncology

A corrigendum on

The risk of heart disease-related death among anaplastic astrocytoma patients after chemotherapy: A SEER population-based analysis

By Lin Q, Bao J-H, Xue F, Qin J-J, Chen Z, Chen Z-R, Li C, Yan Y-X, Fu J, Shen Z-L and Chen X-Z (2022) *Front. Oncol.* 12:870843. doi: 10.3389/fonc.2022.870843

In the published article, there was an error in affiliation 1. Instead of "[1]Department of Neurosurgery, School of Medicine, Shanghai Tenth People's Hospital, Tongji University, Shanghai, China", it should be "Department of Neurosurgery, Shanghai Tenth People's Hospital, Tongji University School of Medicine, Shanghai, China" as above.

The authors apologize for this error and state that this does not change the scientific conclusions of the article in any way. The original article has been updated.

Publisher's note

All claims expressed in this article are solely those of the authors and do not necessarily represent those of their affiliated organizations, or those of the publisher, the editors and the reviewers. Any product that may be evaluated in this article, or claim that may be made by its manufacturer, is not guaranteed or endorsed by the publisher.

frontiers | Frontiers in Pharmacology

ORIGINAL RESEARCH
published: 21 June 2022
doi: 10.3389/fphar.2022.920436

Rapid Determination of 9 Tyrosine Kinase Inhibitors for the Treatment of Hepatocellular Carcinoma in Human Plasma by QuEChERS-UPLC-MS/MS

Wen Jiang[1], *Tingting Zhao*[2], *Xiaolan Zhen*[3], *Chengcheng Jin*[1], *Hui Li*[3]* *and Jing Ha*[1]*

[1]College of Chemistry and Pharmaceutical Engineering, Hebei University of Science and Technology, Shijiazhuang, China, [2]College of Pharmacy, Hebei Medical University, Shijiazhuang, China, [3]Hebei Institute of Drug and Medical Device Inspection, Shijiazhuang, China

A reliable and rapid method employing QuEChERS (Quick, Easy, Cheap, Effective, Rugged, and Safe) pretreatment coupled with ultra-performance liquid chromatography–tandem mass spectrometry (UPLC–MS/MS) was successfully developed and validated for the analysis of nine tyrosine kinase inhibitors (TKIs) in human plasma. Biological samples were extracted with acetonitrile and salted out with 350 mg of anhydrous magnesium sulfate ($MgSO_4$), followed by purification with 40 mg of ethyl enediamine-N-propylsilane (PSA) adsorbents. All analytes and internal standards (IS) were separated on the Hypersil GOLD VANQUISH C18 (2.1 mm × 100 mm, 1.9 μM) column using the mobile phases composed of acetonitrile (phase A) and 0.1% formic acid in water (phase B) for 8.0 min. Detection was performed by selection reaction monitoring (SRM) in the positive ion electrospray mode. Lenvatinib, sorafenib, cabozantinib, apatinib, gefitinib, regorafenib, and anlotinib rendered good linearity over the range of 0.1–10 ng/ml, and 1–100 ng/ml for tivantinib and galunisertib. All linear correlation coefficients for all standard curves were ≥ 0.9966. The limits of detection (LOD) and the limits of quantitation (LOQ) ranged from 0.003 to 0.11 ng/ml and 0.01–0.37 ng/ml, respectively. The method was deemed satisfactory with an accuracy of -7.34–6.64%, selectivity, matrix effect (ME) of 90.48–107.77%, recovery, and stability. The proposed method is simple, efficient, reliable, and applicable for the detection of TKIs in human plasma samples as well as for providing a reference for the clinical adjustment of drug administration regimen by monitoring the drug concentrations in the plasma of patients.

Keywords: tyrosine kinase inhibitors, UPLC-MS/MS, QuEChERS, plasma, hepatocellular carcinoma

OPEN ACCESS

Edited by:
Miao Yan,
Central South University, China

Reviewed by:
Priyanka Shah,
Gujarat University, India
Alessandro Granito,
University of Bologna, Italy

***Correspondence:**
Hui Li
lihui7171@163.com
Jing Ha
hajing02@163.com

Specialty section:
This article was submitted to Pharmacology of Anti-Cancer Drugs, a section of the journal Frontiers in Pharmacology

Received: *14 April 2022*
Accepted: *11 May 2022*
Published: *21 June 2022*

Citation:
Jiang W, Zhao T, Zhen X, Jin C, Li H and Ha J (2022) Rapid Determination of 9 Tyrosine Kinase Inhibitors for the Treatment of Hepatocellular Carcinoma in Human Plasma by QuEChERS-UPLC-MS/MS. Front. Pharmacol. 13:920436. doi: 10.3389/fphar.2022.920436

1 INTRODUCTION

Cancer is a major public health issue across the world, with the associated global burden increasing dramatically owing to the aging of the population, environmental degradation, and undesirable lifestyle behaviors such as smoking and alcoholism (Noorolyai et al., 2019; Wu et al., 2019; Bray et al., 2020). Hepatocellular carcinoma (HCC) is a common malignant tumor with insidious onset, rapid progression, early recurrence, and poor prognosis, as well as consistently high rates of incidence and mortality (Dutta and Mahato, 2017).

TABLE 1 | The MS condition of the 9 tyrosine kinase inhibitors and IS.

Compounds	Parent (m/z)	Product (m/z)	Fragmentor voltage (V)	Collision voltage (eV)	Retention time (min)
LEN	427.1	370.1[a]/312.0	102	27/43	2.61
SOR	465.1	252.1[a]/270.1	113	33/24	3.67
CBZ	502.2	323.1[a]/297.1	139	37/35	3.10
RGF	483.1	270.1[a]/288.1	123	33/24	3.72
APA	398.2	212.1[a]/184.1	81	26/37	3.05
GEF	447.1	128.1[a]/100.1	75	24/47	2.74
ANL	408.2	339.1[a]/304.1	60	18/40	2.78
TIV	370.1	253.1[a]/158.1	65	21/22	3.46
GAL	370.1	336.1[a]/325.1	74	30/29	1.30
PRO	260.1	116.13[a]/183.1	53	18/18	3.05

[a]*Quantification ion.*

Tyrosine kinase inhibitors (TKIs) are small molecule-targeted drugs that target receptor tyrosine kinases. Their action mechanism is based on competing with adenosine triphosphate (ATP) for binding to the ATP-binding site of the kinase domain in order to block or reduce the phosphorylation of tyrosine kinase and, ultimately, exert anti-tumor effects (Cammarota et al., 2022; Yang et al., 2022; Yao et al., 2022). TKIs are widely used in the treatment of small-cell lung cancer (SCLC) (Hwang et al., 2021), non-small cell lung cancer (NSCLC) (Lin et al., 2022; Ten et al., 2022), gastrointestinal mesenchymal tumor (GIST) (Mohammadi and Gelderblom, 2021; Foo et al., 2022; Klug et al., 2022), hepatocellular liver cancer (HCC) (Decraecker et al., 2021), renal cancer (RCC) (Fogli et al., 2020; Pedersen et al., 2021), and other cancers owing to their high selectivity and low adverse effects when compared with those of the traditional cytotoxic anticancer drugs (Xing et al., 2021). Sorafenib is the first first-line oral small molecule TKI approved by the U.S. Food and Drug Administration (FDA) for HCC, ushering in a new era of molecular targeting in HCC (Di et al., 2013; Decraecker et al., 2021). Sorafenib has been followed by other targeted drug studies in search of breakthroughs in molecularly targeted drug therapy for HCC. Currently, the first-line targeted agents include sorafenib and lenvatinib, while the second-line targeted agents for HCC include regorafenib and cabozantinib (Zhao et al., 2020; El-Khoueiry et al., 2021). In addition, results from a randomized, placebo-controlled, double-blind phase-III study of apatinib as the second-line treatment of Chinese patients with advanced HCC demonstrated that apatinib could significantly prolong the survival time of first-line resistant patients with advanced HCC and that it was well tolerated by patients in a safe and manageable manner (Qin et al., 2020; Qin et al., 2021). Tivantinib has been reported to downregulate the MET activity and the expression of downstream signaling pathways in tumor biopsy specimens (Rimassa et al., 2018). The safety and efficacy of galunisertib in combination with sorafenib have been reported in several publications (Yingling et al., 2018; Wick et al., 2020). In addition, it has been reported that the combination of gefitinib treatment for patients with intermediate to advanced HCC who failed to respond to lenvatinib treatment could effectively inhibit the progression of HCC (Jin et al., 2021), while anlotinib has also been demonstrated to be effective in the treatment of intermediate to advanced HCC (Guo et al., 2020). Therefore, all of the nine TKIs mentioned earlier exhibited anti-hepatocellular carcinogenic effects.

A recent review suggested that the specific metabolism (supporting the therapeutic schedule of 3 weeks on and 1 week off/month) of regorafenib may affect the blood levels and therapeutic efficacy (Granito et al., 2021). Patients with HCC may suffer from adverse events or serious adverse events associated with drug therapy owing to drug resistance and drug toxicity. An overview of the study on lenvatinib reported that 82% of patients in the trial reduced their dose or stopped treatment because of adverse effects (Rehman et al., 2021). Patients with mild or moderate renal and hepatic impairment may need to be closely monitored, according to a report of cabozantinib (D'Angelo et al., 2020). It is recommended that tivantinib requires monitoring of therapeutic agents in order to adjust the administered dose on time (Maharati et al., 2022). Therefore, monitoring the above nine TKIs have a significant meaning to improve drug efficacy and safety. It is necessary to develop a reliable, rapid, and sensitive method to monitor the concentration of anti-HCC drugs in order to facilitate clinical medication guidance.

Currently, the analysis of small-molecule tyrosinase inhibitors is mostly performed by liquid chromatography coupled with mass spectrometry (LC-MS), albeit the assay requires a good matrix effect (ME) of the sample. Accordingly, a suitable pretreatment technique needs to be selected to improve the purification efficiency and reduce the effect of the impurities. Based on the detection of TKIs, the commonly used pretreatment techniques include protein precipitation (PP) (Tibben et al., 2019; Ferrer et al., 2020; Iacuzzi et al., 2020; Krens et al., 2020; Aghai et al., 2021), liquid-liquid extraction (LLE) (Ni et al., 2017; Guan et al., 2019; Ezzeldin et al., 2020), salinization-assisted liquid-liquid extraction (SALLE) (Zhou et al., 2021), and solid-liquid extraction (SLE) (Sueshige et al., 2021), among others. While QuEChERS is an emerging pretreatment technique derived from dispersive solid-phase extraction (dSPE), it was initially applied in the field of pesticide residues. Recently, it was applied to the analysis of metabolites and other compounds in biological matrices, such as plasma and urine in parallel with the advancements in this technique.

In this study, we developed and validated the UPLC-MS/MS method combined with an emerging preprocessing technology

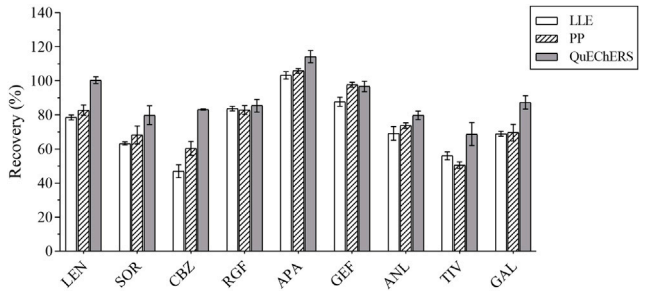

FIGURE 1 | The recovery results of all analytes by the 3 pretreatment methods.

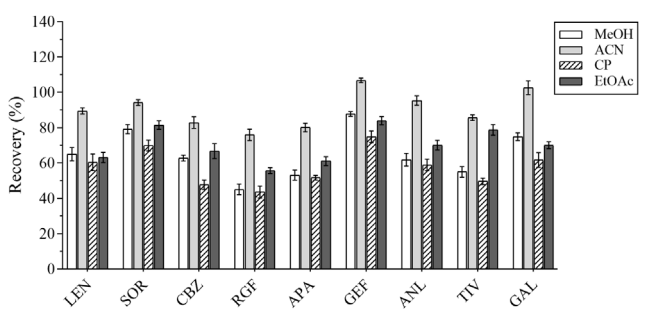

FIGURE 2 | The recovery results of all analytes for different extraction solvents.

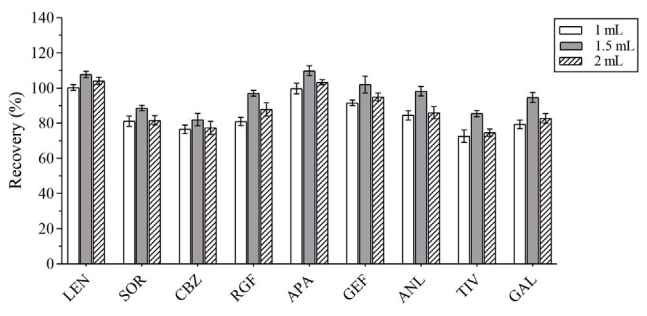

FIGURE 3 | The recovery results of all analytes with different volumes of acetonitrile.

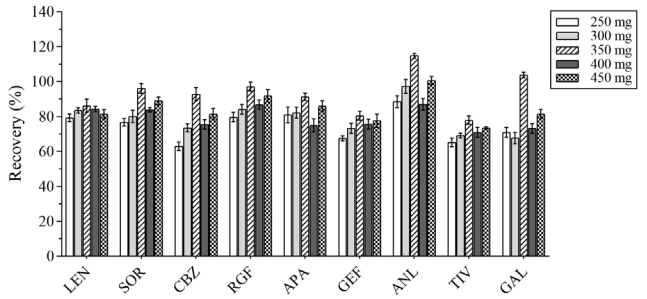

FIGURE 4 | The recovery results of all analytes with different masses of anhydrous magnesium sulfate.

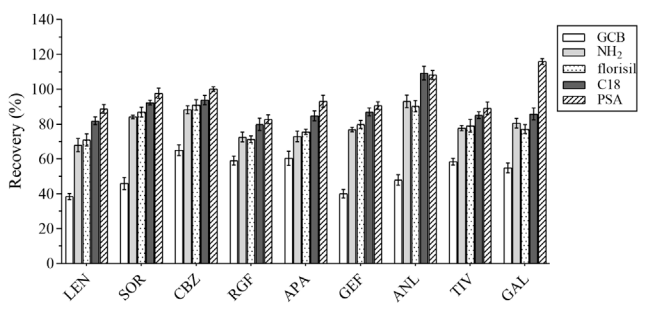

FIGURE 5 | The recovery results of all analytes with 5 adsorbents.

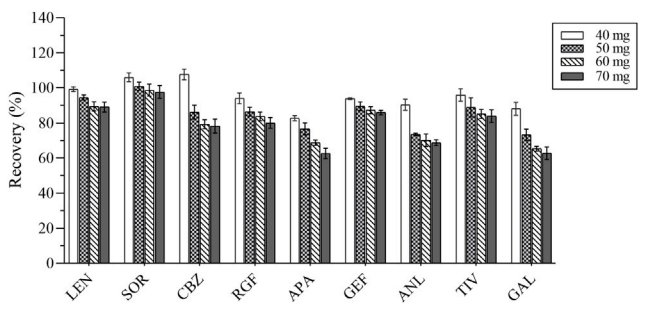

FIGURE 6 | The recovery results of all analytes with different amounts of PSA.

QuEChERS (Quick, Easy, Cheap, Effective, Rugged, and Safe) for the detection of nine anti-HCC TKIs, including lenvatinib (LEN), sorafenib (SOR), cabozantinib (CBZ), apatinib (APA), gefitinib (GEF), regorafenib (RGF), anlotinib (ANL), tivantinib (TIV), and galunisertib (GAL).

2 MATERIALS AND METHODS

2.1 Chemicals and Reagents

A total of nine TKIs standard substances were purchased from the Shanghai Yuanye Biotechnology Co., Ltd. (Shanghai, China). Propranolol was supplied by the China National Institute for China Drug and Biological Products Control. HPLC-grade methanol (MeOH), ethyl acetate (EtOAc), and acetone (CP) were purchased from Merck Drugs & Biotechnology (Darmstadt, Germany). HPLC-grade formic acid (FA) and acetic acid (HOAc) were purchased from Dikma (Beijing, China); LC/MS-grade acetonitrile (ACN) was acquired from ThermoFisher Scientific (Shanghai, China). Analytical-grade anhydrous magnesium sulfate ($MgSO_4$) was purchased from the Tianjin Damao Chemical Reagent Factory (Tianjin, China). Octadecyl bonded silicagel (C18), florisil adsorbents, and graphitized carbon black (GCB) were supplied by Agela

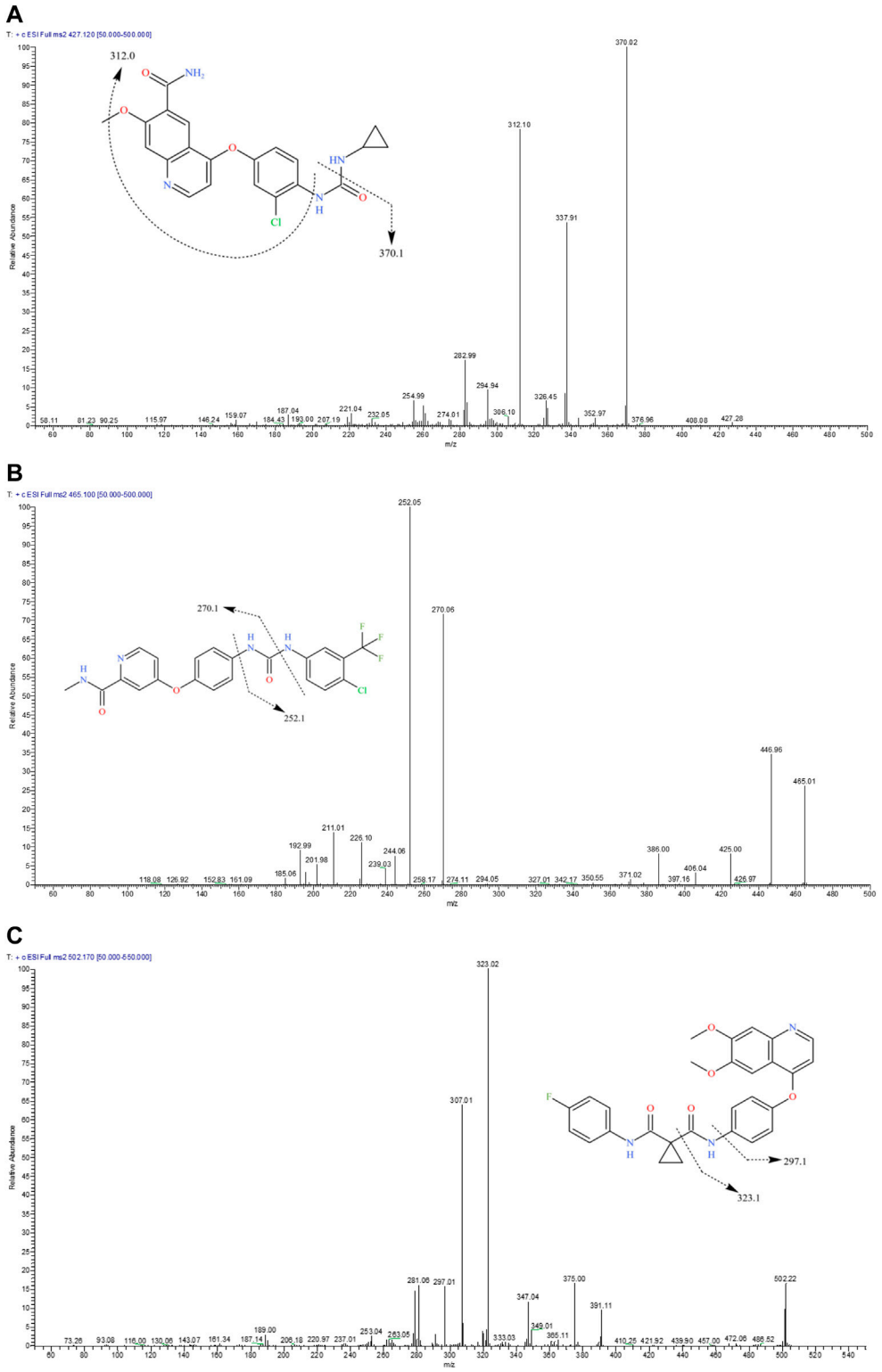

FIGURE 7 | (Continued).

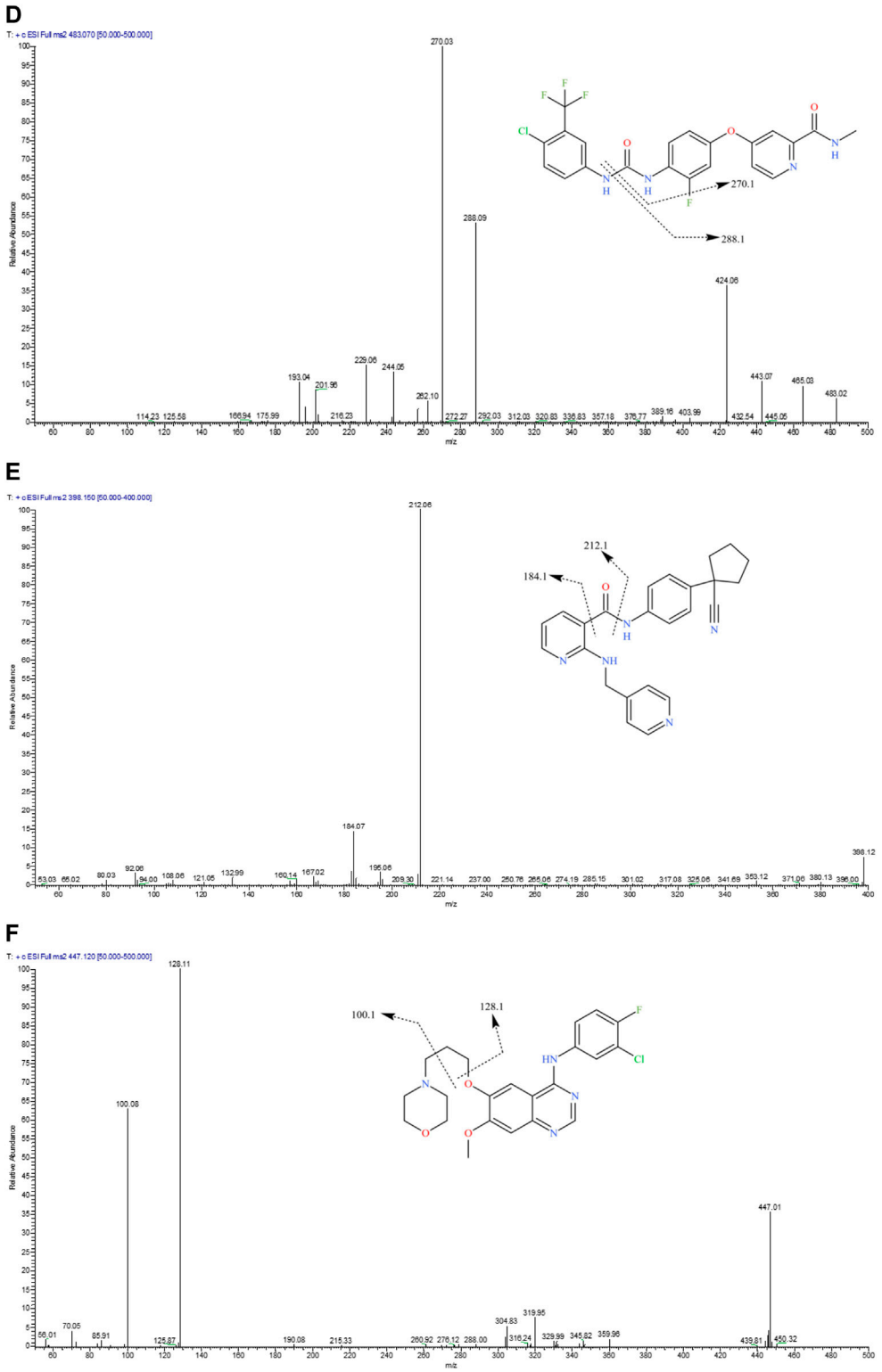

FIGURE 7 | (Continued).

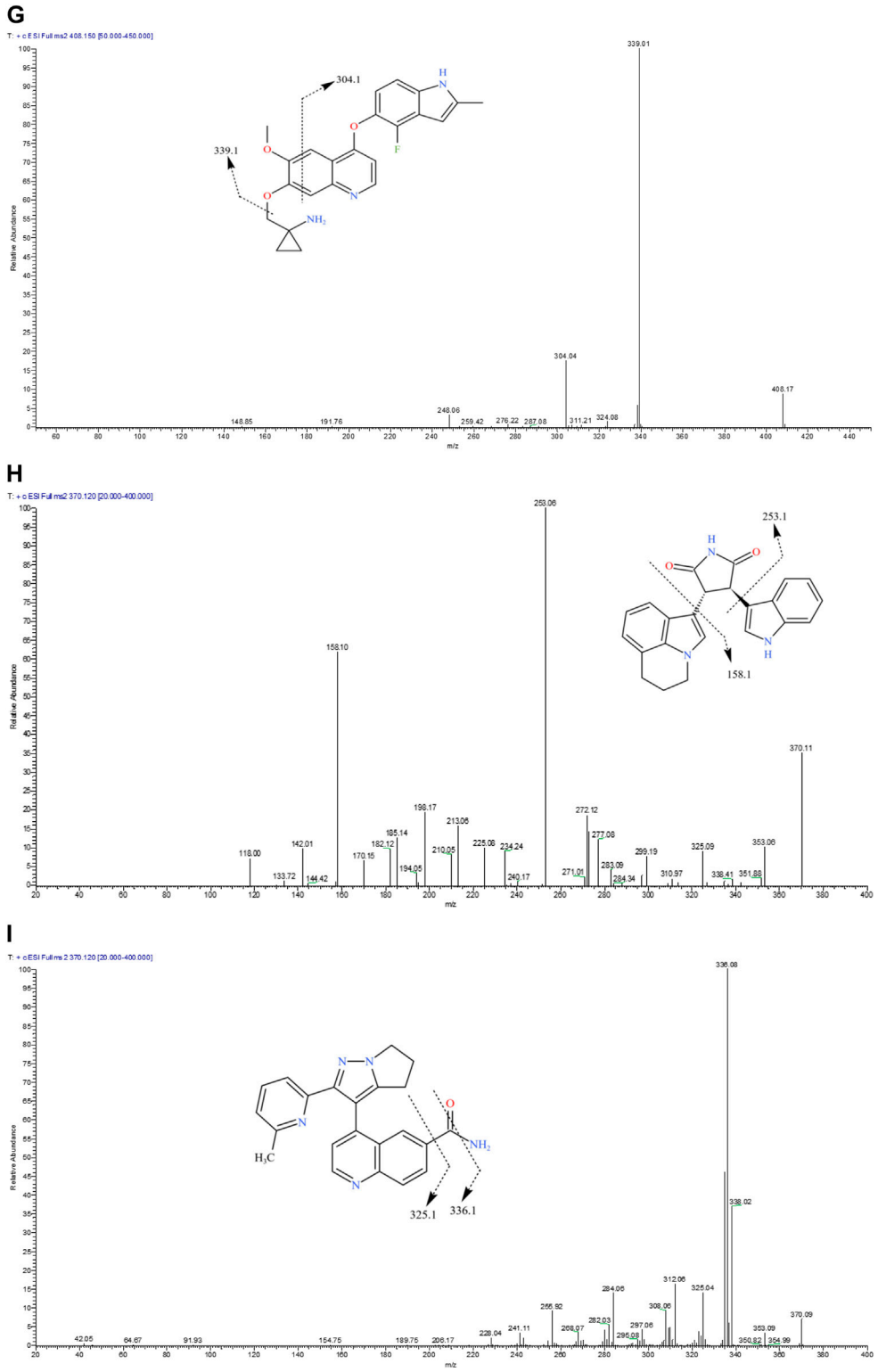

FIGURE 7 | (Continued).

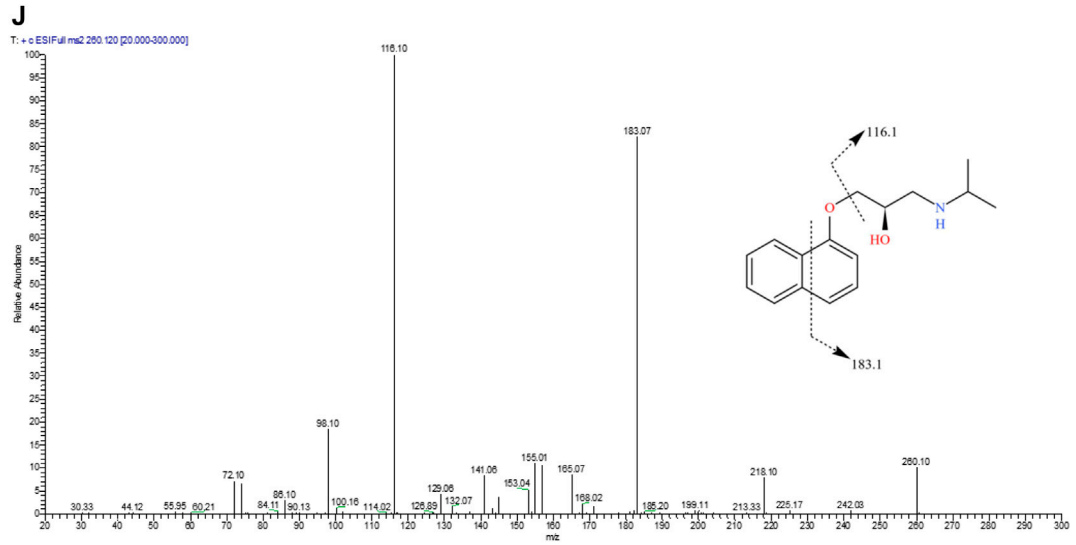

FIGURE 7 | (Continued). The product ion spectra of $[M+H]^+$ of lenvatinib **(A)**, sorafenib **(B)**, cabozantinib **(C)**, regorafenib **(D)**, apatinib **(E)**, gefitinib **(F)**, anlotinib **(G)**, tivantinib **(H)**, galunisertib **(I)** and IS **(J)**, and their chemical structures.

Technologies (Tianjin, China). NH_2 and ethyl enediamine-N-propylsilane (PSA) were purchased from Agilent Technologies (Shanghai, China).

2.2 Instrument

Vanquish Flex Ultra-performance Liquid Chromatography (UPLC) and TSQ Altis Triple Quadrupole Mass Spectrometer (MS) (Thermo Fisher Scientific, United States), nitrogen blowing concentrator (Beijing Politech Instrument Co., Ltd., China), High-speed Refrigerated Centrifuge (Yancheng Kait Experimental Equipment Co., Ltd. China), Vortex Meter (Wiggens, Germany), Milli-Q Purification System (Millipore, United States), KQ-500E Ultrasonic Cleaner (Kunshan Ultrasonic Instrument Co., Ltd. China), and Electronic analytical balance (Mettler Toledo, United States).

2.3 Mass Conditions

The MS was operated in the positive ionization mode with electrospray ionization (ESI) and selection reaction monitoring (SRM) to analyze all compounds. Xcalibur software (Thermo Fisher Scientific) was applicated for data acquisition and processing. The ion source parameters were set as follows: the ionspray voltage was 3500 V, the sheath gas was 45 Arb, the aux gas was 10 Arb, the ion transfer tube temperature was 350°C, and the vaporizer temperature was 400°C. Argon at a pressure of 1.5 mTorr as collision gas for collision-induced dissociation (CID). In this method, the dwell time for per transition was 100 ms. The precursor ions and product ions of each compound, the fragmentor voltage, collision energy, and retention time are displayed in **Table 1**.

2.4 Chromatographic Conditions

Separation and analysis were achieved using the Hypersil GOLD VANQUISH C18 column (100 μM × 2.1 μM; 1.9 μM), and the mobile phase was acetonitrile (phase A) and 0.1% formic acid in water (phase B). The gradient elution was performed as follows: for the first 0.5 min, the mobile phase B was 85%, then the proportion of mobile phase B was decreased from 85 to 5% at 0.5–2 min and held for 4 min, the mobile phase B was restored to 85% within 1 min, and then equilibrated for 1 min in the final. The analytical runtime was 8 min, the flow rate was 0.3 ml/min, and the injection volume for analysis was 5 μL.

2.5 Stock Solutions, Working Solutions, and Quality Control Samples

The stock solutions of sorafenib, cabozantinib, gefitinib, regorafenib, anlotinib, tivantinib, galunisertib (1 mg/ml), lenvatinib (800 μg/ml), and IS (500 μg/ml) were prepared in methanol at room temperature and maintained at -20°C until further use.

Different concentrations of the mixing working stock solutions (100, 10, and 1 μg/ml) were prepared by dilution of the stock solutions in methanol and stored at −20°C until use. The mixed working solutions were diluted with methanol in a certain proportion to prepare a series of calibration curve samples, ranging in concentration from 0.1 to 100 ng/ml (LEN, SOR, CBZ, RGF, APA, GEF, ANL: 0.1, 0.2, 0.5, 1, 2, 5, 8, and 10 ng/ml; TIV, GAL: 1, 2, 5, 10, 20, 50, 80, and 100 ng/ml). The concentration of the final IS solution was 5 ng/ml.

Blank human plasma (200 μL) was spiked with a certain concentration of the mixed working solution (10 μL) in order to obtain the quality control (QC) samples. The low QC (LQC), the medium QC (MQC), and the high QC (HQC) samples were set at 0.2, 5, and 10 ng/ml concentration (TIV and GAL) and at 2, 50, and 100 ng/ml concentration (LEN, SOR, CBZ, RGF, APA, GEF, and ANL), respectively. All working solutions were stored

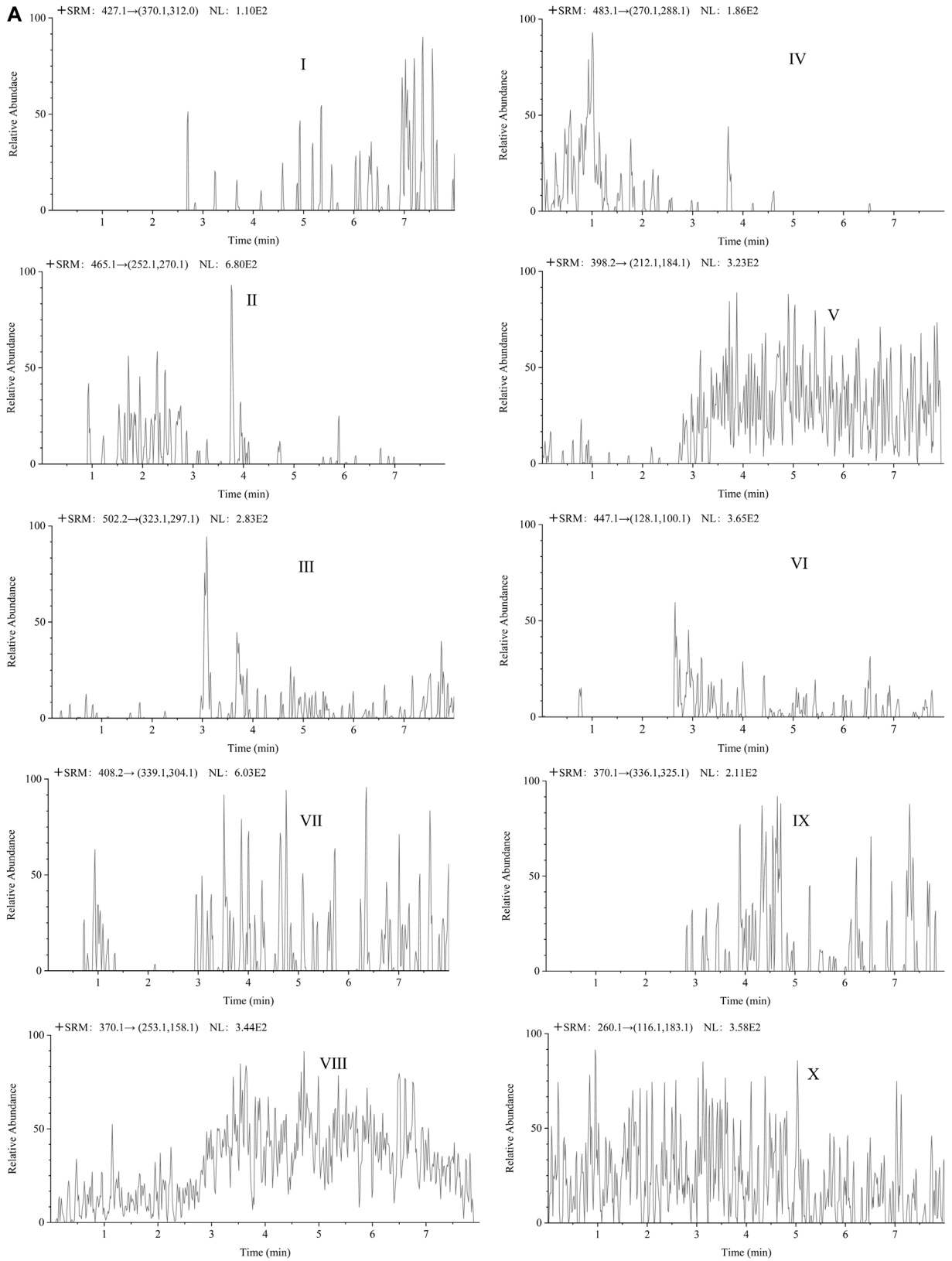

FIGURE 8 | (Continued).

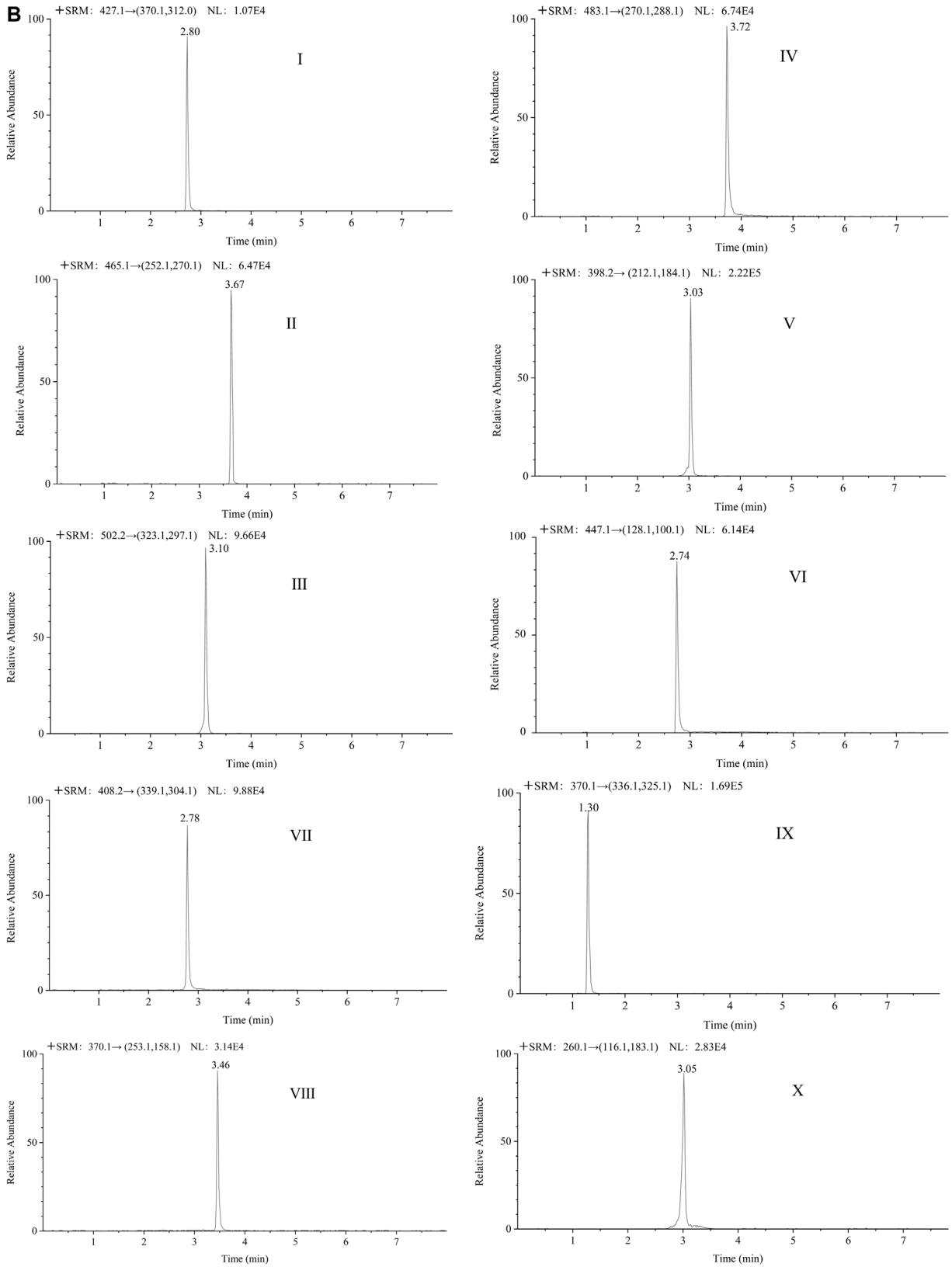

FIGURE 8 | (Continued). The representative chromatograms of lenvatinib **(I)**, sorafenib **(II)**, cabozantinib **(III)**, regorafenib **(IV)**, apatinib **(V)**, gefitinib **(VI)**, anlotinib **(VII)**, tivantinib **(VIII)**, galunisertib **(IX)**, and IS **(X)** in blank plasma samples **(A)**; each analyte in LLOQ samples **(B)**.

in a polypropylene (PP) centrifuge tube at −20°C until further analyses.

2.6 Sample Preparation

The blood of healthy people and hepatocellular carcinoma patients were obtained from the Bethune International Peace Hospital (Hebei, China) to serve as a control.

The received blood samples were centrifuged for 10 min at 3,500 × g at 4°C, and the supernatant was separated in a PP centrifuge tube and stored at −20°C. The plasma was removed before use and then thawed at room temperature. After vortex for 1 min, 200 μL of the plasma sample was added to a 4-ml centrifuge tube, to which 10 μL of the 5 ng/ml IS solution was added and mixed for 10 s. Subsequently, the samples were added to 1.5 ml of acetonitrile for extraction and vortexed for 30 s. Then, 350 mg of the $MgSO_4$ and 40 mg of the PSA were added respectively for salting out and purification. After vortexing for 30 s, the samples were centrifuged at 12,000 × g for 10 min. Then, 1 ml of the supernatant was filtered through a 0.22-μM microporous membrane and transferred into a centrifugal tube, followed by blowing with nitrogen at room temperature until dry. In the final step, the dried extracts were redissolved in 200 μL of the methanol solution and 5 μL of the final solution was injected into the UPLC-MS/MS system.

2.7 Method Validation

The established methods were validated in terms of selectivity, linearity, precision, accuracy, stability, and MEs based on the bioanalytical method validation guidelines by the US Food and Drug Administration (FDA) (U.S., 2018).

2.7.1 Selectivity

The selectivity of the method was evaluated by analyzing six blank blood samples from diverse individuals and six lower limits of quantitation (LLOQ) samples. The resulting chromatograms were compared and the response of interfering components was set to < 20% of the response of the analytes and < 5% of the response of IS (Verougstraete et al., 2021).

2.7.2 Calibration Curve and Lower Limit of the Quantification

Standard samples in different concentration ranges were obtained following "sample preparation" as detailed in **Section 2.6**. The concentration of the analytes was set as the horizontal coordinate (X) and the peak area ratio of the analytes to the internal standard as the vertical coordinate (Y). Then the calibration curves were assessed by a linearly weighted ($1/x^2$) least-squares linear regression analysis (Fresnais et al., 2020). The correlation coefficient (R^2) was > 0.990. The concentration of the calibration standard samples were based on the calibration curve, each calibration level was set to within ±15% of the nominal value, and the LLOQ was accepted for a ±20% range (He et al., 2017).

The limit of detection (LODs) and the limit of quantitation (LOQs) of the instrument was defined by the S/N (signal-to-noise ratio) (Kocan et al., 2018). The S/N of LODs was set to ≥ 3 and the S/N of LOQs to ≥ 10.

2.7.3 Precision and Accuracy

Intra-day precision and accuracy of the method were obtained by analyzing the QC samples at three different levels (i.e., LQC, MQC, and HQC) and the LLOQ samples using six replicates on the same day. The inter-day accuracy and precision were evaluated on three consecutive days (Ferrer et al., 2020). Precision was expressed in terms of relative standard deviation (RSD) and accuracy in terms of relative error (RE). For each QC level, the RSD value was required to be < 15% and the deviation of the RE value was set to be within ±15%. For the LLOQ, the RSD was set to < 20% and RE within ±20% (Reis et al., 2018).

2.7.4 Recovery and MEs

To ensure efficient recovery, six replicates of the three analyte concentration levels (i.e., LQC, MQC, and HQC) and one IS concentration level (5 ng/ml) were assessed. The analytical results of the blank plasma spiked with analyte after extraction (A) were compared to the samples spiked with the analyte before extraction (B). The extent of recovery in this experiment was evaluated based on the ratio of the analytes' peak area to the IS area: (A/B) × 100% (Aghai et al., 2021).

The ratio of the peak area to the internal standard area was compared with QC samples (C) and the matrix-free samples(D). The ME of the QuEChERS-UPLC-MS/MS method was calculated as follows: C/D × 100%, and the RSD was set to be < 15% (Ogawa-Morita et al., 2017; Zheng et al., 2021).

2.7.5 Stability

Stability assessments under different conditions were conducted for the QC (low- and high-concentration) samples, namely at room temperature (25°C) for 24 h, under refrigeration (4°C) for 48 h, in an autosampler for 72 h, under −20°C for 15 days, and in three different freeze-thaw cycles (−20°Cto room temperature); three parallel samples were set for each concentration and then tested. If the RSD was < 15%, stability was considered to be acceptable.

3 RESULTS AND DISCUSSION

3.1 Comparison of the Preprocessing Methods

At the same spiked level, the effects of two frequently used pretreatment methods, that is, LLE and PP, and the emerging pre-treatment method QuEChERS on analyte recovery were evaluated. The recovery of the analytes in these three pretreatment methods is illustrated in **Figure 1**.

The QuEChERS purification method was performed according to the "sample preparation" method, as detailed in **Section 2.6**. Pure acetonitrile was used for PP. The IS solution (10 μL of 5 ng/ml) and 10 μL of the standard solution were added to the blank plasma sample and mixed for 30 s, followed by the use of 1 ml acetonitrile for PP. These results revealed that the acetonitrile PP method was efficient and convenient, although its purification effect was not ideal. Methyl tert-butyl ether was used for LLE, and 10 μL of the IS solution (5 ng/ml) and 10 μL of the

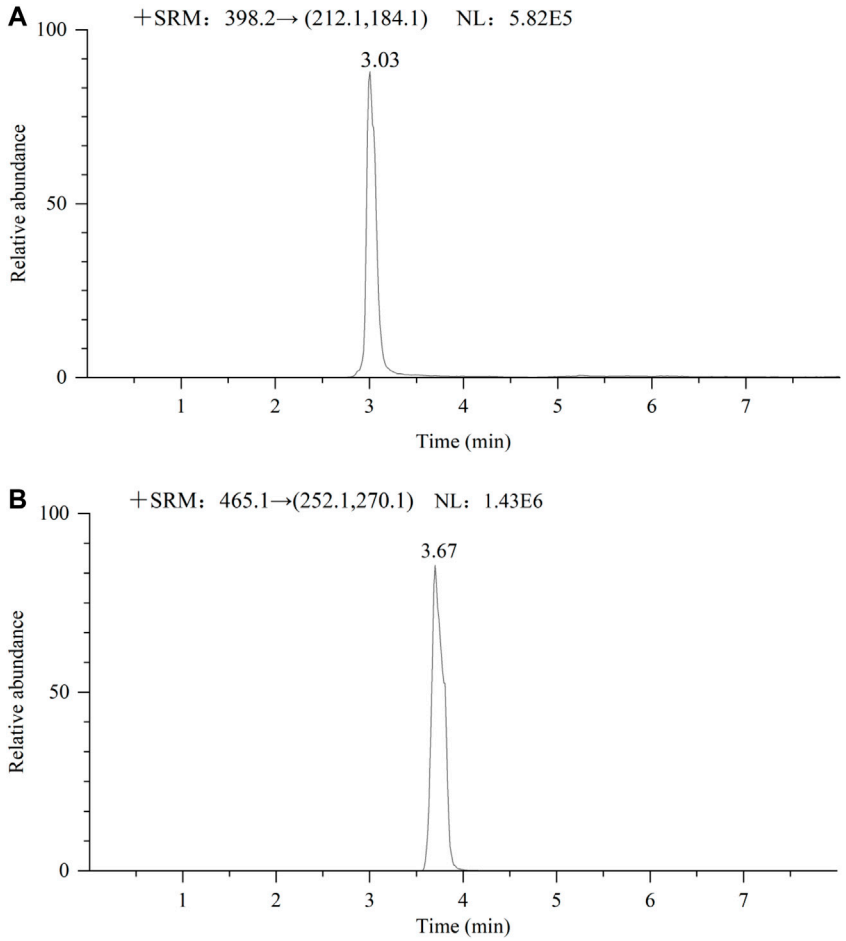

FIGURE 9 | Chromatogram of 2 male patients receiving oral apatinib **(A)** 250 mg and sorafenib **(B)** 400 mg respectively.

standard solution were added to the blank plasma sample and mixed for 30 s, after which 1 ml of methyl tert-butyl ether was added for LLE. The recovery rates of several methods ranged from 47.85 to 95.01%. For instance, when compared with LLE and acetonitrile PP, the QuEchERs method revealed a higher recovery rate for most analytes, just as for the plasma samples used in this study. Accordingly, the QuEchERs method was selected for the pretreatment of plasma samples in this study.

3.2 Optimization of Preprocessing Methods

3.2.1 Optimization of the Extraction Conditions

In the first place, the varieties and amounts of extraction solvents were optimized. Methanol, acetonitrile, ethyl acetate, and acetone were the commonly used extraction solvents (Perestrelo et al., 2019; Kanu et al., 2021; Chen et al., 2021). The recovery results were applied to evaluate the extraction effect of several organic solvents. Equal amounts of the intended analytes and 1 ml of

TABLE 2 | Linear regression equations, LODs, and LOQs of all TKIs.

Analyte	Linear equation	Linear range (ng/ml)	R^2	LODs (ng/ml)	LOQs (ng/ml)
LEN	Y = 0.7709x + 0.2815	0.1–10	0.9968	0.01	0.04
SOR	Y = 0.3739x + 0.1048	0.1–10	0.9996	0.006	0.02
CBZ	Y = 0.0672x + 0.0318	0.1–10	0.9999	0.01	0.04
RGF	Y = 0.4654x + 0.0492	0.1–10	0.9977	0.003	0.01
APA	Y = 1.2796x + 1.0863	0.1–10	0.9982	0.006	0.02
GEF	Y = 0.3259x + 0.0084	0.1–10	0.9973	0.003	0.01
ANL	Y = 0.1886x + 0.0353	0.1–10	0.9975	0.01	0.04
TIV	Y = 0.0618x + 0.0296	1.0–100	0.9966	0.11	0.37
GAL	Y = 0.2120x – 0.2406	1.0–100	0.9992	0.05	0.18

TABLE 3 | Results for intra-day and inter-day precision (RSD) and accuracy (RE) of QC and LLOQ samples (n = 6).

Analyte	Nominal concentration (ng/ml)	Intra-day		Inter-day	
		RSD (%)	RE (%)	RSD (%)	RE (%)
LEN	0.1	7.61	–3.83	8.23	5.85
	0.2	6.57	2.08	7.02	–6.45
	5	4.59	–6.44	5.67	3.65
	10	2.43	4.34	4.21	1.43
SOR	0.1	6.11	–4.43	7.41	4.78
	0.2	5.87	–3.32	7.76	–4.32
	5	2.96	1.70	6.95	5.77
	10	1.45	3.82	2.64	0.97
CBZ	0.1	7.21	4.34	9.09	–7.32
	0.2	6.74	3.90	7.08	3.98
	5	5.67	–1.32	5.28	4.76
	10	3.43	3.31	6.87	3.82
RGF	0.1	5.43	–1.32	8.23	1.34
	0.2	3.08	2.47	6.65	–7.32
	5	3.56	3.95	6.77	2.67
	10	1.22	–2.45	4.01	1.34
APA	0.1	5.35	–6.21	4.34	5.43
	0.2	6.65	4.67	6.64	4.77
	5	5.41	–7.34	5.63	4.98
	10	0.99	3.36	2.81	2.08
GEF	0.1	3.36	–2.24	5.44	2.96
	0.2	1.95	–2.94	2.78	1.77
	5	2.45	–1.95	1.46	2.04
	10	0.87	3.95	2.82	–4.55
ANL	0.1	5.34	4.27	8.45	5.54
	0.2	4.79	3.39	6.78	2.98
	5	3.47	–3.67	6.48	3.01
	10	3.46	6.64	5.73	3.83
TIV	1	6.46	5.99	3.97	–0.78
	2	4.38	2.63	5.56	1.15
	50	1.06	–2.27	2.58	2.97
	100	0.40	–3.82	2.20	1.04
GAL	1	3.36	3.67	3.82	–0.77
	2	4.02	0.30	6.92	5.44
	50	0.92	–2.01	3.02	–2.24
	100	1.29	4.88	2.24	–0.95

the abovementioned organic solvents were then added; the experimental results revealed that the peak shape and the extraction effect of acetonitrile were better than that of the other solvents; the recovery results are shown in **Figure 2**. The extraction efficiency of this method was affected by the amount of extraction solvent and the addition of different volumes of acetonitrile (i.e., 1, 1.5, and 2 ml) respectively. The results are presented in **Figure 3**. The best extraction effect was achieved with the addition of 1.5 ml acetonitrile. Therefore, 1.5 ml of acetonitrile was selected for the extraction of these TKIs.

3.2.2 Optimization of Salting-Out Conditions

The composition of the human plasma matrix is complex and majorly attributable to water, which affects the determination of analytes and causes unnecessary loss to the MS. In this study, anhydrous $MgSO_4$ was selected as the salting-out agent, and its dosage was optimized; the recovery of each analyte served as the evaluation index. Different masses of anhydrous $MgSO_4$ (i.e., 250, 300, 350, 400, and 450 mg) were added for the experiments under the same spiking level (**Figure 4**). The best recovery of each analyte was obtained with 350 mg of anhydrous $MgSO_4$.

3.2.3 Optimization of the Adsorption Conditions

The composition of the plasma is complex, including proteins, lipids, inorganic salts, and amino acids, all of which can influence the MEs. In this study, five adsorbents were selected, including ethyl enediamine-N-propylsilane (PSA), florisil, octadecyl bonded silica gel (C18), NH_2, and graphitized carbon black (GCB). Their results were compared based on the recovery rate (**Figure 5**). GCB exhibited poor purification results outcome not deemed suitable for plasma purification. In contrast, PSA exhibited the best results and was hence recommended for the removal of sugars, fatty acids, and organic acids (Niu et al., 2020). Various amounts of PSA (i.e., 40, 50, 60, and 70 mg) were selected as the optimum amount of the salting-out agent for this assay. The experimental results were compared by recovery and are shown in **Figure 6**. Therefore, 40 mg of PSA was selected as the optimal amount of adsorbent in the QuEChERS pretreatment method.

TABLE 4 | Recovery and matrix effect of the 9 TKIs in the human plasma (n = 6).

Analyte	Concentration (ng/ml)	Recovery %		Matrix effect %	
		Mean	RSD	Mean	RSD
LEN	0.2	94.34	6.54	97.95	3.29
	5	97.72	5.32		
	10	96.82	3.91	99.54	1.91
SOR	0.2	93.83	4.25	102.76	6.24
	5	94.24	4.68		
	10	98.02	3.67	98.34	7.29
CBZ	0.2	96.92	2.73	106.46	5.32
	5	97.29	4.45		
	10	97.02	3.69	107.77	6.20
RGF	0.2	92.92	7.92	97.45	7.02
	5	90.84	5.74		
	10	93.02	5.31	95.88	3.91
APA	0.2	93.54	3.40	96.78	2.29
	5	100.13	3.73		
	10	98.39	2.44	99.34	3.65
GEF	0.2	96.28	5.40	105.29	5.72
	5	93.14	2.71		
	10	97.62	1.85	100.36	8.54
ANL	0.2	92.82	7.52	93.77	2.98
	5	98.94	4.28		
	10	96.02	3.61	98.64	4.92
TIV	2	91.64	9.29	90.48	2.23
	50	92.82	7.42		
	100	98.76	2.24	94.32	5.44
GAL	2	93.39	4.67	97.56	5.42
	50	95.85	6.88		
	100	96.20	3.83	104.67	9.74
IS	5	94.57	6.86		

3.3 Optimization of the Mass Spectrometric

All analytes and IS (1 μg/ml) were directly injected via a needle pump and scanned in the positive ion mode and negative ion mode. We found that the response of each substance was higher in the positive ion mode. Accordingly, nine TKIs were analyzed in the positive ion mode. One quantitative ion and one qualitative ion were selected for each substance. The product spectra and the proposed fragmentation patterns of each analyte and IS are depicted in **Figure 7**.

3.4 Optimization of the Chromatographic Conditions

In this experiment, we attempted to compare the separation performance of 4 columns, which included the Agilent Poroshell 120 EC-C18 (3.0 mm × 50 mm, 2.7 μM) column, Hypersil GOLD VANQUISH C18 (2.1 mm × 100 mm, 1.9 μM) column, the Agilent Eclipse Plus C18 (3.0 mm × 100 mm, 1.8 μM) column, and Agilent Eclipse Plus C18 (4.6 mm × 100 mm, 3.5 μM) column. The columns were evaluated under moderate concentrations of QC samples. The results revealed that the Agilent Poroshell 120 EC-C18 column gave a good peak shape, but a relatively concentrated peak time. The Hypersil GOLD VANQUISH C18 columns were found to be good for the analysis of each determinant, with good separation performance and peak shape. The Agilent Eclipse Plus C18 (3.0 mm × 100 mm, 1.8 μM) column could not separate the analytes adequately owing to the small difference in the polarity of the analytes, resulting in poor peak shape. On the other hand, the Agilent Eclipse Plus C18 (4.6 mm × 100 mm, 3.5 μM) column was longer, and the analytes were slower to the peak. According to the experimental results, the Hypersil GOLD VANQUISH C18 column was selected for use as the analytical column in this experiment.

Moreover, the effects of different combinations of organic and aqueous phases on the peak shapes and response values of the analytes were investigated. Methanol and acetonitrile were examined and the response of the analytes was found to be slightly higher with acetonitrile as the organic phase. Subsequently, different aqueous phases were examined (e.g., water, 0.1% formic acid with water, and

TABLE 5 | Stabilities of the LQC and HQC samples under different storage conditions (n = 6).

Analyte	Concentration (ng/ml)	Expressed % (RSD %)				
		25°C/24 h	4°C/48 h	Autosampler/72 h	3 freeze-Thaw cycles	-20°C/15 days
LEN	0.2	93.38 (7.84)	96.38 (8.63)	96.76 (5.82)	93.24 (11.76)	89.23 (4.23)
	10	97.93 (3.88)	93.86 (4.71)	105.72 (7.65)	95.96 (5.83)	96.37 (6.34)
SOR	0.2	92.83 (6.39)	94.44 (10.67)	100.48 (8.73)	96.62 (6.03)	91.04 (8.04)
	10	104.22 (5.02)	103.26 (5.98)	106.27 (6.78)	97.28 (8.34)	103.75 (6.39)
CBZ	0.2	106.23 (0.89)	102.68 (8.19)	107.41 (10.54)	105.82 (4.73)	100.84 (7.33)
	10	109.02 (3.91)	103.28 (10.60)	108.19 (4.36)	106.25 (7.65)	110.45 (2.08)
RGF	0.2	78.20 (8.92)	87.55 (6.83)	92.56 (6.45)	87.06 (4.09)	76.87 (6.94)
	10	94.88 (6.20)	95.46 (1.82)	96.17 (8.32)	93.28 (5.86)	90.34 (5.98)
APA	0.2	91.05 (12.83)	93.53 (5.92)	96.35 (7.82)	92.43 (6.45)	89.43 (10.47)
	10	103.81 (9.54)	92.58 (3.86)	108.48 (10.27)	93.65 (5.02)	88.28 (8.22)
GEF	0.2	76.87 (2.98)	85.46 (1.38)	88.29 (3.67)	85.66 (5.45)	75.77 (6.38)
	10	87.17 (6.82)	81.25 (6.45)	96.23 (4.65)	88.54 (8.45)	80.65 (1.67)
ANL	0.2	109.55 (1.93)	107.47 (3.87)	111.87 (2.78)	102.68 (6.88)	98.63 (7.45)
	10	100.76 (6.55)	103.17 (8.56)	102.34 (5.85)	104.95 (7.85)	97.46 (9.43)
TIV	2	91.64 (5.92)	89.24 (12.62)	97.16 (11.02)	92.66 (9.44)	96.49 (8.95)
	100	95.76 (5.11)	92.48 (7.38)	99.35 (4.45)	89.54 (2.56)	85.34 (6.44)
GAL	2	104.28 (2.96)	100.66 (6.49)	106.28 (5.34)	95.32 (3.76)	97.56 (1.76)
	100	107.98 (3.81)	98.86 (4.78)	109.45 (2.64)	99.84 (4.87)	96.47 (7.56)

TABLE 6 | Comparison of the proposed method with other published methods for the quantitative detection of TKIs with anti-hepatocellular carcinogenic effects.

Sample Type	Analyte	Detection system	Method	LOQ (ng/ml)	Recovery (%)	Ref
Plasma	9 TKIs	UPLC–MS/MS	QuEChERS	0.01~0.37	90.84~100.13	this work
Plasma	Cabozantinib	LC–MS/MS	PP	25	86.9 ± 5.4	Ferrer et al., (2020)
Serum/plasma	10 TKIs	LC–MS/MS	PP	2–6	89.5–110	Aghai et al., (2021)
Plasma	7 TKIs	UPLC–MS/MS	LLE	5	≥69	Ezzeldin et al., (2020)
Plasma	Galunisertib	LC–MS/MS	PP	0.05	85.96 ± 5.8	Tibben et al., (2019)
Plasma	6 TKIs	HPLC–Q–Orbitrap MS	LLE	0.02–2	88.3–103.4	Ni et al., (2017)
Plasma	7 TKIs and metabolite regorafenib M2	UPLC–MS/MS	PP	6–4,998.7	>70	Krens et al., (2020)
Plasma	sorafenib, regorafenib and their metabolites	LC–MS/MS	PP	30~50	≥85.5	Iacuzzi et al., (2020)
Plasma	Lenvatinib	UPLC–MS/MS	SLE	0.2	98.63 ± 4.55	Sueshige et al., (2021)
Plasma	sorafenib, lenvatinib, and apatinib	UPLC–MS/MS	PP	1.3–312.5	90.5–99.4	Ye et al., (2021)
Plasma	apatinib and metabolites	UPLC–MS/MS	LLE	1	48.9–69.5	Guan et al. (2019)
Plasma	12 TKIs	LC–MS/MS	SALLE	0.5–12.5	83.19–112.04	Zhou et al. (2021)
Dried blood spots	Gefitinib	LC–MS/MS	PP	40	95.7–104.9	Irie et al. (2018)

0.1% acetic acid with water), and the results revealed that the optimal mobile phase was 0.1% formic acid water and acetonitrile.

3.5 Method Validation

3.5.1 Selectivity

In the analysis of blank plasma samples, no interfering peaks from the endogenous substances were detected. Among these, the method was exclusively selective for the TKIs and IS. The representative chromatograms for the LLOQ and blank plasma samples are shown in **Figure 8**. The retention time for LEN, SOR, CBZ, RGF, APA, GEF, ANL, TIV, GAL and IS were 2.80, 3.67, 3.10, 3.72, 3.03, 2.74, 2.78, 3.46, 1.30, and 3.05 min, respectively.

3.5.2 Calibration Curve and the Lower Limit of Quantification

The calibration curve of nine TKIs exhibited satisfactory linearity over the range of 0.1–10 ng/ml for lenvatinib, sorafenib, cabozantinib, apatinib, gefitinib, regorafenib, and anlotinib, and that of 1–100 ng/ml for tivantinib and galunisertib, while the linear correlation coefficients (R2) of all analytes was 0.9966–0.9999. The linearity, LODs, and LOQs of the nine analytes are shown in **Table 2**. LODs and LOQs indicated the sensitivity of the assay, the final results showed that the LODs of these analyzed hepatic agents targeting antineoplastic drugs were 0.003–0.11 ng/ml and the LOQs as 0.01–0.37 ng/ml, respectively. Therefore, the method was determined to be sufficiently sensitive for application in quantitative analyses.

3.5.3 Precision and Accuracy

The results of intra-day and inter-day precision and accuracy at different concentration levels are depicted in **Table 3**. The precision for all TKIs was < 9.09%, whereas the accuracy value was -7.34–6.64%. Thus, this assay was deemed suitable for the detection of these nine TKIs with satisfying accuracy and precision at different concentration levels (LQC, MQC, HQC, and LLOQ).

3.5.4 MEs and Recovery

The recovery outcomes and MEs are depicted in **Table 4**. The recoveries of nine analytes at different concentrations ranged from 90.84 to 100.13%, and the RSD values were 1.85–9.29%. The recoverie of IS was 94.57%, and the RSD value was 6.86%. These results indicated a high extraction efficiency for nine TKIs. The MEs for all analytes ranged from 90.48 to 107.77% at the LQC and HQC levels, and the normalized matrix factors of the internal standard were determined by RSD to be < 9.74%. Therefore, the ME of the established method was negligible.

3.5.5 Stability

Table 5 depicts the stability outcomes of the nine TKIs under five storage conditions. The values of RSD for the stability test were < 12.83%, which is within the acceptance criteria, indicating that all TKIs have acceptable stability under different storage conditions.

3.6 Comparative Analyses With Other Published Methods

This method was compared with other published assays for the TKIs with anti-hepatocellular carcinogenic effects in terms of LOQs and recovery (**Table 6**). The LC-MS/MS method revealed a large dynamic range and high sensitivity, and it is hence the most widely used detection method in the present literature. Among the pretreatment methods tested, the most commonly used methods included PP and LLE. The optimized QuEChERS method employed in this research was compared with other assays to reveal relatively and significantly better recovery and LOQs. Although the recovery rates of particular methods were similar, the LOQs were low. Therefore, finally, the QuEChERS method was used for further analyses considering that it is simple, efficient, and suitable for detection.

3.7 Method Application

This method is currently used only for blood concentration monitoring of apatinib and sorafenib because blood from patients with HCC is more difficult to obtain. The method was validated and has been successfully applied to the quantitative analysis of apatinib and sorafenib in the plasma of patients with HCC. The basic information of the two patients is as follows: sample 1 (male, age: 69 years), taking apatinib 250 mg daily; Sample 2 (male, age: 62 years), taking sorafenib 400 mg daily. **Figures 9A,B** show the chromatograms of apatinib and sorafenib in the plasma of patients with HCC, respectively. The blood drug concentrations were calculated to be 327 ng/ml and 3,842 ng/ml, respectively. The

results suggest that the method is suitable for the detection of the nine TKIs in the plasma of patients with HCC.

4 CONCLUSION

In conclusion, in this study, we established a new method that combines the QuEChERS pretreatment technology with UPLC-MS/MS for the quantitative determination of nine TKIs in human plasma specimens. Accordingly, the factors of chromatographic conditions, MS conditions, and the QuEChERS method were optimized. When compared with the other available methods, the optimized method exhibited the advantages of simplicity, reliability, and rapidity. The LOQs of this method were 0.01–0.37 ng/ml and the total chromatographic run time was 8 min for each analyte. Moreover, the recovery and precision were found to be excellent, and the TKI samples showed acceptable stability under different conditions with negligible ME. Therefore, we recommend the proposed method for use in the routine quantitative assay to evaluate nine TKIs in the human plasma.

DATA AVAILABILITY STATEMENT

The original contributions presented in the study are included in the article/supplementary materials, further inquiries can be directed to the corresponding authors.

ETHICS STATEMENT

The studies involving human participants were reviewed and approved by the Ethics Committee of Hebei Medical University. The patients/participants provided their written informed consent to participate in this study.

AUTHOR CONTRIBUTIONS

WJ performed the experiment and statistical analysis. WJ and TZ wrote the first draft of the manuscript. XZ wrote sections of the manuscript. CJ and LH revised the final version of the article. JH and HL contributed to conception and design of the study. All authors have contributed to, read, and approved this submitted manuscript in its current form.

ACKNOWLEDGMENTS

The authors would like to thank the personnel at the Bethune International Peace Hospital for their assistance in collecting the plasma samples. This work was supported by the Natural Science Foundation of Hebei Province (H2019329002). The authors would like to thank all the reviewers who participated in the review and MJEditor (www.mjeditor.com) for its linguistic assistance during the preparation of this manuscript.

REFERENCES

Aghai, F., Zimmermann, S., Kurlbaum, M., Jung, P., Pelzer, T., Klinker, H., et al. (2021). Development and Validation of a Sensitive Liquid Chromatography Tandem Mass Spectrometry Assay for the Simultaneous Determination of Ten Kinase Inhibitors in Human Serum and Plasma. *Anal. Bioanal. Chem.* 413, 599–612. doi:10.1007/s00216-020-03031-7

Bray, F., Ferlay, J., Soerjomataram, I., Siegel, R. L., Torre, L. A., and Jemal, A. (2020). Erratum: Global Cancer Statistics 2018: GLOBOCAN Estimates of Incidence and Mortality Worldwide for 36 Cancers in 185 Countries. *CA Cancer J. Clin.* 70, 313. doi:10.3322/caac.2149210.3322/caac.21609

Cammarota, A., Zanuso, V., D'Alessio, A., Pressiani, T., Personeni, N., and Rimassa, L. (2022). Cabozantinib Plus Atezolizumab for the Treatment of Advanced Hepatocellular Carcinoma: Shedding Light on the Preclinical Rationale and Clinical Trials. *Expert Opin. Investigational Drugs* 31, 401–413. doi:10.1080/13543784.2022.2032641

Chen, L., Zhang, Y., Zhou, Y., Li, G. H., and Feng, X. S. (2021). Pretreatment and Determination Methods for Benzimidazoles: An Update since 2005. *J. Chromatogr. A* 1644, 462068. doi:10.1016/j.chroma.2021.462068

D'Angelo, A., Sobhani, N., Bagby, S., Casadei-Gardini, A., and Roviello, G. (2020). Cabozantinib as a Second-Line Treatment Option in Hepatocellular Carcinoma. *Expert Rev. Clin. Pharmacol.* 13, 623–629. doi:10.1080/17512433.2020.1767591

Decraecker, M., Toulouse, C., and Blanc, J. F. (2021). Is There Still a Place for Tyrosine Kinase Inhibitors for the Treatment of Hepatocellular Carcinoma at the Time of Immunotherapies? A Focus on Lenvatinib. *Cancers (Basel)* 13, 6310. doi:10.3390/cancers13246310

Di Marco, V., De Vita, F., Koskinas, J., Semela, D., Toniutto, P., and Verslype, C. (2013). Sorafenib: from Literature to Clinical Practice. *Ann. Oncol.* 24 Suppl 2, ii30–7. doi:10.1093/annonc/mdt055

Dutta, R., and Mahato, R. I. (2017). Recent Advances in Hepatocellular Carcinoma Therapy. *Pharmacol. Ther.* 173, 106–117. doi:10.1016/j.pharmthera.2017.02.010

El-Khoueiry, A. B., Hanna, D. L., Llovet, J., and Kelley, R. K. (2021). Cabozantinib: An Evolving Therapy for Hepatocellular Carcinoma. *Cancer Treat. Rev.* 98, 102221. doi:10.1016/j.ctrv.2021.102221

Ezzeldin, E., Iqbal, M., Herqash, R. N., and ElNahhas, T. (2020). Simultaneous Quantitative Determination of Seven Novel Tyrosine Kinase Inhibitors in Plasma by a Validated UPLC-MS/MS Method and its Application to Human Microsomal Metabolic Stability Study. *J. Chromatogr. B Anal. Technol. Biomed. Life Sci.* 1136, 121851. doi:10.1016/j.jchromb.2019.121851

Ferrer, F., Solas, C., Giocanti, M., Lacarelle, B., Deville, J. L., Gravis, G., et al. (2020). A Simple and Rapid Liquid Chromatography-Mass Spectrometry Method to Assay Cabozantinib in Plasma: Application to Therapeutic Drug Monitoring in Patients with Renal Cell Carcinoma. *J. Chromatogr. B Anal. Technol. Biomed. Life Sci.* 1138, 121968. doi:10.1016/j.jchromb.2020.121968

Fogli, S., Porta, C., Del Re, M., Crucitta, S., Gianfilippo, G., Danesi, R., et al. (2020). Optimizing Treatment of Renal Cell Carcinoma with VEGFR-TKIs: a Comparison of Clinical Pharmacology and Drug-Drug Interactions of Anti-angiogenic Drugs. *Cancer Treat. Rev.* 84, 101966. doi:10.1016/j.ctrv.2020.101966

Foo, T., Goldstein, D., Segelov, E., Shapiro, J., Pavlakis, N., Desai, J., et al. (2022). The Management of Unresectable, Advanced Gastrointestinal Stromal Tumours. *Targ. Oncol.* 17, 95–110. doi:10.1007/s11523-022-00869-y

Fresnais, M., Roth, A., Foerster, K. I., Jäger, D., Pfister, S. M., Haefeli, W. E., et al. (2020). Rapid and Sensitive Quantification of Osimertinib in Human Plasma Using a Fully Validated MALDI-IM-MS/MS Assay. *Cancers (Basel)* 12, 1897. doi:10.3390/cancers12071897

Granito, A., Forgione, A., Marinelli, S., Renzulli, M., Ielasi, L., Sansone, V., et al. (2021). Experience with Regorafenib in the Treatment of Hepatocellular Carcinoma. *Ther. Adv. Gastroenterol.* 14, 17562848211016959. doi:10.1177/17562848211016959

Guan, S., Shi, W., Zhao, Z., Wang, F., Jiang, F., Zhang, C., et al. (2019). Determination of Apatinib and its Three Active Metabolites by UPLC-MS/MS in a Phase IV Clinical Trial in NSCLC Patients. *Bioanalysis* 11, 2049–2060. doi:10.4155/bio-2019-0214

Guo, W., Chen, S., Wu, Z., Zhuang, W., and Yang, J. (2020). Efficacy and Safety of Transarterial Chemoembolization Combined with Anlotinib for Unresectable Hepatocellular Carcinoma: A Retrospective Study. *Technol. Cancer Res. Treat.* 19, 1533033820965587. doi:10.1177/1533033820965587

He, Y., Zhou, L., Gao, S., Yin, T., Tu, Y., Rayford, R., et al. (2017). Development and Validation of a Sensitive LC-MS/MS Method for Simultaneous Determination of Eight Tyrosine Kinase Inhibitors and its Application in Mice Pharmacokinetic Studies. *J. Pharm. Biomed. Anal.* 148, 65–72. doi:10.1016/j.jpba.2017.09.013

Hwang, S., Hong, T. H., Park, S., Jung, H. A., Sun, J. M., Ahn, J. S., et al. (2021). Molecular Subtypes of Small Cell Lung Cancer Transformed from Adenocarcinoma after EGFR Tyrosine Kinase Inhibitor Treatment. *Transl. Lung Cancer Res.* 10, 4209–4220. doi:10.21037/tlcr-21-691

Iacuzzi, V., Zanchetta, M., Gagno, S., Poetto, A. S., Orleni, M., Marangon, E., et al. (2020). A LC-MS/MS Method for Therapeutic Drug Monitoring of Sorafenib, Regorafenib and Their Active Metabolites in Patients with Hepatocellular Carcinoma. *J. Pharm. Biomed. Anal.* 187, 113358. doi:10.1016/j.jpba.2020.113358

Irie, K., Shobu, S., Hiratsuji, S., Yamasaki, Y., Nanjo, S., Kokan, C., et al. (2018). Development and Validation of a Method for Gefitinib Quantification in Dried Blood Spots Using Liquid Chromatography-Tandem Mass Spectrometry: Application to Finger-Prick Clinical Blood Samples of Patients with Non-small Cell Lung Cancer. *J. Chromatogr. B Anal. Technol. Biomed. Life Sci.* 1087-1088, 1–5. doi:10.1016/j.jchromb.2018.04.027

Jin, H., Shi, Y., Lv, Y., Yuan, S., Ramirez, C. F. A., Lieftink, C., et al. (2021). EGFR Activation Limits the Response of Liver Cancer to Lenvatinib. *Nature* 595, 730–734. doi:10.1038/s41586-021-03741-7

Kanu, A. B. (2021). Recent Developments in Sample Preparation Techniques Combined with High-Performance Liquid Chromatography: A Critical Review. *J. Chromatogr. A* 1654, 462444. doi:10.1016/j.chroma.2021.462444

Klug, L. R., Khosroyani, H. M., Kent, J. D., and Heinrich, M. C. (2022). New Treatment Strategies for Advanced-Stage Gastrointestinal Stromal Tumours. *Nat. Rev. Clin. Oncol.* 19, 328–341. doi:10.1038/s41571-022-00606-4

Kocan, G. P., Huang, M. Q., Li, F., and Pai, S. (2018). A Sensitive LC-MS-MS Assay for the Determination of Lapatinib in Human Plasma in Subjects with End-Stage Renal Disease Receiving Hemodialysis. *J. Chromatogr. B Anal. Technol. Biomed. Life Sci.* 1097-1098, 74–82. doi:10.1016/j.jchromb.2018.09.005

Krens, S. D., van der Meulen, E., Jansman, F. G. A., Burger, D. M., and van Erp, N. P. (2020). Quantification of Cobimetinib, Cabozantinib, Dabrafenib, Niraparib, Olaparib, Vemurafenib, Regorafenib and its Metabolite Regorafenib M2 in Human Plasma by UPLC-MS/MS. *Biomed. Chromatogr.* 34, e4758. doi:10.1002/bmc.4758

Lin, L., Pan, H., Li, X., Zhao, C., Sun, J., Hu, X., et al. (2022). A Phase I Study of FCN-411, a Pan-HER Inhibitor, in EGFR-Mutated Advanced NSCLC after Progression on EGFR Tyrosine Kinase Inhibitors. *Lung Cancer* 166, 98–106. doi:10.1016/j.lungcan.2022.01.025

Maharati, A., Zanguei, A. S., Khalili-Tanha, G., and Moghbeli, M. (2022). MicroRNAs as the Critical Regulators of Tyrosine Kinase Inhibitors Resistance in Lung Tumor Cells. *Cell Commun. Signal* 20, 27. doi:10.1186/s12964-022-00840-4

Mohammadi, M., and Gelderblom, H. (2021). Systemic Therapy of Advanced/metastatic Gastrointestinal Stromal Tumors: an Update on Progress beyond Imatinib, Sunitinib, and Regorafenib. *Expert Opin. Investig. Drugs* 30, 143–152. doi:10.1080/13543784.2021.1857363

Ni, M. W., Zhou, J., Li, H., Chen, W., Mou, H. Z., and Zheng, Z. G. (2017). Simultaneous Determination of Six Tyrosine Kinase Inhibitors in Human Plasma Using HPLC-Q-Orbitrap Mass Spectrometry. *Bioanalysis* 9, 925–935. doi:10.4155/bio-2017-0031

Niu, Y., Gao, W., Li, H., Zhang, J., and Lian, Y. (2020). Rapid Determination of 17 Phthalate Esters in Capsanthin by QuEChERS Coupled with Gas Chromatography-Mass Spectrometry. *Anal. Sci.* 36, 485–490. doi:10.2116/analsci.19P421

Noorolyai, S., Mokhtarzadeh, A., Baghbani, E., Asadi, M., Baghbanzadeh Kojabad, A., Mogaddam, M. M., et al. (2019). The Role of microRNAs Involved in PI3-Kinase Signaling Pathway in Colorectal Cancer. *J. Cell Physiol.* 234, 5664–5673. doi:10.1002/jcp.27415

Ogawa-Morita, T., Sano, Y., Okano, T., Fujii, H., Tahara, M., Yamaguchi, M., et al. (2017). Validation of a Liquid Chromatography-Tandem Mass Spectrometric Assay for Quantitative Analysis of Lenvatinib in Human Plasma. *Int. J. Anal. Chem.* 2017, 2341876. doi:10.1155/2017/2341876

Pedersen, K. S., Grierson, P. M., Picus, J., Lockhart, A. C., Roth, B. J., Liu, J., et al. (2021). Vorolanib (X-82), an Oral anti-VEGFR/PDGFR/CSF1R Tyrosine Kinase Inhibitor, with Everolimus in Solid Tumors: Results of a Phase I Study. *Invest. New Drugs* 39, 1298–1305. doi:10.1007/s10637-021-01093-7

Perestrelo, R., Silva, P., Porto-Figueira, P., Pereira, J. A. M., Silva, C., Medina, S., et al. (2019). QuEChERS - Fundamentals, Relevant Improvements, Applications and Future Trends. *Anal. Chim. Acta* 1070, 1–28. doi:10.1016/j.aca.2019.02.036

Qin, S., Li, Q., Gu, S., Chen, X., Lin, L., Wang, Z., et al. (2021). Apatinib as Second-Line or Later Therapy in Patients with Advanced Hepatocellular Carcinoma (AHELP): a Multicentre, Double-Blind, Randomised, Placebo-Controlled, Phase 3 Trial. *Lancet Gastroenterol. Hepatol.* 6, 559–568. doi:10.1016/S2468-1253(21)00109-6

Qin, S., Li, Q., Gu, S., Chen, X., Lin, L., Wang, Z., et al. (2020). Apatinib as Second-Line Therapy in Chinese Patients with Advanced Hepatocellular Carcinoma: A Randomized, Placebo-Controlled, Double-Blind, Phase III Study. *J. Clin. Oncol.* 38, 4507.

Rehman, O., Jaferi, U., Padda, I., Khehra, N., Atwal, H., Mossabeh, D., et al. (2021). Overview of Lenvatinib as a Targeted Therapy for Advanced Hepatocellular Carcinoma. *Clin. Exp. Hepatol.* 7 (3), 249–257. doi:10.5114/ceh.2021.109312

Reis, R., Labat, L., Allard, M., Boudou-Rouquette, P., Chapron, J., Bellesoeur, A., et al. (2018). Liquid Chromatography-Tandem Mass Spectrometric Assay for Therapeutic Drug Monitoring of the EGFR Inhibitors Afatinib, Erlotinib and Osimertinib, the ALK Inhibitor Crizotinib and the VEGFR Inhibitor Nintedanib in Human Plasma from Non-small Cell Lung Cancer Patients. *J. Pharm. Biomed. Anal.* 158, 174–183. doi:10.1016/j.jpba.2018.05.052

Rimassa, L., Assenat, E., Peck-Radosavljevic, M., Pracht, M., Zagonel, V., Mathurin, P., et al. (2018). Tivantinib for Second-Line Treatment of MET-High, Advanced Hepatocellular Carcinoma (METIV-HCC): a Final Analysis of a Phase 3, Randomised, Placebo-Controlled Study. *Lancet Oncol.* 19, 682–693. doi:10.1016/S1470-2045(18)30146-3

Sueshige, Y., Shiraiwa, K., Honda, K., Tanaka, R., Saito, T., Tokoro, M., et al. (2021). A Broad Range High-Throughput Assay for Lenvatinib Using Ultra-high Performance Liquid Chromatography Coupled to Tandem Mass Spectrometry with Clinical Application in Patients with Hepatocellular Carcinoma. *Ther. Drug Monit.* 43, 664–671. doi:10.1097/FTD.0000000000000872

Ten Berge, D. M. H. J., Aarts, M. J., Groen, H. J. M., Aerts, J. G. J. V., and Kloover, J. S. (2022). A Population-Based Study Describing Characteristics, Survival and the Effect of TKI Treatment on Patients with EGFR Mutated Stage IV NSCLC in the Netherlands. *Eur. J. Cancer* 165, 195–204. doi:10.1016/j.ejca.2022.01.038

Tibben, M. M., Huijberts, S., Li, W., Schinkel, A. H., Gebretensae, A., Rosing, H., et al. (2019). Liquid Chromatography-Tandem Mass Spectrometric Assay for the Quantification of Galunisertib in Human Plasma and the Application in a Pre-clinical Study. *J. Pharm. Biomed. Anal.* 173, 169–175. doi:10.1016/j.jpba.2019.05.037

U.S. Department of Health and Human Services Food and Drug Administration (2018). Bioanalytical Method Validation Guidance for Industry. Available at: https://www.fda.gov/media/70858/download (Accessed Oct 17, 2019).

Verougstraete, N., Stove, V., Verstraete, A. G., and Stove, C. (2021). Quantification of Eight Hematological Tyrosine Kinase Inhibitors in Both Plasma and Whole Blood by a Validated LC-MS/MS Method. *Talanta* 226, 122140. doi:10.1016/j.talanta.2021.122140

Wick, A., Desjardins, A., Suarez, C., Forsyth, P., Gueorguieva, I., Burkholder, T., et al. (2020). A Phase 1b Study of Transforming Growth Factor-Beta Receptor I in- Hibitor Galunisertib in Combination with Sorafenib in Japanese Patients with Unresectable Hepatocellular Car- Cinoma. *Invest. New Drugs* 37, 118–126. doi:10.1007/s10637-018-0636-3

Wu, C., Li, M., Meng, H., Liu, Y., Niu, W., Zhou, Y., et al. (2019). Analysis of Status and Countermeasures of Cancer Incidence and Mortality in China. *Sci. China Life Sci.* 62, 640–647. doi:10.1007/s11427-018-9461-5

Xing, R., Gao, J., Cui, Q., and Wang, Q. (2021). Strategies to Improve the Antitumor Effect of Immunotherapy for Hepatocellular Carcinoma. *Front. Immunol.* 12, 783236. doi:10.3389/fimmu.2021.7832369

Yang, G., Liu, C., Hu, J., Sun, Y., Hu, P., Liu, L., et al. (2022). The Lifted Veil of Uncommon EGFR Mutation p.L747P in Non-small Cell Lung Cancer: Molecular Feature and Targeting Sensitivity to Tyrosine Kinase Inhibitors. *Front. Oncol.* 12, 843299. doi:10.3389/fonc.2022.843299

Yao, F., Zhan, Y., Li, C., Lu, Y., Chen, J., Deng, J., et al. (2021). Single-Cell RNA Sequencing Reveals the Role of Phosphorylation-Related Genes in Hepatocellular Carcinoma Stem Cells. *Front. Cell Dev. Biol.* 9, 734287. doi:10.3389/fcell.2021.734287

Ye, Z., Wu, L., Zhang, X., Hu, Y., and Zheng, L. (2021). Quantification of Sorafenib, Lenvatinib, and Apatinib in Human Plasma for Therapeutic Drug Monitoring by UPLC-MS/MS. *J. Pharm. Biomed. Anal.* 202, 114161. doi:10.1016/j.jpba.2021.114161

Yingling, J. M., McMillen, W. T., Yan, L., Huang, H., Sawyer, J. S., Graff, J., et al. (2018). Preclinical Assessment of Galunisertib (LY2157299 Monohydrate), a First-In-Class Transforming Growth Factor-β Receptor Type I Inhibitor. *Oncotarget* 9, 6659–6677. doi:10.18632/oncotarget.23795

Zhao, Y., Zhang, Y. N., Wang, K. T., and Chen, L. (2020). Lenvatinib for Hepatocellular Carcinoma: From Preclinical Mechanisms to Anti-cancer Therapy. *Biochim. Biophys. Acta Rev. Cancer* 1874, 188391. doi:10.1016/j.bbcan.2020.188391

Zheng, M., Zhang, C., Wang, L., Wang, K., Kang, W., Lian, K., et al. (2021). Determination of Nine Mental Drugs in Human Plasma Using Solid-phase Supported Liquid-Liquid Extraction and HPLC-MS/MS. *Microchem. J.* 160, 105647. doi:10.1016/j.microc.2020.105647

Zhou, L., Wang, S., Chen, M., Huang, S., Zhang, M., Bao, W., et al. (2021). Simultaneous and Rapid Determination of 12 Tyrosine Kinase Inhibitors by LC-MS/MS in Human Plasma: Application to Therapeutic Drug Monitoring in Patients with Non-small Cell Lung Cancer. *J. Chromatogr. B Anal. Technol. Biomed. Life Sci.* 1175, 122752. doi:10.1016/j.jchromb.2021.122752

Conflict of Interest: The authors declare that the research was conducted in the absence of any commercial or financial relationships that could be construed as a potential conflict of interest.

Publisher's Note: All claims expressed in this article are solely those of the authors and do not necessarily represent those of their affiliated organizations, or those of the publisher, the editors and the reviewers. Any product that may be evaluated in this article, or claim that may be made by its manufacturer, is not guaranteed or endorsed by the publisher.

frontiers | Frontiers in Pharmacology

ORIGINAL RESEARCH
published: 22 June 2022
doi: 10.3389/fphar.2022.918219

Genetic Polymorphisms in CYP2C19 Cause Changes in Plasma Levels and Adverse Reactions to Anlotinib in Chinese Patients With Lung Cancer

*Tingfei Tan[1], Gongwei Han[2], Ziwei Cheng[3], Jiemei Jiang[1], Li Zhang[4], Zitong Xia[2], Xinmeng Wang[1] and Quan Xia[1]**

[1]Department of Pharmacy, The First Affiliated Hospital of Anhui Medical University, Hefei, China, [2]School of Pharmacy, Anhui Medical University, Hefei, China, [3]School of Pharmacy, Anhui University of Chinese Medicine, Hefei, China, [4]Department of Pharmacy, The Second Affiliated Hospital of Bengbu Medical College, Bengbu, China

Background: Anlotinib is a small molecular multi-targeting tyrosine kinase inhibitor. Growing evidence indicates that treatment efficacy, and toxicity varies considerably between individuals. Therefore, this study aimed to investigate the relationship between cytochrome P450 (CYP450) gene polymorphisms, drug concentrations, and their adverse reactions in anlotinib-treated patients with lung cancer.

Methods: We enrolled 139 patients with lung cancer, treated with anlotinib. Twenty loci in the following five genes of the CYP450 family were genotyped: CYP450 family 3 subfamily A member 5 (CYP3A5), 3 subfamily A member 4 (CYP3A4), 2 subfamily C member 9 (CYP2C9), 2 subfamily C member 19 (CYP2C19), and 1 subfamily A member 2 (CYP1A2). Data on adverse reactions were collected from patients, and plasma anlotinib concentrations were measured.

Results: There were significant variances in plasma trough concentration (3.95–52.88 ng/ml) and peak plasma concentration (11.53–42.8 ng/ml) following administration of 8 mg anlotinib. Additionally, there were significant differences in the plasma trough concentration (5.65–81.89 ng/ml) and peak plasma concentration (18.01–107.18 ng/ml) following administration of 12 mg anlotinib. Furthermore, for CYP2C19-rs3814637, the peak plasma concentrations of mutant allele T carriers (TT+CT) were significantly higher than those of wildtypes (CC). For CYP2C19-rs11568732, the peak plasma concentrations of the mutant allele G carriers (GT+GG) were significantly higher than those of the wild-type (TT). More importantly, the incidence rates of hypertension and hemoptysis (peripheral lung cancer) with TT+CT in rs3814637 and GT+GG in rs11568732 were significantly higher than those with CC and TT.

Conclusions: The plasma trough and peak concentrations varied significantly for both 8 and 12 mg of anlotinib. Single-nucleotide polymorphisms in CYP2C19 are significantly associated with hypertension, hemoptysis, and anlotinib peak concentrations. Polymorphisms in CYP450 may explain inter-individual differences in anlotinib-related adverse reactions.

Keywords: anlotinib, lung cancer, CYP450 gene polymorphisms, plasma concentration, adverse reactions

OPEN ACCESS

Edited by:
Miao Yan,
Central South University, China

Reviewed by:
Wei-Wei Jia,
Chinese Academy of Sciences (CAS), China
Yiming Zhao,
Sun Yat-sen Memorial Hospital, China
Salih Ibrahem,
University of Kirkuk, Iraq

****Correspondence:***
Quan Xia
xiaquan2010@163.com

Specialty section:
This article was submitted to Pharmacology of Anti-Cancer Drugs, a section of the journal Frontiers in Pharmacology

Received: *12 April 2022*
Accepted: *31 May 2022*
Published: *22 June 2022*

Citation:
Tan T, Han G, Cheng Z, Jiang J, Zhang L, Xia Z, Wang X and Xia Q (2022) Genetic Polymorphisms in CYP2C19 Cause Changes in Plasma Levels and Adverse Reactions to Anlotinib in Chinese Patients With Lung Cancer. Front. Pharmacol. 13:918219. doi: 10.3389/fphar.2022.918219

INTRODUCTION

Lung cancer is one of the most common cancers, killing approximately 1.8 million people worldwide each year (Sung et al., 2021). It is also one of the most common causes of cancer-related deaths in China and worldwide (Cao et al., 2021). In addition to traditional drugs, new cytotoxic drugs, molecular-targeted therapies, and immune checkpoint inhibitors have provided new approaches for cancer treatment (Wu et al., 2021). Among them, molecular-targeted therapies have high specificity for tumor cells and low toxicity, and are considered promising cancer treatments (Herbst et al., 2018). Tyrosine kinase (TK) is an important component of the intracellular signal transduction system, transmitting conditional information from the extracellular domain or cytoplasm to the nucleus. TK is dysregulated in many tumor cells. Therefore, tyrosine kinase inhibitors (TKIs) have emerged as an effective approach for molecular-targeted therapies (Krause and Van Etten, 2005; Ferguson and Gray, 2018).

Anlotinib, a small molecular multi-targeted TKI, can inhibit tumor angiogenesis and proliferation (Syed, 2018). *In vitro* studies have shown that anlotinib inhibits tumor cell growth by inhibiting platelet-derived growth factor receptor β (PDGFRβ), vascular endothelial growth factor receptor 2/3 (VEGFR2/3), and stem cell factor receptor (c-Kit) (Chi et al., 2018; Lin et al., 2018; Liu et al., 2018). *In vivo*, anlotinib displayed broad activity in human tumor xenograft models (Sun et al., 2016). Anlotinib has shown promise in several cancer clinical trials. Consequently, anlotinib has been approved in China as a third-line treatment for patients with advanced non-small cell lung cancer (NSCLC), and small cell lung cancer. Despite the numerous benefits of anlotinib treatment, there is an increasing number of cases of treatment failure due to drug resistance and toxicity. Hypertension, elevated thyroid-stimulating hormone (TSH) levels, hand-foot syndrome (HFS), hepatotoxicity, and hemoptysis are the most prevalent adverse reactions to anlotinib (Han et al., 2018a; Han et al., 2018b). With the widespread use of anlotinib in clinical practice, adverse reactions have become increasingly concerning.

Currently, research on advanced lung cancer focuses on identifying the biological predictors of efficacy and adverse events, which lead to the individualization of treatment. Systemic exposure or intracellular drug concentrations can influence drug efficacy and adverse reactions, resulting in interpatient variation (Decosterd et al., 2015). Furthermore, the level of drug exposure is significantly associated with the pharmacokinetic properties (absorption, distribution, and metabolism) of the drug. Therefore, inter-individual variations in pharmacokinetics may influence the efficacy and adverse reactions of anlotinib.

Growing evidence suggests that genetic polymorphisms in cytochrome P450 (CYP450) may significantly influence inter-individual differences in drug responses and disposition (Evans and McLeod, 2003). The activities of these drug-metabolizing enzymes determine how quickly the drug is metabolized and can therefore influence the occurrence of adverse reactions. CYP450 oxidizes approximately half of the widely prescribed medications as well as most oral small-molecule anticancer medicines, such as TKIs (Parra-Guillen et al., 2017). It has been shown that the adverse reactions of TKI correlate with drug concentrations and metabolic enzyme gene polymorphisms (Liao et al., 2020), such as CYP3A5*3 for sorafenib-related severe hepatic and renal damage (Guo et al., 2018), and CYP3A4-rs4646437 and CYP3A5-rs776746 for sunitinib-related hypertension (Garcia-Donas et al., 2011; Diekstra et al., 2015; Diekstra et al., 2017). Studies have shown that P450-mediated oxidation is a key factor that affects the oral bioavailability, exposure, half-life, and interspecific differences in anlotinib. A variety of CYP450 enzymes are involved in anlotinib metabolism *in vitro*, with CYP3A4 and CYP3A5 being the most readily metabolized enzymes (Zhong et al., 2018). Wei *et al.* investigated the effects of anlotinib on CYP1A2, CYP2C6, CYP2D1, CYP2D2, and CYP3A1/2 in animals and discovered that anlotinib strongly induces CYP2D1 and CYP3A1/2 (Sun et al., 2017). Although *in vitro* and *in vivo* experiments have confirmed the effect of CYP450 enzymes on anlotinib metabolism, the relationship between CYP450 gene polymorphisms, plasma concentrations and clinical adverse reactions of anlotinib in patients with lung cancer remains unclear.

Accordingly, for the first time, we propose that individual differences in plasma drug concentrations, and adverse reactions in patients with lung cancer treated with anlotinib may be correlated with CYP450 polymorphisms. To validate this hypothesis, we examined the plasma concentrations of anlotinib in subjects, analyzing single-nucleotide polymorphisms (SNPs) at high-frequency mutation sites in CYP450. In addition, we examined the correlations between polymorphisms of these genes, plasma concentrations, and adverse reactions.

MATERIALS AND METHODS

Patient Eligibility

This single-center retrospective study was conducted in accordance with the Helsinki Declaration of the First Affiliated Hospital of Anhui Medical University, Hefei, China, between January 2020, and August 2021. The study protocol was reviewed and approved by the institutional ethics committee (No. Quick-PJ2019-14-15). Written informed consent was obtained from all patients. The inclusion criteria were as follows: *1*) patients aged 18–80 years *2*) gender was not limited; *3*) patients taking more than two courses of anlotinib, with trackable complete information about adverse reactions during treatment; and *4*) patients with clear pathological and imaging diagnoses of lung cancer, including non-small cell lung cancer and small cell lung cancer. The exclusion criteria were as follows: *1*) moderate-to-severe hepatic and renal insufficiency, *2*) allergy to anlotinib, *3*) missing basic or adverse reaction information, *4*) pregnant or lactating women, and *5*) poor compliance.

Plasma Anlotinib Concentration Determination

Patients received a 2-week on/1-week off (2/1) schedule and a 12 or 8 mg once-daily dose for our study. As second-line treatment,

anlotinib was combined with immune checkpoint inhibitors (carryilizumab and pabrolizumab). In addition, anlotinib alone was used as third-line treatment. None of the enrolled patients was taking drugs that affected the plasma levels of anlotinib (e.g., rifampicin, ketoconazole, and itraconazole). Peak concentration blood samples were collected at 8 a.m. on the day after the end of the course of treatment (day 15). Blood samples were collected 30 min before the start of the new course (day 22). The collected blood samples were centrifuged at 3,000 rpm for 5 min. The supernatant in the centrifuge tubes was collected and stored at −80°C until analysis, while the remaining samples were used for gene polymorphism analysis. An ACQUITY ultra-performance liquid chromatograph (UPLC, Waters, United States) combined with a Xevo TQ-S triple quadrupole mass spectrometer (Waters, United States) was used to determine the plasma concentrations of anlotinib. Gradient separation was performed on a PACQUITY UPLC BEH C18 column (1.7 μm 2.1 × 50 mm) (Waters, United States) at a temperature of 40°C and a flow rate of 0.5 ml/min. Data processing was performed using MassLynxV4.1 a data workstation (Waters, United States). A standard curve was established according to an internal reference to calculate the plasma concentrations of anlotinib. The results of methodological validation are presented in **Supplementary Material S3**.

Genotype Identification

DNA was extracted from the blood samples of patients using a blood genomic DNA extraction kit (Tiangen Biotechnology, Beijing, China) and stored at −80°C until analysis. The quality of the extracted DNA was strictly controlled using Nanodrop 2000 (Thermo Scientific, United States) and capillary electrophoresis (Qiagen, Switzerland). In this study, 20 loci in five different CYP450 genes were selected for polymorphism detection, including rs2242480, rs35599367, rs4646437, rs3735451, and rs4646460 in CYP3A4; rs1419745, rs4646450, rs15524, and rs3800959 in CYP3A5; rs11568732, rs12248560, rs12769205, rs3814637, rs4244285, and rs4986893 in CYP2C19; rs2069526, rs2470890, rs4646425, and rs4646427 in CYP1A2; and rs9332113 in CYP2C9. Primers for all gene loci in patients were designed using Sequenom (Assay Design Suite V2.0) online software. MassARRAY Analyzer Compac mass spectrometry was used to detect gene locus information. TYPER software was used to analyze the results and obtain the genotyping data.

Data Collection

All patients were followed-up in special clinics or wards between January 2020, and August 2021 to monitor anlotinib-induced adverse reactions. Adverse reactions were graded using the Common Terminology Criteria for Adverse Events version 5.0 (CTCAE 5.0). The results were recorded during an adverse reaction assessment.

Statistical Analysis

All statistical analyses were performed using Statistical Products and Services Solutions, version 26 (SPSS 26.0). Descriptive statistics were used to summarize the demographic data and baseline characteristics of the patients receiving anlotinib. The mean and standard deviation were calculated for normally distributed data. Comparisons between groups for continuous variables were performed using an independent-sample *t*-test or one-way ANOVA. If the variance was not uniform, the Mann-Whitney *U* test was used. Chi-square and Fisher's exact tests were used to compare differences in the Hardy-Weinberg balance test and adverse reactions among different genotypes. For all statistical analyses, a p-value < 0.05 was considered statistically significant.

TABLE 1 | Patient characteristics.

Characteristics	No. of patients (%)
Mean age (years)	62.97 ± 10.9
Gender	
Male	87 (62.6%)
Female	52 (37.4%)
Cancer-related family history	
Yes	4 (2.9%)
No	135 (97.1%)
Smoking status	
Non-smoker	115 (82.7%)
Ever smoker	24 (17.3%)
Dosage	
8 mg	73 (52.5%)
12 mg	66 (47.5%)
ECOG score	
0	38 (27.3%)
1	85 (61.2%)
≥2	16 (11.5%)
Histology	
Adenocarcinoma	77 (55.4%)
Squamous cell carcinoma	27 (19.4%)
Small cell	21 (15.1%)
Others	14 (10.1%)
Clinical stage *n* (%)	
IIIB	19 (13.7%)
IV	120 (86.3%)
Treatment line	
<3rd line	47 (33.8%)
≥3rd line	92 (66.2%)
EGFR mutation	
Yes	17 (12.2%)
No	87 (62.6%)
Unknown	35 (25.2%)
Prior targeted therapy	
Yes	41 (29.5%)
No	98 (70.5%)
Prior thoracic radiotherapy	
Yes	39 (28.1%)
No	100 (71.9%)
Prior anti-angiogenesis treatment	
Yes	44 (31.7%)
No	95 (68.3%)
Surgical history	
Yes	101 (72.7%)
No	38 (27.3%)

RESULTS

Patient Characteristics

In the current study, 139 patients were enrolled in the follow-up trials. The mean age of the study population was 62.97 ±

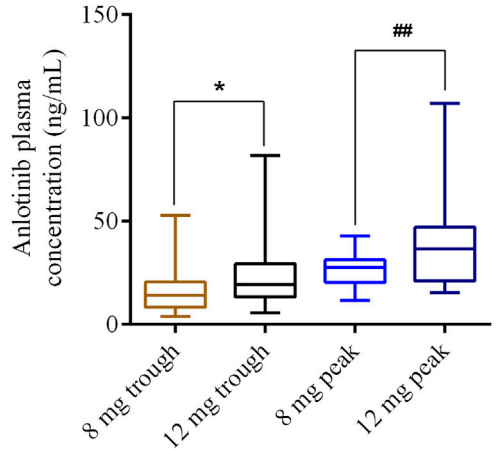

FIGURE 1 | Distribution of anlotinib trough or peak concentrations for 8 and 12 mg dosages, respectively. *$p < 0.05$; ##$p < 0.01$.

10.9 years. Of the patients, 87 (62.6%) were male and 52 (37.4%) were female. Only four patients (2.9%) had a family history of tumors. Twenty-four (17.3%) patients had a history of smoking. The detailed demographic and clinical characteristics of the patients are shown in **Table 1**.

Plasma Anlotinib Concentration

A total of 73 of 139 patients with lung cancer received 8 mg anlotinib per day, and 66 patients received 12 mg anlotinib per day. The plasma concentrations of anlotinib are shown in **Figure 1**. The trough and peak concentrations of anlotinib (8 mg) were 17.59 ± 12.55 and 27.01 ± 7.97 ng/ml, ranging from 3.95 to 52.88 ng/ml and 11.53–42.8 ng/ml, respectively. In contrast, the trough and peak concentrations after 12 mg of anlotinib dosing were 23.51 ± 14.83 and 41.22 ± 27.15 ng/ml, ranging from 5.65 to 81.89 ng/ml and 18.01–107.18 ng/ml, respectively. There were significant differences between the trough and peak concentrations at a dosage of 8 versus 12 mg of anlotinib per day ($p < 0.05$).

Genotype Frequencies

The genotype status of 20 CYP450 loci was determined in 139 patients. For the CYP3A5-rs15524 polymorphism, the frequencies of the A and G alleles were 69.42 and 30.58%, respectively. The frequencies of the G and A alleles for rs4646450 were 71.22 and 28.78%, respectively. The frequencies of the C and T alleles for rs1419745 were 28.42 and 71.58%, and the frequencies of the A and G alleles for rs3800959 were 82.37 and 17.63%, respectively. For the CYP3A4-rs2242480 polymorphism, the frequencies of the T and C alleles were 25.54 and 74.46%, respectively. The frequencies of the C and T alleles of rs43735451 were 31.29 and 68.71%, respectively. The frequencies of the A and G alleles for rs4646437 were 11.87 and 88.13%, respectively, and those of the A and G alleles for rs4646440 were 24.10 and 75.90%, respectively. For the CYP2C9-rs9332113 polymorphism, the frequencies of the G and C alleles were 65.83 and 34.17%, respectively. For the CYP2C19-rs12769205 polymorphism, the frequencies of the G and A alleles were 33.81 and 66.19%, respectively. The frequencies of the T and C alleles of rs12248560 were 1.44 and 98.56%, respectively. The frequencies of the T and C alleles of rs3814637 were 8.27 and 91.73%, respectively. The frequencies of the A and G alleles of rs4986893 were 5.76 and 94.24%, respectively. The frequencies of the G and T alleles for rs11568732 were 8.27 and 91.73%, and those of the A and G alleles for rs4244285 were 33.45 and 66.55%, respectively. For the CYP1A2-rs4646427 polymorphism, the frequencies of the C and T alleles were 6.47 and 93.53% respectively. The frequencies of the G and T alleles were 6.47 and 93.53% for rs2069526, respectively. The frequencies of the T and C alleles were 13.67 and 86.33% for rs2470890 and 93.53 and 6.47% for rs4646425, respectively. All alleles followed–y the Weinberg equilibrium, except for CYP340-rs35599367. Genotype and allele frequencies of the study population are shown in **Table 2**.

Influence of Different Genotypes on Anlotinib Peak Plasma Concentration

Correlation analysis between different genotypes and the peak plasma concentrations of anlotinib showed that CYP2C19-rs3814637 and -rs11568732 were significantly associated with peak plasma concentrations. For CYP2C19-rs3814637, the peak plasma concentrations of the mutant allele T carriers (TT+CT) were significantly higher than those of the wildtypes (CC) ($p = 0.035$). For CYP2C19-rs11568732, the peak plasma concentrations of mutant allele G carriers (GT+GG) were significantly higher than those of the wild-type (TT) ($p = 0.035$), as shown in **Table 3**. The differences between the plasma concentrations of the other genotypes and that of anlotinib were not statistically significant.

Effect of Genetic Polymorphisms on Adverse Reactions of Anlotinib

After analyzing the correlation between different genotypes and adverse reactions of anlotinib, for all 20 of the SNPs, only the mutations of CYP2C19-rs3814637 and -rs11568732 genotypes were significantly associated with the occurrence of hypertension and hemoptysis (peripheral lung cancer) in the study population.

The incidence rate of hypertension in mutant allele T carriers (CT + TT) of rs3814637 was significantly higher than that in the wildtype (CC) ($p = 0.034$, odds ratio (OR) = 0.316, 95% confidence interval (CI): 0.12–0.835). The incidence rate of hypertension in mutated allele G carriers (GT + GG) of rs11568732 was significantly higher than that in the wild type (TT) ($p = 0.034$, OR = 0.316, 95% CI: 0.12–0.835).

The incidence rate of hemoptysis (peripheral lung cancer) in mutated allele G carriers (GT + GG) of rs11568732 was significantly higher than that in the wild type (TT) ($p = 0.043$, OR = 0.13, 95% CI: 0.02–0.845). The incidence rate of hemoptysis (peripheral lung cancer) in mutant allele T carriers (CT + TT) of rs3814637 was significantly higher than that in the wild type (CC) ($p = 0.043$, OR = 0.13, 95% CI: 0.02–0.845). There was no

TABLE 2 | Observed genotype and allele frequency of SNPs in the present study.

Gene	SNP-ID	Genotype	*n*	Identified Frequency %	Allele	Allele frequency %
CYP3A5	rs15524	AG	68	48.92	A	69.42
		AA	63	45.32	G	30.58
		GG	8	5.76	—	—
CYP3A5	rs4646450	GG	67	48.20	G	71.22
		AA	8	5.76	A	28.78
		AG	64	46.04	—	—
CYP3A5	rs1419745	CT	65	46.76	C	28.42
		TT	67	48.20	T	71.58
		CC	7	5.04	—	—
CYP3A5	rs3800959	AA	93	66.91	A	82.37
		AG	43	30.94	G	17.63
		GG	3	2.16	—	—
CYP3A4	rs35599367	GG	139	100.00	G	100.00
CYP3A4	rs2242480	TT	7	5.04	T	25.54
		CC	75	53.96	C	74.46
		CT	57	41.01	—	—
CYP3A4	rs3735451	CC	9	6.47	C	31.29
		TT	62	44.60	T	68.71
		CT	68	48.92	—	—
CYP3A4	rs4646437	GG	107	76.98	A	11.87
		AG	31	22.30	G	88.13
		AA	1	0.72	—	—
CYP3A4	rs4646440	AA	7	5.04	A	24.10
		AG	53	38.13	G	75.90
		GG	79	56.83	—	—
CYP2C9	rs9332113	CG	69	49.64	G	65.83
		GG	57	41.01	C	34.17
		CC	13	9.35	—	—
CYP2C19	rs12769205	GG	12	8.63	G	33.81
		AG	70	50.36	A	66.19
		AA	57	41.01	—	—
CYP2C19	rs12248560	CT	3	2.16	T	1.44
		CC	136	97.84	C	98.56
CYP2C19	rs3814637	CC	117	84.17	T	8.27
		TT	1	0.72	C	91.73
		CT	21	15.11	—	—
CYP2C19	rs4986893	GG	123	88.49	A	5.76
		AG	16	11.51	G	94.24
CYP2C19	rs11568732	GG	1	0.72	G	8.27
		GT	21	15.11	T	91.73
		TT	117	84.17	—	—
CYP2C19	rs4244285	GG	57	41.01	A	33.45
		AA	12	8.63	G	66.55
		AG	70	50.36	—	—
CYP1A2	rs4646427	CT	18	12.95	C	6.47
		TT	121	87.05	T	93.53
CYP1A2	rs2069526	GT	18	12.95	G	6.47
		TT	121	87.05	T	93.53
CYP1A2	rs2470890	CC	103	74.10	T	13.67
		TT	2	1.44	C	86.33
		CT	34	24.46	—	—
CYP1A2	rs4646425	CC	121	87.05	C	93.53
		CT	18	12.95	T	6.47

SNPs, single nucleotide polymorphisms; n*, the numbers of patients.*

significant difference between rs11568732 and rs3814637 genotypes in the incidence of hemoptysis between central lung cancer ($p > 0.05$). **Table 4** presents the results.

There were no significant differences in the incidence of proteinuria, hepatotoxicity, or other adverse reactions among the 20 SNP genotypes ($p > 0.05$).

DISCUSSION

Anlotinib is a multitarget drug that has been developed and marketed independently in China. A phase I clinical trial confirmed that anlotinib showed controlled toxicity at a dose of 12 mg once daily in a 2-week on/1-week off schedule (2/1) (Sun

TABLE 3 | Correlation between different genotypes and anlotinib plasma peak concentration.

Gene	SNP_ID	Genotype	*n*	Mean ± SD (ng/ml)	*p* value
CYP2C19	rs3814637	CC	35	30.29 ± 16.42	—
		CT+TT	5	49.52 ± 30.32	0.035[a]
	rs11568732	TT	35	30.29 ± 16.42	—
		GT+GG	5	49.52 ± 30.32	0.035[a]

[a]*Significant at* p < *0.05.*

et al., 2016). However, adverse reactions to anlotinib in clinical practice often leads to dose reductions, or treatment discontinuation. In the present study, the most common adverse reactions associated with anlotinib were hypertension, hemoptysis, elevated TSH levels, hepatotoxicity, hypertriglyceridemia, proteinuria, dyspepsia, and HFS. Notably, hypertension was the most common adverse reaction during anlotinib treatment, which is consistent with the results of a phase II trial (Han et al., 2018b). In this study, plasma anlotinib concentrations showed large individual variations. In addition, 11 patients developed a grade 3 or higher incidence of hypertension during treatment, resulting in dose reductions in five patients and drug changes in six patients. This dramatic change can be explained not only by drug interactions and acquired factors but also by genetic factors, such as CYP450 gene polymorphisms. As CYP450 is regulated by genes, once the gene is mutated, CYP450 is regulated and synthesized, and drug metabolism *via* the enzyme is subsequently altered. Therefore, polymorphisms in CYP450 are the basis of race and individual differences in drug metabolism. In this study, we used a candidate gene approach to investigate the correlation between polymorphisms in genes encoding drug-metabolizing enzymes and anlotinib toxicity.

In humans, CYP3A4/5 has the largest impact on drug biotransformation, followed by CYP2D6, CYP2C6, CYP1A2, and other enzymes (Zanger and Schwab, 2013). Similarly, TKIs are metabolized by CYP450 enzymes, which affects drug concentrations. Imatinib is a cytochrome of CYP3A4 and CYP2C8 substrates that markedly increases plasma CYP3A4 substrate concentrations and reduces hepatic CYP3A4 activity in humans (Filppula et al., 2012). According to previous *in vitro* investigations, erlotinib is largely metabolized by CYP3A4, whereas CYP1A2 makes a minor contribution (Endo-Tsukude et al., 2018). The major metabolic enzymes of anlotinib are similar to those of imatinib and erlotinib. CYP3A4 and CYP3A5 play important roles in the metabolism of anlotinib.

It is known to all that the genetic mutations of metabolic enzymes do not necessarily lead to corresponding changes in blood exposure to substrate drugs. Currently, there is no evidence of the influence of CYP3A4/5 gene mutations on blood exposure to anlotinib. Anlotinib metabolism is regulated by multiple enzymes. In addition, as mentioned in the previous paragraph, even if CYP3A4/5 gene mutation alters its enzyme activity, this single degree of enzyme activity change does not necessarily affect the pharmacokinetic characteristics of anlotinib (Zhong et al., 2018). This process involves many complex mechanisms. For example, as the largest part (82%) of the intestinal CYP450 family, intestinal CYP3A is inhibited by anlotinib during intestinal absorption (the first site of drug exposure in the body's metabolic system) and probably results in increased systemic exposure to anlotinib (Kaminsky and Zhang, 2003; Paine et al., 2006). There are many other factors.

This study provides evidence that anlotinib blood exposure is clinically associated not with CYP3A4 and CYP3A5 mutations but with CYP2C19 mutations. This is an interesting phenomenon, and further mechanistic evidence is required.

Previous *in vivo* studies have demonstrated that efficacy and adverse reactions are closely linked to genetic factors. However, few drug-metabolizing enzyme gene polymorphisms have been used as predictive factors of TKI toxicity (Scott, 2011; Patel, 2016). In this study, we found that the CYP2C19-rs3814637 and -rs11568732 genotypes were significantly associated with the occurrence of hypertension and hemoptysis. Studies have shown that CYP2C19 genotype can guide antiplatelet therapy (Martin et al., 2020). In addition, polymorphisms in the CYP2C19 gene have been reported to be positively associated with cardiovascular diseases, such as coronary artery disease and atherosclerosis (Ercan et al., 2008; Yang et al., 2010). Further studies showed that CYP2C19-rs11568732 was significantly associated with bleeding in patients with ST-segment elevation myocardial infarction who underwent primary percutaneous coronary intervention and treatment with clopidogrel (Novkovic et al., 2018). This finding is consistent with the results of our study, which showed that CYP2C19-rs11568732 was significantly associated with the occurrence of hemoptysis. Additionally, studies have shown that the CYP2C19*3 defective allele may contribute to a reduced risk of developing essential hypertension (Shin et al., 2012). However, few studies have investigated the correlation between CYP2C19-rs3814637 and -rs11568732 polymorphisms and hypertension. In this study, no association was observed between the different genotypes of other CYP450 loci and adverse reactions to anlotinib.

The epidermal growth factor receptor (EGFR) is a ligand receptor for epidermal growth factor (EGF). When EGF binds to EGFR, the signaling pathway is activated, leading to cell proliferation and differentiation. EGFR overexpression due to mutations or structural changes promotes carcinogenesis, invasion, and metastasis. Studies have shown that common mutations are associated with sensitivity to EGFR tyrosine kinase inhibitors (TKI) (Lynch et al., 2004; Paez et al., 2004). Anlotinib is a small-molecule, multi-target TKI. Currently, there is no evidence for an association between anlotinib and EGFR mutations. In this study, 17 patients were found to have EGFR mutations; however, no correlation was found between EGFR mutations and anlotinib-induced adverse reactions.

Based on this study, it is reasonable to speculate that inter-individual differences in anlotinib-related adverse reactions may be explained by CYP450 gene polymorphisms or different exposures, caused by CYP450 gene polymorphisms. Thus, the clinical application of anlotinib should be based on the genotyping of CYP450 in lung cancer, particularly for rs3814637 and rs11568732 of CYP2C19. This strategy may reduce the incidence of anlotinib-related adverse reactions. However, the underlying mechanisms by which CYP450 gene polymorphisms influence the variation in anlotinib-related

TABLE 4 | Correlation between genetic polymorphisms and adverse reactions.

Adverse reactions	Gene	SNP-ID	Genotype	Abnormal group (*n*)	Normal group (*n*)	*p* value	OR	95%CI
Hypertension	CYP2C19	rs3814637	CC	21 (0.179)	96 (0.821)	—	—	—
			TT+CT	9 (0.409)	13 (0.591)	0.034[a]	0.316	0.12–0.84
		rs11568732	TT	9 (0.409)	13 (0.591)	—	—	—
			GT+GG	21 (0.179)	96 (0.821)	0.034[a]	0.316	0.12–0.84
	CYP3A4	rs2242480	CC	17 (0.227)	58 (0.773)	—	—	—
			CT+TT	13 (0.203)	51 (0.797)	0.737	0.87	0.39–1.96
		rs3735451	TT	13 (0.206)	49 (0.794)	—	—	—
			CC+CT	17 (0.224)	60 (0.776)	0.874	0.936	0.42–2.12
		rs4646437	GG	22 (0.206)	85 (0.794)	—	—	—
			AG+AA	8 (0.250)	24 (0.750)	0.592	0.776	0.31–1.96
		rs4646440	GG	18 (0.228)	61 (0.772)	—	—	—
			AA+AG	12 (0.200)	48 (0.800)	0.693	0.847	0.37–1.93
	CYP3A5	rs1419745	TT	14 (0.209)	53 (0.791)	—	—	—
			CC+CT	16 (0.222)	56 (0.778)	0.849	0.925	0.41–2.08
		rs15524	AA	13 (0.206)	50 (0.794)	—	—	—
			GG+AG	17 (0.224)	59 (0.776)	0.805	1.108	0.49–2.50
		rs3800959	AA	22 (0.237)	71 (0.763)	—	—	—
			AG+GG	8 (0.174)	38 (0.826)	0.398	0.679	0.28–1.67
		rs4646450	GG	14 (0.209)	53 (0.791)	—	—	—
			AG+AA	16 (0.222)	56 (0.778)	0.849	1.082	0.48–2.43
Hemoptysis (Peripheral lung cancer)	CYP2C19	rs11568732	TT	2 (0.025)	77 (0.975)	—	—	—
			GT+GG	3 (0.167)	15 (0.833)	0.043[a]	0.13	0.02–0.85
		rs3814637	CC	2 (0.025)	77 (0.975)	—	—	—
			CT+TT	3 (0.167)	15 (0.833)	0.043[a]	0.13	0.02–0.85
	CYP3A4	rs2242480	CC	2 (0.041)	47 (0.959)	—	—	—
			CT+TT	3 (0.063)	45 (0.938)	0.981	0.638	0.10–4.00
		rs3735451	TT	2 (0.050)	38 (0.950)	—	—	—
			CC+CT	3 (0.053)	54 (0.947)	1.000	0.947	0.15–5.95
		rs4646437	GG	4 (0.056)	68 (0.944)	—	—	—
			AG+AA	1 (0.040)	24 (0.960)	1.000	1.412	0.15–13.26
		rs4646440	GG	2 (0.038)	50 (0.962)	—	—	—
			AA+AG	3 (0.067)	42 (0.933)	0.868	0.560	0.09–3.51
	CYP3A5	rs1419745	TT	2 (0.048)	40 (0.952)	—	—	—
			CC+CT	3 (0.055)	52 (0.945)	1.000	0.867	0.14–5.44
		rs15524	AA	2 (0.049)	39 (0.951)	—	—	—
			GG+AG	3 (0.054)	53 (0.946)	1.000	0.906	0.14–5.68
		rs3800959	AA	5 (0.070)	66 (0.930)	—	—	—
			AG+GG	0 (0.000)	26 (1.000)	0.384	0.93	0.87–0.99
		rs4646450	GG	2 (0.048)	40 (0.952)	—	—	—
			AG+AA	3 (0.055)	52 (0.945)	1.000	0.867	0.14–5.44
Hemoptysis (central lung cancer)	CYP2C19	rs11568732	TT	6 (0.158)	32 (0.842)	—	—	—
			GT+GG	1 (0.250)	3 (0.750)	0.532	0.563	0.05–6.36
		rs3814637	CC	6 (0.158)	32 (0.842)	—	—	—
			CT+TT	1 (0.250)	3 (0.750)	0.532	0.563	0.05–6.36
	CYP3A4	rs2242480	CC	3 (0.115)	23 (0.885)	—	—	—
			CT+TT	4 (0.250)	12 (0.750)	0.447	0.391	0.08–2.04
		rs3735451	TT	3 (0.136)	19 (0.864)	—	—	—
			CC+CT	4 (0.200)	16 (0.800)	0.89	0.632	0.12–3.25
		rs4646437	GG	6 (0.171)	29 (0.829)	—	—	—
			AG+AA	1 (0.143)	6 (0.857)	1.000	1.241	0.13–12.29
		rs4646440	GG	3 (0.111)	24 (0.889)	—	—	—
			AA+AG	4 (0.267)	11 (0.733)	0.388	0.344	0.07–1.81
	CYP3A5	rs1419745	TT	3 (0.120)	22 (0.880)	—	—	—
			CC+CT	4 (0.235)	13 (0.765)	0.574	0.443	0.09–2.30
		rs15524	AA	3 (0.136)	19 (0.864)	—	—	—
			GG+AG	4 (0.200)	16 (0.800)	0.890	0.632	0.12–3.25
		rs3800959	AA	4 (0.182)	18 (0.818)	—	—	—
			AG+GG	3 (0.150)	17 (0.850)	1.000	1.259	0.25–6.47
		rs4646450	GG	3 (0.120)	22 (0.880)	—	—	—
			AG+AA	4 (0.235)	13 (0.765)	0.574	0.443	0.09–2.30

[a]*Significant at* $p < 0.05$. *OR, odd ratio; 95%CI, 95%confidence interval.*

adverse reactions and toxicity between individuals remain unclear, and could be a direction for further research.

Nevertheless, our study has a few limitations. First, it was a single-center prospective study with limited patient enrolment. Second, owing to the short follow-up time of the patients, there was no statistical information about progression-free survival and overall survival. Third, the anlotinib concentration may be influenced by other factors (e.g., coffee and drugs), which was not studied separately.

CONCLUSION

In summary, some CYP450 genotypes are significantly associated with adverse reactions to anlotinib in clinical practice, including hypertension and hemoptysis. Our results show that these genetic variants in CYP450 can explain inter-individual differences in anlotinib adverse reactions. Therefore, identifying CYP450 gene polymorphisms, particularly CYP2C19-rs3814637 and -rs11568732, before anlotinib treatment might be a potential personalized treatment approach.

DATA AVAILABILITY STATEMENT

The original contributions presented in the study are included in the article/**Supplementary Materials**, further inquiries can be directed to the corresponding author.

ETHICS STATEMENT

The studies involving human participants were reviewed and approved by The Ethics Committee of the First Affiliated Hospital of Anhui Medical University approved this study. The patients/participants provided their written informed consent to participate in this study.

AUTHOR CONTRIBUTIONS

QX conceptualized and supervised the project; TT and GH carried out the study and interpreted the results; ZC and JJ drafted the initial version of the manuscript; LZ and ZX searched the literature and collected data; QX and XW modified the revised manuscript; All authors read and approved the manuscript.

FUNDING

This study was supported by the Clinical Research Fund of Wu Jieping Medical Foundation (320.6750.2020-03-6) and the Program of National Natural Science Foundation of China (82174011).

ACKNOWLEDGMENTS

We would like to take the opportunity to thank the patients, their families, and all of the research members in this study.

SUPPLEMENTARY MATERIAL

The Supplementary Material for this article can be found online at: https://www.frontiersin.org/articles/10.3389/fphar.2022.918219/full#supplementary-material

REFERENCES

Cao, W., Chen, H. D., Yu, Y. W., Li, N., and Chen, W. Q. (2021). Changing Profiles of Cancer Burden Worldwide and in China: a Secondary Analysis of the Global Cancer Statistics 2020. *Chin. Med. J. Engl.* 134 (7), 783–791. doi:10.1097/CM9.0000000000001474

Chi, Y., Fang, Z., Hong, X., Yao, Y., Sun, P., Wang, G., et al. (2018). Safety and Efficacy of Anlotinib, a Multikinase Angiogenesis Inhibitor, in Patients with Refractory Metastatic Soft-Tissue Sarcoma. *Clin. Cancer Res.* 24 (21), 5233–5238. doi:10.1158/1078-0432.CCR-17-3766

Decosterd, L. A., Widmer, N., Zaman, K., Cardoso, E., Buclin, T., and Csajka, C. (2015). Therapeutic Drug Monitoring of Targeted Anticancer Therapy. *Biomark. Med.* 9 (9), 887–893. doi:10.2217/bmm.15.78

Diekstra, M. H., Belaustegui, A., Swen, J. J., Boven, E., Castellano, D., Gelderblom, H., et al. (2017). Sunitinib-induced Hypertension in CYP3A4 Rs4646437 A-Allele Carriers with Metastatic Renal Cell Carcinoma. *Pharmacogenomics J.* 17 (1), 42–46. doi:10.1038/tpj.2015.100

Diekstra, M. H., Swen, J. J., Boven, E., Castellano, D., Gelderblom, H., Mathijssen, R. H., et al. (2015). CYP3A5 and ABCB1 Polymorphisms as Predictors for Sunitinib Outcome in Metastatic Renal Cell Carcinoma. *Eur. Urol.* 68 (4), 621–629. doi:10.1016/j.eururo.2015.04.018

Endo-Tsukude, C., Sasaki, J. I., Saeki, S., Iwamoto, N., Inaba, M., Ushijima, S., et al. (2018). Population Pharmacokinetics and Adverse Events of Erlotinib in Japanese Patients with Non-small-cell Lung Cancer: Impact of Genetic Polymorphisms in Metabolizing Enzymes and Transporters. *Biol. Pharm. Bull.* 41 (1), 47–56. doi:10.1248/bpb.b17-00521

Ercan, B., Ayaz, L., Çiçek, D., and Tamer, L. (2008). Role of CYP2C9 and CYP2C19 Polymorphisms in Patients with Atherosclerosis. *Cell Biochem. Funct.* 26 (3), 309–313. doi:10.1002/cbf.1437

Evans, W. E., and McLeod, H. L. (2003). Pharmacogenomics--drug Disposition, Drug Targets, and Side Effects. *N. Engl. J. Med.* 348 (6), 538–549. doi:10.1056/NEJMra020526

Ferguson, F. M., and Gray, N. S. (2018). Kinase Inhibitors: the Road Ahead. *Nat. Rev. Drug Discov.* 17 (5), 353–377. doi:10.1038/nrd.2018.21

Filppula, A. M., Laitila, J., Neuvonen, P. J., and Backman, J. T. (2012). Potent Mechanism-Based Inhibition of CYP3A4 by Imatinib Explains its Liability to Interact with CYP3A4 Substrates. *Br. J. Pharmacol.* 165 (8), 2787–2798. doi:10.1111/j.1476-5381.2011.01732.x

Garcia-Donas, J., Esteban, E., Leandro-García, L. J., Castellano, D. E., González del Alba, A., Climent, M. A., et al. (2011). Single Nucleotide Polymorphism Associations with Response and Toxic Effects in Patients with Advanced Renal-Cell Carcinoma Treated with First-Line Sunitinib: a Multicentre, Observational, Prospective Study. *Lancet Oncol.* 12 (12), 1143–1150. doi:10.1016/S1470-2045(11)70266-2

Guo, X. G., Wang, Z. H., Dong, W., He, X. D., Liu, F. C., and Liu, H. (2018). Specific CYP450 Genotypes in the Chinese Population Affect Sorafenib Toxicity in HBV/HCV-associated Hepatocellular Carcinoma Patients. *Biomed. Environ. Sci.* 31 (8), 586–595. doi:10.3967/bes2018.080

Han, B., Li, K., Wang, Q., Zhang, L., Shi, J., Wang, Z., et al. (2018a). Effect of Anlotinib as a Third-Line or Further Treatment on Overall Survival of Patients with Advanced Non-small Cell Lung Cancer: The ALTER 0303 Phase 3 Randomized Clinical Trial. *JAMA Oncol.* 4 (11), 1569–1575. doi:10.1001/jamaoncol.2018.3039

Han, B., Li, K., Zhao, Y., Li, B., Cheng, Y., Zhou, J., et al. (2018b). Anlotinib as a Third-Line Therapy in Patients with Refractory Advanced Non-small-cell Lung Cancer: a Multicentre, Randomised Phase II Trial (ALTER0302). *Br. J. Cancer* 118 (5), 654–661. doi:10.1038/bjc.2017.478

Herbst, R. S., Morgensztern, D., and Boshoff, C. (2018). The Biology and Management of Non-small Cell Lung Cancer. *Nature* 553 (7689), 446–454. doi:10.1038/nature25183

Kaminsky, L. S., and Zhang, Q. Y. (2003). The Small Intestine as a Xenobiotic-Metabolizing Organ. *Drug Metab. Dispos.* 31 (12), 1520–1525. doi:10.1124/dmd.31.12.1520

Krause, D. S., and Van Etten, R. A. (2005). Tyrosine Kinases as Targets for Cancer Therapy. *N. Engl. J. Med.* 353 (2), 172–187. doi:10.1056/NEJMra044389

Liao, D., Liu, Z., Zhang, Y., Liu, N., Yao, D., Cao, L., et al. (2020). Polymorphisms of Drug-Metabolizing Enzymes and Transporters Contribute to the Individual Variations of Erlotinib Steady State Trough Concentration, Treatment Outcomes, and Adverse Reactions in Epidermal Growth Factor Receptor-Mutated Non-small Cell Lung Cancer Patients. *Front. Pharmacol.* 11, 664. doi:10.3389/fphar.2020.00664

Lin, B., Song, X., Yang, D., Bai, D., Yao, Y., and Lu, N. (2018). Anlotinib Inhibits Angiogenesis via Suppressing the Activation of VEGFR2, PDGFRβ and FGFR1. *Gene* 654, 77–86. doi:10.1016/j.gene.2018.02.026

Liu, Z., Wang, J., Meng, Z., Wang, X., Zhang, C., Qin, T., et al. (2018). CD31-labeled Circulating Endothelial Cells as Predictor in Anlotinib-Treated Non-small-cell Lung Cancer: Analysis on ALTER-0303 Study. *Cancer Med.* 7, 3011–3021. doi:10.1002/cam4.1584

Lynch, T. J., Bell, D. W., Sordella, R., Gurubhagavatula, S., Okimoto, R. A., Brannigan, B. W., et al. (2004). Activating Mutations in the Epidermal Growth Factor Receptor Underlying Responsiveness of Non-small-cell Lung Cancer to Gefitinib. *N. Engl. J. Med.* 350 (21), 2129–2139. doi:10.1056/NEJMoa040938

Martin, J., Williams, A. K., Klein, M. D., Sriramoju, V. B., Madan, S., Rossi, J. S., et al. (2020). Frequency and Clinical Outcomes of CYP2C19 Genotype-Guided Escalation and De-escalation of Antiplatelet Therapy in a Real-World Clinical Setting. *Genet. Med.* 22 (1), 160–169. doi:10.1038/s41436-019-0611-1

Novkovic, M., Matic, D., Kusic-Tisma, J., Antonijevic, N., Radojkovic, D., and Rakicevic, L. (2018). Analysis of the CYP2C19 Genotype Associated with Bleeding in Serbian STEMI Patients Who Have Undergone Primary PCI and Treatment with Clopidogrel. *Eur. J. Clin. Pharmacol.* 74 (4), 443–451. doi:10.1007/s00228-017-2401-5

Paez, J. G., Jänne, P. A., Lee, J. C., Tracy, S., Greulich, H., Gabriel, S., et al. (2004). EGFR Mutations in Lung Cancer: Correlation with Clinical Response to Gefitinib Therapy. *Science* 304 (5676), 1497–1500. doi:10.1126/science.1099314

Paine, M. F., Hart, H. L., Ludington, S. S., Haining, R. L., Rettie, A. E., and Zeldin, D. C. (2006). The Human Intestinal Cytochrome P450 "pie". *Drug Metab. Dispos.* 34 (5), 880–886. doi:10.1124/dmd.105.008672

Parra-Guillen, Z. P., Berger, P. B., Haschke, M., Donzelli, M., Winogradova, D., Pfister, B., et al. (2017). Role of Cytochrome P450 3A4 and 1A2 Phenotyping in Patients with Advanced Non-small-cell Lung Cancer Receiving Erlotinib Treatment. *Basic Clin. Pharmacol. Toxicol.* 121 (4), 309–315. doi:10.1111/bcpt.12801

Patel, J. N. (2016). Cancer Pharmacogenomics, Challenges in Implementation, and Patient-Focused Perspectives. *Pharmgenomics Pers. Med.* 9, 65–77. doi:10.2147/PGPM.S62918

Scott, S. A. (2011). Personalizing Medicine with Clinical Pharmacogenetics. *Genet. Med.* 13 (12), 987–995. doi:10.1097/GIM.0b013e318238b38c

Shin, D. J., Kwon, J., Park, A. R., Bae, Y., Shin, E. S., Park, S., et al. (2012). Association of CYP2C19*2 and *3 Genetic Variants with Essential Hypertension in Koreans. *Yonsei Med. J.* 53 (6), 1113–1119. doi:10.3349/ymj.2012.53.6.1113

Sun, W., Wang, Z., Chen, R., Huang, C., Sun, R., Hu, X., et al. (2017). Influences of Anlotinib on Cytochrome P450 Enzymes in Rats Using a Cocktail Method. *Biomed. Res. Int.* 2017, 3619723. doi:10.1155/2017/3619723

Sun, Y., Niu, W., Du, F., Du, C., Li, S., Wang, J., et al. (2016). Safety, Pharmacokinetics, and Antitumor Properties of Anlotinib, an Oral Multi-Target Tyrosine Kinase Inhibitor, in Patients with Advanced Refractory Solid Tumors. *J. Hematol. Oncol.* 9 (1), 105. doi:10.1186/s13045-016-0332-8

Sung, H., Ferlay, J., Siegel, R. L., Laversanne, M., Soerjomataram, I., Jemal, A., et al. (2021). Global Cancer Statistics 2020: GLOBOCAN Estimates of Incidence and Mortality Worldwide for 36 Cancers in 185 Countries. *CA Cancer J. Clin.* 71 (3), 209–249. doi:10.3322/caac.21660

Syed, Y. Y. (2018). Anlotinib: First Global Approval. *Drugs* 78 (10), 1057–1062. doi:10.1007/s40265-018-0939-x

Wu, F., Wang, L., and Zhou, C. (2021). Lung Cancer in China: Current and Prospect. *Curr. Opin. Oncol.* 33 (1), 40–46. doi:10.1097/CCO.0000000000000703

Yang, Y. N., Wang, X. L., Ma, Y. T., Xie, X., Fu, Z. Y., Li, X. M., et al. (2010). Association of Interaction between Smoking and CYP 2C19*3 Polymorphism with Coronary Artery Disease in a Uighur Population. *Clin. Appl. Thromb. Hemost.* 16 (5), 579–583. doi:10.1177/1076029610364522

Zanger, U. M., and Schwab, M. (2013). Cytochrome P450 Enzymes in Drug Metabolism: Regulation of Gene Expression, Enzyme Activities, and Impact of Genetic Variation. *Pharmacol. Ther.* 138 (1), 103–141. doi:10.1016/j.pharmthera.2012.12.007

Zhong, C. C., Chen, F., Yang, J. L., Jia, W. W., Li, L., Cheng, C., et al. (2018). Pharmacokinetics and Disposition of Anlotinib, an Oral Tyrosine Kinase Inhibitor, in Experimental Animal Species. *Acta Pharmacol. Sin.* 39 (6), 1048–1063. doi:10.1038/aps.2017.199

Conflict of Interest: The authors declare that the research was conducted in the absence of any commercial or financial relationships that could be construed as a potential conflict of interest.

Publisher's Note: All claims expressed in this article are solely those of the authors and do not necessarily represent those of their affiliated organizations, or those of the publisher, the editors and the reviewers. Any product that may be evaluated in this article, or claim that may be made by its manufacturer, is not guaranteed or endorsed by the publisher.

frontiers | Frontiers in Pharmacology

ORIGINAL RESEARCH
published: 23 June 2022
doi: 10.3389/fphar.2022.931495

Toward Therapeutic Drug Monitoring of Lenalidomide in Hematological Malignancy? Results of an Observational Study of the Exposure-Safety Relationship

Zaiwei Song[1,2†], Lan Ma[3†], Li Bao[4], Yi Ma[1,2], Ping Yang[1,2], Dan Jiang[1,2], Aijun Liu[5], Lu Zhang[6], Yan Li[3], Yinchu Cheng[1,2], Fei Dong[3], Rongsheng Zhao[1,2] and Hongmei Jing[3]**

[1]Department of Pharmacy, Peking University Third Hospital, Beijing, China, [2]Therapeutic Drug Monitoring and Clinical Toxicology Center, Peking University, Beijing, China, [3]Department of Hematology, Peking University Third Hospital, Beijing, China, [4]Department of Hematology, Beijing Jishuitan Hospital, Beijing, China, [5]Department of Hematology, Beijing Chaoyang Hospital, Capital Medical University, Beijing, China, [6]Department of Hematology, State Key Laboratory of Complex Severe and Rare Diseases, Peking Union Medical College Hospital, Chinese Academy of Medical Sciences and Peking Union Medical College, Beijing, China

OPEN ACCESS

Edited by:
Miao Yan,
Central South University, China

Reviewed by:
Samuel Yamshon,
Weill Cornell Medical Center, NewYork-Presbyterian, United States
Masatomo Miura,
Akita University Hospital, Japan

***Correspondence:**
Rongsheng Zhao
zhaorongsheng@bjmu.edu.cn
Hongmei Jing
hongmeijing@bjmu.edu.cn

[†]These authors have contributed equally to this work

Specialty section:
This article was submitted to Pharmacology of Anti-Cancer Drugs, a section of the journal Frontiers in Pharmacology

Received: 29 April 2022
Accepted: 31 May 2022
Published: 23 June 2022

Citation:
Song Z, Ma L, Bao L, Ma Y, Yang P, Jiang D, Liu A, Zhang L, Li Y, Cheng Y, Dong F, Zhao R and Jing H (2022) Toward Therapeutic Drug Monitoring of Lenalidomide in Hematological Malignancy? Results of an Observational Study of the Exposure-Safety Relationship. Front. Pharmacol. 13:931495. doi: 10.3389/fphar.2022.931495

Objective: Continuous lenalidomide (LEN) therapy is important to achieve a therapeutic effect in patients with multiple myeloma (MM) and non-Hodgkin lymphoma (NHL). However, despite dose adjustment according to kidney function, many patients discontinue LEN therapy because of hematological toxicity. To date, therapeutic drug monitoring (TDM) of LEN has not been performed in oncology, and no target concentration level has been yet defined. The aim of this study was to evaluate the exposure-safety relationship of LEN and determine the target concentration for toxicity.

Materials and Methods: A prospective observational study was designed and implemented. Blood samples were collected at 0.5 h (trough concentration, C_{min}) before oral administration and 1 h (C_{1h}) thereafter on the day. Clinical data were gathered from patients' medical records and laboratory reports. Outcome measures of hematological toxicity were defined by the Common Terminology Criteria for Adverse Events. The concentration values were dichotomized by receiver operating characteristic (ROC) curve analysis, and the association between exposure and outcome was determined using the logistic regression model.

Results: Out of the 61 patients enrolled in this study, 40 (65.57%) had MM, and 21 (34.43%) had NHL. Hematological toxicity was reported in 15 (24.59%) patients. The LEN C_{min} showed remarkable differences (p = 0.031) among patients with or without hematological toxicity, while no association between C_{1h} values and toxicity was noted (p>0.05). By ROC analysis, a C_{min} threshold of 10.95 ng/mL was associated with the best sensitivity/specificity for toxicity events (AUC = 0.687; sensitivity = 0.40; specificity = 0.935). By multivariate logistic regression, an LEN C_{min} below 10.95 ng/mL was associated with a markedly decreased risk of hematological toxicity (<10.95 ng/mL vs. >10.95 ng/mL: OR = 0.023, 95% CI = 0.002–0.269; p = 0.003).

Conclusions: We demonstrate that the LEN trough concentration correlates with hematological toxicity, and the C_{min} threshold for hematological toxicity (10.95 ng/mL) is proposed. Altogether, LEN TDM appears to be a new approach to improve medication safety and achieve continuous treatment for patients with NHL or MM in routine clinical care.

Keywords: lenalidomide, hematological toxicity, therapeutic drug monitoring, trough concentration, hematological malignancies

INTRODUCTION

Non-Hodgkin's lymphoma (NHL) is a cancer that develops in white blood cells called lymphocytes, representing the most frequent hematological malignancy. It is estimated that NHL was responsible for 544,000 new cases and 260,000 deaths worldwide in 2020 (Sung et al., 2021). Multiple myeloma (MM), the second most common hematologic malignancy, is a plasma cell malignancy in which monoclonal plasma cells proliferate in bone marrow (Mitsiades et al., 2004). Currently, projections suggest that, as the two most common hematologic malignancies, the incidence of both NHL and MM will continue to increase (Cai et al., 2021; Zhou et al., 2021).

The past years have witnessed a dramatic shift in the treatment of NHL and MM, from chemotherapy to chemoimmunotherapeutic regimens, and now biological and targeted strategies. One such treatment option is lenalidomide (LEN), which is a thalidomide derivative known as an immunomodulatory drug (List et al., 2005). LEN's significant activity in hematological malignancy has led to its incorporation into multiple treatment regimens (Gribben et al., 2015), such as the LEN plus rituximab (R^2) regimen for NHL (Leonard et al., 2019), as well as regimens based on LEN plus dexamethasone for MM (Mateos et al., 2013). As an oral targeted antineoplastic agent, long-term and continuous LEN treatment is important to achieve a therapeutic effect (Kado et al., 2020).

However, a close link has been established between LEN therapy and severe hematological toxicities, including neutropenia, thrombocytopenia, anemia, and leukopenia. Almost half of the patients experienced hematological toxicity of any grade across studies, and the incidence of high-grade hematologic toxicity might be 30% or higher (Cheson et al., 2020). During real clinical practice, despite dose adjustments according to baseline kidney function, unacceptable hematological toxicity is still the most common factor preventing continuous therapy with LEN. In addition to possibly causing treatment interruption, LEN-related hematological toxicity can affect patient adherence to treatment, increase the relapse risk and increase healthcare costs.

Therapeutic drug monitoring (TDM) is the clinical practice of measuring drug exposure at designated intervals to tailor drug doses, thereby optimizing outcomes in individual patients. The process of TDM is predicated on the assumption that there is a definable relationship between concentration and therapeutic or adverse effects (Kang and Lee, 2009). In terms of LEN, dose-limiting hematological toxicity has been observed, and dose modification or treatment interruption according to the severity of myelosuppression is recommended (Ludwig et al., 2018). Furthermore, a high area under the plasma concentration-time curve (AUC) of LEN has been shown to result in severe adverse events (Chen et al., 2013; Kobayashi et al., 2018). However, accurate measurement of the AUC requires collecting and analyzing multiple blood samples, which is both costly and time consuming for patients and clinical staff. Consequently, AUC-based TDM could be difficult to implement in clinical practice. There still exists a gap in the optimal index for TDM of hematological toxicity that can be used in clinical settings.

Herein, in the present study, we aimed to investigate the association between LEN exposure and its hematological toxicity and to determine concentration targets, which could be used in the TDM of LEN in patients with NHL or MM.

MATERIALS AND METHODS

Patients

This was a prospective observational study that was in compliance with the Declaration of Helsinki and approved by the hospital medical science research ethics committee (No. M2021573). Patients provided written informed consent prior to enrollment. Adult patients with MM and NHL taking LEN capsules (Revlimid®, Celgene Corporation) for at least 3 days (steady state) and performing LEN concentration measurements during therapy between October 2021 and February 2022 were enrolled in this study. Patients taking any dose of LEN, pretreated with or without LEN, were eligible.

Patients were excluded if they had incomplete data, making it unable to assess whether the outcome event occurred; the clinical diagnosis was unclear; they had impaired kidney function with creatinine clearance (CCr) < 45 mL/min; they had impaired liver function with alanine aminotransferase (ALT) or aspartate aminotransferase (AST) greater than 5 times the upper limits of normal (ULN); they failed to take medicine as prescribed; they did not perform blood sample collection according to the prescribed time; and the plasma concentration of LEN was below the detection limit of 1 ng/mL.

Data Collection

Data were gathered from patients' medical records and laboratory reports, which included patients' demographics, clinical data on the diagnosis (subtype and stage of MM or NHL), history of previous chemotherapy, details of LEN therapy (including number of courses, duration days, dosage, antineoplastic agents combined),

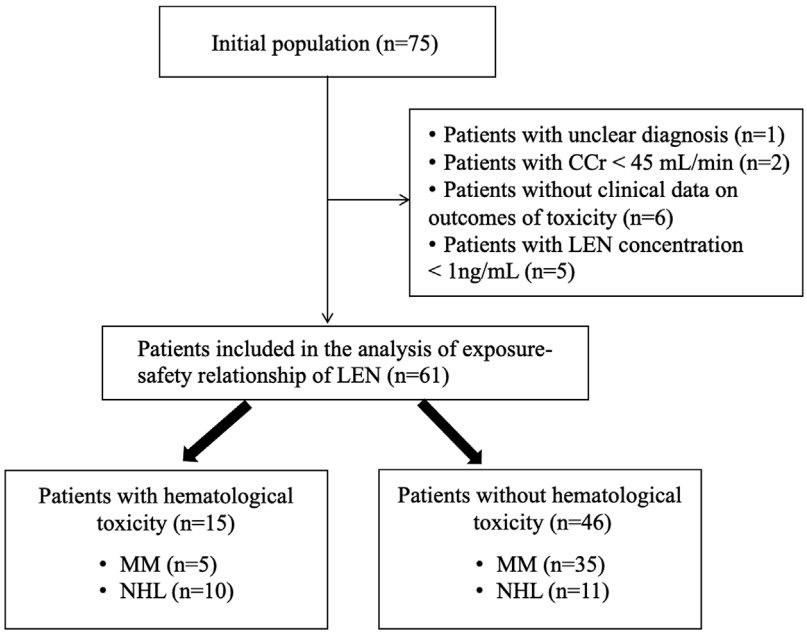

FIGURE 1 | Flow chart of the study.

other concomitant drugs, and biological results. The biological data of complete blood count (CBC, including white cells, neutrophils, platelets, hemoglobin) were tested and collected on the day blood plasma concentration was measured, whereas the baseline CBC was collected before taking LEN of this cycle. In addition, other laboratory test data, including serum creatinine (SCr), total protein, albumin, alanine aminotransferase (ALT), aspartate aminotransferase (AST), and alkaline phosphatase (ALP) values, were also collected. The creatinine clearance (CCr) was estimated using the Cockcroft-Gault formula.

Measurement of Lenalidomide Concentration

Given that the half-life of LEN is approximately 3–5 h (Chen et al., 2017), LEN was considered to have achieved a steady-state plasma concentration after 3 days. Only patients who achieved steady state were included in the analysis; thus, we accepted that the blood samples could be collected on day 3 after starting the LEN therapy. Blood samples were collected at 0.5 h (trough concentration, C_{min}) before oral administration and 1 h (C_{1h}) thereafter on the day. The two blood samples need to be collected before meals in the morning to avoid the influence of food on drug absorption and plasma concentration, although LEN was administered without regard to food intake in daily clinical practice. Blood samples were drawn into EDTA tubes.

The plasma was stored at −80°C until analysis. LEN concentrations were measured using a validated high-performance liquid chromatography tandem-mass spectrometry method (HPLC–MS/MS). LEN-$^{13}C_5$ was used as the internal standard. The analyte was separated on a Waters Atlantis® HILIC silica column (5 μm, 2.1 mm × 150 mm). The selected reaction monitoring transitions were 260.1→149.1 for LEN and 265.1→149.1 for the internal standard. The lower limit of quantification is 1 ng/mL for LEN. This method was developed and validated according to regulatory requirements. The inter-run precision and accuracy were less than 11.8% and 5.0%, respectively.

Outcome Definition

Attending physicians and pharmacists evaluated and graded the hematological toxicity according to the Common Terminology Criteria for Adverse Events Version 5.0 (NCI-CTCAE), and the highest grade of all decreased blood cells was defined as the grade of severity of hematological toxicity in this study. The clinical outcome was classified into two categories: a group with hematological toxicity and a group with no hematological toxicity.

In patients with normal baseline counts, hematological toxicity was defined as grade 2 or higher hematological adverse events, including leukopenia (decreased white blood cell count), neutropenia (decreased neutrophil count), thrombocytopenia (decreased platelet count) and anemia (decreased hemoglobin count). In patients with abnormal baseline counts, hematological toxicity was defined as a count <75% of baseline and grade 2 or higher hematological adverse events.

Statistical Analysis

The statistical analyses were performed with SPSS software version 27.0 (IBM Corp., Armonk, NY, United States). For quantitative data following a normal distribution, we calculated the mean with standard deviations (mean ± SD) and used a T test to determine the difference between the groups. For nonnormally distributed data, we calculated the median with interquartile range [median (IQR)] and used the Mann–Whitney U test to compare the difference between the

TABLE 1 | Baseline demographic and clinical characteristics of the included patients.

Characteristic	No-Hematology toxicity group (n = 46) n (%)	Hematology toxicity group (n = 15) n (%)	Total (n = 61) n (%)
Gender			
Female	24 (52.17%)	10 (66.67%)	34 (55.74%)
Male	22 (47.83%)	5 (33.33%)	27 (44.26%)
Median age (IQR), years	62 (56–67)	59 (53–68)	62 (56–68)
Median weight (IQR), kg	64 (58–70)	65 (59–74)	64 (58–70)
Median BMI (IQR), kg/m^2	23.50 (21.49–25.07)	23.80 (22.35–26.67)	23.51 (22.04–25.51)
Median BSA (IQR), m^2	1.73 (1.59–1.83)	1.77 (1.62–1.87)	1.74 (1.60–1.84)
Diagnosis			
Multiple myeloma (MM)	35 (76.09%)	5 (33.33%)	40 (65.57%)
Non-Hodgkin lymphoma (NHL)	11 (23.91%)	10 (66.67%)	21 (34.43%)
Median SCr (IQR), μmol/L	61.5 (52.0–69.8)	61.0 (50.5–69.5)	61.0 (52.0–70.0)
Median CCr (IQR), mL/min	97.8 (74.5–109.3)	94.2 (72.7–102.7)	96.3 (74.5–108.5)
Median total protein (IQR), g/L	65.4 (60.2–69.6)	62.0 (59.3–73.1)	65.0 (59.8–70.0)
Median albumin (IQR), g/L	37.9 (35.7–41.0)	42.0 (36.8–43.1)	38.2 (35.7–41.9)
Median ALT (IQR), U/L	22.8 (13.3–27.2)	15.0 (10.0–35.5)	20.0 (11.1–30.0)
Median AST (IQR), U/L	22.0 (16.6–25.8)	17.0 (14.5–24.5)	21.0 (15.0–25.0)
Median ALP (IQR), U/L	79.0 (61.6–94.5)	69.0 (62.0–78.5)	76.5 (61.8–91.0)
Median courses of Lenalidomide (IQR), n	1 (1–3)	1 (1–3)	1 (1–3)
Median Lenalidomide duration (IQR), days	5 (5–7)	5 (5–6)	5 (5–6)
Dosage of Lenalidomide			
10 mg QD	5 (10.87%)	4 (26.67%)	9 (14.75%)
12.5 mg QD	4 (8.70%)	0	4 (6.56%)
25 mg QD	33 (71.74%)	11 (73.33%)	44 (72.13%)
25 mg QOD	4 (8.70%)	0	4 (6.56%)
Antineoplastic agents combined			
Targeted therapy[a]	41 (89.13%)	10 (66.67%)	51 (83.61%)
Glucocorticoids	36 (78.26%)	8 (53.33%)	44 (72.13%)
Cytotoxic antitumor drugs	4 (8.70)	5 (33.33%)	9 (14.75%)
Other concomitant drugs			
Aspirin	21 (45.65%)	9 (60.00%)	30 (49.18%)
Antiviral agents	19 (41.30%)	4 (26.67%)	23 (37.70%)
Antibacterial agents	7 (15.22%)	4 (26.67%)	11 (18.03%)
PPI or H2RA	5 (10.87%)	5 (33.33%)	10 (16.39%)

Abbreviations; IQR, Interquartile range; BMI,Body mass index; BSA, Body surface area; SCr, Serum creatinine; CCr, Creatinine clearance; ALT, Alanine aminotransferase; AST, Aspartate aminotransferase; ALP, Alkaline phosphatase; QD, Once a day; QOD, Every other day; PPI, Proton pump inhibitor; H2RA, H2 receptor antagonist.
[a]*Targeted therapy includes bortezomib, isazomi, ibrutinib, zanubrutinib, orelabrutinib, rituximab and obinutuzumab.*

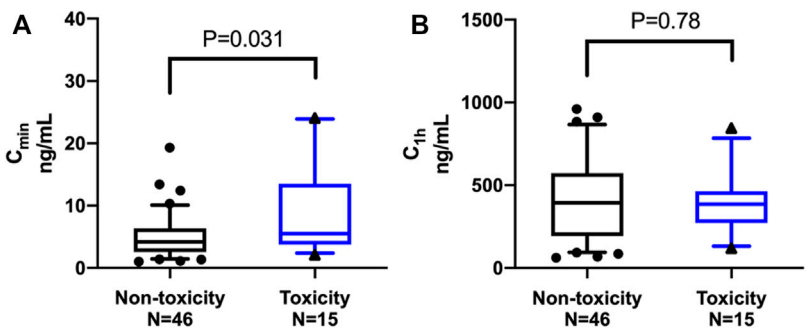

FIGURE 2 | Comparison of lenalidomide plasma concentrations between the groups. The middle line represents the median in each group. **(A)** The trough concentration (C_{min}), expressed as the median (IQR), was significantly higher in the toxicity group than in the non-toxicity group [5.53 (3.97–13.05) ng/mL versus 4.17 (1.03–6.33) ng/mL; $p = 0.031$]. **(B)** The plasma concentration at 1 h (C_{1h}) after oral administration, expressed as the mean (SD), showed no significant difference between the toxicity group and the non-toxicity group [396.67 (206.73) ng/mL versus 416.98 (254.05) ng/mL; $p = 0.78$].

groups. Categorical variables were expressed as frequencies and proportions (%), and the chi-squared test was used to compare the differences between the groups.

If a statistically significant difference in LEN concentrations was observed between the groups, receiver operating characteristic (ROC) curves were constructed to determine a

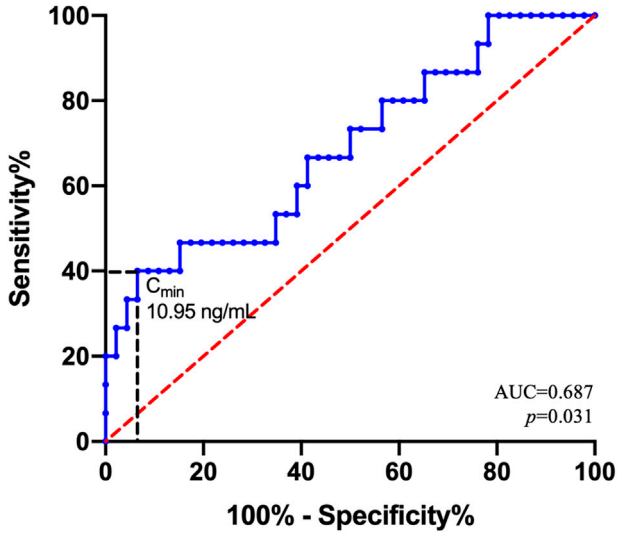

FIGURE 3 | Receiver operating characteristic (ROC) curve for hematological toxicity. ROC curve estimates for the 61 patients. AUC is the area under the ROC curve. With regard to the C_{min} threshold value of 10.95 ng/mL, the sensitivity and specificity were 0.4 and 0.935, respectively.

concentration threshold associated with hematological toxicity. The best threshold was chosen using the Youden index, identifying the target concentration that might result in hematological toxicity. Patients' exposure to LEN was dichotomized depending on this threshold.

To account for various potential risk factors for developing hematological toxicity and to reduce other potential bias, the associations between concentrations and hematological toxicity were further adjusted by the logistic regression model. First, univariate analysis was performed to identify possible factors. Variables with statistical significance (defined as p <0.05) in the univariate analysis, as well as those determined by reading relevant literature and combining clinical experience, including gender, age, weight, CCr, albumin, diagnosis (NHL or MM), and co-administration of cytotoxic antitumor drugs, were then included in the multivariate logistic regression using the Enter method. All statistical analyses were two-tailed, and p <0.05 was considered statistically significant.

RESULTS

Patient Characteristics

A total of 75 patients were screened initially, and only 61 (34 male, 55.74%) were included in the study. The other 14 patients were excluded as a result of unclear diagnosis, impaired kidney function with CCr less than 45 mL/min, missing clinical data, or LEN concentration below the detection limit of 1 ng/mL (**Figure 1**).

The demographic and clinical characteristics of the included patients are listed in **Table 1**. Out of the 61 patients enrolled in this study, hematological toxicity was observed in 15 (24.59%) patients. Patient demographics of the no-hematology toxicity group and hematology toxicity group were similar. Regarding the clinical diagnosis, 40 (65.57%) patients had MM, of which 26 were newly diagnosed; 21 (34.43%) patients had NHL, of which 5 were newly diagnosed. The median number of previous courses of immunochemotherapy was 0 (IQR, 0–5). Among 40 MM patients, the most common type was IgG (n = 19), followed by light chain (n = 15), IgA (n = 5), and IgD (n = 1). The most common Durie-Salmon (DS) stage was stage III (n = 33), followed by stage II (n = 5) and stage I (n = 2). Regarding the International Staging System (ISS), 23 patients had stage I disease, followed by stage III (n = 9) and stage I (n = 8) disease. Among 21 NHL patients, most had diffuse large B-cell lymphoma (DLBCL) (n = 11) and follicular lymphoma (FL) (n = 9), and only one had high-grade B-cell lymphoma (HGBL). According to the Ann Arbor Staging Classification, 19 and 2 patients had stage IV and stage II disease, respectively, of which almost half (n = 10) had B symptoms.

The median number of LEN treatment courses was 1 (range 1–15), and the median days of LEN duration in this current cycle was 5 (range 3–21). The LEN dosage was classified into four categories: 10 mg QD, 12.5 mg QD, 25 mg QD, and 25 mg QOD. In terms of antineoplastic agents combined, LEN was combined with other targeted therapies (e.g., bortezomib, ibrutinib, rituximab) and glucocorticoids in most patients, and LEN monotherapy was administered in only 7 patients. In addition, patients were concomitant with other medications, including aspirin, antiviral agents, antibacterial agents, proton pump inhibitors (PPI) or H2 receptor antagonists (H2RA) and other drugs.

Comparison of Plasma Concentrations

Figure 2 shows the comparison of LEN plasma concentrations between the groups. The trough concentration of LEN at 0.5 h before oral administration (C_{min}), expressed as the median (IQR), was significantly higher in the toxicity group [5.53 (3.97–13.05) ng/mL] than in the no-toxicity group [4.17 (1.03–6.33) ng/mL; p = 0.031]. Regarding the plasma concentration of LEN at 1 h after oral administration (C_{1h}), expressed as the mean (SD), there was no significant difference between the toxicity group [396.67 (206.73) ng/mL] and the no-toxicity group [416.98 (254.05) ng/mL; p = 0.78].

ROC Curve for Hematological Toxicity

Using the ROC curve (**Figure 3**), the LEN C_{min} threshold predicting hematological toxicity was 10.95 ng/mL with an area under the curve (AUC) of 0.687 [95% confidence interval (95% CI) = 0.527–0.847; p = 0.031]. Considering the threshold value of 10.95 ng/mL, the sensitivity and specificity were 0.4 and 0.935, respectively.

Then, the LEN C_{min} was binarized according to the 10.95 ng/mL threshold as "high exposure" when C_{min} was above this value and as "low exposure" when below. Compared to the "low exposure" group (n = 9/52, 17.31%), there was a significantly increased risk of toxicity in the "high exposure" group (n = 6/9, 66.67%; p = 0.006).

Factors Associated With Hematological Toxicity

Logistic regression analysis was used to identify independent factors influencing hematological toxicity. The results of the

TABLE 2 | Univariate and multivariate analyses of factors influencing hematological toxicity.

Characteristics	Univariate analysis		Multivariate analysis	
	OR (95% CI)	*p* value	OR (95% CI)	*p* value
Male (vs. female)	0.545 (0.161–1.847)	0.330	0.255 (0.030–2.185)	0.212
Age (years)	0.976 (0.925–1.030)	0.374	0.998 (0.911–1.093)	0.965
Weight (kg)	1.025 (0.971–1.082)	0.374	0.991 (0.898–1.092)	0.850
BMI (kg/m^2)	1.098 (0.917–1.314)	0.310		
BSA (m^2)	3.393 (0.103–112.125)	0.494		
MM (vs. NHL)	0.157 (0.044–0.559)	0.004*	0.342 (0.057–2.046)	0.240
SCr (μmol/L)	1.004 (0.972–1.037)	0.807		
CCr (mL/min)	1.007 (0.990–1.025)	0.428	1.012 (0.973–1.053)	0.541
Total protein (g/L)	1.004 (0.958–1.052)	0.873		
Albumin (g/L)	1.131 (0.981–1.304)	0.090	1.182 (0.918–1.522)	0.195
ALT (U/L)	1.010 (0.977–1.043)	0.558		
AST (U/L)	0.976 (0.915–1.041)	0.466		
ALP (U/L)	0.978 (0.950–1.007)	0.142		
Courses of Lenalidomide (n)	0.966 (0.785–1.188)	0.742		
Lenalidomide duration (days)	0.965 (0.828–1.126)	0.655		
Lenalidomide dosage				
25 mg QD	References			
Less than 25 mg QOD	0.923 (0.249–3.428)	0.905		
Co-administration of targeted therapy[a] (vs. no)	0.244 (0.059–1.008)	0.051		
Co-administration of glucocorticoids (vs. no)	0.317 (0.093–1.089)	0.068		
Co-administration of cytotoxic antitumor drugs (vs. no)	5.250 (1.190–23.171)	0.029*	8.331 (0.905–76.703)	0.061
Co-administration of aspirin (vs. no)	1.786 (0.546–5.839)	0.337		
Co-administration of antiviral agents (vs. no)	0.517 (0.143–1.870)	0.314		
Co-administration of antibacterial agents (vs. no)	2.026 (0.500–8.207)	0.323		
Co-administration of PPI or H2RA (vs. no)	4.100 (0.992–16.950)	0.051		
C_{min} (<10.95 vs. >10.95 ng/mL)	0.143 (0.029–0.700)	0.016*	0.023 (0.002–0.269)	0.003*
C_{1h} (ng/mL)	1.000 (0.997–1.002)	0.776		

Abbreviations; CI, Confidence interval; BMI, body mass index; BSA, body surface area; MM, Multiple myeloma; NHL, Non-Hodgkin lymphoma; SCr, Serum creatinine; CCr, Creatinine clearance; ALT, Alanine aminotransferase; AST, Aspartate aminotransferase; ALP, Alkaline phosphatase; QD, Once a day; QOD, Every other day; PPI, Proton pump inhibitor; H2RA, H2 Receptor Antagonist.

[a]*Targeted therapy includes bortezomib, isazomi, ibrutinib, zanubrutinib, orelabrutinib, rituximab and obinutuzumab.*

univariate and multivariate analyses are presented in **Table 2**. The dichotomized LEN C_{min} was retained in the final model. In line with previous analysis, a LEN C_{min} threshold below 10.95 ng/mL was significantly associated with a decreased risk of hematological toxicity (<10.95 ng/mL vs. >10.95 ng/mL: OR = 0.023, 95% CI = 0.002–0.269; p = 0.003). In other words, compared to "low exposure" (C_{min}<10.95 ng/mL), "high exposure" (C_{min}>10.95 ng/mL) was associated with an apparent increase in the odds of developing hematological toxicity.

DISCUSSION

General Findings and Trends

LEN, a non-chemotherapy immunomodulator, has been extensively used in the treatment of MM and NHL, and the mechanism involves direct cytotoxicity as well as indirect effects on tumor immunity (Gribben et al., 2015). With the expanding role of LEN in hematologic malignancies, the management of its hematological toxicity has become a wide clinical concern and research focus (Cheson et al., 2020). Despite dose adjustments according to the severity of myelosuppression, unacceptable hematological toxicity is still the most common factor preventing continuous therapy with LEN. To date, there is no established and feasible marker that can be used as a predictive factor in routine clinical practice to inform a high risk of developing hematological toxicity. Therefore, we paid more attention to the association between hematological toxicity and its plasma concentration in this study.

This current study revealed that only C_{min} was independently associated with hematological toxicity. We found that LEN over-exposure contributed to its hematological toxicity, which is similar to previous investigations on the cumulative exposure (AUC) of LEN (Komrokji et al., 2012; Chen et al., 2013; Kobayashi et al., 2018). Given that a C_{min} higher than 10.95 ng/mL was associated with a remarkable increase in the risk of developing toxicity, a C_{min} of 10.95 ng/mL was determined as the upper limit to prevent hematological toxicity. This threshold was associated with a specificity of 93.5% and a sensitivity of 40%.

Conversely, no apparent association was observed between LEN C_{1h} and its hematological toxicity in our study, which corresponds to the findings in a previous investigation on the relationship of peak serum concentration (C_{max}) and hematological toxicity (Bridoux et al., 2016). However, it is notable that the inter-individual variability of the time to reach C_{max} (T_{max}) could not be excluded; thus, C_{1h} cannot be equal to C_{max} in our study.

As similar pharmacokinetic profiles of LEN have been previously shown in patients with various types of hematological malignancies (Chen et al., 2017), the two most common hematologic malignancies, MM and NHL, were simultaneously included in our study population.

Interestingly, the results of univariate analysis suggested that patients with MM might have a lower risk of hematological toxicity than those with NHL, which needs to be studied further. In addition, the univariate analysis suggested a possible tendency toward an increased risk of hematological toxicity in patients co-administered cytotoxic antitumor drugs. However, it was not an independent factor affecting hematological toxicity in the multivariate analysis, which also enhances the reliability of the observed association between C_{min} and hematological toxicity.

Key Strengths and Significance

With regard to TDM, sampling trough concentrations at steady state (C_{min}) is often performed in clinical practice and is currently the most precise approach, as it avoids the shrinkage of individual information to the population mean (Mueller- Schoell et al., 2021). To the best of our knowledge, the present study is the first to establish and highlight a relationship between LEN C_{min} and its hematological toxicity. Furthermore, multivariate logistic analysis confirmed the significance of this cut-off value of LEN C_{min}, and we propose it as an optimal index for TDM of LEN hematological toxicity. In comparison, TDM based on cumulated AUC requires collecting and analyzing multiple blood samples, whereas dense blood sampling is rarely feasible in the clinical setting.

Of note, despite TDM's value in oncology becoming more recognized, it is still not commonly used in antineoplastic treatment compared to other therapeutic areas (e.g., antimicrobial and antiepileptic) (Wicha et al., 2015; Velghe and Stove, 2018; Mueller- Schoell et al., 2021). The present study provides exploratory evidence for LEN TDM in patients with NHL and MM, which contributes to further promoting the extensive use of TDM in the field of oncology. Additionally, the exposure-safety relationship was established based on real-world data from patients' medical records in our study. Evidence from the real-world setting can help to establish a broad picture of TDM implementation in everyday clinical practice.

Recommendations for Clinical Practice

From a clinician's or pharmacist's point of view, the hematological toxicity of LEN has become a wide clinical concern. Herein, we discuss recommendations regarding the clinical management of the hematological toxicity of LEN. First, prior to the initiation of LEN treatment, the assessment of patients' baseline kidney function, complete blood count (CBC), and other concomitant drugs causing myelosuppression (e.g., cytotoxic drugs) should be performed. These aforementioned factors should be taken into consideration when determining the initial dose. Second, early measurement of LEN C_{min} on at least day 3 after starting LEN therapy (that is, at least 2 days of dosing) would help to inform a high risk of developing hematological toxicity. Then, individual dose adjustments can be made if necessary. Last but not least, patients should be well trained and motivated to take their medication correctly. Additionally, patients should have CBC assessment regularly to monitor for hematological toxicity, particularly neutropenia.

Limitations and Future Perspectives

Several limitations should be considered for our study. First, we included only a relatively small number of patients; thus, the findings need to be confirmed in a larger and independent population. The outcome measure of hematology toxicity was defined as grade 2 and a higher level in this study, whereas the relationship between exposure and severe hematology toxicity (grade 3 and above) still deserves further consideration. Second, it was unfeasible to assess the exposure-response relationship due to lack of follow-up on long-term efficacy. More particularly, efficacy is a multifactorial and more complex process than toxicity events. Future well-designed studies are warranted to explore the exposure-response relationship. Third, patients were required to delay the breakfast on the morning of the blood sample, but it was difficult to be sure that these instructions were followed. However, it is unlikely that this would alter our conclusions of C_{min}.

CONCLUSION

In conclusion, we demonstrate that the LEN trough concentration correlates with hematological toxicity, and the C_{min} threshold for hematological toxicity (10.95 ng/mL) is proposed. These findings provide the first elements of proof in favor of C_{min}-based TDM in NHL or MM patients receiving LEN therapy. Altogether, LEN TDM appears to be a new approach to improve medication safety and achieve continuous treatment for NHL or MM patients in routine clinical care.

DATA AVAILABILITY STATEMENT

The original contributions presented in the study are included in the article/supplementary material, further inquiries can be directed to the corresponding authors.

ETHICS STATEMENT

The studies involving human participants were reviewed and approved by Peking University Third Hospital Medical Science Research Ethics Committee. The patients/participants provided their written informed consent to participate in this study.

AUTHOR CONTRIBUTIONS

RZ, HJ, and ZS conceived and designed the study. LM, LB, AL, LZ, YL and, FD enrolled patients. ZS, YM, DJ, and YC collected the data and performed the statistical analysis. PY measured concentrations. ZS and LM wrote the article. ZS and DJ prepared the pictures and tables. RZ, HJ, and FD provided suggestions and participated in the

revision of the article. All authors read and approved the final manuscript.

FUNDING

This work was supported by the National Natural Science Foundation of China (NSFC) (72074005).

ACKNOWLEDGMENTS

We would like to express our gratitude to Wei Zhao, Qihui Li, Ping Yang, Wei Wan, Fang Bao and Lingli Wang from Peking University Third Hospital for help with enrolling patients. We are also grateful to Libo Zhao and Xianhua Zhang from Peking University Third Hospital for consultation, and Yang Hu from Peking University Third Hospital for help with editing.

REFERENCES

Bridoux, F., Chen, N., Moreau, S., Arnulf, B., Moumas, E., Abraham, J., et al. (2016). Pharmacokinetics, Safety, and Efficacy of Lenalidomide Plus Dexamethasone in Patients with Multiple Myeloma and Renal Impairment. *Cancer Chemother. Pharmacol.* 78, 173–182. doi:10.1007/s00280-016-3068-9

Cai, W., Zeng, Q., Zhang, X., and Ruan, W. (2021). Trends Analysis of Non-hodgkin Lymphoma at the National, Regional, and Global Level, 1990-2019: Results from the Global Burden of Disease Study 2019. *Front. Med.* 8, 738693. doi:10.3389/fmed.2021.738693

Chen, N., Zhou, S., and Palmisano, M. (2017). Clinical Pharmacokinetics and Pharmacodynamics of Lenalidomide. *Clin. Pharmacokinet.* 56, 139–152. doi:10.1007/s40262-016-0432-1

Chen, N., Ette, E., Zhou, S., Weiss, D., and Palmisano, M. (2013). Population Pharmacokinetics and Exposure-Safety of Lenalidomide in Patients with Multiple Myeloma, Myelodysplastic Syndromes and Mantle Cell Lymphoma. *Blood* 122, 3234. doi:10.1182/blood.v122.21.3234.3234

Cheson, B. D., Morschhauser, F., and Martin, P. (2020). Management of Adverse Events from the Combination of Rituximab and Lenalidomide in the Treatment of Patients with Follicular and Low-Grade Non-hodgkin Lymphoma. *Clin. Lymphoma Myeloma Leuk.* 20, 563–571. doi:10.1016/j.clml.2020.03.009

Gribben, J. G., Fowler, N., and Morschhauser, F. (2015). Mechanisms of Action of Lenalidomide in B-Cell Non-hodgkin Lymphoma. *J. Clin. Oncol.* 33, 2803–2811. doi:10.1200/JCO.2014.59.5363

Kado, Y., Tsujimoto, M., Fuchida, S. I., Okano, A., Hatsuse, M., Murakami, S., et al. (2020). Factors Associated with Dose Modification of Lenalidomide Plus Dexamethasone Therapy in Multiple Myeloma. *Biol. Pharm. Bull.* 43, 1253–1258. doi:10.1248/bpb.b20-00337

Kang, J. S., and Lee, M. H. (2009). Overview of Therapeutic Drug Monitoring. *Korean J. Intern Med.* 24, 1–10. doi:10.3904/kjim.2009.24.1.1

Kobayashi, T., Miura, M., Niioka, T., Abumiya, M., Ito, F., Kobayashi, I., et al. (2018). Phase II Clinical Trial of Lenalidomide and Dexamethasone Therapy in Japanese Elderly Patients with Newly Diagnosed Multiple Myeloma to Determine Optimal Plasma Concentration of Lenalidomide. *Ther. Drug Monit.* 40, 301–309. doi:10.1097/FTD.0000000000000499

Komrokji, R. S., Lancet, J. E., Swern, A. S., Chen, N., Paleveda, J., Lush, R., et al. (2012). Combined Treatment with Lenalidomide and Epoetin Alfa in Lower-Risk Patients with Myelodysplastic Syndrome. *Blood* 120, 3419–3424. doi:10.1182/blood-2012-03-415661

Leonard, J. P., Trneny, M., Izutsu, K., Fowler, N. H., Hong, X., Zhu, J., et al. (2019). AUGMENT: A Phase III Study of Lenalidomide Plus Rituximab Versus Placebo Plus Rituximab in Relapsed or Refractory Indolent Lymphoma. *J. Clin. Oncol.* 37, 1188–1199. doi:10.1200/JCO.19.00010

List, A., Kurtin, S., Roe, D. J., Buresh, A., Mahadevan, D., Fuchs, D., et al. (2005). Efficacy of Lenalidomide in Myelodysplastic Syndromes. *N. Engl. J. Med.* 352, 549–557. doi:10.1056/NEJMoa041668

Ludwig, H., Delforge, M., Facon, T., Einsele, H., Gay, F., Moreau, P., et al. (2018). Prevention and Management of Adverse Events of Novel Agents in Multiple Myeloma: a Consensus of the European Myeloma Network. *Leukemia* 32, 1542–1560. doi:10.1038/s41375-018-0040-1

Mateos, M. V., Hernández, M. T., Giraldo, P., de la Rubia, J., de Arriba, F., López Corral, L., et al. (2013). Lenalidomide Plus Dexamethasone for High-Risk Smoldering Multiple Myeloma. *N. Engl. J. Med.* 369, 438–447. doi:10.1056/NEJMoa1300439

Mitsiades, C. S., Mitsiades, N., Munshi, N. C., and Anderson, K. C. (2004). Focus on Multiple Myeloma. *Cancer Cell* 6, 439–444. doi:10.1016/j.ccr.2004.10.020

Mueller-Schoell, A., Groenland, S. L., Scherf-Clavel, O., van Dyk, M., Huisinga, W., Michelet, R., et al. (2021). Therapeutic Drug Monitoring of Oral Targeted Antineoplastic Drugs. *Eur. J. Clin. Pharmacol.* 77, 441–464. doi:10.1007/s00228-020-03014-8

Sung, H., Ferlay, J., Siegel, R. L., Laversanne, M., Soerjomataram, I., Jemal, A., et al. (2021). Global Cancer Statistics 2020: GLOBOCAN Estimates of Incidence and Mortality Worldwide for 36 Cancers in 185 Countries. *CA Cancer J. Clin.* 71, 209–249. doi:10.3322/caac.21660

Velghe, S., and Stove, C. P. (2018). Volumetric Absorptive Microsampling as an Alternative Tool for Therapeutic Drug Monitoring of First-Generation Anti-epileptic Drugs. *Anal. Bioanal. Chem.* 410, 2331–2341. doi:10.1007/s00216-018-0866-4

Wicha, S. G., Kees, M. G., Solms, A., Minichmayr, I. K., Kratzer, A., and Kloft, C. (2015). TDMx: a Novel Web-Based Open-Access Support Tool for Optimising Antimicrobial Dosing Regimens in Clinical Routine. *Int. J. Antimicrob. Agents* 45, 442–444. doi:10.1016/j.ijantimicag.2014.12.010

Zhou, L., Yu, Q., Wei, G., Wang, L., Huang, Y., Hu, K., et al. (2021). Measuring the Global, Regional, and National Burden of Multiple Myeloma from 1990 to 2019. *BMC Cancer* 21, 606. doi:10.1186/s12885-021-08280-y

Conflict of Interest: The authors declare that the research was conducted in the absence of any commercial or financial relationships that could be construed as a potential conflict of interest.

Publisher's Note: All claims expressed in this article are solely those of the authors and do not necessarily represent those of their affiliated organizations, or those of the publisher, the editors and the reviewers. Any product that may be evaluated in this article, or claim that may be made by its manufacturer, is not guaranteed or endorsed by the publisher.

frontiers | Frontiers in Pharmacology

TYPE Original Research
PUBLISHED 12 August 2022
DOI 10.3389/fphar.2022.953178

OPEN ACCESS

EDITED BY
Miao Yan,
Second Xiangya Hospital, Central South University, China

REVIEWED BY
Yubo Li,
Tianjin University of Traditional Chinese Medicine, China
Nili Schamroth Pravda,
Rabin Medical Center, Israel
Rossella Rella,
ASL Roma, Italy

*CORRESPONDENCE
Ellen Thompson,
ethompson@marshall.edu

SPECIALTY SECTION
This article was submitted to Pharmacology of Anti-Cancer Drugs, a section of the journal Frontiers in Pharmacology

RECEIVED 25 May 2022
ACCEPTED 28 July 2022
PUBLISHED 12 August 2022

CITATION
Pillai SS, Pereira DG, Bonsu G, Chaudhry H, Puri N, Lakhani HV, Tirona MT, Sodhi K and Thompson E (2022), Biomarker panel for early screening of trastuzumab -induced cardiotoxicity among breast cancer patients in west virginia.
Front. Pharmacol. 13:953178.
doi: 10.3389/fphar.2022.953178

Biomarker panel for early screening of trastuzumab -induced cardiotoxicity among breast cancer patients in west virginia

Sneha S. Pillai[1], Duane G. Pereira[1], Gloria Bonsu[1], Hibba Chaudhry[1], Nitin Puri[1], Hari Vishal Lakhani[1], Maria Tria Tirona[2], Komal Sodhi[1] and Ellen Thompson[3]*

[1]Departments of Surgery and Biomedical Sciences, Marshall University Joan C. Edwards School of Medicine, Huntington, WV, United States, [2]Department of Oncology, Edwards Comprehensive Cancer Center, Marshall University Joan C. Edwards School of Medicine, Huntington, WV, United States, [3]Division of Cardiology, Department of Internal Medicine, Marshall University Joan C. Edwards School of Medicine, Huntington, WV, United States

Cardiotoxicity is a well-known pathophysiological consequence in breast cancer patients receiving trastuzumab. Trastuzumab related cardiotoxicity typically results in an overall decline in cardiac function, primarily characterized by reduction in left ventricular ejection fraction (LVEF) and development of symptoms associated with heart failure. Current strategies for the monitoring of cardiac function, during trastuzumab therapy, includes serial echocardiography, which is cost ineffective as well as offers limited specificity, while offering limited potential in monitoring early onset of cardiotoxicity. However, biomarkers have been shown to be aberrant prior to any detectable functional or clinical deficit in cardiac function. Hence, this study aims to develop a panel of novel biomarkers and circulating miRNAs for the early screening of trastuzumab induced cardiotoxicity. Patients with clinical diagnosis of invasive ductal carcinoma were enrolled in the study, with blood specimen collected and echocardiography performed prior to trastuzumab therapy initiation at baseline, 3- and 6-months post trastuzumab therapy. Following 6-months of trastuzumab therapy, about 18% of the subjects developed cardiotoxicity, as defined by reduction in LVEF. Our results showed significant upregulation of biomarkers and circulating miRNAs, specific to cardiac injury and remodeling, at 3- and 6-months post trastuzumab therapy. These biomarkers and circulating miRNAs significantly correlated with the cardiac injury specific markers, troponin I and T. The findings in the present study demonstrates the translational applicability of the proposed biomarker panel in early preclinical diagnosis of trastuzumab induced cardiotoxicity, further allowing management of cardiac function decline and improved health outcomes for breast cancer patients.

KEYWORDS

Cardiotoxicity after chemotherapy, biomarkers, Cardiac dysfunction, microRNA, breast cancer

Introduction

The manifestation of cardiotoxicity induced by chemotherapeutic agents is a well-established pathophysiological consequence which may lead to chronic, progressive and often irreversible cardiac damage (Florescu et al., 2013). The mitigation of the cancerous growth using conventional course of treatment by cytotoxic chemotherapeutic agents often presents with cardiovascular risks. Hence, it is essential to identify strategies to prevent chemotherapy related cardiac dysfunction (CRCD) and improve long term health outcomes for patients. This is particularly relevant for female population afflicted with breast cancer, which accounted for more than 2 million new cases worldwide in 2020, making it the most common form of cancer detected amongst women (Lukasiewicz et al., 2021). Given the rural and poor socioeconomic characteristics of West Virginia, the factors such as obesity, diabetes, and access to mammography screening will influence the poorer outcomes for women with breast cancer in West Virginia (Abraham et al., 2009). Hence the unusually high incidence of breast cancer has a strong inverse correlation with both annual income and educational achievement, which resulted in ranking West Virginia as 41st in the United States (Vona-Davis et al., 2008). Furthermore, approximately 1 in 4 women in West Virginia have been afflicted with breast cancer, according to the West Virginia Department of Health and Human Resources (WV DHHR). While treatment options for breast cancer varies depending on the differentiated subtypes, trastuzumab remains one of the common therapeutic regimens, a humanized monoclonal antibody engineered to specifically target human epidermal growth factor receptor 2 (HER2) proteins (Kitani et al., 2019; Waks and Winer, 2019)

Although administering trastuzumab to early and metastatic HER2+ breast cancer patients along with other chemotherapeutic treatments improves their survival by 50%, patients often develop early cardiomyopathy which can later progress to ventricular dysfunction succeeding treatment completion (Portera et al., 2008). This is suggested to be partially attributed to the mechanism of action through which trastuzumab regulates HER2 proteins. More specifically, the cardiotoxic effects are proposed to be induced by trastuzumab interfering with HER2 function in cardiomyocytes thereby impeding their cardioprotective effects as well as the increased production of reactive oxygen species (ROS) (Mohan et al., 2017). The cumulative line of evidence suggests that trastuzumab induces type II reversible cardiotoxicity thereby suggesting that the risk of developing cardiac damage is dose-dependent and can typically be reversed through modulation of treatment (Onitilo et al., 2014). These cardiotoxic effects are exhibited through decreased left ventricular ejection fraction (LVEF) as well as heart failure in more severe cases (Huszno et al., 2013; Nowsheen et al., 2018). In fact, nearly 25% of HER2+ breast cancer patients experience a significant decline in asymptomatic LVEF and as many as 4.0% of patients experience symptomatic heart failure (Romond et al., 2012; Goldhirsch et al., 2013).

Several strategies have been proposed to reduce trastuzumab-induced cardiotoxicity, though none are studied in controlled clinical trials. These strategies include establishing stringent LVEF criteria for patient selection, monitoring cardiac function during therapy, discontinuing potentially cardiotoxic therapy when cardiotoxicity arises, and instituting heart failure medications early (Armenian et al., 2017). Current standards of monitoring CRCD suggests performing periodic echocardiography, which not only merely identifies cardiac damage once it has already developed, but also lacks the sensitivity and specificity required to serve as an effective prognostic tool that can be utilized for early screening (Jensen et al., 2002; Swain et al., 2003; Lakhani et al., 2018). Furthermore, given the poor cost-effectiveness of this conventional method of serial echocardiography, there have been limited implementation of such strategy, which poses economic burden, in a rural community like West Virginia. It is important to identify alternative and more cost-effective strategies allowing a prompt identification of drug-induced cardiotoxicity to prevent their aggravation.

In this study, we aim to create a panel of biomarkers and circulating miRNAs, to detect trastuzumab induced cardiotoxicity, prior to manifestation of clinical deficits in cardiac function. These biomarkers, including cardiac myosin light chain 1 (cMLC1), growth differentiation factor 15 (GDF-15) and placental growth factor (PIGF), have been shown to be aberrant prior to any detectable functional or clinical deficit in cardiac function. In addition, integration of miRNAs, including miR-34a, miR-21, miR-133, miR-1 and miR-30e, which are having significant role in cardiac function, will offer a superior prognostic modality. The prognostic approach using comprehensive assessment of panel of biomarkers is minimally invasive, highly cost effective and provides high specificity, proving to be a superior modality over conventionally utilized serial echocardiography (Mayeux, 2004; Cho, 2011). The effective utilization of this panel of biomarker may allow early detection of cardiotoxicity, resulting in early implementation of treatment and/or chemotherapy cessation.

Material and methods

Study design and patient population

All studies were performed in accordance with the guidelines and regulations outlined in the Declaration of Helsinki on the use and enrollment of human research subjects. The study was approved by the institutional review board (IRB) and ethics committee of Cabell Huntington Hospital and Marshall University Joan C. Edwards School of Medicine, WV (IRB

No.: 866164). Trained hospital personnel reviewed the electronic medical records (EMR) and ensured an appropriate selection of the eligible patients, with rigorous confidentiality measures and HIPAA compliance. All subjects voluntarily participating in the study were briefed about the use of blood sample for this clinical study, signed the informed consent form (ICF) and agreed to the study follow up protocols.

Specifically, a total of 17 Caucasian female subjects were recruited for the study, who were visiting the Edwards Comprehensive Cancer Center at Cabell Huntington Hospital, WV. All patients of age >18 years and <80 years having a new clinical diagnosis of invasive ductal carcinoma, Stages IA (T1b-1c) to III A, having positive HER-2 receptor status (by IHC or FISH), scheduled to receive anti-HER2 therapy consisting of trastuzumab (with or without pertuzumab) were included in the study. The first 12 to 18 weeks of trastuzumab was given in combination with taxanes (weekly paclitaxel x 12 weeks or docetaxel (with or without carboplatin) every 3 weeks x 6 cycles). The trastuzumab regimen was administered at 4 mg/kg intravenous (IV) loading dose on week 1 followed by 2 mg/kg IV weekly in combination with weekly paclitaxel starting week 1 for a total of 12 doses followed by maintenance dose of trastuzumab at 6 mg/kg IV q3 weeks to complete one year of treatment ; or 8 mg/kg IV loading dose on day 1 followed by 6 mg/kg q3 weeks in combination with docetaxel x 6 cyces followed by maintenance dose of trastuzumab at 6 mg/kg IV q3 weeks to complete one year in the adjuvant setting.

Blood specimens were collected, and periodic echocardiography was performed on patients consenting to the participation in the study, at predetermined intervals: prior to the initiation of trastuzumab therapy (baseline; T0), at 3-months (T1) and 6-months (T2) post-initiation of the trastuzumab therapy. According to the exclusion criteria, any patient <18 years or >80 years old, patients with any second cancer, concurrent or prior history of chemotherapy and/or chest radiation therapy, history of myocardial infarction, cardiomyopathy or any cardiovascular dysfunction, hereditary iron metabolism disorder and hyaluronan synthase 3 gene (HAS3) polymorphisms, hematologic disorder, autoimmune disease, or any chronic diseases were excluded from the study during the patient screening process, as described previously (Lakhani et al., 2021). In addition, patients with LVEF ≤50%, as determined by echocardiography, history of symptomatic or asymptomatic heart failure, use of antihypertensive medications, antibiotics, weight loss medications or use of any medication for a chronic disease were also excluded from the study during the review of EMR for patient eligibility (Lakhani et al., 2021). Based on the periodic echocardiography at the predetermined intervals, including baseline, 3-months and 6-months post trastuzumab therapy initiation, cardiotoxicity was determined in the subjects according to the guidelines set forth by Cardiac Review and Evaluation Committee: symptomatic heart failure with a reduction of ≥5% to <55% from baseline in LVEF or an asymptomatic heart failure with a reduction of ≥10% to <55% from baseline in LVEF (Sawaya et al., 2011; Sawaya et al., 2012; Florescu et al., 2013; Ky et al., 2014).

Another set of 17 female subjects were also enrolled which served as the healthy controls. These age and sex matched healthy controls were enrolled, having no new onset of invasive ductal carcinoma or prior clinical history of any form of cancer, cardiovascular disease, in addition to applicability of all the exclusion criteria defined above. The appropriate confidentiality measures and consenting protocols, using ICF, were followed as detailed above. Patients wishing to participate in the study consented to the withdrawal of blood specimen and echocardiography procedure.

Collection of blood specimen

Blood specimen was collected from all the eligible patients meeting the inclusion/exclusion criteria, consenting to participate in the study, as described previously (Lakhani et al., 2018; Pillai et al., 2020; Lakhani et al., 2021). As defined in the study protocol, patient follow up was maintained and blood specimen was collected, by trained hospital personnel, at baseline (before initiation of trastuzumab therapy), at 3-months and 6-months post trastuzumab therapy initiation. At each study interval, approximately 10mL of blood was withdrawn from antecubital vein and collected in the BD Vacutainer tubes, as described previously (Lakhani et al., 2021). Within 30 min of collection, each blood specimen was processed by centrifugation at 4000 rpm for 10 min under temperature of 4°C. Plasma obtained from these samples was further aliquoted in appropriately labelled Eppendorf tubes to avoid continuous freeze-thaw cycles at the time of their use. All aliquots were stored at -80°C and utilized for the quantitative measurement of biomarker levels and assessment of circulating levels of miRNA expression.

Quantitative assessment of plasma biomarkers

Plasma samples were used for the quantitative assessment of biomarkers by enzyme linked immunosorbent assays (ELISAs). Commercially available kits were used and the manufacturer's protocol was followed for each of the following biomarkers: Human GDF-15 (Abcam, United States), Human PIGF (Abcam, United States), Human cardiac MLC1 (MyBioSource, United States), Human cardiac Troponin T (MyBioSource, United States) and Human cardiac Troponin I (Abcam, United States). Each assay was performed using technical duplicates for each sample to minimize statistical error. The manufacturer's

provided antigen-specific coated 96-well plate was used for each assay, and the color produced at the end of the assay was read at 450nm wavelength in BioTek ELx900 Absorbance Reader, as described previously. The concentrations for each biomarker in each sample was calculated based on the standard curve, and the resulting equation from the line of best fit.

Expression of circulating plasma miRNA

Total RNA was extracted from human plasma samples using miRNeasy Serum/Plasma Kit (Qiagen, United States), according to the manufacturer's protocol, followed by synthesis of cDNA using miRCURY LNA RT Kit (Qiagen, United States) with a total of 50 ng RNA for each reaction, as described previously. Next, miRNA specific primers were used, combined with SYBR Green master mix, to perform RT-PCR reaction of 7,500 Fast Real Time PCR System (Applied Biosystems, United States). The miRNA expression was normalized using an internal control and a synthetic spike-in. For every sample, two technical replicates were used for the qRT-PCR amplification, to minimize the statistical error. The averages of the comparative threshold cycle (C_t) values were used to calculate the amplification and relative fold change expression in the final analysis. Following is the sequence of human miRNA primers (Qiagen, United States), used in the study:

hsa-miR-34a-5p -5′UGGCAGUGUCUUAGCUGGUUGU

hsa-miR-21–5p -5′UAGCUUAUCAGACUGAUGUUGA

has-miR-133a-3p -5′UUUGGUCCCCUUCAACCAGCUG

hsa-miR-1-3p -5′UGGAAUGUAAAGAAGUAUGUAU

has-miR-30e-5p -5′UGUAAACAUCCUUGACUGGAAG

Transthoracic echocardiography assessment

Transthoracic echocardiography was performed in the Cardiology Clinic at Cabell Huntington Hospital, WV. Echocardiography was performed on all healthy controls as well as each subject with breast cancer, at predetermined intervals (baseline, 3-months and 6-months), as outlined above in the study protocol. 2D Doppler and color flow imaging was used by a certified echocardiography technician using Philip TE 33 with S transducer in an ICAEL-accredited laboratory, as described previously (Lakhani et al., 2018; Lakhani et al., 2021). Echocardiography procedures were performed in accordance with the guidelines set forth by the American Society of Echocardiography (Nagueh et al., 2016). Each echocardiography image was read by the physicians who were blinded to the study groups and subjects. The LVEF was further calculated by 2D imaging, as described previously (Shaver et al., 2016).

Statistical Analysis

The study was designed, conducted, recorded, analyzed, and interpreted without any bias, further ensuring that all results and data generated are reproducible. The statistical analysis, for all the data for each biomarker and circulating miRNA expression, was performed using GraphPad Prism 8.0. Bartlett's test was used for data for each biomarker at each study interval to ensure equal variance. The data was tested for normality and subjected to parametric analysis. To identify the statistical significance among the mean plasma levels of biomarkers and circulating miRNA expression, one-way ANOVA was performed, followed by Tukey's post-hoc t-test for multiple comparison. All significance was assigned at $p<0.05$ or $p<0.01$ for confidence interval of 95% or 99%, respectively. Each bar represents values as means ± standard error or mean (SEM). Correlation analysis was performed between cardiac injury specific markers, cardiac troponin I and cardiac troponin T, and each biomarker and circulating miRNA expression. The extent of correlation was determined by Pearson's *r* coefficient using a 95% confidence interval and choosing two-tailed p-value to determined significance (alpha = 0.05), as described previously (Pillai et al., 2020; Lakhani et al., 2021).

Results

Patient demographics, clinical profile and echocardiography assessment

The subjects with breast cancer had an average tumor size of 2.97 cm ± 0.53 (Table 1). The assessment of clinical parameters in the laboratory panel, showed no significant difference at any of the study intervals, baseline, 3- and 6-months (Table 1). These clinical parameters included albumin, alkaline phosphatase, alanine transaminase (ALT), aspartate aminotransferase (AST), total bilirubin, blood urea nitrogen (BUN), creatinine, total protein, and N-terminal (NT)-pro B-type natriuretic peptide (BNP). Furthermore, assessment of echocardiography parameters also showed no significant difference at any of the study intervals, suggestive of no apparent cardiac function decline in the overall population (Table 1). Since numerous clinical trials have defined cardiotoxicity as the serial decline in LVEF (Alexander et al., 1979; Schwartz et al., 1987; Seidman et al., 2002; Cocco et al., 2022), it is important to note that when each subject was assessed, there were 3 isolated events of cardiotoxicity noted. Specifically, these 3 subjects (approximately 18% of the total population) met the criteria of cardiotoxicity, defined by the Cardiac Review and Evaluation Committee, at 6-months post trastuzumab therapy showing a significant LVEF decline of 19% (LVEF of 42% at 6-months), 24% (LVEF of 50% at 6-month) and 6.6%

TABLE 1 Summary of patient demographics, clinical parameters, and echocardiography measurements. This table provides demographics of the study subjects including their clinical profile and echocardiography measurements at each study interval of baseline (prior to trastuzumab therapy initiation), 3-months and 6-months post trastuzumab therapy initiation. There was no statistical significance among any of the parameters at any defined study interval. Values are presented as means ± SEM.

	Healthy Controls	Invasive ductal Carcinoma
Sample Size (n)	17	17
Age (years)	61.2 ± 2.0	51.6 ± 3.2
Tumor Size (cm)	N/A	2.97 ± 0.53

Clinical Data (Patients with Invasive Ductal Carcinoma)

	Baseline (Prior to trastuzumab therapy)	3-months (After trastuzumab therapy)	6-months (After trastuzumab therapy)
Albumin (g/dl)	3.7 ± 0.1	3.6 ± 0.1	3.3 ± 0.2
Alkaline Phosphatase (U/L)	85.8 ± 6.6	82.0 ± 5.7	82.7 ± 6.8
SGPT (ALT) (U/L)	25.4 ± 4.1	33.3 ± 9.2	28.4 ± 6.3
SGOT (AST)	17.6 ± 2.9	17.9 ± 2.4	19.2 ± 2.6
Bilirubin, Total (mg/dl)	0.51 ± 0.09	0.36 ± 0.06	0.44 ± 0.08
BUN (mg/dl)	12.9 ± 1.4	11.7 ± 1.3	13.1 ± 1.1
Creatinine (mg/dl)	0.85 ± 0.03	0.80 ± 0.04	0.87 ± 0.05
Protein, Total (g/dl)	7.6 ± 0.1	7.4 ± 0.1	7.3 ± 0.1
NT-proBNP (pg/ml)	141.1 ± 42.4	179.6 ± 68.8	146.9 ± 89.3

Echocardiography (Patients with Invasive Ductal Carcinoma)

	Baseline (Prior to trastuzumab therapy)	3-months (After trastuzumab therapy)	6-months (After trastuzumab therapy)
Systolic Blood Pressure (mmHg)	135.4 ± 3.6	131.9 ± 4.5	130.8 ± 3.8
Diastolic Blood Pressure (mmHg)	81.6 ± 1.4	80.4 ± 1.9	78.6 ± 2.5
Heart Rate (bpm)	78.6 ± 3.3	86.4 ± 2.2	85.1 ± 3.9
LV Ejection Fraction (%)	62.0 ± 1.3	58.4 ± 1.4	57.8 ± 2.0
LV Diastolic Volume (ml)	77.4 ± 3.9	78.5 ± 5.4	79.9 ± 5.0
LV Systolic Volume (ml)	29.8 ± 2.0	31.2 ± 2.9	33.9 ± 2.8
LV Stroke Volume (ml)	47.6 ± 2.5	47.3 ± 2.9	46.0 ± 3.3
LV Cardiac Output (L/min)	3.7 ± 0.2	4.1 ± 0.3	3.8 ± 0.3
LV Cardiac Index (L/min/m2)	1.9 ± 0.1	2.1 ± 0.1	1.9 ± 0.1

(LVEF of 54% at 6-months) from baseline, developing either symptomatic or asymptomatic heart failure.

Assessment of plasma biomarkers

Our results showed significantly upregulated levels of cardiac troponin I and troponin T, which are highly specific markers of myocardial injury, at 3-months and 6-months post trastuzumab initiation, as compared to healthy controls (Figures 1A,B). When compared to baseline, the levels of cardiac troponin I was significantly upregulated at 6-months, while level of cardiac troponin T was significantly upregulated at 3- and 6-months (Figures 1A,B). Furthermore, we observed a significant upregulation of a pro-angiogenic marker, PIGF, at 3-month and 6-months post trastuzumab initiation, as compared to healthy controls and baseline (Figure 1C). Subsequently, the level of cMLC1, a marker of cardiomyocyte damage and injury, was also significantly upregulated at 3-months and 6-months, as compared to healthy controls (Figure 1D). Oxidative stress is one of the important mechanisms through which trastuzumab promotes cardiotoxicity, while previous studies have elucidated the functional role of GDF-15 in mediating oxidative stress. To this end, our study showed significantly elevated levels of GDF-15 at 3-and 6-months post-trastuzumab initiation, as compared to healthy controls

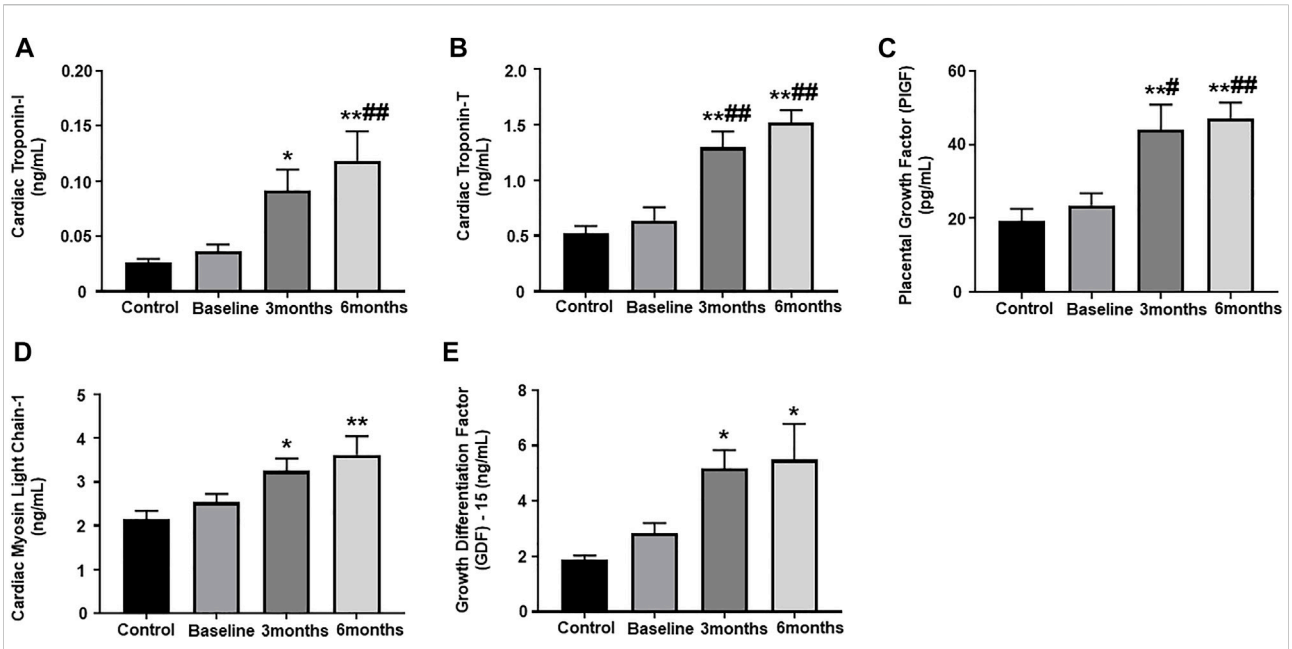

FIGURE 1
Assessment of plasma biomarkers. Quantitative analysis of plasma biomarker concentrations by ELISA: **(A)** cardiac troponin I, **(B)** cardiac troponin T, **(C)** placental growth factor (PlGF), **(D)** cardiac myosin light chain 1 (cMLC1), **(E)** growth differentiation factor 15 (GDF-15). Values represent means ± SEM. *$p < 0.05$ vs. Control, **$p < 0.01$ vs. Control, #$p < 0.05$ vs. Baseline, ##$p < 0.01$ vs. Baseline.

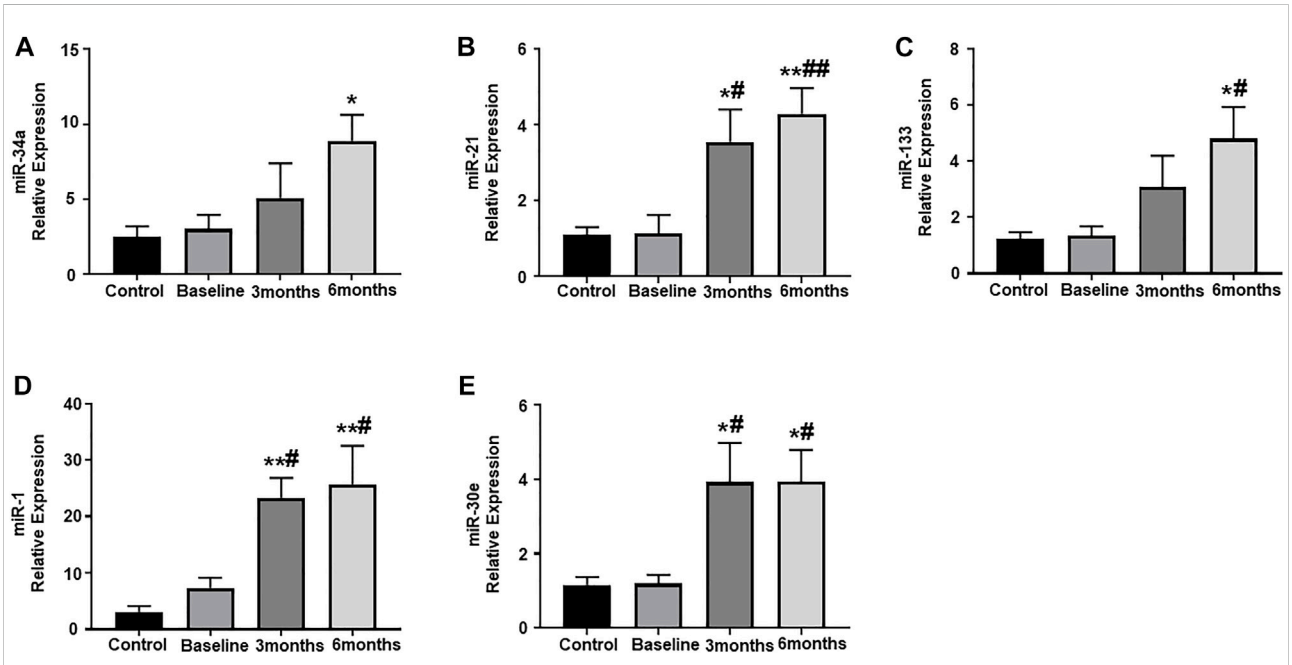

FIGURE 2
Assessment of circulating plasma miRNA expression. Quantitative analysis of circulating plasma miRNA expression by qRT-PCR: **(A)** miR-34a, **(B)** miR-21, **(C)** miR-133, **(D)** miR-1, **(E)** miR-30e. Values represent means ± SEM. *$p < 0.05$ vs. Control, **$p < 0.01$ vs. Control, #$p < 0.05$ vs. Baseline, ##$p < 0.01$ vs. Baseline.

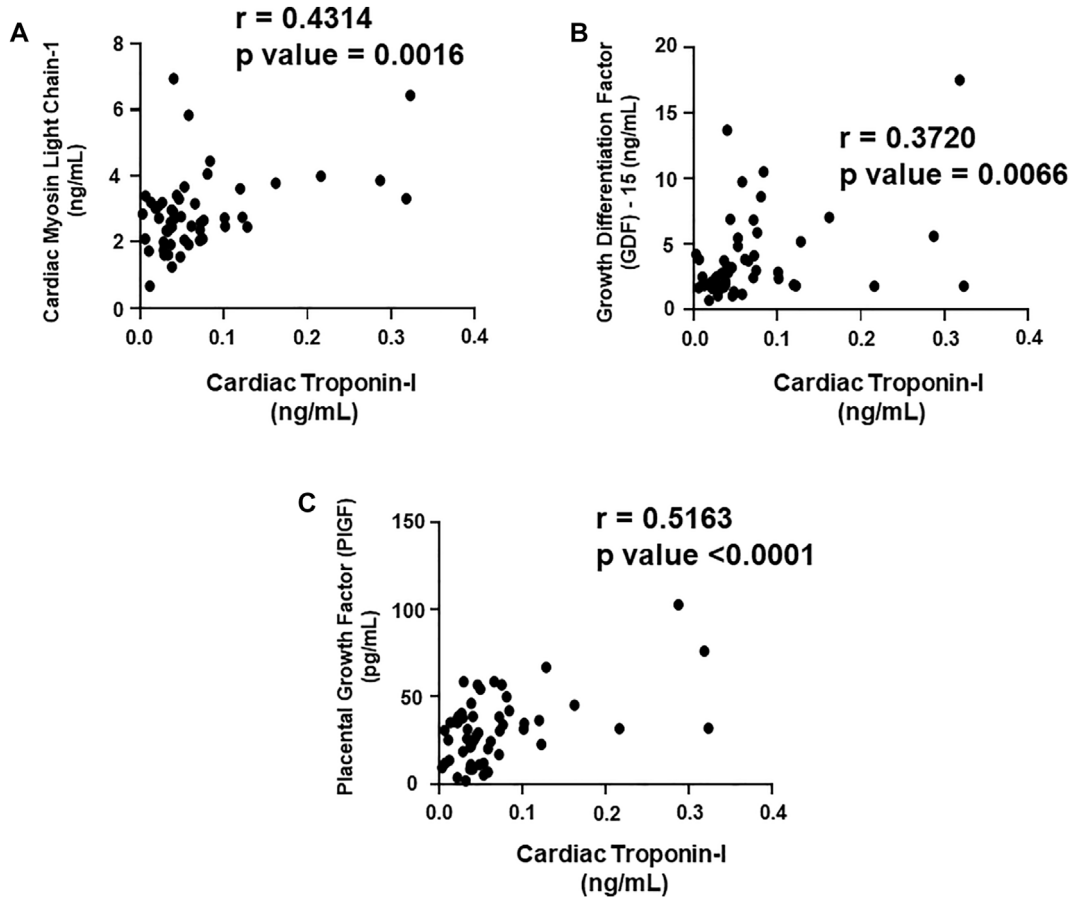

FIGURE 3
Correlation analysis of cardiac troponin I with plasma biomarkers. Correlation analysis was performed using a scatter plot between cardiac troponin I and plasma biomarkers, **(A)** cardiac myosin light chain 1 (cMLC1), **(B)** growth differentiation factor 15 (GDF-15) and **(C)** placental growth factor (PlGF). Pearson's *r* coefficient was used to determine the extent of correlation and statistical significance was obtained by two-tailed *p*-value. Each plot independently demonstrates the correlation (Pearson's *r* coefficient) and significance (*p*—value).

(Figure 1E). There was no significant difference and progression in the levels of any of these biomarkers between 3-months and 6-months.

Assessment of circulating plasma miRNA expression

Plasma samples from our study subjects, obtained at pre-determined study intervals, were assessed for the expression of some important circulating miRNAs, which have been shown to play a crucial role in cardiac remodeling and exacerbation of cardiac dysfunction. In the present study, the expression of circulating miR-34a was significantly upregulated at 6-months post trastuzumab therapy initiation, as compared to healthy controls (Figure 2A). Subsequently, there was also significant upregulation in the expression of miR-21 at 3-and 6-month post trastuzumab therapy, as compared to baseline and healthy control (Figure 2B). The relative expression of miR-133 also showed marked increase at 6-months, as compared to baseline and healthy controls (Figure 2C). Next, we assessed the expression of miR-1 and miR-30e, which showed significant upregulation at 3- and 6-months, as compared to baseline and healthy controls (Figures 2D,E). There was no significant difference and progression in the levels of any of these circulating miRNAs between 3-months and 6-months.

Correlation of cardiac Troponin I and T with the plasma biomarkers and circulating miRNAs

We aimed to establish a correlation of our panel of biomarkers and miRNAs with cardiac Troponin I and T, which have been demonstrated to offer high sensitivity and specificity in response to changes in the left ventricular (LV)

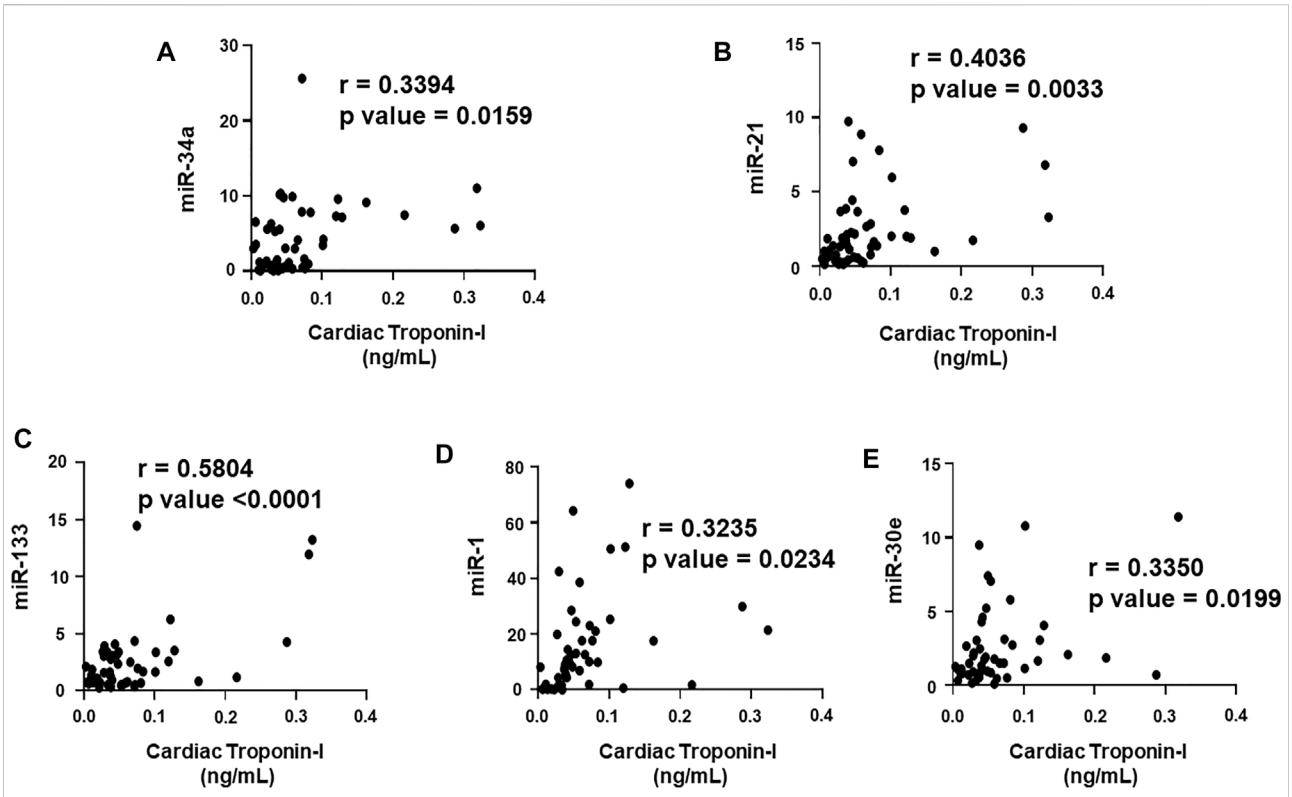

FIGURE 4
Correlation analysis of cardiac troponin I with circulating plasma miRNAs. Correlation analysis was performed using a scatter plot between cardiac troponin I and plasma miRNAs, **(A)** miR-34a, **(B)** miR-21, **(C)** miR-133, **(D)** miR-1, **(E)** miR-30e. Pearson's *r* coefficient was used to determine the extent of correlation and statistical significance was obtained by two-tailed *p*-value. Each plot independently demonstrates the correlation (Pearson's *r* coefficient) and significance (*p*—value).

function. The extent of correlation was established by plotting each biomarker against either cardiac troponin I or troponin T and determining the Pearson's *r* coefficient. Our results showed significant and positive correlation of cardiac troponin I with each biomarker, cMLC1 (r = 0.4314), GDF-15 (r = 0.3720) and PIGF (r = 0.5163), offering confidence interval of >99% (Figures 3A–C). Subsequently, cardiac troponin I also showed strong positive correlation with all miRNAs, miR-34a (r = 0.3394), miR-21 (r = 0.4036), miR-133 (r = 0.5804), miR-1 (r = 0.3235) and miR-30e (r = 0.3350) (Figures 4A–E). Furthermore, high sensitive cardiac troponin T also showed a significant and positive correlation with cMLC1 (r = 0.3006), GDF-15 (r = 0.3784) and PIGF (r = 0.3745) (Figures 5A–C). Finally, a significant positive correlation was observed between cardiac troponin T with each miRNA, miR-34a (r = 0.3882), miR-21 (r = 0.4744), miR-133 (r = 0.4242), miR-1 (r = 0.4372) and miR-30e (r = 0.4920), all at confidence interval of >99% (Figures 6A–E). Our correlation analysis offers strong evidence for the viability and utility of this panel of biomarkers for the early screening of trastuzumab induced cardiotoxicity in breast cancer patients.

Discussion

Cardiotoxicity emerges as one of the most prevalent and a well-known pathophysiological consequence of chemotherapy in breast cancer patients. The chemotherapy induced cardiotoxicity is characterized by reduction in LVEF, which is often augmented by the progressive cardiac damage caused by the mechanisms specific to the chemotherapeutic regimens, including trastuzumab (Figure 7). Although the rates for new female breast cancer cases have been steadily increasing in the past four decades, the mortality have only slightly decreased, which is attributed to the development of effective multimodality treatments. Cardiac comorbidity present high risk for the patient receiving adjuvant and neoadjuvant therapies consisting of trastuzumab (Onitilo et al., 2014), thereby hindering the potential benefits posed by these chemotherapeutic treatments by significantly reducing the quality of life for survivors. However, trastuzumab-induced cardiotoxicity is dose-dependent (Copeland-Halperin et al., 2019), indicating that appropriate cardiac surveillance during chemotherapy may enable prevention as well as attenuation of intrinsic cardiac damage prior to its onset. The current standard

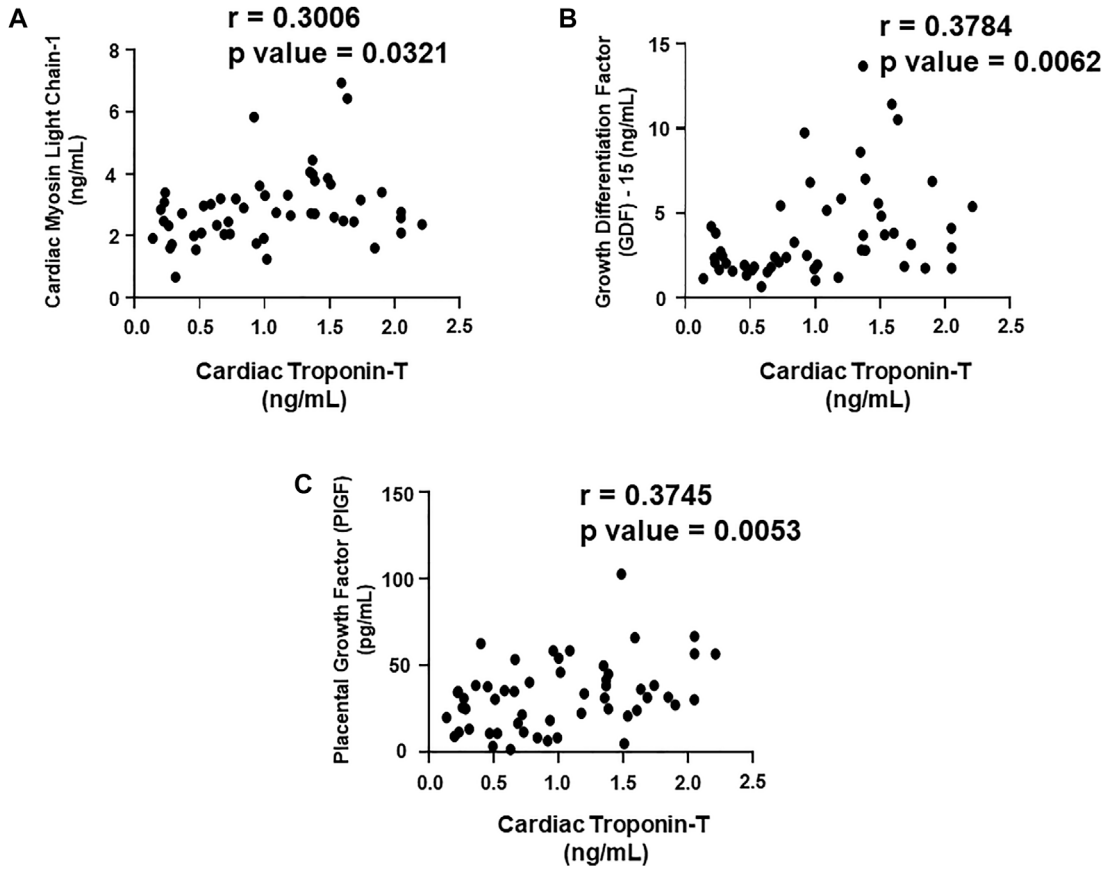

FIGURE 5
Correlation analysis of cardiac troponin T with plasma biomarkers. Correlation analysis was performed using a scatter plot between cardiac troponin T and plasma biomarkers, **(A)** cardiac myosin light chain 1 (cMLC1), **(B)** growth differentiation factor 15 (GDF-15) and **(C)** placental growth factor (PlGF). Pearson's *r* coefficient was used to determine the extent of correlation and statistical significance was obtained by two-tailed *p*-value. Each plot independently demonstrates the correlation (Pearson's *r* coefficient) and significance (*p*—value).

of detection is by serial echocardiography, a non-invasive procedure that is conducted every three to six months (Tan and Scherrer-Crosbie, 2014). Although this method is effective at detecting cardiotoxicity, it lacks the specificity required to for the prognosis of progressive cardiac degeneration before it manifests into detectable cardiac dysfunction (Sawaya et al., 2012). Global longitudinal strain (GLS) is also another technique being used in clinical practice in order to detect early changes in left ventricular myocardial contractile function in chemotherapy-induced cardiotoxicity (Gripp et al., 2018; Karlsen et al., 2019; Cocco et al., 2022). Cardiac biomarkers offers high sensitivity and specificity, and provides the added benefit of cost-effectiveness, hence blood samples can be tested for biomarkers at closer intervals (Shams-Vahdati et al., 2014). Based on the current limitations in achieving consensus on reliable prognostic tools for early screening of trastuzumab induced cardiotoxicity, the present study identifies a novel panel of biomarkers and circulating plasma miRNAs, which have the potential of providing a superior prognostic modality than conventional approaches. In the present study, patients with breast cancer, receiving trastuzumab therapy, were monitored for progressive cardiac function decline at several time intervals, including pre-chemotherapy initiation, 3-months and 6-months post-chemotherapy initiation. Our results showed significant upregulation of cardiac troponin I and troponin T, which are well established and highly specific predictive markers of cardiac injury and cardiac function decline. These results were in concordance with our previously published findings that showed upregulation of cardiac troponin I and troponin T in anthracyclines induced cardiotoxicity at 3-months and 6-months post chemotherapy initiation (Kitayama et al., 2017; Simoes et al., 2018). The high prognostic efficacy of cardiac troponins has also been confirmed by multiple studies that have shown utilization of these markers for the early assessment of myocardial injury, cardiac degeneration, and remodeling, becoming an effective translational biomarker for cardiotoxicity in humans (Reagan

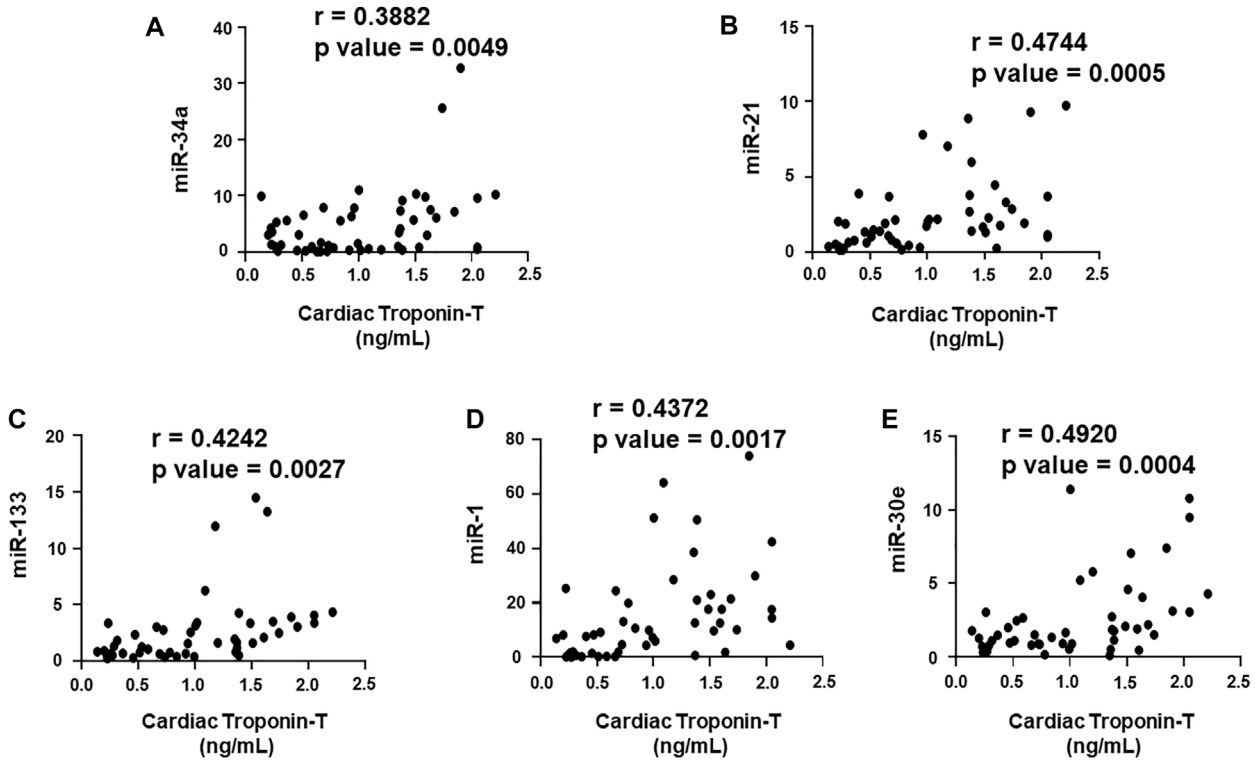

FIGURE 6
Correlation analysis of cardiac troponin T with circulating plasma miRNAs. Correlation analysis was performed using a scatter plot between cardiac troponin T and plasma miRNAs, **(A)** miR-34a, **(B)** miR-21, **(C)** miR-133, **(D)** miR-1, **(E)** miR-30e. Pearson's *r* coefficient was used to determine the extent of correlation and statistical significance was obtained by two-tailed *p*-value. Each plot independently demonstrates the correlation (Pearson's *r* coefficient) and significance (*p*—value).

et al., 2013). Hence, utility of these highly sensitive cardiac troponin markers may be highly effective in predicting early onset of cardiotoxicity.

Our study further sets out the prominence of an important pro-angiogenic biomarker, PIGF, which showed significant upregulation at 3-months and 6-months post-trastuzumab therapy initiation. In tumor cells, the expression of PIGF protein have been shown to undergo an angiogenic switch that promotes tumor vascularization (Chau et al., 2017; Saman et al., 2020). This upregulation of PIGF sustains the survival and metastasis of tumor cells while stimulating cardiac angiogenesis (Chau et al., 2017). The anti-metastatic and anti-angiogenic activity of trastuzumab targets the overexpression of HER2 receptors and vascular endothelial growth factor (VEGF) proteins, including PIGF, thereby inhibiting the cardioprotective effects of the HER neuroregulin-1 (NRG-1) ligand, as well as those induced by the cardiac angiogenesis of PIGF (Han et al., 2017). As a result, breast cancer patients administered chemotherapeutic treatments consisting of trastuzumab may be more inclined to develop cardiotoxic effects. Furthermore, a previous study has also shown upregulation of PIGF in breast cancer patients, undergoing combination therapy of anthracyclines and trastuzumab, followed by sensitivity analysis which showed increased risk of developing cardiotoxicity with an increase in the level of PIGF (Putt et al., 2015). Hence, the upregulation of PIGF, as noted in the present study, may be highly relevant to the pathophysiology of trastuzumab-induced cardiotoxicity and could potentially serve as a prognostic marker for cardiac dysfunction following trastuzumab exposure.

Apart from that, upregulated levels of GDF-15 have been predominately studied in relation to major adverse cardiac incidents such as myocardial infarction or heart failure (Kempf et al., 2007; Wollert et al., 2017). GDF-15, a protein member of TGF-β superfamily, have been shown to be highly elevated as a result of cardiomyocytes secreting these proteins in response to stimuli indicative of oxidative stress, myocardial ischemia, proinflammatory cytokines, lower peripheral blood mononuclear cell (PBMC) telomerase activity and cancer (Adela and Banerjee, 2015; Liu et al., 2021). Since oxidative stress is fundamental to the mechanism through which trastuzumab induces cardiotoxicity, the use of this important biomarker is viable in early screening of CRCD. Our results showed significant upregulation of GDF-15 at 3-months and 6-

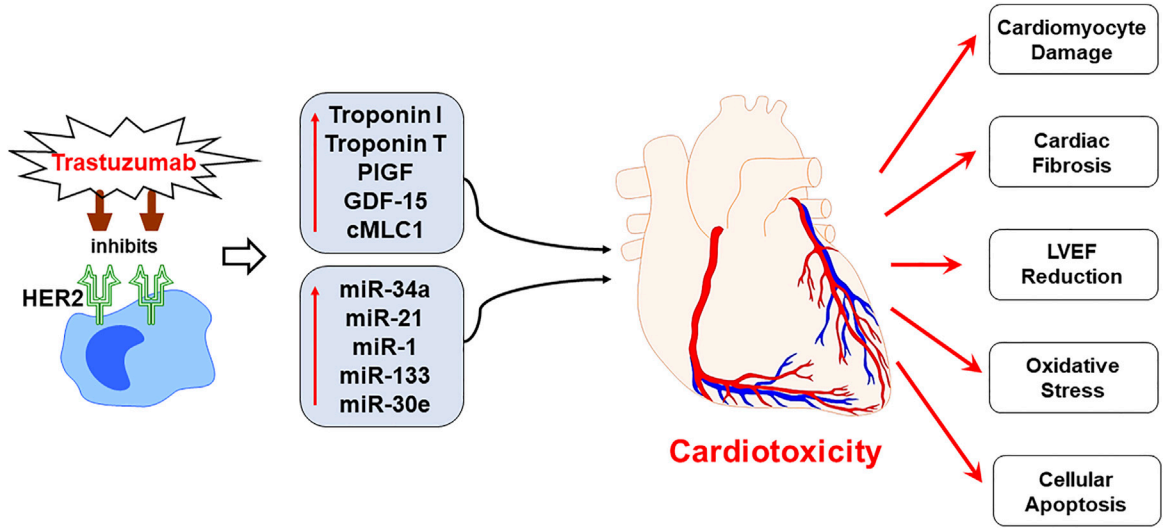

FIGURE 7
Schematic representation demonstrating the progression of trastuzumab induced cardiotoxicity. Chemotherapeutic regimen, trastuzumab, specifically inhibits the human epidermal growth factor receptor 2 (HER2) receptor to negate the cancerous cell growth and survival, as a mechanism of action. However, trastuzumab treatment upregulates the expression of plasma biomarkers and circulating miRNA, that are primarily involved in the regulation of cardiac function. The mechanistic action of trastuzumab induces cardiotoxicity by cardiomyocyte damage, cardiac fibrosis, LVEF decline, oxidative stress and cellular apoptosis. Since the panel of proposed biomarkers and miRNAs is specifically involved in the cardiac remodeling and regulation of cardiac function, their upregulated expression can predict cardiotoxicity before it is apparent on echocardiography. Hence, the utility of the proposed panel in clinical practice is viable for the early prognosis of trastuzumab induced cardiotoxicity.

months post chemotherapy initiation, which was in line with the functional role of this biomarker. The findings in the present study were also in concordance with previous studies that positively correlated elevated levels of GDF-15 with cardiac dysfunction in breast cancer patients (Tromp et al., 2020), receiving chemotherapeutic agents, further supporting the predictive utility of this biomarker. Subsequently, the present study also elucidates the potential role of cMLC1, as a biomarker of trastuzumab induced cardiotoxicity. The component of a multimeric protein complex, myosin, cMLC1 is known to facilitate cardiac muscle contractions (England and Loughna, 2013). The circulating levels of cMLC1 has been shown to be upregulated during the injury or damage of cardiomyocytes, as this induces the myocardium to secrete these proteins into circulation (Stejskal et al., 2005). Our study showed significant upregulation of cMLC1 at 3- and 6-months post trastuzumab initiation, suggestive of myocardial damage and progressive decline in cardiac function. These findings were in concordance with previous studies in murine models, which showed that mice treated with trastuzumab exhibited significant damage to cardiac myofibers, suggesting that the structural changes induced by the cardiotoxic effects of trastuzumab diminishes the contractile potential of the heart (Elzarrad et al., 2013). Furthermore, the study also showed significant decline in the cardiac function, which was evident by the echocardiography assessment of these trastuzumab treated mice. Hence, the findings in the presents study and the evidence from literature advocates the potential use of cMLC1 as a predictive biomarker for trastuzumab-induced cardiotoxicity.

The role of miRNAs, as biomarkers, have been increasingly gaining attention as they regulate the transcription of genes associated with the disease progression and offer high sensitivity in detecting early pathophysiological changes associated with the diseased condition (Cho, 2011). The present study further elucidates the intrinsic role and translational applicability of plasma miRNAs in cardiac remodeling, subsequently providing evidence of their prognostic utility in predicting risks of trastuzumab induced cardiotoxicity. Several studies have shown the important clinical utility of highly sensitive miRNAs, due to their specific roles in cardiac injury, inflammation, fibrosis and apoptosis (Cho, 2011). To this end, our results showed significant upregulation of miR-34a, which is primarily expressed in cardiac tissues, after 6-months of trastuzumab therapy. Several studies have shown pro-apoptotic effects of miR-34a on cardiomyocytes as well as mediator of oxidative stress, subsequently showing a positive correlation of elevated expression of miR-34a with cardiotoxicity (Piegari et al., 2016; Pellegrini et al., 2020). Our previous study also showed upregulation of miR-34a in anthracyclines induced cardiotoxicity (Lakhani et al., 2021). Although the role of

miRNA-34a in response to trastuzumab has not yet been elucidated in detail, the present study supports the prospective utility of this miRNA in monitoring the cardiotoxic effects induced by trastuzumab treatment, prior to cardiac dysfunction. Apart from that, we also assessed the role of miR-21, which is primarily dysregulated in response to ischemic injury of the heart, precipitated by oxidative stress or inflammation (Wu et al., 2015). Studies have shown that the inhibition of miR-21 expression improves interstitial fibrosis and cardiac function, suggestive of its role in cardiac structural remodeling (Surina et al., 2021). The cardiotoxic effects of trastuzumab is most notably manifested through reduced LVEF, which is characterized by myocardial interstitial fibrosis. Hence, suggesting that circulating levels of miR-21 may serve as a potential predictor trastuzumab induced cardiotoxicity. Notably, our results also showed marked upregulation of miR-21 at 3-months and 6-months post trastuzumab initiation. In addition, our results also showed significant upregulation of miR-133 after 6-months of trastuzumab therapy. The clinical utility of miR-133, as prognostic marker of trastuzumab induced cardiotoxicity, is supported by the evidence in the literature that shows expression of this miRNA primarily in muscle tissues (Yu et al., 2014). Furthermore, miR-133 have been shown to participate in cardiac remodeling, specifically causing cardiac fibrosis and hypertrophy, due to its role in cellular proliferation, hypertrophic growth and electrical remodeling, affecting cardiac dysfunction (Xiao et al., 2019). Hence, cardiac changes ascertained by miR-133 support its role as a prognostic marker for cardiotoxicity. The cumulative line of evidence also showed an important role of miR-1 in chemotherapy induced cardiotoxicity. The upregulation of miR-1 has been shown to cause redox imbalance by direct suppression of antioxidant factors in cardiomyocytes, hence promoting oxidant stress as well as subsequent apoptotic activity leading to cardiac damage (Ai et al., 2010; Zhou et al., 2013). Previous studies have also demonstrated the potential role of miR-1 in causing anthracyclines induced cardiotoxicity, offering superior modality than cardiac troponin I (Rigaud et al., 2017). While the role of miR-1 has not been previously explored in trastuzumab induced cardiotoxicity, our results are in concordance with previous observations, suggesting its utility as a viable prognostic marker. Subsequently, our results showed upregulation of miR-30e in trastuzumab administered breast cancer subjects. Studies have shown that miR-30e has a functional role as a pro-apoptotic factor and promotes autophagy (Zheng et al., 2018). The increased expression of miR-30e and subsequent excessive autophagy results in the cardiomyocyte death during myocardial injury (Li et al., 2018).

Together, the present study demonstrates strong translational utility of the proposed biomarker panel in predicting early onset of trastuzumab induced cardiotoxicity in patients with breast cancer. Despite the strong statistical outcomes of the present study, there were several limitations of the study. The viability of the proposed panel can be further strengthened by confirming the present findings in a large population prior to implementation in a clinical practice. As taxane itself has cardiotoxicity properties, the initial combination therapy with taxane may interfere with the cardiotoxicity induced by trastuzumab therapy. Furthermore, another limitation of the study was the short follow up period of up to 6-months only, since cardiotoxicity can become apparent as the treatment progresses, hence, also affect the level of the proposed biomarkers. Despite the small sample size and shorter follow up period, our results showed apparent cardiotoxicity in about 18% of the patients after only 6-months of trastuzumab therapy. However, the present study still offers crucial evidence and a cost effective, non-invasive predictive modality demonstrating the efficacy of the proposed panel of biomarkers. With advances in the understanding the mechanisms operant in trastuzumab induced cardiotoxicity, more biomarkers may be added to this panel that may be highly specific to the molecular changes in cardiac tissues, induced by trastuzumab therapy. Furthermore, the utilization of this panel in patients with highest risk of cardiotoxicity, due to comorbidities, may allow to monitor cardiotoxic manifestation by trastuzumab therapy. The proposed panel offers a viable guide to the clinicians in developing mitigation strategies, including dose adjustments, mitigation of cardiovascular risks, or alternate treatment therapies. These mitigation strategies can be tailored based on the cumulative evidence including, susceptibility of the patients to develop cardiotoxicity, prior risk factors, presence of other acute or chronic conditions, and finally levels of these biomarkers. The panel will help monitor high risk group for cardiotoxicity, which may need more surveillance during therapy. Nevertheless, the implementation of this panel of biomarkers may improve health outcomes and reduce mortality associated with chemotherapy induced cardiotoxicity.

Data availability statement

The original contributions presented in the study are included in the article/supplementary material, further inquiries can be directed to the corresponding author.

Ethics statement

The studies involving human participants were reviewed and approved by The institutional review board (IRB) and ethics committee of Cabell Huntington Hospital and Marshall University Joan C. Edwards School of Medicine, WV (IRB No.: 866164). The patients/participants provided their written informed consent to participate in this study.

Author contributions

Conceptualization: KS, MT, and ET; writing—original draft preparation: SP; investigation/methodology: SP, DP, GB, HC, NP, and HL; writing—review and editing, NP, MT, ET, and KS; supervision: ET; funding acquisition: KS.

Funding

This research was supported by NIH Bench-to-Bedside award made possible by the Office of Research on Women's Health (ORWH) 736214 (to K.S.) and Cancer Research Fund by The Edwards Foundation Inc.

Acknowledgments

We would also like to acknowledge Keshia Bowen, RN and Lora Maynard, RN, from Edwards Comprehensive Cancer Center of Cabell Huntington Hospital for their contribution and assistance in patient enrollment and blood collection.

Conflict of interest

The authors declare that the research was conducted in the absence of any commercial or financial relationships that could be construed as a potential conflict of interest.

Publisher's note

All claims expressed in this article are solely those of the authors and do not necessarily represent those of their affiliated organizations, or those of the publisher, the editors and the reviewers. Any product that may be evaluated in this article, or claim that may be made by its manufacturer, is not guaranteed or endorsed by the publisher.

References

Abraham, J., Flanagan, M., Hazard, H., Jubelirer, S., Tirona, M. T., and Vona-Davis, L. (2009). *Triple-negative breast cancer in West Virginia*, *W V. Med. J.*, 105. 54–59.

Adela, R., and Banerjee, S. K. (2015). GDF-15 as a target and biomarker for diabetes and cardiovascular diseases: A translational prospective. *J. Diabetes Res.* 2015, 490842. doi:10.1155/2015/490842

Ai, J., Zhang, R., Li, Y., Pu, J., Lu, Y., Jiao, J., et al. (2010). Circulating microRNA-1 as a potential novel biomarker for acute myocardial infarction. *Biochem. Biophys. Res. Commun.* 391, 73–77. doi:10.1016/j.bbrc.2009.11.005

Alexander, J., Dainiak, N., Berger, H. J., Goldman, L., Johnstone, D., Reduto, L., et al. (1979). Serial assessment of doxorubicin cardiotoxicity with quantitative radionuclide angiocardiography. *N. Engl. J. Med.* 300, 278–283. doi:10.1056/NEJM197902083000603

Armenian, S. H., Lacchetti, C., Barac, A., Carver, J., Constine, L. S., Denduluri, N., et al. (2017). Prevention and monitoring of cardiac dysfunction in survivors of adult cancers: American society of clinical oncology clinical practice guideline. *J. Clin. Oncol.* 35, 893–911. doi:10.1200/JCO.2016.70.5400

Chau, K., Hennessy, A., and Makris, A. (2017). Placental growth factor and pre-eclampsia. *J. Hum. Hypertens.* 31, 782–786. doi:10.1038/jhh.2017.61

Cho, W. C. (2011). Circulating MicroRNAs as minimally invasive biomarkers for cancer theragnosis and prognosis. *Front. Genet.* 2, 7. doi:10.3389/fgene.2011.00007

Cocco, L. D., Chiaparini, A. F., Saffi, M. a. L., and Leiria, T. L. L. (2022). Global longitudinal strain for the early detection of chemotherapy-induced cardiotoxicity: A systematic review and meta-analysis. *Clin. Oncol.* 34, 514–525. doi:10.1016/j.clon.2022.05.001

Copeland-Halperin, R. S., Liu, J. E., and Yu, A. F. (2019). Cardiotoxicity of HER2-targeted therapies. *Curr. Opin. Cardiol.* 34, 451–458. doi:10.1097/HCO.0000000000000637

Elzarrad, M. K., Mukhopadhyay, P., Mohan, N., Hao, E., Dokmanovic, M., Hirsch, D. S., et al. (2013). Trastuzumab alters the expression of genes essential for cardiac function and induces ultrastructural changes of cardiomyocytes in mice. *PLoS One* 8, e79543. doi:10.1371/journal.pone.0079543

England, J., and Loughna, S. (2013). Heavy and light roles: Myosin in the morphogenesis of the heart. *Cell. Mol. Life Sci.* 70, 1221–1239. doi:10.1007/s00018-012-1131-1

Florescu, M., Cinteza, M., and Vinereanu, D. (2013). Chemotherapy-induced cardiotoxicity. *Maedica (Bucur)* 8, 59–67.

Goldhirsch, A., Gelber, R. D., Piccart-Gebhart, M. J., De Azambuja, E., Procter, M., Suter, T. M., et al. (2013). 2 years versus 1 year of adjuvant trastuzumab for HER2-positive breast cancer (HERA): An open-label, randomised controlled trial. *Lancet* 382, 1021–1028. doi:10.1016/S0140-6736(13)61094-6

Gripp, E. A., Oliveira, G. E., Feijo, L. A., Garcia, M. I., Xavier, S. S., and Sousa, A. S. (2018). Global longitudinal strain accuracy for cardiotoxicity prediction in a cohort of breast cancer patients during anthracycline and/or trastuzumab treatment. *Arq. Bras. Cardiol.* 110, 140–150. doi:10.5935/abc.20180021

Han, X., Zhou, Y., and Liu, W. (2017). Precision cardio-oncology: Understanding the cardiotoxicity of cancer therapy. *NPJ Precis. Oncol.* 1, 31. doi:10.1038/s41698-017-0034-x

Huszno, J., Les, D., Sarzyczny-Slota, D., and Nowara, E. (2013). Cardiac side effects of trastuzumab in breast cancer patients - single centere experiences. *Contemp. Oncol.* 17, 190–195. doi:10.5114/wo.2013.34624

Jensen, B. V., Skovsgaard, T., and Nielsen, S. L. (2002). Functional monitoring of anthracycline cardiotoxicity: A prospective, blinded, long-term observational study of outcome in 120 patients. *Ann. Oncol.* 13, 699–709. doi:10.1093/annonc/mdf132

Karlsen, S., Dahlslett, T., Grenne, B., Sjoli, B., Smiseth, O., Edvardsen, T., et al. (2019). Global longitudinal strain is a more reproducible measure of left ventricular function than ejection fraction regardless of echocardiographic training. *Cardiovasc. Ultrasound* 17, 18. doi:10.1186/s12947-019-0168-9

Kempf, T., Von Haehling, S., Peter, T., Allhoff, T., Cicoira, M., Doehner, W., et al. (2007). Prognostic utility of growth differentiation factor-15 in patients with chronic heart failure. *J. Am. Coll. Cardiol.* 50, 1054–1060. doi:10.1016/j.jacc.2007.04.091

Kitani, T., Ong, S. G., Lam, C. K., Rhee, J. W., Zhang, J. Z., Oikonomopoulos, A., et al. (2019). Human-induced pluripotent stem cell model of trastuzumab-induced cardiac dysfunction in patients with breast cancer. *Circulation* 139, 2451–2465. doi:10.1161/CIRCULATIONAHA.118.037357

Kitayama, H., Kondo, T., Sugiyama, J., Kurimoto, K., Nishino, Y., Kawada, M., et al. (2017). High-sensitive troponin T assay can predict anthracycline- and trastuzumab-induced cardiotoxicity in breast cancer patients. *Breast Cancer* 24, 774–782. doi:10.1007/s12282-017-0778-8

Ky, B., Putt, M., Sawaya, H., French, B., Januzzi, J. L., Jr., Sebag, I. A., et al. (2014). Early increases in multiple biomarkers predict subsequent cardiotoxicity in patients with breast cancer treated with doxorubicin, taxanes, and trastuzumab. *J. Am. Coll. Cardiol.* 63, 809–816. doi:10.1016/j.jacc.2013.10.061

Lakhani, H. V., Khanal, T., Gabi, A., Yousef, G., Alam, M. B., Sharma, D., et al. (2018). Developing a panel of biomarkers and miRNA in patients with myocardial

infarction for early intervention strategies of heart failure in West Virginian population. *PLoS One* 13, e0205329. doi:10.1371/journal.pone.0205329

Lakhani, H. V., Pillai, S. S., Zehra, M., Dao, B., Tirona, M. T., Thompson, E., et al. (2021). Detecting early onset of anthracyclines-induced cardiotoxicity using a novel panel of biomarkers in West-Virginian population with breast cancer. *Sci. Rep.* 11, 7954. doi:10.1038/s41598-021-87209-8

Li, X., Hu, X., Wang, J., Xu, W., Yi, C., Ma, R., et al. (2018). Inhibition of autophagy via activation of PI3K/Akt/mTOR pathway contributes to the protection of hesperidin against myocardial ischemia/reperfusion injury. *Int. J. Mol. Med.* 42, 1917–1924. doi:10.3892/ijmm.2018.3794

Liu, H., Huang, Y., Lyu, Y., Dai, W., Tong, Y., and Li, Y. (2021). GDF15 as a biomarker of ageing. *Exp. Gerontol.* 146, 111228. doi:10.1016/j.exger.2021.111228

Lukasiewicz, S., Czeczelewski, M., Forma, A., Baj, J., Sitarz, R., and Stanislawek, A. (2021). Breast cancer-epidemiology, risk factors, classification, prognostic markers, and current treatment strategies-an updated review. *Cancers (Basel)* 13, 4287. doi:10.3390/cancers13174287

Mayeux, R. (2004). Biomarkers: Potential uses and limitations. *NeuroRx* 1, 182–188. doi:10.1602/neurorx.1.2.182

Mohan, N., Jiang, J., and Wu, W. J. (2017). Implications of autophagy and oxidative stress in trastuzumab-mediated cardiac toxicities. *Austin Pharmacol. Pharm.* 2, 1005.

Nagueh, S. F., Smiseth, O. A., Appleton, C. P., Byrd, B. F., 3rd, Dokainish, H., Edvardsen, T., et al. (2016). Recommendations for the evaluation of left ventricular diastolic function by echocardiography: An update from the American society of echocardiography and the European association of cardiovascular imaging. *J. Am. Soc. Echocardiogr.* 29, 277–314. doi:10.1016/j.echo.2016.01.011

Nowsheen, S., Aziz, K., Park, J. Y., Lerman, A., Villarraga, H. R., Ruddy, K. J., et al. (2018). Trastuzumab in female breast cancer patients with reduced left ventricular ejection fraction. *J. Am. Heart Assoc.* 7, e008637. doi:10.1161/JAHA.118.008637

Onitilo, A. A., Engel, J. M., and Stankowski, R. V. (2014). Cardiovascular toxicity associated with adjuvant trastuzumab therapy: Prevalence, patient characteristics, and risk factors. *Ther. Adv. Drug Saf.* 5, 154–166. doi:10.1177/2042098614529603

Pellegrini, L., Sileno, S., D'agostino, M., Foglio, E., Florio, M. C., Guzzanti, V., et al. (2020). *MicroRNAs in Cancer Treatment-Induced Cardiotoxicity*, 12.*Cancers (Basel)*

Piegari, E., Russo, R., Cappetta, D., Esposito, G., Urbanek, K., Dell'aversana, C., et al. (2016). MicroRNA-34a regulates doxorubicin-induced cardiotoxicity in rat. *Oncotarget* 7, 62312–62326. doi:10.18632/oncotarget.11468

Pillai, S. S., Lakhani, H. V., Zehra, M., Wang, J., Dilip, A., Puri, N., et al. (2020). Predicting nonalcoholic fatty liver disease through a panel of plasma biomarkers and MicroRNAs in female West Virginia population. *Int. J. Mol. Sci.* 21, E6698. doi:10.3390/ijms21186698

Portera, C. C., Walshe, J. M., Rosing, D. R., Denduluri, N., Berman, A. W., Vatas, U., et al. (2008). Cardiac toxicity and efficacy of trastuzumab combined with pertuzumab in patients with [corrected] human epidermal growth factor receptor 2-positive metastatic breast cancer. *Clin. Cancer Res.* 14, 2710–2716. doi:10.1158/1078-0432.CCR-07-4636

Putt, M., Hahn, V. S., Januzzi, J. L., Sawaya, H., Sebag, I. A., Plana, J. C., et al. (2015). Longitudinal changes in multiple biomarkers are associated with cardiotoxicity in breast cancer patients treated with doxorubicin, taxanes, and trastuzumab. *Clin. Chem.* 61, 1164–1172. doi:10.1373/clinchem.2015.241232

Reagan, W. J., York, M., Berridge, B., Schultze, E., Walker, D., and Pettit, S. (2013). Comparison of cardiac troponin I and T, including the evaluation of an ultrasensitive assay, as indicators of doxorubicin-induced cardiotoxicity. *Toxicol. Pathol.* 41, 1146–1158. doi:10.1177/0192623313482056

Rigaud, V. O., Ferreira, L. R., Ayub-Ferreira, S. M., Avila, M. S., Brandao, S. M., Cruz, F. D., et al. (2017). Circulating miR-1 as a potential biomarker of doxorubicin-induced cardiotoxicity in breast cancer patients. *Oncotarget* 8, 6994–7002. doi:10.18632/oncotarget.14355

Romond, E. H., Jeong, J. H., Rastogi, P., Swain, S. M., Geyer, C. E., Jr., Ewer, M. S., et al. (2012). Seven-year follow-up assessment of cardiac function in NSABP B-31, a randomized trial comparing doxorubicin and cyclophosphamide followed by paclitaxel (ACP) with ACP plus trastuzumab as adjuvant therapy for patients with node-positive, human epidermal growth factor receptor 2-positive breast cancer. *J. Clin. Oncol.* 30, 3792–3799. doi:10.1200/JCO.2011.40.0010

Saman, H., Raza, S. S., Uddin, S., and Rasul, K. (2020). Inducing angiogenesis, a key step in cancer vascularization, and treatment approaches. *Cancers (Basel)* 12, E1172. doi:10.3390/cancers12051172

Sawaya, H., Sebag, I. A., Plana, J. C., Januzzi, J. L., Ky, B., Cohen, V., et al. (2011). Early detection and prediction of cardiotoxicity in chemotherapy-treated patients. *Am. J. Cardiol.* 107, 1375–1380. doi:10.1016/j.amjcard.2011.01.006

Sawaya, H., Sebag, I. A., Plana, J. C., Januzzi, J. L., Ky, B., Tan, T. C., et al. (2012). Assessment of echocardiography and biomarkers for the extended prediction of cardiotoxicity in patients treated with anthracyclines, taxanes, and trastuzumab. *Circ. Cardiovasc. Imaging* 5, 596–603. doi:10.1161/CIRCIMAGING.112.973321

Schwartz, R. G., Mckenzie, W. B., Alexander, J., Sager, P., D'souza, A., Manatunga, A., et al. (1987). Congestive heart failure and left ventricular dysfunction complicating doxorubicin therapy. Seven-year experience using serial radionuclide angiocardiography. *Am. J. Med.* 82, 1109–1118. doi:10.1016/0002-9343(87)90212-9

Seidman, A., Hudis, C., Pierri, M. K., Shak, S., Paton, V., Ashby, M., et al. (2002). Cardiac dysfunction in the trastuzumab clinical trials experience. *J. Clin. Oncol.* 20, 1215–1221. doi:10.1200/JCO.2002.20.5.1215

Shams-Vahdati, S., Vand-Rajavpour, Z., Paknezhad, S. P., Piri, R., Moghaddasi-Ghezeljeh, E., Mirabolfathi, S., et al. (2014). Cost-effectiveness of cardiac biomarkers as screening test in acute chest pain. *J. Cardiovasc. Thorac. Res.* 6, 29–33. doi:10.5681/jcvtr.2014.006

Shaver, A., Nichols, A., Thompson, E., Mallick, A., Payne, K., Jones, C., et al. (2016). Role of serum biomarkers in early detection of diabetic cardiomyopathy in the West virginian population. *Int. J. Med. Sci.* 13, 161–168. doi:10.7150/ijms.14141

Simoes, R., Silva, L. M., Cruz, A., Fraga, V. G., De Paula Sabino, A., and Gomes, K. B. (2018). Troponin as a cardiotoxicity marker in breast cancer patients receiving anthracycline-based chemotherapy: A narrative review. *Biomed. Pharmacother.* 107, 989–996. doi:10.1016/j.biopha.2018.08.035

Stejskal, D., Lacnak, B., Andelova, K., Skvarilova, M., and Bartek, J. (2005). MCL-1 (myosin light chains-1) in differential diagnosis of dyspnea. *Biomed. Pap. Med. Fac. Univ. Palacky. Olomouc Czech. Repub.* 149, 89–91. doi:10.5507/bp.2005.010

Surina, S., Fontanella, R. A., Scisciola, L., Marfella, R., Paolisso, G., and Barbieri, M. (2021). miR-21 in human cardiomyopathies. *Front. Cardiovasc. Med.* 8, 767064. doi:10.3389/fcvm.2021.767064

Swain, S. M., Whaley, F. S., and Ewer, M. S. (2003). Congestive heart failure in patients treated with doxorubicin: A retrospective analysis of three trials. *Cancer* 97, 2869–2879. doi:10.1002/cncr.11407

Tan, T. C., and Scherrer-Crosbie, M. (2014). Cardiac complications of chemotherapy: Role of imaging. *Curr. Treat. Options Cardiovasc. Med.* 16, 296. doi:10.1007/s11936-014-0296-3

Tromp, J., Boerman, L. M., Sama, I. E., Maass, S., Maduro, J. H., Hummel, Y. M., et al. (2020). Long-term survivors of early breast cancer treated with chemotherapy are characterized by a pro-inflammatory biomarker profile compared to matched controls. *Eur. J. Heart Fail.* 22, 1239–1246. doi:10.1002/ejhf.1758

Vona-Davis, L., Rose, D. P., Hazard, H., Howard-Mcnatt, M., Adkins, F., Partin, J., et al. (2008). Triple-negative breast cancer and obesity in a rural Appalachian population. *Cancer Epidemiol. Biomarkers Prev.* 17, 3319–3324. doi:10.1158/1055-9965.EPI-08-0544

Waks, A. G., and Winer, E. P. (2019). Breast cancer treatment: A review. *JAMA* 321, 288–300. doi:10.1001/jama.2018.19323

Wollert, K. C., Kempf, T., and Wallentin, L. (2017). Growth differentiation factor 15 as a biomarker in cardiovascular disease. *Clin. Chem.* 63, 140–151. doi:10.1373/clinchem.2016.255174

Wu, K., Li, L., and Li, S. (2015). Circulating microRNA-21 as a biomarker for the detection of various carcinomas: An updated meta-analysis based on 36 studies. *Tumour Biol.* 36, 1973–1981. doi:10.1007/s13277-014-2803-2

Xiao, Y., Zhao, J., Tuazon, J. P., Borlongan, C. V., and Yu, G. (2019). MicroRNA-133a and myocardial infarction. *Cell Transpl.* 28, 831–838. doi:10.1177/0963689719843806

Yu, H., Lu, Y., Li, Z., and Wang, Q. (2014). microRNA-133: expression, function and therapeutic potential in muscle diseases and cancer. *Curr. Drug Targets* 15, 817–828. doi:10.2174/1389450115666140627104151

Zheng, J., Li, J., Kou, B., Yi, Q., and Shi, T. (2018). MicroRNA-30e protects the heart against ischemia and reperfusion injury through autophagy and the Notch1/Hes1/Akt signaling pathway. *Int. J. Mol. Med.* 41, 3221–3230. doi:10.3892/ijmm.2018.3548

Zhou, X., Mao, A., Wang, X., Duan, X., Yao, Y., and Zhang, C. (2013). Urine and serum microRNA-1 as novel biomarkers for myocardial injury in open-heart surgeries with cardiopulmonary bypass. *PLoS One* 8, e62245. doi:10.1371/journal.pone.0062245

frontiers | Frontiers in Pharmacology

TYPE Original Research
PUBLISHED 30 August 2022
DOI 10.3389/fphar.2022.944342

OPEN ACCESS

EDITED BY
Miao Yan,
Second Xiangya Hospital, Central South University, China

REVIEWED BY
Xiaojing Guo,
Second Military Medical University, China
Amit Krishna De,
Indian Science Congress Association, India

*CORRESPONDENCE
Chunxia Su,
susu_mail@126.com

SPECIALTY SECTION
This article was submitted to Pharmacology of Anti-Cancer Drugs, a section of the journal Frontiers in Pharmacology

RECEIVED 15 May 2022
ACCEPTED 04 August 2022
PUBLISHED 30 August 2022

CITATION
Chen J, Wen Y, Chu X, Liu Y and Su C (2022), Pulmonary adverse events associated with hypertension in non-small cell lung cancer patients receiving PD-1/PD-L1 inhibitors. *Front. Pharmacol.* 13:944342. doi: 10.3389/fphar.2022.944342

Pulmonary adverse events associated with hypertension in non-small cell lung cancer patients receiving PD-1/PD-L1 inhibitors

Jianing Chen[1,2], Yaokai Wen[1,2], Xiangling Chu[1,2], Yuzhi Liu[1,3] and Chunxia Su[1,2]*

[1]School of Medicine, Tongji University, Shanghai, China, [2]Department of Medical Oncology, Shanghai Pulmonary Hospital & Thoracic Cancer Institute, Tongji University, School of Medicine, Shanghai, China, [3]Department of Oncology, Shanghai East Hospital, Tongji University, School of Medicine, Shanghai, China

Introduction: Non-small cell lung cancer patients have gained therapeutic benefits from immune checkpoint inhibitors, although immune-related adverse events (irAEs) could be inevitable. Whether irAEs are associated with chronic diseases is still unclear, our study aims to clarify the distinct adverse events in NSCLC patients with concomitant hypertension.

Methods: Adverse event cases were searched and collected in the Food and Drug Administration (FDA) Adverse Event Reporting System (FAERS) database from January 2015 to December 2021. We performed disproportionality analysis to detect safety signals by calculating reporting odds ratios (ROR) and corresponding 95% confidence intervals (95% CIs), information component (IC), and the lower bound of the information component 95% credibility interval (IC_{025}).

Results: Among 17,163 NSCLC patients under treatment with single-agent anti-programmed death-1/programmed death ligand-1 (PD-1/PD-L1) inhibitor (nivolumab, pembrolizumab, cemiplimab, durvalumab, atezolizumab, and avelumab), 497 patients had hypertension while 16,666 patients had no hypertension. 4,283 pulmonary AEs were reported, including 166 patients with hypertension and 4,117 patients without hypertension. Compared with patients without hypertension, patients with hypertension were positively associated with increased reporting of interstitial lung disease (ROR = 3.62, 95%CI 2.68–4.89, IC = 1.54, IC_{025} = 0.57) among patients receiving anti-PD-1 treatment. The median duration of onset from the time of initiation of anti-PD-1 administration was 28 days (IQR, 12.00–84.25).

Conclusion: Our pharmacovigilance analysis showed the profile of pulmonary toxicities in NSCLC patients with hypertension caused by anti-PD-1/PD-L1 inhibitors. Interstitial lung disease was the statistically significant reporting adverse event in patients with hypertension receiving anti-PD-1 treatment.

KEYWORDS
pharmacovigilance, immune checkpoint inhibitor, hypertension, NSCLC, FAERS

Introduction

Immune checkpoint inhibitors (ICIs) that target the programmed death 1 receptor (PD-1) and programmed death-ligand 1 (PD-L1) have brought a durable long-term survival response to patients with malignant tumors. Nivolumab, pembrolizumab, cemiplimab, durvalumab, atezolizumab, and avelumab have been approved for non-small cell lung cancer (NSCLC). These approvals accelerated prescribing of these drugs in routine oncological practices. However, anti-tumor treatments also generate a series of unique dysimmune toxicities, which are termed as immune-related adverse events (irAEs) (Nishino et al., 2015; Tirumani et al., 2015; Michot et al., 2016). ICI-induced toxicities can cause suspension of the anti-tumor treatment, and some severe irAEs would impair life quality, even leading to death (Combs Scott and Pennell, 2017; Wang et al., 2018). Theoretically, irAEs can involve all organs and tissues (Champiat et al., 2016; Weber et al., 2017; Postow et al., 2018). Skin (Minkis et al., 2013; Abdel-Rahman et al., 2015), gastrointestinal tract (Di Giacomo et al., 2009; Gentile et al., 2013; Cheng et al., 2015), endocrine glands (Ryder et al., 2014; Albarel et al., 2015; Gaudy et al., 2015), and pulmonary system (Berthod et al., 2012; Barjaktarevic et al., 2013) are the most affected organs. The effective predictive biomarkers of irAEs are required to identify the risk for patients receiving anti-PD-1/PD-L1 administration. Patients with specific physical conditions are often at a high risk of irAEs. Therefore, before receiving immunotherapy, doctors need to carefully ask patients about their physical status. Patients with autoimmune disease (Kyi et al., 2014; Pedersen et al., 2014) and chronic infection (Sharma et al., 2013) are mentioned with a high risk of developing irAEs. Recently, biomarkers to predict irAEs have been reported, such as sex (Valpione et al., 2018), cytokines (Tarhini et al., 2015), autoantibodies (Duarte et al., 2018; Cortellini et al., 2019), TMB (Bomze et al., 2019), gut microbiome (Chaput et al., 2017), and multi-omics (Jing et al., 2020). However, the identification of candidate risk factors that prelude to irAEs is still a realm of highly unmet need.

Chronic conditions often lead to higher morbidity and mortality of malignant tumors. Aged patients with NSCLC are often associated with comorbidities, such as COPD, diabetes mellitus, hyperlipidemia, and hypertension. Hypertension, as a clinical factor, is the most frequently reported comorbidity in patients with malignancy, which has a reported prevalence of 38% (Piccirillo et al., 2004; Mouhayar and Salahudeen, 2011). Besides, hypertension is emerging as one of the most common side effects in NSCLC patients receiving immunotherapy (Garon et al., 2019). Its incidence increases significantly when combined with angiogenesis inhibitors including the anti-vascular endothelial growth factor (VEGF) monoclonal antibody bevacizumab (Jain et al., 2006; Ranpura et al., 2010; Syrigos et al., 2011) and certain small molecular inhibitors of tyrosine kinase (sunitinib, sorafenib, and pazopanib) (Riely and Miller, 2007).

The number of patients with lung cancer complicated with chronic diseases is very large, and the safety of immunotherapy in this population should not be ignored. However, patients with comorbidities such as uncontrolled hypertension are often excluded from oncological clinical trials. Whether patients with hypertension have a higher risk of irAEs is a lack of knowledge. Therefore, we aimed to investigate the association between irAEs and hypertension. Herein, we investigated the characteristics and risk factors of pulmonary ICI-related AEs through the FAERS database. Numerous researches suggested that the use of angiogenesis inhibitors can increase the risk of hypertension in cancer patients (Wu et al., 2008; Ranpura et al., 2010). In order to exclude the interference of other drug factors, our study only included reports of pulmonary adverse reactions after receiving single-agent immunotherapy.

Methods

Data Source and study design

Adverse event reports are available on FAERS database which is submitted by healthcare professionals, consumers, and manufacturers. The FAERS database contains demographic information, drug information, patient outcomes, and preferred terms (PTs) coded for the adverse events. These PTs are categorized into their primary system organ classes (SOCs) in the MedDRA and SOCs are equivalent to systematic classification in other medical terms. Our study was designed as a retrospective pharmacovigilance study. 14,072,154 FAERS records from January 2015 to December 2021 were included. According to the FDA's recommendation, duplicate reports were removed by case number in this study, with only the most recent case version adopted. After extraction and de-duplication of case reports, there were 112,764 unique reports for patients who used anti-PD-1 (nivolumab, pembrolizumab, and cemiplimab) or anti-PD-L1 (durvalumab, atezolizumab, avelumab), then we excluded adverse events caused by combined therapies, only 63,055 cases receiving monotherapy included. 17,163 cases of non-small cell lung cancer (lung adenocarcinoma, lung squamous cell carcinoma/squamous cell carcinoma of lung, adenosquamous cell lung cancer, large cell lung cancer, sarcoid carcinoma, and not specified type of NSCLC) were finally included in our study, including 4,283 respiratory, thoracic and mediastinal AE reports.

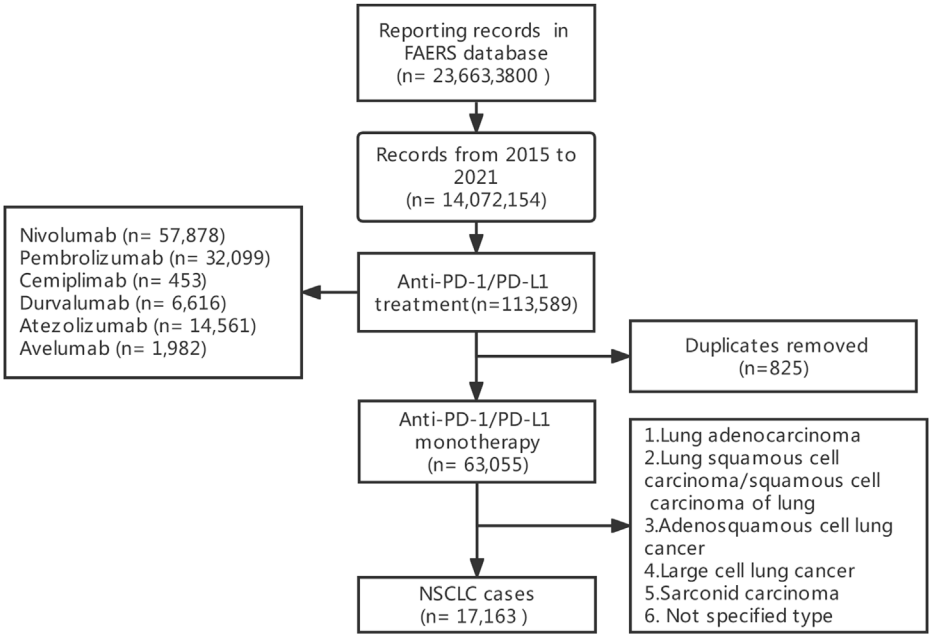

FIGURE 1
Flowchart of screening and inclusion of adverse reactions.

Severe adverse events were defined as death, life-threatening, disability, hospitalization, required for intervention, or any other outcomes.

Statistical Analysis

Disproportionality analysis was applied to measure safety signals for patients who used anti-PD-1/PD-L1 therapy with hypertension under study (Almenoff et al., 2007). We calculated reporting odds ratios (ROR), 95% confidence intervals (95% CIs) and the lower bound of a two-sided 95% interval of information component (IC_{025}) to detect potential associations between hypertension and irAEs (Bate et al., 1998; Bate et al., 2002; Bate and Evans, 2009). The calculation formulas for ROR and 95% CI were as follows: ROR = (a/c)/(b/d), 95% CI = $e^{\ln(ROR) \pm 1.96SQRT(1/a + 1/b + 1/c + 1/d)}$. a = Number of patients with hypertension who received anti-PD1/PD-L1 therapy and developed the target irAEs. b = No. of hypertensive patients receiving anti-PD1/PD-L1 therapy with other adverse effects. c = No. of patients without hypertension who received anti-PD1/PD-L1 therapy and developed the target irAEs. d = No. of patients without hypertension receiving anti-PD1/PD-L1 therapy with other adverse effects. The safety signal was considered to be statistically significant when the ROR was greater than 1.0, IC more than zero and $IC_{025} > 0$. We also calculated the time-to onset of adverse events. The formula of the time-to-onset of events was as follows: Time-to-onset = Event onset date–Therapy start date. The median and interquartile ranges (IQR) were also calculated to show the time to onset.

RStudio (version 4.1.1; Boston, MA, United States) was used for all statistical analyses and for generating graphs in our study.

Result

Descriptive Analysis

From 2015 to 2021, a total of 17,163 records were extracted (Figure 1), 497 patients were also diagnosed with hypertension 16,666 patients were diagnosed without hypertension. 4,283 (24.95%) were reported as respiratory thoracic and mediastinal AEs after using ICI regimes. Among them, 166 NSCLC patients were also diagnosed with hypertension. All demographic and clinical characteristics of patients were presented in Table 1. In the hypertensive and non-hypertensive groups, the proportion of males was higher than that of females. In the hypertensive group, the proportion of men (80.12%) was higher than that (67.09%) of the non-hypertensive group. In addition, compared to those aged younger than 65 years, higher percentage of patients older than 65 years in both cohorts (74.7%, 52.5%). Due to the severity of pulmonary irAEs, death was the most frequent

TABLE 1 Clinical characteristics of NSCLC patients with ICIs induced pulmonary toxicity, N (%).

	Hypertension (n = 166)	Without hypertension (n = 4,117)
Gender		
Male	133 (80.12)	2,762 (67.09)
Female	32 (19.28)	1,083 (26.31)
Missing	1 (0.60)	272 (6.61)
Age		
<65	34 (20.48)	1,134 (27.54)
≥65	124 (74.70)	2,176 (52.85)
Missing	8 (4.82)	807 (19.60)
Reporting year		
2015	16 (9.64)	164 (3.98)
2016	5 (3.01)	561 (13.63)
2017	38 (22.89)	728 (17.68)
2018	52 (31.33)	608 (14.77)
2019	35 (21.08)	506 (12.29)
2020	7 (4.22)	255 (6.19)
2021	3 (1.81)	156 (3.79)
Anti-PD-1		
Nivolumab	22 (13.25)	1784 (43.33)
Pembrolizumab	92 (55.42)	1,398 (33.96)
Cemiplimab	1 (0.60)	4 (0.10)
Anti-PD-L1		
Atezolizumab	20 (12.05)	325 (7.89)
Durvalumab	30 (18.07)	600 (14.57)
Avelumab	1 (0.60)	6 (0.15)
Outcome		
Death	76 (45.78)	1,437 (34.9)
Life-threatening	9 (5.42)	199 (4.83)
Hospitalization	68 (40.96)	1,270 (30.85)
Disability	2 (1.20)	19 (0.46)
Other serious	11 (6.63)	1,032 (25.07)
Non-Serious	0 (0)	160 (3.89)

report. Death (n = 76) was the most common outcome in hypertension cohort. Furthermore, death accounted for a larger proportion in hypertensive patients than that in non-hypertensive patients.

The number of adverse events for each drug

The distribution of SOCs for NSCLC patients was shown in Table 2. In total, general disorders (n = 4,493) and pulmonary disorders (n = 4,283) had the largest number of AEs. For patients receiving nivolumab, cemiplimab, or atezolizumab, the main irAEs were general disorders. For patients taking pembrolizumab, durvalumab or avelumab, the number of pulmonary disorders was the largest.

The spectrum of pulmonary irAEs differed in PD-1 inhibitors.

The pulmonary signal spectrum of different anti-PD-1 therapies was shown in Figure 2 and Supplemetary Table S1. Cumulative event rates of irAEs since the initiation of ICI were shown in Figure 3. According to ROR and Bayesian confidence propagation neural network (BCPNN) algorithm, interstitial lung disease (ROR = 3.62, 95%CI 2.68–4.89, IC = 1.54, IC_{025} = 0.57) with median time-to-onset of 28 (12.00–84.25) days (Supplemetary

TABLE 2 System Organ Classes (SOCs) for adverse events of PD-1/PD-L1 inhibitors, N (%).

SOCs	Total	Nivolumab	Pembrolizumab	Cemiplimab	Durvalumab	Atezolizumab	Avelumab
General disorders and administration site conditions	4,493 (0.13)	2,268 (13.86)	1,325 (0.11)	6 (0.10)	464 (0.12)	424 (0.15)	6 (0.10)
Respiratory, thoracic and mediastinal disorders	4,283 (0.12)	1806 (11.03)	1,490 (0.12)	5 (0.08)	630 (0.17)	345 (0.12)	7 (0.12)
Neoplasms benign, malignant and unspecified	3,827 (0.11)	1730 (10.57)	1,404 (0.11)	0 (0)	558 (0.15)	135 (0.05)	0 (0)
Gastrointestinal disorders	2,578 (0.07)	1,286 (7.86)	917 (0.07)	5 (0.08)	160 (0.04)	202 (0.07)	8 (0.13)
Infections and infestations	2,456 (0.07)	1,148 (7.01)	828 (0.07)	7 (0.12)	237 (0.06)	231 (0.08)	5 (0.08)
Nervous system disorders	1953 (0.05)	926 (5.66)	677 (0.05)	3 (0.05)	144 (0.04)	199 (0.07)	4 (0.07)
Investigations	1823 (0.05)	810 (4.95)	665 (0.05)	3 (0.05)	167 (0.04)	173 (0.06)	5 (0.08)
Injury, poisoning and procedural complications	1904 (0.05)	786 (4.80)	457 (0.04)	1 (0.02)	578 (0.15)	79 (0.03)	3 (0.05)
Musculoskeletal and connective tissue disorders	1,512 (0.04)	785 (4.80)	503 (0.04)	1 (0.02)	119 (0.03)	102 (0.04)	2 (0.03)
Skin and subcutaneous tissue disorders	1,650 (0.05)	746 (4.56)	666 (0.05)	3 (0.05)	108 (0.03)	125 (0.04)	2 (0.03)
Cardiac disorders	1,257 (0.04)	589 (3.60)	422 (0.03)	4 (0.07)	121 (0.03)	119 (0.04)	2 (0.03)
Metabolism and nutrition disorders	1,284 (0.04)	582 (3.56)	464 (0.04)	5 (0.08)	69 (0.02)	159 (0.06)	5 (0.08)
Blood and lymphatic system disorders	1,071 (0.03)	518 (3.16)	374 (0.03)	5 (0.08)	70 (0.02)	103 (0.04)	1 (0.02)
Endocrine disorders	1,107 (0.03)	469 (2.87)	477 (0.04)	2 (0.03)	89 (0.02)	67 (0.02)	3 (0.05)
Hepatobiliary disorders	1,253 (0.04)	434 (2.65)	584 (0.05)	8 (0.14)	95 (0.02)	131 (0.05)	1 (0.02)
Renal and urinary disorders	912 (0.03)	371 (2.27)	398 (0.03)	0 (0)	41 (0.01)	102 (0.04)	0 (0)
Vascular disorders	616 (0.02)	296 (1.81)	208 (0.02)	0 (0)	58 (0.02)	53 (0.02)	1 (0.02)
Surgical and medical procedures	325 (0.01)	272 (1.66)	43 (<0.01)	0 (0)	7 (<0.01)	3 (<0.01)	0 (0)
Psychiatric disorders	435 (0.01)	186 (1.14)	170 (0.01)	1 (0.02)	34 (0.01)	44 (0.02)	0 (0)
Eye disorders	349 (0.01)	175 (1.07)	129 (0.01)	0 (0)	20 (0.01)	25 (0.01)	0 (0)
Immune system disorders	333 (0.01)	90 (0.55)	182 (0.01)	0 (0)	21 (0.01)	37 (0.01)	3 (0.05)
Ear and labyrinth disorders	86 (<0.01)	49 (0.30)	15 (<0.01)	0 (0)	11 (<0.01)	10 (<0.01)	1 (0.02)
Reproductive system and breast disorders	53 (<0.01)	23 (0.14)	17 (<0.01)	0 (0)	6 (<0.01)	7 (<0.01)	0 (0)
Product issues	21 (<0.01)	9 (0.05)	9 (<0.01)	0 (0)	1 (<0.01)	1 (<0.01)	1 (0.02)
Social circumstances	19 (<0.01)	7 (0.04)	8 (<0.01)	0 (0)	4 (<0.01)	0 (0)	0 (0)
Congenital, familial and genetic disorders	23 (<0.01)	6 (0.04)	13 (<0.01)	0 (0)	3 (<0.01)	1 (<0.01)	0 (0)

Table S5), was the only one statistically positively associated with hypertension in patients receiving PD-1 inhibitors. Pneumonitis (ROR = 2.57, 95%CI 1.18–5.63, IC = 1.02, IC_{025} = −1.42) was not significantly correlated with hypertension in NSCLC patients receiving nivolumab. Interstitial lung disease (ROR = 3.04, 95% CI 2.19–4.23, IC = 1.25, IC_{025} = 0.20) was the mostly reported among the statistically significant reported adverse event in pembrolizumab subgroup. 54 patients with hypertension developed interstitial lung disease, with a disease severity rate of 100%, a mortality rate of 63%, and a hospitalization rate of 83%. Besides, we performed the disproportionality analysis of NSCLC patients without hypertension receiving anti-PD-1 treatment. The results demonstrated that no statistically significant signal was detected in the group without hypertension (Supplemetary Table S3,S4).

The spectrum of pulmonary irAEs differed in PD-L1 inhibitors.

The safety signal spectrum of different anti-PD-L1 treatments was presented in Figure 4 and Supplemetary Table S2. Using the ROR algorithm, haemoptysis (ROR 3.23, 95%CI 1.12–9.31) and acute respiratory failure (ROR 5.63, 95% CI 1.57–20.17) were mostly reported among the statistically significant reported adverse events in patients receiving PD-L1 inhibitors. However, when we used the Bayesian algorithm to estimate drug safety signals, neither of these achieved statistical significance (IC = 0.19, IC_{025} = −1.55; IC = 0.28, IC_{025} = −1.89). The median (IQR) time from therapy start to the onset of interstitial lung disease, pneumonitis, dyspnoea, pleural effusion and respiratory failure were 55 (29.00–58.00) days, 31

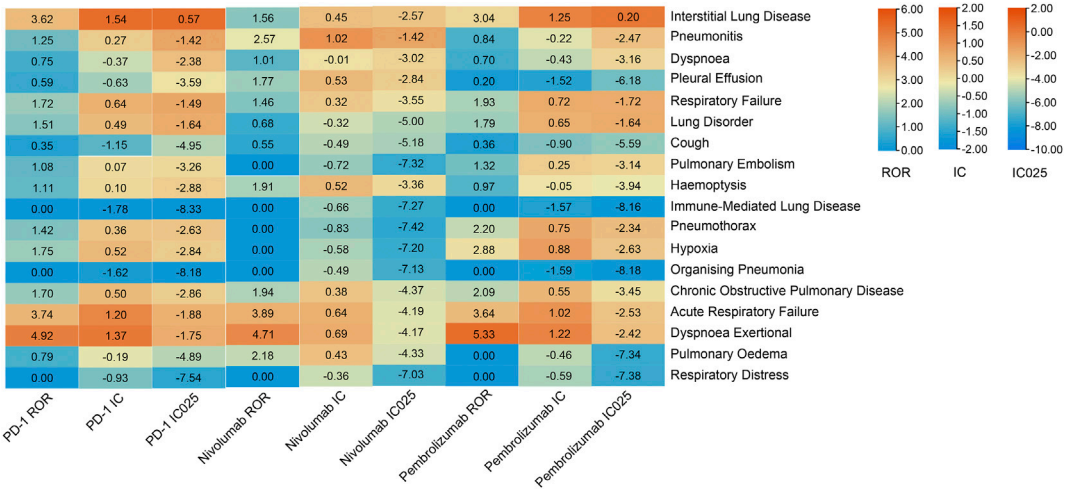

FIGURE 2
Safety signals of anti-PD-1 treatment in the NSCLC group with hypertension. ROR, reporting odds ratios; IC, information component; IC025, the lower limit of the 95% confidence interval of IC. ROR was greater than 1.0, the lower limit of 95% CI was above 1.0, IC more than zero and IC025 > 0. The value of each column is represented by a different color, the more orange the color, the larger the value. A signal is defined as ROR >1.0, IC > 0, and IC025 > 0.

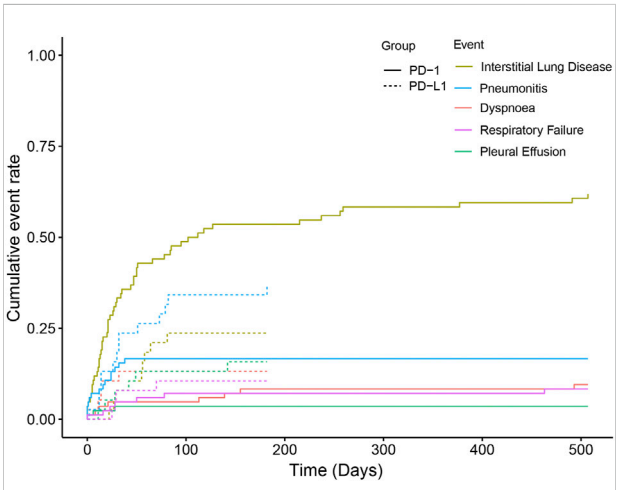

FIGURE 3
Time from initiation of ICI administration to onset of pulmonary adverse events.

(14.00–67.50) days, 14 (11.00–14.00) days, 35 (20.50–47.25) days, 28.5 (27.25–39.25) days (Figure 3; Supplemetary Table S5).

Discussion

Hypertension is one of the common chronic degenerative diseases, that involves remodeling and inflammation of arterial walls, and has an intricate relationship with cancer. Both of them share some same risk factors including smoking, diabetes mellitus, and physical inactivity (Battistoni et al., 2015; Ameri et al., 2018). Adjunctive therapies concurrently administered with antineoplastic agents can promote the development of hypertension or worsen previously controlled hypertension (Tonia et al., 2012; Cohen et al., 2019). Meanwhile, high blood pressure increases the risk of cancer development (Sanfilippo et al., 2014; Seretis et al., 2019). Dyer et al. (1977) firstly pointed out that hypertension might be a risk factor for cancer mortality, which was confirmed by other studies (Stocks et al., 2012; Berger et al., 2016; Harding et al., 2016) that hypertension could accelerate the biological process of aging which favors carcinogenesis. The metabolic disorders of hypertension increase oxidative stress and result in an irreversible proinflammatory state that reduces intracellular antioxidant capacity and predisposes it to malignant transformation (Federico et al., 2007). As hypertension is the most prevalent comorbidity in patients diagnosed with cancer (Piccirillo et al., 2004), patients with lung cancer coexisting with hypertension do not affect anti-tumor responses, nor does it affect the survival time (Yan et al., 2018). Common antihypertensive drugs, such as renin–angiotensin system inhibitors (RASi), angiotensin-converting enzyme inhibitors (ACEI), angiotensin II receptor blockers (ARBs) and direct renin inhibitors have no impact on clinical outcomes with anti-PD1/PD-L1 inhibitors (Bangalore et al., 2011; Cui et al., 2019).

Immunotherapeutic agents that target immune checkpoint pathways have shown great promise. Despite extensive research efforts, few biomarkers had a high accuracy and ubiquity to predict irAEs. Patients often receive additional concomitant therapies, which bring a lot of confounding factors to the risk of irAEs to immunotherapy. Concomitant medications in the

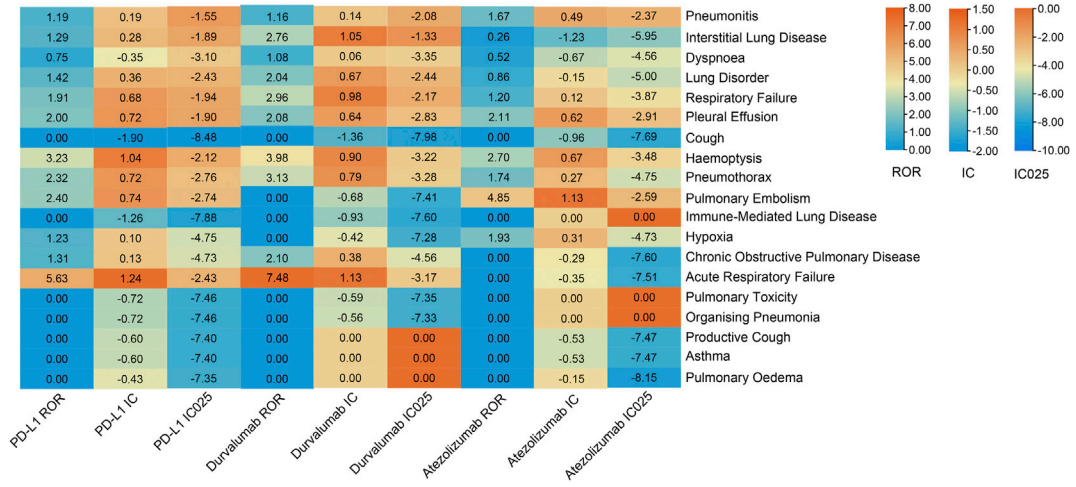

FIGURE 4
Safety signals of anti-PD-L1 therapy in the NSCLC group with hypertension. ROR, reporting odds ratios; IC, information component; IC025, the lower limit of the 95% confidence interval of IC. The value of each column is represented by a different color, the more orange the color, the larger the value. A signal is defined as ROR >1.0, IC > 0, and IC025 > 0.

treatment of malignant tumors have different effects on response to immunotherapy (Arbour et al., 2018; Fuca et al., 2019). Some reports found that antibiotics had detrimental efficacy and toxicity effects on ICIs. In fact, compare with patients without receiving extra agents, patients receiving baseline concomitant medication had worse outcomes (Cortellini et al., 2020). We have already known that antibiotics could increase the risk of irAE by changing the gut microbiome (Pinato et al., 2019). Not only is hypertension a common adverse reaction, frequently reported in clinical trials, but also a common comorbidity in patients with non-small cell lung cancer. However, the safety of antineoplastic therapy in these patients with hypertension has been rarely reported. As a common adverse reaction, the incidence of arterial hypertension is associated with the clinical outcome of antiangiogenetic-targeted treatment modalities in patients with tumors. (Scartozzi et al., 2009). As there were growing reports on the relationship between the occurrence of irAEs and tumor response, the anti-tumor treatments of ICI were associated with a reduced incidence of irAEs (Teraoka et al., 2017; Sato et al., 2018). We speculated that there is a potential link between high blood pressure and adverse reactions.

Although the causative pathogenic mechanism of hypertension-associated irAEs was poorly understood, studies have suggested that activation or reactivation of tissue-resident autoreactive T cells is thought to be a dominant prime factor in the development of irAEs (June et al., 2017; Dougan et al., 2021). Shared antigens between the specified organs and vessels could lead to *de novo* T cell activation and precipitate unwanted effects. High blood pressure caused endothelial dysfunction and vascular oxidative stress, leading to vasoconstriction. Neoantigens generated and then T cells were activated by binding specific antigens presented in major histocompatibility complex molecules on specific antigen-presenting cells, thereby activating of the adaptive immune system (Vinh et al., 2010). Activated T cells infiltrated blood vessels and produced cytokines, which promoted endothelial dysfunction and low-grade chronic inflammation (Idris-Khodja et al., 2014). Beyond increased perivascular immune cells accumulation and intravascular infiltration, circulating levels of certain cytokines and chemokines are abnormally elevated. Multiple chemokines recruited and stimulated the infiltration of T cells and monocytes and macrophages during hypertension (Guzik et al., 2007; Moore et al., 2015; Mikolajczyk et al., 2016). Besides, elevated circulatory levels of cytokines, C-reactive proteins, and immunoglobulins in patients with hypertension have also been reported. furthermore, autoreactive antibodies to vascular wall antigens have been detected (Martinez Amenos et al., 1985; Blake et al., 2003; Alexander et al., 2019). Recent investigations demonstrated that circulating antibody levels are elevated in both essential and pregnancy-related hypertension (Dib et al., 2012; Chan et al., 2014). Together, these studies indicated that T cells could be activated when self-peptides are presented through epitopes spread by antigen-presenting cells. Pre-existing autoreactive T cells have already existed and be kept in check through immune checkpoint molecules. When receiving immune checkpoint inhibitors, immune cells were over-activated, resulting in a low-level inflammatory response in tumor patients being amplified, further leading to immune-related adverse reactions.

To our knowledge, irAEs after receiving PD-1/PD-L1 inhibitors have never been reported in the context of cancer patients under chronic diseases. According to real-world data, we found a high reporting frequency of respiratory AEs associated with PD-1/PD-L1 inhibitors. Meanwhile, every PD-1/PD-L1 inhibitor has respective profiles of toxicities. Our

study showed statistical evidence regarding the association between pulmonary irAEs and hypertension, which needs to be interpreted cautiously and further verified in pharmacology and clinical aspects. Beyond that, there may be some other potential mechanisms that could affect the safety of immunotherapies. Chronic diseases, particularly in aged patients, have an indirect causative effect on the occurrence of irAE. They need to pay attention to pulmonary adverse reactions during immunotherapy. Our study could help to recognize and manage irAEs in clinical practice. Further observational studies are required to establish the safety of ICIs in hypertensive patients.

We acknowledged several limitations in our study beyond its retrospective and observative nature, with reporting bias, missing data, and confounding bias on the FAERS database, specific grades of hypertension, and cancer outcomes. We would prospectively assess the physical condition of NSCLC patients and investigated interactions between hypertension and irAEs in our center to validate our results. In addition, we need to further analyze the clinical outcomes in NSCLC patients with hypertension.

Conclusion

NSCLC patients with hypertension receiving PD-1/PD-L1 inhibitors have higher reporting odds of pulmonary adverse events. Clinicians should pay special attention to the occurrence of interstitial lung disease when using immunotherapy for these patients, and should intervene in time if lung disease occurs. Other adverse events such as pneumonitis and haemoptysis, which were highly reported without significance by the Bayesian IC algorithm, should not be ignored in clinical practice.

Data availability statement

The original contributions presented in the study are included in the article/Supplementary Material, further inquiries can be directed to the corresponding authors.

Author contributions

JC: the conception and design of the study; acquisition of data, analysis of data, drafting the article. YW: Manuscript revision, interpretation of data. XC: analysis and interpretation of data. YL: acquisition of data. CS: the conception and design of the study. All authors read and approved the final manuscript.

Funding

This study was supported by the National Natural Science Foundation of China (Grant number: 82072568) and Shanghai Shenkang Hospital Development Center (Grant Number: SHDC12020110).

Conflict of interest

The authors declare that the research was conducted in the absence of any commercial or financial relationships that could be construed as a potential conflict of interest.

Publisher's note

Supplementary material

The Supplementary Material for this article can be found online at: https://www.frontiersin.org/articles/10.3389/fphar.2022.944342/full#supplementary-material

References

Abdel-Rahman, O., ElHalawani, H., and Fouad, M. (2015). Risk of cutaneous toxicities in patients with solid tumors treated with immune checkpoint inhibitors: A meta-analysis. *Future Oncol.* 11, 2471–2484. doi:10.2217/fon.15.118

Albarel, F., Gaudy, C., Castinetti, F., Carre, T., Morange, I., Conte-Devolx, B., et al. (2015). Long-term follow-up of ipilimumab-induced hypophysitis, a common adverse event of the anti-CTLA-4 antibody in melanoma. *Eur. J. Endocrinol.* 172, 195–204. doi:10.1530/EJE-14-0845

Alexander, M. R., Norlander, A. E., Elijovich, F., Atreya, R. V., Gaye, A., Gnecco, J. S., et al. (2019). Human monocyte transcriptional profiling identifies IL-18 receptor accessory protein and lactoferrin as novel immune targets in hypertension. *Br. J. Pharmacol.* 176, 2015–2027. doi:10.1111/bph.14364

Almenoff, J. S., Pattishall, E. N., Gibbs, T. G., DuMouchel, W., Evans, S. J. W., and Yuen, N. (2007). Novel statistical tools for monitoring the safety of marketed drugs. *Clin. Pharmacol. Ther.* 82, 157–166. doi:10.1038/sj.clpt.6100258

Ameri, P., Canepa, M., Anker, M., Belenkov, Y., Bergler-Klein, J., Cohen-Solal, A., et al. (2018). Cancer diagnosis in patients with heart failure: Epidemiology, clinical implications and gaps in knowledge. *Eur. J. Heart Fail.* 20, 879–887. doi:10.1002/ejhf.1165

Arbour, K. C., Mezquita, L., Long, N., Rizvi, H., Auclin, E., Ni, A., et al. (2018). Impact of baseline steroids on efficacy of programmed cell death-1 and programmed death-ligand 1 blockade in patients with non-small-cell lung cancer. *J. Clin. Oncol.* 36, 2872–2878. doi:10.1200/JCO.2018.79.0006

Bangalore, S., Kumar, S., Kjeldsen, S. E., Makani, H., Grossman, E., Wetterslev, J., et al. (2011). Antihypertensive drugs and risk of cancer: Network meta-analyses and trial sequential analyses of 324 168 participants from randomised trials. *Lancet. Oncol.* 12, 65–82. doi:10.1016/S1470-2045(10)70260-6

Barjaktarevic, I. Z., Qadir, N., Suri, A., Santamauro, J. T., and Stover, D. (2013). Organizing pneumonia as a side effect of ipilimumab treatment of melanoma. *Chest* 143, 858–861. doi:10.1378/chest.12-1467

Bate, A., and Evans, S. J. W. (2009). Quantitative signal detection using spontaneous ADR reporting. *Pharmacoepidemiol. Drug Saf.* 18, 427–436. doi:10.1002/pds.1742

Bate, A., Lindquist, M., Edwards, I. R., Olsson, S., Orre, R., Lansner, A., et al. (1998). A Bayesian neural network method for adverse drug reaction signal generation. *Eur. J. Clin. Pharmacol.* 54, 315–321. doi:10.1007/s002280050466

Bate, A., Lindquist, M., Edwards, I. R., and Orre, R. (2002). A data mining approach for signal detection and analysis. *Drug Saf.* 25, 393–397. doi:10.2165/00002018-200225060-00002

Battistoni, A., Mastromarino, V., and Volpe, M. (2015). Reducing cardiovascular and cancer risk: How to address global primary prevention in clinical practice. *Clin. Cardiol.* 38, 387–394. doi:10.1002/clc.22394

Berger, S. M., Gislason, G., Moore, L. L., Andersson, C., Torp-Pedersen, C., Denis, G. V., et al. (2016). Associations between metabolic disorders and risk of cancer in Danish men and women - a nationwide cohort study. *Bmc Cancer* 16, 133. doi:10.1186/s12885-016-2122-7

Berthod, G., Lazor, R., Letovanec, I., Romano, E., Noirez, L., Stalder, J. M., et al. (2012). Pulmonary sarcoid-like granulomatosis induced by ipilimumab. *J. Clin. Oncol.* 30, E156–E159. doi:10.1200/JCO.2011.39.3298

Blake, G. J., Rifai, N., Buring, J. E., and Ridker, P. M. (2003). Blood pressure, C-reactive protein, and risk of future cardiovascular events. *Circulation* 108, 2993–2999. doi:10.1161/01.CIR.0000104566.10178.AF

Bomze, D., Ali, O. H., Bate, A., and Flatz, L. (2019). Association between immune-related adverse events during anti-PD-1 therapy and tumor mutational burden. *JAMA Oncol.* 5, 1633–1635. doi:10.1001/jamaoncol.2019.3221

Champiat, S., Lambotte, O., Barreau, E., Belkhir, R., Berdelou, A., Carbonnel, F., et al. (2016). Management of immune checkpoint blockade dysimmune toxicities: A collaborative position paper. *Ann. Oncol.* 27, 559–574. doi:10.1093/annonc/mdv623

Chan, C. T., Lieu, M., Toh, B. H., Kyaw, T. S., Bobik, A., Sobey, C. G., et al. (2014). Antibodies in the pathogenesis of hypertension. *Biomed. Res. Int.* 2014, 504045. doi:10.1155/2014/504045

Chaput, N., Lepage, P., Coutzac, C., Soularue, E., Le Roux, K., Monot, C., et al. (2017). Baseline gut microbiota predicts clinical response and colitis in metastatic melanoma patients treated with ipilimumab. *Ann. Oncol.* 28, 1368–1379. doi:10.1093/annonc/mdx108

Cheng, R., Cooper, A., Kench, J., Watson, G., Bye, W., McNeil, C., et al. (2015). Ipilimumab-induced toxicities and the gastroenterologist. *J. Gastroenterol. Hepatol.* 30, 657–666. doi:10.1111/jgh.12888

Cohen, J. B., Geara, A. S., Hogan, J. J., and Townsend, R. R. (2019). Hypertension in cancer patients and survivors epidemiology, diagnosis, and management. *JACC. CardioOncol.* 1, 238–251. doi:10.1016/j.jaccao.2019.11.009

Combs Scott, S., and Pennell, N. (2017). PS02.09 Use of systemic corticosteroids during the first month of nivolumab therapy in patients with advanced non-small cell lung cancer. *J. Thorac. Oncol.* 12, S1567. doi:10.1016/j.jtho.2017.09.047

Cortellini, A., Buti, S., Santini, D., Perrone, F., Giusti, R., Tiseo, M., et al. (2019). Clinical outcomes of patients with advanced cancer and pre-existing autoimmune diseases treated with anti-programmed death-1 immunotherapy: A real-world transverse study. *Oncologist* 24, E327–E337. doi:10.1634/theoncologist.2018-0618

Cortellini, A., Tucci, M., Adamo, V., Stucci, L. S., Russo, A., Tanda, E. T., et al. (2020). Integrated analysis of concomitant medications and oncological outcomes from PD-1/PD-L1 checkpoint inhibitors in clinical practice. *J. Immunother. Cancer* 8, e001361. doi:10.1136/jitc-2020-001361

Cui, Y., Wen, W., Zheng, T., Li, H., Gao, Y.-T., Cai, H., et al. (2019). Use of antihypertensive medications and survival rates for breast, colorectal, lung, or stomach cancer. *Am. J. Epidemiol.* 188, 1512–1528. doi:10.1093/aje/kwz106

Di Giacomo, A. M., Danielli, R., Guidoboni, M., Calabro, L., Carlucci, D., Miracco, C., et al. (2009). Therapeutic efficacy of ipilimumab, an anti-CTLA-4 monoclonal antibody, in patients with metastatic melanoma unresponsive to prior systemic treatments: Clinical and immunological evidence from three patient cases. *Cancer Immunol. Immunother.* 58, 1297–1306. doi:10.1007/s00262-008-0642-y

Dib, H., Tamby, M. C., Bussone, G., Regent, A., Berezne, A., Lafine, C., et al. (2012). Targets of anti-endothelial cell antibodies in pulmonary hypertension and scleroderma. *Eur. Respir. J.* 39, 1405–1414. doi:10.1183/09031936.00181410

Dougan, M., Luoma, A. M., Dougan, S. K., and Wucherpfennig, K. W. (2021). Understanding and treating the inflammatory adverse events of cancer immunotherapy. *Cell* 184, 1575–1588. doi:10.1016/j.cell.2021.02.011

Duarte, J. D., Parakh, S., Andrews, M. C., Woods, K., Pasam, A., Tutuka, C., et al. (2018). Autoantibodies may predict immune-related toxicity: Results from a phase I study of intralesional Bacillus calmette-guerin followed by ipilimumab in patients with advanced metastatic melanoma. *Front. Immunol.* 9, 411. doi:10.3389/fimmu.2018.00411

Dyer, A., Berkson, D., Stamler, J., Lindberg, H., and Stevens, E. (1975). High blood-pressure: A risk factor for cancer mortality? *Lancet (London, Engl.* 305, 1051–1056. doi:10.1016/s0140-6736(75)91826-7

Federico, A., Morgillo, F., Tuccillo, C., Ciardiello, F., and Loguercio, C. (2007). Chronic inflammation and oxidative stress in human carcinogenesis. *Int. J. Cancer* 121, 2381–2386. doi:10.1002/ijc.23192

Fuca, G., Galli, G., Poggi, M., Lo Russo, G., Proto, C., Imbimbo, M., et al. (2019). Modulation of peripheral blood immune cells by early use of steroids and its association with clinical outcomes in patients with metastatic non-small cell lung cancer treated with immune checkpoint inhibitors. *Esmo Open* 4, e000457. doi:10.1136/esmoopen-2018-000457

Garon, E. B., Hellmann, M. D., Rizvi, N. A., Carcereny, E., Leighl, N. B., Ahn, M. J., et al. (2019). Five-year overall survival for patients with advanced non-small-cell lung cancer treated with pembrolizumab: Results from the phase I KEYNOTE-001 study. *J. Clin. Oncol.* 37, 2518–2527. doi:10.1200/JCO.19.00934

Gaudy, C., Clevy, C., Monestier, S., Dubois, N., Preau, Y., Mallet, S., et al. (2015). Anti-PD1 pembrolizumab can induce exceptional fulminant type 1 diabetes. *Diabetes Care* 38, E182–E183. doi:10.2337/dc15-1331

Gentile, N. M., D'Souza, A., Fujii, L. L., Wu, T. T., and Murray, J. A. (2013). Association between ipilimumab and celiac disease. *Mayo Clin. Proc.* 88, 414–417. doi:10.1016/j.mayocp.2013.01.015

Guzik, T. J., Hoch, N. E., Brown, K. A., McCann, L. A., Rahman, A., Dikalov, S., et al. (2007). Role of the T cell in the genesis of angiotensin II-induced hypertension and vascular dysfunction. *J. Exp. Med.* 204, 2449–2460. doi:10.1084/jem.20070657

Harding, J. L., Sooriyakumaran, M., Anstey, K. J., Adams, R., Balkau, B., Brennan-Olsen, S., et al. (2016). Hypertension, antihypertensive treatment and cancer incidence and mortality: A pooled collaborative analysis of 12 Australian and New Zealand cohorts. *J. Hypertens.* 34, 149–155. doi:10.1097/HJH.0000000000000770

Idris-Khodja, N., Mian, M. O. R., Paradis, P., and Schiffrin, E. L. (2014). Dual opposing roles of adaptive immunity in hypertension. *Eur. Heart J.* 35, 1238–1244. -+. doi:10.1093/eurheartj/ehu119

Jain, R. K., Duda, D. G., Clark, J. W., and Loeffler, J. S. (2006). Lessons from phase III clinical trials on anti-VEGF therapy for cancer. *Nat. Clin. Pract. Oncol.* 3, 24–40. doi:10.1038/ncponc0403

Jing, Y., Liu, J., Ye, Y. Q., Pan, L., Deng, H., Wang, Y. S., et al. (2020). Multi-omics prediction of immune-related adverse events during checkpoint immunotherapy. *Nat. Commun.* 11, 4946. doi:10.1038/s41467-020-18742-9

June, C. H., Warshauer, J. T., and Bluestone, J. A. (2017). Is autoimmunity the Achilles' heel of cancer immunotherapy? *Nat. Med.* 23, 540–547. doi:10.1038/nm.4321

Kyi, C., Carvajal, R. D., Wolchok, J. D., and Postow, M. A. (2014). Ipilimumab in patients with melanoma and autoimmune disease. *J. Immunother. Cancer* 2, 35–44. doi:10.1186/s40425-014-0035-z

Martinez Amenos, A., Buendia, E., Carreras, L., Font, I., Mestre, M., Rama, H., et al. (1985). Humoral and cellular immunological abnormalities in hypertensive patients. *J. Clin. Hypertens.* 1, 153–160.

Michot, J. M., Bigenwald, C., Champiat, S., Collins, M., Carbonnel, F., Postel-Vinay, S., et al. (2016). Immune-related adverse events with immune checkpoint blockade: A comprehensive review. *Eur. J. Cancer* 54, 139–148. doi:10.1016/j.ejca.2015.11.016

Mikolajczyk, T. P., Nosalski, R., Szczepaniak, P., Budzyn, K., Osmenda, G., Skiba, D., et al. (2016). Role of chemokine RANTES in the regulation of perivascular inflammation, T-cell accumulation, and vascular dysfunction in hypertension. *Faseb J.* 30, 1987–1999. doi:10.1096/fj.201500088R

Minkis, K., Garden, B. C., Wu, S. H., Pulitzer, M. P., and Lacouture, M. E. (2013). The risk of rash associated with ipilimumab in patients with cancer: A systematic review of the literature and meta-analysis. *J. Am. Acad. Dermatology* 69, E121–E128. doi:10.1016/j.jaad.2012.12.963

Moore, J. P., Vinh, A., Tuck, K. L., Sakkal, S., Krishnan, S. M., Chan, C. T., et al. (2015). M2 macrophage accumulation in the aortic wall during angiotensin II infusion in mice is associated with fibrosis, elastin loss, and elevated blood pressure. *Am. J. Physiol. Heart Circ. Physiol.* 309, H906–H917. doi:10.1152/ajpheart.00821.2014

Mouhayar, E., and Salahudeen, A. (2011). Hypertension in cancer patients. *Tex. Heart Inst. J.* 38, 263–265.

Nishino, M., Tirumani, S. H., Ramaiya, N. H., and Hodi, F. S. (2015). Cancer immunotherapy and immune-related response assessment: The role of radiologists in the new arena of cancer treatment. *Eur. J. Radiol.* 84, 1259–1268. doi:10.1016/j.ejrad.2015.03.017

Pedersen, M., Andersen, R., Norgaard, P., Jacobsen, S., Thielsen, P., Straten, P. T., et al. (2014). Successful treatment with Ipilimumab and Interleukin-2 in two patients with metastatic melanoma and systemic autoimmune disease. *Cancer Immunol. Immunother.* 63, 1341–1346. doi:10.1007/s00262-014-1607-y

Piccirillo, J. F., Tierney, R. M., Costas, I., Grove, L., and Spitznagel, E. L. (2004). Prognostic importance of Comorbidity in a hospital-based cancer registry. *Jama-Journal Am. Med. Assoc.* 291, 2441–2447. doi:10.1001/jama.291.20.2441

Pinato, D. J., Gramenitskaya, D., Altmann, D. M., Boyton, R. J., Mullish, B. H., Marchesi, J. R., et al. (2019). Antibiotic therapy and outcome from immune-checkpoint inhibitors. *J. Immunother. Cancer* 7, 287. doi:10.1186/s40425-019-0775-x

Postow, M. A., Sidlow, R., and Hellmann, M. D. (2018). Immune-related adverse events associated with immune checkpoint blockade. *N. Engl. J. Med. Overseas. Ed.* 378, 158–168. doi:10.1056/nejmra1703481

Ranpura, V., Pulipati, B., Chu, D., Zhu, X. L., and Wu, S. H. (2010). Increased risk of high-grade hypertension with bevacizumab in cancer patients: A. Meta-analysis. *Am. J. Hypertens.* 23, 460–468. doi:10.1038/ajh.2010.25

Riely, G., and Miller, V. A. (2007). Vascular endothelial growth factor trap in non-small cell lung cancer. *Clin. Cancer Res.* 13, 4623S–4627S. doi:10.1158/1078-0432.ccr-07-0544

Ryder, M., Callahan, M., Postow, M. A., Wolchok, J., and Fagin, J. A. (2014). Endocrine-related adverse events following ipilimumab in patients with advanced melanoma: A comprehensive retrospective review from a single institution. *Endocr. Relat. Cancer* 21, 371–381. doi:10.1530/ERC-13-0499

Sanfilippo, K. M., McTigue, K. M., Fidler, C. J., Neaton, J. D., Chang, Y., Fried, L. F., et al. (2014). Hypertension and obesity and the risk of kidney cancer in 2 large cohorts of US men and women. *Hypertension* 63, 934–941. doi:10.1161/HYPERTENSIONAHA.113.02953

Sato, K., Akamatsu, H., Murakami, E., Sasaki, S., Kanai, K., Hayata, A., et al. (2018). Corrigendum to "Correlation between immune-related adverse events and efficacy in non-small cell lung cancer treated with nivolumab" [Lung Cancer 115 (2018) 71–74]. *Lung Cancer* 126, 230–231. doi:10.1016/j.lungcan.2018.11.007

Scartozzi, M., Galizia, E., Chiorrini, S., Giampieri, R., Berardi, R., Pierantoni, C., et al. (2009). Arterial hypertension correlates with clinical outcome in colorectal cancer patients treated with first-line bevacizumab. *Ann. Oncol.* 20, 227–230. doi:10.1093/annonc/mdn637

Seretis, A., Cividini, S., Markozannes, G., Tseretopoulou, X., Lopez, D. S., Ntzani, E. E., et al. (2019). Association between blood pressure and risk of cancer development: A systematic review and meta-analysis of observational studies. *Sci. Rep.* 9, 8565. doi:10.1038/s41598-019-45014-4

Sharma, A., Thompson, J. A., Repaka, A., and Mehnert, J. M. (2013). Ipilimumab administration in patients with advanced melanoma and hepatitis B and C. *J. Clin. Oncol.* 31, E370–E372. doi:10.1200/JCO.2012.47.1946

Stocks, T., Van Hemelrijck, M., Manjer, J., Bjorge, T., Ulmer, H., Hallmans, G., et al. (2012). Blood pressure and risk of cancer incidence and mortality in the metabolic syndrome and cancer project. *Hypertension* 59, 802–810. doi:10.1161/HYPERTENSIONAHA.111.189258

Syrigos, K. N., Karapanagiotou, E., Boura, P., Manegold, C., and Harrington, K. (2011). Bevacizumab-induced hypertension pathogenesis and management. *BioDrugs.* 25, 159–169. doi:10.2165/11590180-000000000-00000

Tarhini, A. A., Zahoor, H., Lin, Y., Malhotra, U., Sander, C., Butterfield, L. H., et al. (2015). Baseline circulating IL-17 predicts toxicity while TGF-β1 and IL-10 are prognostic of relapse in ipilimumab neoadjuvant therapy of melanoma. *J. Immunother. Cancer* 3, 39–46. doi:10.1186/s40425-015-0081-1

Teraoka, S., Fujimoto, D., Morimoto, T., Kawachi, H., Ito, M., Sato, Y., et al. (2017). Early immune-related adverse events and association with outcome in advanced non-small cell lung cancer patients treated with nivolumab: A prospective cohort study. *J. Thorac. Oncol.* 12, 1798–1805. doi:10.1016/j.jtho.2017.08.022

Tirumani, S. H., Ramaiya, N. H., Keraliya, A., Bailey, N. D., Ott, P. A., Hodi, F. S., et al. (2015). Radiographic profiling of immune-related adverse events in advanced melanoma patients treated with ipilimumab. *Cancer Immunol. Res.* 3, 1185–1192. doi:10.1158/2326-6066.CIR-15-0102

Tonia, T., Mettler, A., Robert, N., Schwarzer, G., Seidenfeld, J., Weingart, O., et al. (2012). Erythropoietin or darbepoetin for patients with cancer. *Cochrane database Syst. Rev.* 12:CD003407. doi:10.1002/14651858.cd003407.pub5

Valpione, S., Pasquali, S., Campana, L. G., Piccin, L., Mocellin, S., Pigozzo, J., et al. (2018). Sex and interleukin-6 are prognostic factors for autoimmune toxicity following treatment with anti-CTLA4 blockade. *J. Transl. Med.* 16, 94–10. doi:10.1186/s12967-018-1467-x

Vinh, A., Chen, W., Blinder, Y., Weiss, D., Taylor, W. R., Goronzy, J. J., et al. (2010). Inhibition and genetic ablation of the B7/CD28 T-cell costimulation Axis prevents experimental hypertension. *Circulation* 122, 2529–2537. doi:10.1161/CIRCULATIONAHA.109.930446

Wang, D. Y., Salem, J.-E., Cohen, J. V., Chandra, S., Menzer, C., Ye, F., et al. (2018). Fatal toxic effects associated with immune checkpoint inhibitors: A systematic review and meta-analysis. *JAMA Oncol.* 4, 1721–1728. doi:10.1001/jamaoncol.2018.3923

Weber, J. S., Hodi, F. S., Wolchok, J. D., Topalian, S. L., Schadendorf, D., Larkin, J., et al. (2017). Safety profile of nivolumab monotherapy: A pooled analysis of patients with advanced melanoma. *J. Clin. Oncol.* 35, 785–792. doi:10.1200/JCO.2015.66.1389

Wu, S. H., Chen, J. J., Kudelka, A., Lu, J., and Zhu, X. L. (2008). Incidence and risk of hypertension with sorafenib in patients with cancer: A systematic review and meta-analysis. *Lancet Oncol.* 9, 117–123. doi:10.1016/s1470-2045(08)70003-2

Yan, L. Z., Dressler, E. V., and Adams, V. R. (2018). Association of hypertension and treatment outcomes in advanced stage non-small cell lung cancer patients treated with bevacizumab or non-bevacizumab containing regimens. *J. Oncol. Pharm. Pract.* 24, 209–217. doi:10.1177/1078155217690921

frontiers | Frontiers in Pharmacology

TYPE Original Research
PUBLISHED 04 November 2022
DOI 10.3389/fphar.2022.986357

OPEN ACCESS

EDITED BY
Jennifer Martin,
The University of Newcastle, Australia

REVIEWED BY
Eli Ehrenpreis,
Advocate Lutheran General Hospital, United States
Pengfei Li,
Capital Medical University, China

*CORRESPONDENCE
Xinan Wu,
wuxinan@boe.com.cn

SPECIALTY SECTION
This article was submitted to Pharmacology of Anti-Cancer Drugs, a section of the journal Frontiers in Pharmacology

RECEIVED 05 July 2022
ACCEPTED 25 October 2022
PUBLISHED 04 November 2022

CITATION
Wang F, Wei Q and Wu X (2022), Cardiac arrhythmias associated with immune checkpoint inhibitors: A comprehensive disproportionality analysis of the FDA adverse event reporting system. *Front. Pharmacol.* 13:986357. doi: 10.3389/fphar.2022.986357

Cardiac arrhythmias associated with immune checkpoint inhibitors: A comprehensive disproportionality analysis of the FDA adverse event reporting system

Feifei Wang[1], Qi Wei[2] and Xinan Wu[1]*

[1]Department of Pharmacy, Hefei BOE Hospital, Hefei, China, [2]Department of Cardiology, Lu'an Hospital of Traditional Chinese Medicine, Lu'an, China

Introduction: With the widespread application of Immune checkpoint inhibitors (ICIs), it is important to explore the association between ICIs and cardiac arrhythmias and to characterize the clinical features of ICI-associated cardiac arrhythmias in real-world studies.

Objective: The purpose of this study was to characterize the main features of ICI-related cardiac arrhythmias.

Methods: From January 2017 to June 2021, data in the Food and Drug Administration Adverse Event Reporting System (FAERS) database were retrieved to conduct the disproportionality analysis. For the ICI-related cardiac arrhythmia detection, signals were detected by reporting odds ratio (ROR) and information component (IC), calculated using two-by-two contingency tables The clinical characteristics of patients reported with ICI-related cardiac arrhythmias were compared between fatal and non-fatal groups, and the time to onset (TTO) following different ICI regimens was further investigated. Multivariate logistic regression was used to evaluate the association between concurrent cardiotoxicities and ICI-associated arrhythmias.

Results: We identified a total of 1957 ICI–associated cardiac arrhythmias reports which appeared to influence more men (64.44%) than women (30.76%), with a median age of 68 [interquartile range (IQR) 60–75] years. Cardiac arrhythmias were reported most often in patients with lung, pleura, thymus and heart cancers (38.02% of 1957 patients). Compared with the full database, ICIs were detected with pharmacovigilance of cardiac arrhythmias (ROR025 = 1.16, IC025 = 0.19). Anti-PD-1 and anti-PD-L1 monotherapies were found to be related to higher reporting of arrhythmias, corresponding to ROR025 = 1.03, IC025 = 0.06 and ROR025 = 1.27, IC025 = 0.29, respectively, with the exception of anti-CTLA-4 monotherapies (ROR025 = 0.57, IC025 = −1.21). The spectrum of arrhythmias induced by ICIs differed among therapeutic regimens. There was no significant difference in the onset time between monotherapy and combination regimen. Moreover, reports of ICI-associated arrhythmias were

associated with other concurrent cardiotoxicity, including cardiac failure [ROR 2.61 (2.20–3.09)], coronary artery disorders [ROR 2.28 (1.83–2.85)], myocardial disorders [ROR 5.25 (4.44–6.22)], pericardial disorders [ROR 2.76 (2.09–3.64)] and cardiac valve disorders [ROR 3.21 (1.34–7.68)].

Conclusion: ICI monotherapy and combination therapy can lead to cardiac arrhythmias that can result in serious outcomes and tend to occur early. Our findings underscore the importance of early recognition and management of ICI-related cardiac arrhythmias.

KEYWORDS

immune checkpoint inhibitors, adverse event reporting system, cardiac arrhythmias, CTLA-4, PD-1, PD-L1

Introduction

Immune checkpoint inhibitors (ICIs) are novel therapeutic agents that have revolutionized the treatment of numerous cancer types (Ferris et al., 2016; Reck et al., 2016; Larkin et al., 2019). ICIs target a range of costimulatory signaling molecules on T lymphocytes and antigen-presenting cells, such as cytotoxic T-lymphocyte antigen-4 (CTLA-4) and programmed cell death 1/ligand 1 (PD-1/PD-L1) (Mahmood et al., 2018; Ball et al., 2019).

Whereas, immune-related adverse events (irAEs) can affect multiple organ systems (Zhai et al., 2019; Hu et al., 2020; Mikami et al., 2021; Bomze et al., 2022), including the cardiovascular system (Salem et al., 2018; Ma et al., 2021). Due to its rarity, primary evidence regarding ICIs-associated cardiac arrhythmias is derived from case reports (Katsume et al., 2018; Bukamur et al., 2019; Prevel et al., 2020; Alhumaid et al., 2021; Savarapu et al., 2021) and clinical trials (Joseph et al., 2021), which have not systematically focused on ICI-induced arrhythmias. Cardiac arrhythmias associated with ICIs have been reported to occur in the setting of myocarditis (Katsume et al., 2018), which implies that ICI-related arrhythmias may be associated with concurrent cardiotoxicity. Besides, the overviewed relationship between arrhythmias and ICIs, the spectrum of potential signals, the factors related to fatality, as well as the clinical information of ICI-associated arrhythmias remain unknown.

In this pharmacovigilance study, we investigated the FDA's Adverse Event Reporting System (FAERS) to identify the association between arrhythmias and different ICI regimens, detect a comprehensive spectrum of 17 potential signals, and present comprehensive information (patient characterizations, prognosis outcomes, the onset time and the association between concurrent cardiotoxicities and ICI-associated arrhythmias).

Methods

Data source

We conducted a retrospective pharmacovigilance study based on data from January 2017 to June 2021 in the FAERS database. The FAERS database is a spontaneous reporting system (SRS), which collects adverse events (AEs) reports by health professionals, consumers, pharmaceutical manufacturers, patients, and other non-healthcare workers. OpenVigil FDA, a pharmacovigilance tool, was adapted to extract FAERS data using the openFDA API for accessing the FDA drug-event database with the additional openFDA duplicate detection functionality.

Procedures

The report of the FAERS database is coded using preferred terms (PTs) from Medical Dictionary for Regulatory Activities (MedDRA). We considered the following PTs as related to cardiac arrhythmias: "atrioventricular block complete (10003673)," "bundle branch block right (10006582)," "atrioventricular block (10003671)," "Bundle branch block left (10006580)," "arrhythmia (10003119)," "bradycardia (10006093)," "tachycardia (10043071)," "atrial fibrillation (10003658)," "sinus tachycardia (10040752)," "atrial flutter (10003662)," "sinus node dysfunction (10075889)," "supraventricular tachycardia (10042604)," "cardiac arrest (10007515)," "sudden death (10042434)," "ventricular tachycardia (10047302)," "cardio-respiratory arrest (10007617)," and "ventricular fibrillation (10047290)." The above PT level adverse events belonged to the following four High Level Terms (HLTs): "Cardiac conduction disorders (10000032)," "Rate and rhythm disorders NEC (10037908)," "Supraventricular arrhythmias (10042600)," and "Ventricular arrhythmias and cardiac arrest (10047283)." Concurrent cardiac AEs are entered using terms in the MedDRA terminology (provided in Supplementary Tables S1–S5). In this study, the following data concerning ICIs were retrieved from FAERS, including demographic information about the patient (e.g., gender, age), drug name, AEs and their outcomes, the country and year of reporting, the type of reporter, indications of use and the time to onset (TTO).

Statistical analysis

We used descriptive statistics to present the clinical characteristics of the ICI-associated arrhythmias. A comparison of categorical variables was made between fatal and non-fatal group using the chi-squared test. We used *t* test and non-parametric test to analyze the normally distributed and not normally distributed continuous variables respectively, and $p < 0.05$ was considered significant. Multivariate logistic regression was used to examine concurrent cardiotoxicities related to ICI-related arrhythmias. The reporting odds ratio (ROR) with 95% confidence intervals (CIs) and Bayesian confidence propagation neural networks of information components (IC) were two specific indices to calculate disproportionality in pharmacovigilance (Noren et al., 2013; Zhai et al., 2019), which could detect potential signals in our investigation. The calculation formulas for ROR and IC are as follows:

$$\mathrm{ROR} = \frac{N_{\mathrm{observed}} + 0.5}{N_{\mathrm{expected}} + 0.5}$$

$$95\%\mathrm{CI} = e^{\mathrm{In}(ROR) \pm 1.96\sqrt{\frac{1}{a}+\frac{1}{b}+\frac{1}{c}+\frac{1}{d}}}$$

$$N_{\mathrm{expected}} = \frac{N_{\mathrm{drug}} * N_{\mathrm{event}}}{N_{\mathrm{total}}}$$

$$\mathrm{IC} = \log 2 \frac{N_{\mathrm{observed}} + 0.5}{N_{\mathrm{expected}} + 0.5}$$

$$\mathrm{IC}_{025} = \mathrm{IC} - 3.3 \times (N_{\mathrm{observed}} + 0.5)^{-0.5} - 2 \times (N_{\mathrm{observed}} + 0.5)^{-1.5}$$

$$\mathrm{IC}_{975} = \mathrm{IC} + 2.4 \times (N_{\mathrm{observed}} + 0.5)^{-0.5} - 0.5 \times (N_{\mathrm{observed}} + 0.5)^{-1.5}$$

N_{expected}: the number of case reports expected for the target drug AEs. N_{observed}: the observed number of case reports for the target drug AEs. N_{drug}: the total number of case reports for the target drug, regardless of adverse reactions. N_{event}: the total number of case reports for the target AEs, regardless of drug. N_{total}: the total number of case reports in the database. For IC, a significant signal was considered when the lower limit of the IC 95% confidence interval (IC_{025}) value was greater than zero (Bate et al., 1998; Noren et al., 2013). For ROR, a significant signal was considered when the lower end of the 95% credibility interval (ROR_{025}) exceeded 1, with at least 3 cases (Rothman et al., 2004). One of the two algorithms meeting the criteria should be considered as a positive signal of arrhythmia. All the data analysis was performed by SPSS 24.0 (SPSS Inc, Chicago, IL, United States).

Results

Descriptive analysis

The FAERS database recorded 81,643 adverse events related to ICIs and 111,384 reports related to cardiac arrhythmias between 1 January 2017 and 30 June 2021. We identified 1957 reports of suspected ICI-related arrhythmias and summarized the clinical characteristics of patients in Table 1. The number of reported cases had gradually increased from 2017 to 2020. Males presented a larger proportion of arrhythmias than female patients (64.44% vs. 30.76%). The median age was 68 years [interquartile range (IQR) 60–75]. Physician submitted the highest number of case reports (808, 41.29%). The majority of reports were from North America (799, 40.83%), Europe (661, 33.78%) and Asian (388, 19.83%). Reports of ICI–associated arrhythmias were most frequently reported in lung, pleura, thymus and heart cancer patients (744, 38.02%). Nivolumab monotherapy generated the most reports associated with arrhythmias (659, 33.67%), followed by pembrolizumab monotherapy (479, 24.48%), and nivolumab plus ipilimumab (349, 17.83%). Only 77.77% of arrhythmias reports were isolated, with the overwhelmingly majority associated with concurrent cardiotoxicity, including cardiac failure (9.10%), coronary artery disorders (5.06%), myocardial disorders (9.66%), pericardial disorders (3.17%) and cardiac valve disorders (0.46%).

As shown in Table 1, no significant differences were found in patient age, reporter and reporting year for fatal vs non-fatal reports. Use of different ICI regimens were similar in fatal vs. non-fatal ICI-related arrhythmia reports. There was a significant difference between fatal and non-fatal reports in tumor indications ($p = 0.002$), with the highest percentage of reported deaths (45.38%, 59/130) in digestive system patients. Notably, patient gender was statistically different between the two groups ($p = 0.009$), and the proportion of fatal reports in male patients was higher than that in female patients (69.85 vs. 25.93%). Concurrent cardiotoxicity was also different in fatal vs. non-fatal ICI-related arrhythmias reports ($p = 0.001$). Moreover, there was a significant difference in the reporting region between the two groups ($p < 0.001$), with the highest percentage of fatality occurring in South America (42.59%, 23/54).

Signal values related to different immunotherapy regimens

In general, ICIs were significantly associated with the reporting frequency of arrhythmias [ROR 1.20 (1.16–1.24), IC025 0.19] (Table 2). Concerning reports of cardiac arrhythmias, a significant increased ROR was found for anti-PD-1 monotherapy [ROR 1.11 (1.03–1.21), IC025 0.06] and anti-PD-L1 monotherapy [ROR 1.37 (1.27–1.49), IC025 0.29], with the exception of anti-CTLA-4 monotherapy [ROR 0.62 (0.57–0.67), IC025 −1.21]. As for ICI combination therapy, nivolumab plus ipilimumab detected with pharmacovigilance signals of cardiac arrhythmias [ROR 1.52 (1.37–1.69), IC025 0.43], which was not seen in tremelimumab plus durvalumab [ROR 1.19 (0.82–1.72), IC025 −0.37]. Further analysis showed that combination regimen was associated with a higher risk of

TABLE 1 Characteristics of patients with ICI-associated cardiac arrhythmias sourced from the FAERS database (January 2017 to June 2021).

Characteristics		Total reports, *n* (%)	Fatal cases, *n* (%)	Non-fatal cases, *n* (%)	*p*-value
Total		1957	617	1340	
Patient age (year)	—				*NS*
	Median (IQR)	68 (60-75)	69 (61-75)	68 (60-75)	
	< 18	28 (1.43%)	13 (2.11%)	15 (1.12%)	
	18–64	591 (30.20%)	174 (28.20%)	417 (31.12%)	
	65–74	631 (32.24%)	200 (32.41%)	431 (32.16%)	
	≥75	445 (22.74%)	146 (23.66%)	299 (22.31%)	
	Unknown	262 (13.39%)	84 (13.61%)	178 (13.28%)	
Gender	—				*0.009*
	Female	602 (30.76%)	160 (25.93%)	442 (32.99%)	
	Male	1261 (64.44%)	431 (69.85%)	830 (61.94%)	
	Unknown	94 (4.80%)	26 (4.21%)	68 (5.07%)	
Reporting year	—				*NS*
	2017	262 (13.39%)	88 (14.26%)	174 (12.99%)	
	2018	461 (23.56%)	151 (24.47%)	310 (23.13%)	
	2019	528 (26.98%)	160 (25.93%)	368 (27.46%)	
	2020	562 (28.72%)	174 (28.20%)	388 (28.96%)	
	2021	144 (7.36%)	44 (7.13%)	100 (7.46%)	
Tumor Indications	—				*0.002*
	Lung, pleura, thymus and heart	744 (38.02%)	262 (42.46%)	482 (35.97%)	
	Urinary system and male genital organs	310 (15.84%)	85 (13.78%)	225 (16.79%)	
	Digestive system	130 (6.64%)	59 (9.56%)	71 (5.30%)	
	Haematopoietic and lymphoid tissues	88 (4.50%)	28 (4.54%)	60 (4.48%)	
	Head and neck	61 (3.12%)	25 (4.05%)	36 (2.69%)	
	Endocrine organs	25 (1.28%)	3 (0.49%)	22 (1.64%)	
	Gynecologic organs	96 (4.91%)	19 (3.08%)	77 (5.75%)	
	Skin	267 (13.64%)	76 (12.32%)	191 (14.25%)	
	Central nervous system	15 (0.77%)	3 (0.49%)	12 (0.90%)	
	Unspecified or unknown indication	221 (11.29%)	57 (9.24%)	164 (12.24%)	
Area	—				*p < 0.001*
	Africa	4 (0.20%)	1 (0.16%)	3 (0.22%)	
	Asia	388 (19.83%)	163 (26.42%)	225 (16.79%)	
	Europe	661 (33.78%)	190 (30.79%)	471 (35.15%)	
	North America	799 (40.83%)	233 (37.76%)	566 (42.24%)	
	Oceania	47 (2.40%)	6 (0.97%)	41 (3.06%)	
	South America	54 (2.76%)	23 (3.73%)	31 (2.31%)	
	Unknown	4 (0.20%)	1 (0.16%)	3 (0.22%)	
Reporters	—				*NS*
	Physician	808 (41.29%)	273 (44.25%)	535 (39.93%)	
	Pharmacist	120 (6.13%)	32 (5.19%)	88 (6.57%)	
	Other health–professional	666 (34.03%)	194 (31.44%)	472 (35.22%)	
	Consumer or Non–health professional	344 (17.58%)	109 (17.67%)	235 (17.54%)	
	Unknown	19 (0.97%)	9 (1.46%)	10 (0.75%)	
ICI drug as suspected drug	—				*NS*
	Monotherapy	1579 (80.68%)	490 (79.42%)	1089 (81.27%)	*NS*
	Anti–CTLA–4 monotherapy	40 (2.04%)	12 (1.94%)	28 (2.09%)	
	Ipilimumab	37 (1.89%)	12 (1.94%)	25 (1.87%)	

(Continued on following page)

TABLE 1 (*Continued*) Characteristics of patients with ICI-associated cardiac arrhythmias sourced from the FAERS database (January 2017 to June 2021).

Characteristics		Total reports, *n* (%)	Fatal cases, *n* (%)	Non-fatal cases, *n* (%)	*p*-value
	Tremelimumab	3 (0.15%)	0 (0.00%)	3 (0.22%)	
	Anti–PD–1 monotherapy	1145 (58.51%)	345 (55.92%)	800 (59.70%)	
	Nivolumab	659 (33.67%)	193 (31.28%)	466 (34.78%)	
	Pembrolizumab	479 (24.48%)	148 (23.99%)	331 (24.70%)	
	Cemiplimab	7 (0.36%)	4 (0.65%)	3 (0.22%)	
	Anti–PD–L1 monotherapy	394 (20.13%)	133 (21.56%)	261 (19.48%)	
	Atezolizumab	246 (12.57%)	81 (13.13%)	165 (12.31%)	
	Avelumab	51 (2.61%)	19 (3.08%)	32 (2.39%)	
	Durvalumab	97 (4.96%)	33 (5.35%)	64 (4.78%)	
	Combination therapy	378 (19.32%)	127 (20.58%)	251 (18.73%)	*NS*
	Ipilimumab+Nivolumab	349 (17.83%)	111 (17.99%)	238 (17.76%)	
	Tremelimumab+Durvalumab	29 (1.48%)	16 (2.59%)	13 (0.97%)	
Concurrent cardiotoxicity					*0.001*
	Cardiac failure	178 (9.10%)	59 (9.53%)	119 (8.85%)	
	Coronary artery disorders	99 (5.06%)	31 (5.01%)	68 (5.06%)	
	Myocardial disorders	189 (9.66%)	55 (8.89%)	134 (9.97%)	
	Pericardial disorders	62 (3.17%)	13 (2.10%)	49 (3.65%)	
	Cardiac valve disorders	9 (0.46%)	0 (0.00%)	9 (0.67%)	

Abbreviations: FAERS, Food and Drug Administration's Adverse Event Reporting System; ICI, immune checkpoint inhibitor; IQR: interquartile range; N: number of records.

TABLE 2 Associations of different ICI regimens with cardiac arrhythmias.

	Drug	N	ROR	ROR_{025}	ROR_{975}	IC	IC_{025}
Total	Total ICIs	1957	1.20	1.16	1.24	0.26	0.19
Monotherap	Anti–CTLA–4 monotherapy	40	0.62	0.57	0.67	−0.69	−1.21
	Ipilimumab	37	0.58	0.42	0.80	−0.81	−1.36
	Tremelimumab	3	3.57	1.07	11.97	1.84	−0.23
	Anti–PD–1 monotherapy	1145	1.11	1.03	1.21	0.16	0.06
	Nivolumab	659	1.13	1.04	1.22	0.17	0.04
	Pembrolizumab	479	1.11	1.01	1.21	0.15	0.00
	Cemiplimab	7	0.65	0.31	1.37	−0.62	−1.92
	Anti–PD–L1 monotherapy	394	1.37	1.27	1.49	0.46	0.29
	Atezolizumab	246	1.35	1.19	1.53	0.43	0.22
	Avelumab	51	1.68	1.27	2.22	0.75	0.28
	Durvalumab	97	1.30	1.06	1.59	0.38	0.04
Combination therapy	Combination therapy	378	1.49	1.37	1.62	0.57	0.40
	Ipilimumab+Nivolumab	349	1.52	1.37	1.69	0.60	0.43
	Tremelimumab+Durvalumab	29	1.19	0.82	1.72	0.25	−0.37
Anti-PD-1vs anti-ctla-4	—	1145	1.80	1.44	2.26	0.85	0.75
Anti-PD-L1vs anti-ctla-4	—	394	2.22	1.76	2.80	1.15	0.98
Anti-PD-1 vs anti-PD-L1	—	1145	0.81	0.75	0.88	−0.30	−0.40
Combination vs monotherapy therapy	—	378	1.30	1.20	1.41	0.38	0.21

Abbreviations N: number of records; ROR025: the lower end of the 95% confidence interval of ROR. ROR975: the upper end of the 95% confidence interval of IC; IC025: the lower end of the 95% confidence interval of IC.

TABLE 3 Arrhythmia Signal Profiles of Different ICI Strategies.

$IC_{025}>0$	Ipilimumab	Tremelimumab	Nivolumab	Pembrolizumab	Cemiplimab	Atezolizumab	Avelumab	Durvalumab	Ipilimumab + Nivolumab	Tremelimumab + Durvalumab
Atrioventricular block complete	—	—	1.17	2.00	—	0.73	—	0.29	1.09	—
Bundle branch block right	—	—	−1.57	−1.67	—	—	—	—	−0.02	—
Atrioventricular block	—	—	0.50	0.18	—	−1.49	—	—	0.90	—
Bundle branch block left	—	—	—	−1.16	—	−0.63	—	—	−0.89	—
Arrhythmia	—	—	−0.33	−0.75	−1.03	−2.47	—	−2.70	−1.58	—
Bradycardia	—	—	−1.46	−1.70	—	−1.95	0.51	−2.96	−3.06	—
Tachycardia	−2.18	0.48	−0.89	−0.45	—	−0.83	−1.15	−0.58	−0.61	—
Atrial fibrillation	−0.66	—	0.19	0.12	—	0.80	−0.51	0.36	0.78	−2.80
Sinus tachycardia	—	—	−0.26	−0.61	—	0.14	—	−1.66	1.76	—
Atrial flutter	—	—	0.62	−0.44	—	0.53	—	—	0.24	1.35
Sinus node dysfunction	—	—	0.71	−1.84	—	−0.90	—	—	—	—
Supraventricular tachycardia	—	—	0.43	0.43	—	1.36	—	−1.17	0.42	—
Cardiac arrest	−1.38	—	−0.35	−1.03	—	−0.95	0.20	−0.49	0.01	0.47
Sudden death	—	—	1.34	1.34	—	1.08	1.17	−1.21	1.90	0.45
Ventricular tachycardia	—	—	−0.90	0.59	—	—	—	—	−0.61	—
Cardio-respiratory arrest	—	—	−0.54	−0.87	—	−1.00	—	−0.74	−1.59	—
Ventricular fibrillation	—	—	−1.32	−0.90	—	—	—	—	—	—

10.3389/fphar.2022.986357

reports of cardiac arrhythmias compared with monotherapy [ROR 1.30 (1.20–1.41), IC025 0.21].

The signal spectrum of cardiac arrhythmias differs in immune therapies

The cardiac arrhythmia signal spectrum of different ICI strategies was shown in Table 3, where the IC 025 was regarded as an indicator. As shown in Table 3, ipilimumab plus nivolumab presented a broadest spectrum of cardiac arrhythmias AEs with 8 PTs detected as signals, ranging from cardiac arrest (IC 025 = 0.01) to sudden death (IC 025 = 1.90). For nivolumab, a total of 7 PTs as signals were observed, with signal values ranging from IC 025 = 0.19 (atrial fibrillation) to IC 025 = 1.34 (sudden death). There were 6 PTs both statistically associated with pembrolizumab and atezolizumab receiving. However, the drug with the least PTs were ipilimumab and cemiplimab, with no signal detected, followed by tremelimumab, with only one signal (tachycardia, IC 025 = 0.48) detected. Interestingly, both drugs (ipilimumab and tremelimumab) were all anti-CTLA-4 drugs, with no or only one reported AEs. Cemiplimab, as one of the three anti-PD-1 drugs, presented no signal due to the rare application.

Atrioventricular block complete, atrial fibrillation and sudden death were three overlapping PTs. Among these, sudden death was the most frequent PT, also detected as the second strongest signal (IC 025 = 1.90). Both atrioventricular block complete and atrial fibrillation were found significantly associated with nivolumab, pembrolizumab, atezolizumab, avelumab, and ipilimumab plus nivolumab, with atrioventricular block complete detected as the strongest signal in pembrolizumab (IC 025 = 2.00).

Time to cardiac arrhythmias onset

A total of 1353 ICI-associated cardiac arrhythmias reported TTO, as shown in Table 4 (There were few data on tremelimumab, which was not shown in Table 4). Among ICI monoregimens, we found no significant difference in the reporting onset time of cardiac arrhythmias (p = 0.061). The median time to onset was 47 days for ipilimumab (IQR 19–67), 35 days for nivolumab (IQR 12–135), 25 days for pembrolizumab (IQR 7–76), 56 days for cemiplimab (IQR 22–99), 34 days for atezolizumab (IQR 12–168), 18 days for avelumab (IQR 1–103), and 35 days for durvalumab (IQR 9–100), respectively. In addition, there was no significant difference in the onset time between monotherapy and combination regimen (ipilimumab vs. ipilimumab plus nivolumab, p = 0.606; nivolumab vs. nivolumab plus ipilimumab, p = 0.550; tremelimumab vs. tremelimumab plus durvalumab, p = 0.620; durvalumab vs. tremelimumab plus durvalumab, p = 0.061).

Associations between concurrent cardiotoxicity and ICI-associated arrhythmias

Table 5 showed the associations between concurrent cardiotoxicity reports and ICI-associated arrhythmias reports. In the multivariate logistic regression model, the following concurrent cardiotoxicities reports were associated with ICI-associated arrhythmias reports: cardiac failure (OR = 2.61, 95% CI 2.20–3.09, $p < 0.001$), coronary artery disorders (OR = 2.28, 95% CI 1.83–2.85, $p < 0.001$), myocardial disorders (OR = 5.25, 95% CI 4.44–6.22, $p < 0.001$), pericardial disorders (OR = 2.76, 95% CI 2.09–3.64, $p < 0.001$) and cardiac valve disorders (OR = 3.21, 95% CI 1.34–7.68, $p < 0.001$). As the MedDRA classification "cardiac arrhythmias" encompasses a broad range of diseases, we subgrouped the 1957 reports by the four MedDRA HLT classifications: "rate and rhythm disorders NEC," "cardiac conduction disorders," "ventricular arrhythmias," and "supraventricular arrhythmias" for further analysis (the MedDRA abbreviation "NEC" denotes "Not Elsewhere Classified"). The associations between concurrent cardiotoxicity reports and specific arrhythmias reports under each HLT was diverse, with myocardial disorders having significantly elevated reporting of four specific arrhythmias in HLT level but cardiac valve disorders only increasing the risk of supraventricular arrhythmias.

Discussion

To the best of our knowledge, this is the first pharmacovigilance study on cardiac arrhythmias reports associated with ICIs based on the FAERS database. Our research presented a comprehensive description on cardiac arrhythmias associated to different ICI regimens, resulting in certain systematical and accurate conclusions.

Importantly, our study detected a significant signal between cardiac arrhythmias and ICI therapy. Notably, our study revealed that immune-mediated arrhythmias were disproportionately more frequent reported in concurrent cardiotoxicity, which was concordant to what is observed in prior studies (Johnson et al., 2016; Salem et al., 2018; Herrmann, 2020; Nso et al., 2020; Baik et al., 2021; Stein-Merlob et al., 2021). The ICI-associated arrhythmias reports indicated a complicated clinical course, which prompted an evaluation for the presence of other cardiotoxicities. Similarly, all patients presenting with symptoms concerning for ICI-associated cardiotoxicity should have a 12-lead ECG to assess for arrhythmias.

In our study, concurrent cardiotoxicity increasing the reporting risk of ICI-related arrhythmias included cardiac failure [ROR 2.61 (2.20–3.09)], coronary artery disorders [ROR 2.28 (1.83–2.85)], myocardial disorders [ROR 5.25

TABLE 4 Onset time of ICIs–associated arrhythmias.

	Ipilimumab (*n* = 37)	Tremelimumab (*n*= 3)	Nivolumab (*n* = 659)	Pembrolizumab (*n* = 479)	Cemiplimab (*n* = 7)	Atezolizumab (*n* = 246)	Avelumab (*n*=51)	Durvalumab (*n* = 97)	Ipilimumab +Nivolumab (*n* = 349)	Tremelimumab +Durvalumab (*n* = 29)
Median (IQR)	47 (19–67)	143 (140–143)	35 (12–135)	25 (7–76)	56 (22–99)	34 (12–168)	18 (1–103)	35 (9-100)	31 (12-84)	135 (10–323)
0–30	8 (21.62%)	0 (0.00%)	214 (32.47%)	148 (30.90%)	2 (28.57%)	90 (36.59%)	25 (49.02%)	36 (37.11%)	128 (36.68%)	6 (20.69%)
31–60	9 (24.32%)	0 (0.00%)	79 (11.99%)	42 (8.77%)	0 (0.00%)	25 (10.16%)	7 (13.73%)	13 (13.40%)	49 (14.05%)	3 (10.34%)
61–90	4 (10.81%)	0 (0.00%)	26 (3.95%)	17 (3.55%)	1 (14.29%)	14 (5.69%)	0 (0.00%)	8 (8.25%)	23 (6.59%)	0(0.00%)
91–120	2 (5.41%)	0 (0.00%)	14 (2.12%)	8 (1.67%)	1 (14.29%)	8 (3.25%)	3 (5.88%)	3 (3.09%)	16 (4.58%)	1 (3.45%)
121–150	0 (0.00%)	1 (33.33%)	24 (3.64%)	6 (1.25%)	0 (0.00%)	6 (2.44%)	1 (1.96%)	3 (3.09%)	4 (1.15%)	3 (10.34%)
151–180	0 (0.00%)	2 (66.67%)	9 (1.37%)	8 (1.67%)	0 (0.00%)	3 (1.22%)	1 (1.96%)	1 (1.03%)	5 (1.43%)	1 (3.45%)
181–360	1 (2.70%)	0 (0.00%)	51 (7.74%)	19 (3.97%)	0 (0.00%)	23 (9.35%)	3 (5.88%)	8 (8.25%)	22 (6.30%)	3 (10.34%)
Greater than 360	1 (2.70%)	0 (0.00%)	42 (6.37%)	19 (3.97%)	0 (0.00%)	23 (9.35%)	4 (7.84%)	5 (5.15%)	14 (4.01%)	4 (13.79%)
Unknown	12 (32.43%)	0 (0.00%)	200 (30.35%)	212 (44.26%)	3 (42.86%)	54 (21.95%)	7 (13.73%)	20 (20.62%)	88 (25.21%)	8 (27.59%)

Abbreviations: N: number of records; IQR: interquartile range; ICI, immune checkpoint inhibitor.

10.3389/fphar.2022.986357

TABLE 5 The multivariate analysis of concurrent cardiotoxicity and ICI-associated arrhythmias.

Concurrent cardiotoxicity	Arrhythmias		Cardiac conduction disorders		Rate and rhythm disorders NEC		Supraventricular arrhythmias		Ventricular arrhythmias and cardiac arrest	
	OR (95%CI)	*p-value*	OR (95%CI)	*p-value*	OR (95%CI)	*p-value*	OR (95%CI)	*p-valuee*	OR (95%CI)	*p-value*
Cardiac failure	2.61 (2.20–3.09)	*p*<0.001	1.24 (0.73-2.12)	0.427	2.79 (2.02-3.84)	*p*<0.001	3.40 (2.68–4.32)	*p*<0.001	2.42 (1.79–3.28)	*p*<0.001
Coronary artery disorders	2.28 (1.83–2.85)	*p*<0.001	3.04 (1.81-5.11)	*p*<0.001	3.34 (2.32-4.80)	*p*<0.001	2.04 (1.45–2.89)	*p*<0.001	1.50 (0.96–2.34)	0.075
Myocardial disorders	5.25 (4.44–6.22)	*p*<0.001	35.51 (25.82-48.85)	*p*<0.001	2.45 (1.64-3.64)	*p*<0.001	2.73 (2.01–3.69)	*p*<0.001	5.90 (4.47–7.78)	*p*<0.001
Pericardial disorders	2.76 (2.09–3.64)	*p*<0.001	0.78 (0.24-2.54)	0.683	2.53 (1.49-4.31)	0.001	4.47 (3.18–6.28)	*p*<0.001	1.23 (0.65–2.35)	0.523
Cardiac valve disorders	3.21 (1.34–7.68)	*p*<0.001	—	—	0.80 (0.10-6.37)	0.833	5.79 (2.29–14.68)	*p*<0.001	1.82 (0.40–8.31)	0.441

Abbreviations: CI, confidence interval; OR, odds ratio; eGFR, estimated glomerular filtration rate.

(4.44–6.22)], pericardial disorders [ROR 2.76 (2.09–3.64)] and cardiac valve disorders [ROR 3.21 (1.34–7.68)]. Different types of reports of ICI-associated arrhythmia, including conduction delays, rate and rhythm disorders, supraventricular and ventricular arrhythmias (Escudier et al., 2017; Mir et al., 2018; Stein-Merlob et al., 2021), presented consistent association with concurrent myocardial disorders and different correlation with other four kinds of concurrent cardiotoxicity. Previous studies suggested that reports of supraventricular arrhythmias following ICI therapy were associated with other concurrent irAEs (Salem et al., 2018) or T-lymphocyte-mediated inflammation in the sinoatrial and atrioventricular nodes (Johnson et al., 2016; Nso et al., 2020). Rate and rhythm disorders reports (including arrhythmia, bradycardia and tachycardia) could be seen in the setting of high degrees of conduction block. In patients receiving ICI therapy, ventricular arrhythmias and conduction block might be a result of the T-lymphocyte-mediated inflammatory infiltration into the myocardium (Johnson et al., 2016; Herrmann, 2020; Baik et al., 2021; Stein-Merlob et al., 2021). Whereas, precise mechanisms underlying of ICI-associated arrhythmias remain to be elucidated. It is unclear whether the increased reporting of arrhythmias following ICI therapy was due to concurrent cardiotoxicities *versus* due to ICI treatment itself.

This study showed that ICI-associated arrhythmias were over-reported for anti-PD-1/PD-L1 vs anti-CTLA-4 monotherapy [ROR: 1.80 (1.44–2.26) and 2.22 (1.76–2.80), respectively]. In addition, there was increased risk of reports of arrhythmias with dual ICI combination therapy [ROR: 1.30 (1.20–1.41)]. Anti-CTLA-4 agents were not associated with over-reporting frequencies of reporting arrhythmias [ROR: 0.62 (0.57–0.67)], consistent with previous findings showing that anti-CTLA-4 was not associated with risk of reporting pericardial toxicities and less susceptible to myocarditis (Zhou et al., 2019; Ma et al., 2021). The non-susceptibility of anti-CTLA-4 to pericarditis and myocarditis was due to the difference of disease-specific effects (Salem et al., 2018; Ma et al., 2021) and mechanism (Grabie et al., 2019), respectively. Due to the correlation between ICI related arrhythmias and the both two concurrent cardiotoxicities, the low reporting risk of anti-CTLA-4 in myocarditis and pericarditis may lead to low reporting risk of arrhythmias. Owing to a lack of studies on immunotherapy-induced arrhythmias, the rationale for no signal for anti-CTLA-4 drugs need to be further elucidated and explored.

Our study showed that most reports of ICI-associated arrhythmias occurred early after ICI initiation, with no significant difference between different ICI regimens. The median time to onset of arrhythmias reports associated with ICIs was 32 (IQR 10–109) days, and most reports (33.57%) appeared within the first 30 days after the initiation of ICI, which suggested the importance of cardiac monitoring during the higher-risk time window of 30 days. The median onset time reported with dual ICI therapies were 32.5 (IQR 12–96.25) days, and no earlier onset of arrhythmias was reported with ICI combination therapies than with ICI monotherapies. This finding was inconsistent with those of previously published case reports of ICI-associated cardiotoxicity, which reported that cardiotoxicity occurred earlier when two ICIs were combined (Zhou et al., 2019).

This study involves certain limitations that should be recognized. Firstly, resulting from the signal mining of FAERS database, our study may be associated with inevitable underreporting and selective reporting. Firstly, as a spontaneous reporting system (SRS), there are some

limitations inherent to FAERS database, including missing data, partial clinical features of AEs, and reporting bias (e.g., inevitable underreporting, selective reporting and the potential for the data to be misunderstood). Secondly, it is difficult to control for confounding factors such as history of arrhythmias or concomitant medications, both of which might influence the risk of cardiac arrhythmias. Lastly, due to lack of the number of patients exposed to ICIs without AEs, FAERS data can neither be used to calculate the incidence of an adverse reaction nor quantify adverse reaction signals based on the total number of AEs.

Conclusion

This study comprehensively evaluated the relationship between ICIs and cardiac arrhythmias based on the FAERS database, as well as exploring the associations between concurrent cardiotoxicity and ICI-related arrhythmias, which can assist medication monitoring, clinical practice, and future investigations. Further studies are needed to address the mechanisms underlying ICI-related arrhythmias and to validate the results in our study.

Data availability statement

The original contributions presented in the study are included in the article/Supplementary Material, further inquiries can be directed to the corresponding author.

Author contributions

The manuscript was designed and written by FW and XW. The data acquisition, statistical analysis and revising were performed by FW and QW. All authors read and approved the final manuscript.

Conflict of interest

The authors declare that the research was conducted in the absence of any commercial or financial relationships that could be construed as a potential conflict of interest.

Publisher's note

All claims expressed in this article are solely those of the authors and do not necessarily represent those of their affiliated organizations, or those of the publisher, the editors and the reviewers. Any product that may be evaluated in this article, or claim that may be made by its manufacturer, is not guaranteed or endorsed by the publisher.

Supplementary material

The Supplementary Material for this article can be found online at: https://www.frontiersin.org/articles/10.3389/fphar.2022.986357/full#supplementary-material

References

Alhumaid, W., Yogasundaram, H., and Senaratne, J. M. (2021). Slow bidirectional ventricular tachycardia as a manifestation of immune checkpoint inhibitor myocarditis. *Eur. Heart J.* 42 (29), 2868. doi:10.1093/eurheartj/ehab219

Baik, A. H., Tsai, K. K., Oh, D. Y., and Aras, M. A. (2021). Mechanisms and clinical manifestations of cardiovascular toxicities associated with immune checkpoint inhibitors. *Clin. Sci.* 135 (5), 703–724. doi:10.1042/CS20200331

Ball, S., Ghosh, R. K., Wongsaengsak, S., Bandyopadhyay, D., Ghosh, G. C., Aronow, W. S., et al. (2019). Cardiovascular toxicities of immune checkpoint inhibitors: JACC review topic of the week. *J. Am. Coll. Cardiol.* 74 (13), 1714–1727. doi:10.1016/j.jacc.2019.07.079

Bate, A., Lindquist, M., Edwards, I. R., Olsson, S., Orre, R., Lansner, A., et al. (1998). A Bayesian neural network method for adverse drug reaction signal generation. *Eur. J. Clin. Pharmacol.* 54 (4), 315–321. doi:10.1007/s002280050466

Bomze, D., Meirson, T., Hasan Ali, O., Goldman, A., Flatz, L., and Habot-Wilner, Z. (2022). Ocular adverse events induced by immune checkpoint inhibitors: A comprehensive pharmacovigilance analysis. *Ocul. Immunol. Inflamm.* 30 (1), 191–197. doi:10.1080/09273948.2020.1773867

Bukamur, H. S., Mezughi, H., Karem, E., Shahoub, I., and Shweihat, Y. (2019). Nivolumab-induced third degree atrioventricular block in a patient with stage IV squamous cell lung carcinoma. *Cureus* 11 (6), e4869. doi:10.7759/cureus.4869

Escudier, M., Cautela, J., Malissen, N., Ancedy, Y., Orabona, M., Pinto, J., et al. (2017). Clinical features, management, and outcomes of immune checkpoint inhibitor-related cardiotoxicity. *Circulation* 136 (21), 2085–2087. doi:10.1161/CIRCULATIONAHA.117.030571

Ferris, R. L., Blumenschein, G., Fayette, J., Guigay, J., Colevas, A. D., Licitra, L., et al. (2016). Nivolumab for recurrent squamous-cell carcinoma of the head and neck. *N. Engl. J. Med.* 375 (19), 1856–1867. doi:10.1056/NEJMoa1602252

Grabie, N., Lichtman, A. H., and Padera, R. (2019). T cell checkpoint regulators in the heart. *Cardiovasc. Res.* 115 (5), 869–877. doi:10.1093/cvr/cvz025

Herrmann, J. (2020). Adverse cardiac effects of cancer therapies: Cardiotoxicity and arrhythmia. *Nat. Rev. Cardiol.* 17 (8), 474–502. doi:10.1038/s41569-020-0348-1

Hu, Y., Gong, J., Zhang, L., Li, X., Li, X., Zhao, B., et al. (2020). Colitis following the use of immune checkpoint inhibitors: A real-world analysis of spontaneous reports submitted to the FDA adverse event reporting system. *Int. Immunopharmacol.* 84, 106601. doi:10.1016/j.intimp.2020.106601

Johnson, D. B., Balko, J. M., Compton, M. L., Chalkias, S., Gorham, J., Xu, Y., et al. (2016). Fulminant myocarditis with combination immune checkpoint blockade. *N. Engl. J. Med.* 375 (18), 1749–1755. doi:10.1056/NEJMoa1609214

Joseph, L. (2021). Incidence of cancer treatment induced arrhythmia associated with immune checkpoint inhibitors. *J. Atr. Fibrillation* 13 (5), 2461. doi:10.4022/jafib.2461

Katsume, Y., Isawa, T., Toi, Y., Fukuda, R., Kondo, Y., Sugawara, S., et al. (2018). Complete atrioventricular block Associated with pembrolizumab-induced acute myocarditis: The need for close cardiac monitoring. *Intern. Med.* 57 (21), 3157–3162. doi:10.2169/internalmedicine.0255-17

Larkin, J., Chiarion-Sileni, V., Gonzalez, R., Grob, J. J., Rutkowski, P., Lao, C. D., et al. (2019). Five-year survival with combined nivolumab and ipilimumab in advanced melanoma. *N. Engl. J. Med.* 381 (16), 1535–1546. doi:10.1056/NEJMoa1910836

Ma, Z., Pei, J., Sun, X., Liu, L., Lu, W., Guo, Q., et al. (2021). Pericardial toxicities associated with immune checkpoint inhibitors: A pharmacovigilance analysis of the FDA adverse event reporting system (FAERS) database. *Front. Pharmacol.* 12, 663088. doi:10.3389/fphar.2021.663088

Mahmood, S. S., Fradley, M. G., Cohen, J. V., Nohria, A., Reynolds, K. L., Heinzerling, L. M., et al. (2018). Myocarditis in patients treated with immune checkpoint inhibitors. *J. Am. Coll. Cardiol.* 71 (16), 1755–1764. doi:10.1016/j.jacc.2018.02.037

Mikami, T., Liaw, B., Asada, M., Niimura, T., Zamami, Y., Green-LaRoche, D., et al. (2021). Neuroimmunological adverse events associated with immune checkpoint inhibitor: A retrospective, pharmacovigilance study using FAERS database. *J. Neurooncol.* 152 (1), 135–144. doi:10.1007/s11060-020-03687-2

Mir, H., Alhussein, M., Alrashidi, S., Alzayer, H., Alshatti, A., Valettas, N., et al. (2018). Cardiac complications associated with checkpoint inhibition: A systematic review of the literature in an important emerging area. *Can. J. Cardiol.* 34 (8), 1059–1068. doi:10.1016/j.cjca.2018.03.012

Noren, G. N., Hopstadius, J., and Bate, A. (2013). Shrinkage observed-to-expected ratios for robust and transparent large-scale pattern discovery. *Stat. Methods Med. Res.* 22 (1), 57–69. doi:10.1177/0962280211403604

Nso, N., Antwi-Amoabeng, D., Beutler, B. D., Ulanja, M. B., Ghuman, J., Hanfy, A., et al. (2020). Cardiac adverse events of immune checkpoint inhibitors in oncology patients: A systematic review and meta-analysis. *World J. Cardiol.* 12 (11), 584–598. doi:10.4330/wjc.v12.i11.584

Prevel, R., Colin, G., Cales, V., Renault, P. A., and Mazieres, J. (2020). Third degree atrio-ventricular blockade during a myocarditis occurring under anti-PD1 : Case report and literature review. *Rev. Med. Interne* 41 (4), 284–288. doi:10.1016/j.revmed.2019.12.023

Reck, M., Rodriguez-Abreu, D., Robinson, A. G., Hui, R., Csoszi, T., Fulop, A., et al. (2016). Pembrolizumab versus chemotherapy for PD-L1-positive non-small-cell lung cancer. *N. Engl. J. Med.* 375 (19), 1823–1833. doi:10.1056/NEJMoa1606774

Rothman, K. J., Lanes, S., and Sacks, S. T. (2004). The reporting odds ratio and its advantages over the proportional reporting ratio. *Pharmacoepidemiol. Drug Saf.* 13 (8), 519–523. doi:10.1002/pds.1001

Salem, J. E., Manouchehri, A., Moey, M., Lebrun-Vignes, B., Bastarache, L., Pariente, A., et al. (2018). Cardiovascular toxicities associated with immune checkpoint inhibitors: An observational, retrospective, pharmacovigilance study. *Lancet. Oncol.* 19 (12), 1579–1589. doi:10.1016/S1470-2045(18)30608-9

Savarapu, P., Abdelazeem, B., Isa, S., Kesari, K., and Kunadi, A. (2021). Ipilimumab and Nivolumab induced ventricular tachycardia in a patient with metastatic renal cell carcinoma. *J. Community Hosp. Intern. Med. Perspect.* 11 (6), 874–876. doi:10.1080/20009666.2021.1965708

Stein-Merlob, A. F., Rothberg, M. V., Ribas, A., and Yang, E. H. (2021). Cardiotoxicities of novel cancer immunotherapies. *Heart* 107 (21), 1694–1703. doi:10.1136/heartjnl-2020-318083

Zhai, Y., Ye, X., Hu, F., Xu, J., Guo, X., Zhuang, Y., et al. (2019). Endocrine toxicity of immune checkpoint inhibitors: A real-world study leveraging US Food and drug administration adverse events reporting system. *J. Immunother. Cancer* 7 (1), 286. doi:10.1186/s40425-019-0754-2

Zhou, Y. W., Zhu, Y. J., Wang, M. N., Xie, Y., Chen, C. Y., Zhang, T., et al. (2019). Immune checkpoint inhibitor-associated cardiotoxicity: Current understanding on its mechanism, diagnosis and management. *Front. Pharmacol.* 10, 1350. doi:10.3389/fphar.2019.01350

frontiers | Frontiers in Oncology

TYPE Brief Research Report
PUBLISHED 10 November 2022
DOI 10.3389/fonc.2022.959741

OPEN ACCESS

EDITED BY
Miao Yan,
Second Xiangya Hospital, Central South University, China

REVIEWED BY
Claire Knezevic,
Johns Hopkins University, United States
Gregory Sivolapenko,
University of Patras, Greece
Satoshi Noda,
Shiga University of Medical Science Hospital, Japan

*CORRESPONDENCE
Jana Stojanova
jana.stojanova@svha.org.au

SPECIALTY SECTION
This article was submitted to Pharmacology of Anti-Cancer Drugs, a section of the journal Frontiers in Oncology

RECEIVED 02 June 2022
ACCEPTED 07 October 2022
PUBLISHED 10 November 2022

CITATION
Stojanova J, Carland JE, Murnion B, Seah V, Siderov J and Lemaitre F (2022) Therapeutic drug monitoring in oncology - What's out there: A bibliometric evaluation on the topic. *Front. Oncol.* 12:959741. doi: 10.3389/fonc.2022.959741

Therapeutic drug monitoring in oncology - What's out there: A bibliometric evaluation on the topic

Jana Stojanova[1,2]*, Jane E. Carland[1,3], Bridin Murnion[1,4], Vincent Seah[1], Jim Siderov[5] and Florian Lemaitre[6,7]

[1]Department of Clinical Pharmacology and Toxicology, St. Vincent's Hospital, Sydney, NSW, Australia, [2]Interdisciplinary Centre for Health Studies (CIESAL), Universidad de Valparaiíso, Valparaiíso, Chile, [3]School of Clinical Medicine, Faculty of Medicine and Health, Sydney, NSW, Australia, [4]Faculty of Medicine and Health, University of Sydney, Sydney, NSW, Australia, [5]Pharmacy Department, Austin Health, Heidelberg, VIC, Australia, [6]Université de Rennes, CHU Rennes, Inserm, EHESP, Irset (Institut de recherche en santé, environnement et travail), Rennes, France, [7]INSERM, Centre d'Investigation Clinique, Rennes, France

Pharmacological therapy is the mainstay of treatment for cancer patients. Despite wide interpatient variability in systemic drug concentrations for numerous antineoplastics, dosing based on body size remains the predominant approach. Therapeutic drug monitoring (TDM) is used for few antineoplastics in specific scenarios. We conducted a rapid bibliometric evaluation of TDM in oncology to capture a snapshot of research in this area over time and explore topics that reflect development in the field. Reports with the composite, indexed term 'therapeutic drug monitoring' in the title and abstract were extracted from MEDLINE (inception to August 2021). Reports related to applications in cancer were selected for inclusion and were tagged by study design, antineoplastic drugs and concepts related to TDM. We present a timeline from 1980 to the present indicating the year of first report of antineoplastic agents and key terms. The reports in our sample primarily reflected development and validation of analytical methods with few relating to clinical outcomes to support implementation. Our work emphasises evidence gaps that may contribute to poor uptake of TDM in oncology.

KEYWORDS

therapeutic drug monitoring, pharmacokinetic, antineoplastic agents, kinase inhibitors, bibliometric analysis

Introduction

Therapeutic drug monitoring (TDM) is the practice of determining systemic drug concentrations to optimise patient outcomes, mainly by adjusting drug dosage. It has been shown to be of benefit for drugs with a narrow therapeutic window, significant inter- and intra-individual pharmacokinetic variability, an established concentration-effect relationship and where information about circulating drug concentrations is helpful for clinical management (1). Although TDM has been used to support dosing decisions for some antineoplastics since the 1970s (1), it is not universally applied. TDM guided dosing is accepted for specific antineoplastics in specific clinical contexts, including high-dose methotrexate, busulfan and thiopurines (2). However, dosing based on weight and/or body surface area (BSA) continues to be the dominant approach despite observation of wide interpatient variability in systemic drug concentrations (2).

While there are many aspects to consider when evaluating the suitability of concentration-based dosing in oncology, one issue is that exposure-response relationships are not systematically evaluated during regulatory approval. This is illustrated by an examination of US Food and Drug Administration's clinical pharmacology reviews for biologicals used in oncology; of 15 agents registered between 2005 and 2016, only five had documented exposure-response relationships (3). Following commercialisation in the post-marketing authorisation setting, most exposure-response work is performed through academic initiatives. As a result, it is difficult to determine whether an individual therapeutic agent is a poor candidate for concentration-based dosing in a particular clinical context, or simply that evidence is lacking or of poor quality.

The recent boom in targeted oral and biological therapeutics has changed clinical practice in cancer therapy and has resulted in numerous novel agents entering the market annually. For the targeted oral agents, a single, maximally tolerated universal dose is typically marketed, however most of these drugs are substrates of metabolic enzymes and drug transporters. Of note, dosage adjustment is suggested for managing adverse drug reactions in the summary of product characteristics sheet for a number of these drugs, implicitly suggesting an exposure-response relationship; two examples are regorafenib and ibrutinib (4, 5). Large interpatient variability in systemic concentrations is increasingly recognised, provoking numerous initiatives to evaluate the suitability of concentration-based dosing for these agents (6, 7). While available targeted oral agents outnumber antineoplastic biologicals (both targeted agents and checkpoint inhibitors), the latter are increasingly used. These are similarly marketed at a single, maximally tolerated fixed dose. Although drug exposure is less likely to be impacted by a patient's physiological characteristics, concentrations have been related to effect for some agents (8). For the most part, research initiatives are academic and the evidence base has unfolded according to the clinical need and specialist areas of particular research groups.

Both traditional and targeted agents are approved following clinical trials involving participants that are relatively homogenous in terms of age, body size and ethnicity, and a lower degree of complex comorbidities. It is therefore often through research initiatives after introduction of the drug to routine clinical practice that the impact of obesity, extremes in age, comorbidities and genetic differences, among other aspects, are evaluated.

We conducted a rapid bibliometric evaluation of the literature referring to the TDM of antineoplastic agents, to capture a snapshot of the research in this area over time and explore topics that reflect development in the field. We characterised studies by publication type to explore the degree to which clinical evaluations have been undertaken within the greater body of literature. We sought to evaluate the impact of technological developments and novel approaches, such as alternative sampling strategies, over time. We were also interested in the timing and frequency of reports for agents that involved special populations, where the application of concentration-based dosing may be particularly important.

Methods

Search strategy

Reports with the composite, indexed term 'therapeutic drug monitoring' in the title and abstract were extracted from MEDLINE, from inception to August 3, 2021. This was a rapid scoping exercise. A subset of reports that included specific terms related to the fields of oncology/haematology and a list of antineoplastic agents were extracted (Appendix 1).

Selection criteria and screening

Studies were included if they reported on TDM in oncology. There was no restriction on the type of report or language, except for corrigendum or errata which were not included. Reports related to myeloablation for hematopoietic stem cell transplantation, or those referring to agents that have not reached global markets to date were excluded. Screening of titles and abstracts, and initial tagging, was performed using Rayyan by four reviewers (9). Discrepancies were discussed and resolved by the review team.

Tagging of therapeutic agents and key concepts

Tagging for therapeutic agents and key concepts was performed in Microsoft Excel. A column was assigned to each term and the presence of the term in the title and/or abstract was indicated. Additional terms were identified through iterations of the process. Tagging of a term was nonspecific; for example, occasionally therapeutic agents were referred to in the abstract as an auxiliary agent, such as co-therapy or an internal standard, rather than the object of the report. We did not correct for such instances and accepted this limitation. Tagging of words with different spelling was performed individually, but reported together, for example, pediatric/paediatric or haematology/hematology. Tagging of words and their most common acronyms was performed individually, but reported together, for example tandem mass spectroscopy/'MS/MS'. For reports without an abstract (n=25), the full text was reviewed to identify the publication type and the antineoplastic agent that was the object of the report, however concept terms were not reviewed for these reports. We did not tag for type of malignancy.

Categorization and grouping

Tags related to study design were grouped into four categories: assay development and validation; modelling and simulation; clinical trials and primary studies; and reviews and perspectives (Appendix 2). Pharmacological agents were grouped into categories: cytotoxic antineoplastics; kinase inhibitors; hormonal antineoplastics; monoclonal antibodies and other non-cytotoxic antineoplastics.

Data analysis and presentation

Data summaries were developed in R version 4.12 (10). Time series figures were prepared using Prism 9 (GraphPad, San Diego, CA).

Results

There were 8860 reports with the term 'therapeutic drug monitoring' in titles and abstracts, and 1750 were identified for screening. Of the total set, 686 (7.7%) were included as referring to TDM in oncology (Figure 1). Reports were identified that related to 27 cytotoxic antineoplastics, 25 kinase inhibitors, 8 hormonal antineoplastics, 7 biological targeted agents and 3 other non-cytotoxic antineoplastics. Twenty-three reports (3%) did not refer to any specific neoplastic agent, most of which were general reviews or perspectives on the topic.

Most publications concerned analytical aspects (n=278, 40.5%); 23.9% were clinical or cost-effectiveness studies (n=164), 26.8% were reviews and perspectives (n=184) and 10.9% concerned modelling and simulation (n=72). Most clinical studies were observational: case reports (n=44), prospective cohort (n=41), retrospective cohort (n=35), case series (n=25); only 0.9% of all identified reports were randomized or non-randomized controlled trials where TDM was the intervention (n=6); these were conducted 2011-2021. Cost-effectiveness was the objective of 25 reports. Twelve reports were categorised into two of the four publication categories.

The first report identified was published in 1980 and concerned methotrexate (Figure 2A). A relatively low publication rate on the topic of TDM in oncology (1-20 per

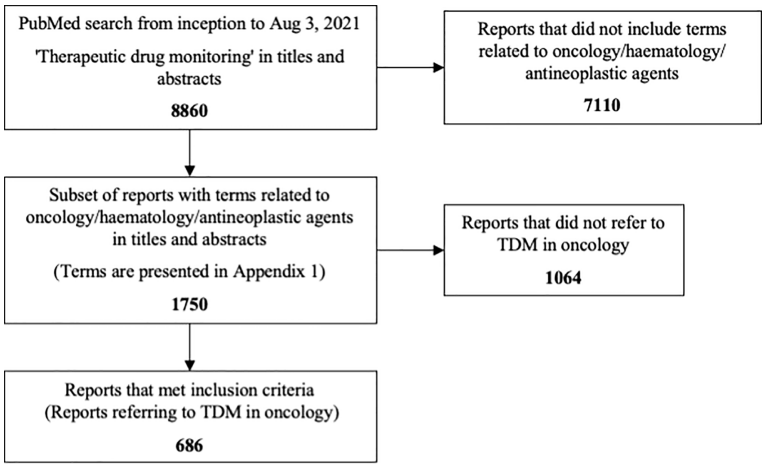

FIGURE 1
Flow chart presenting the study inclusion process.

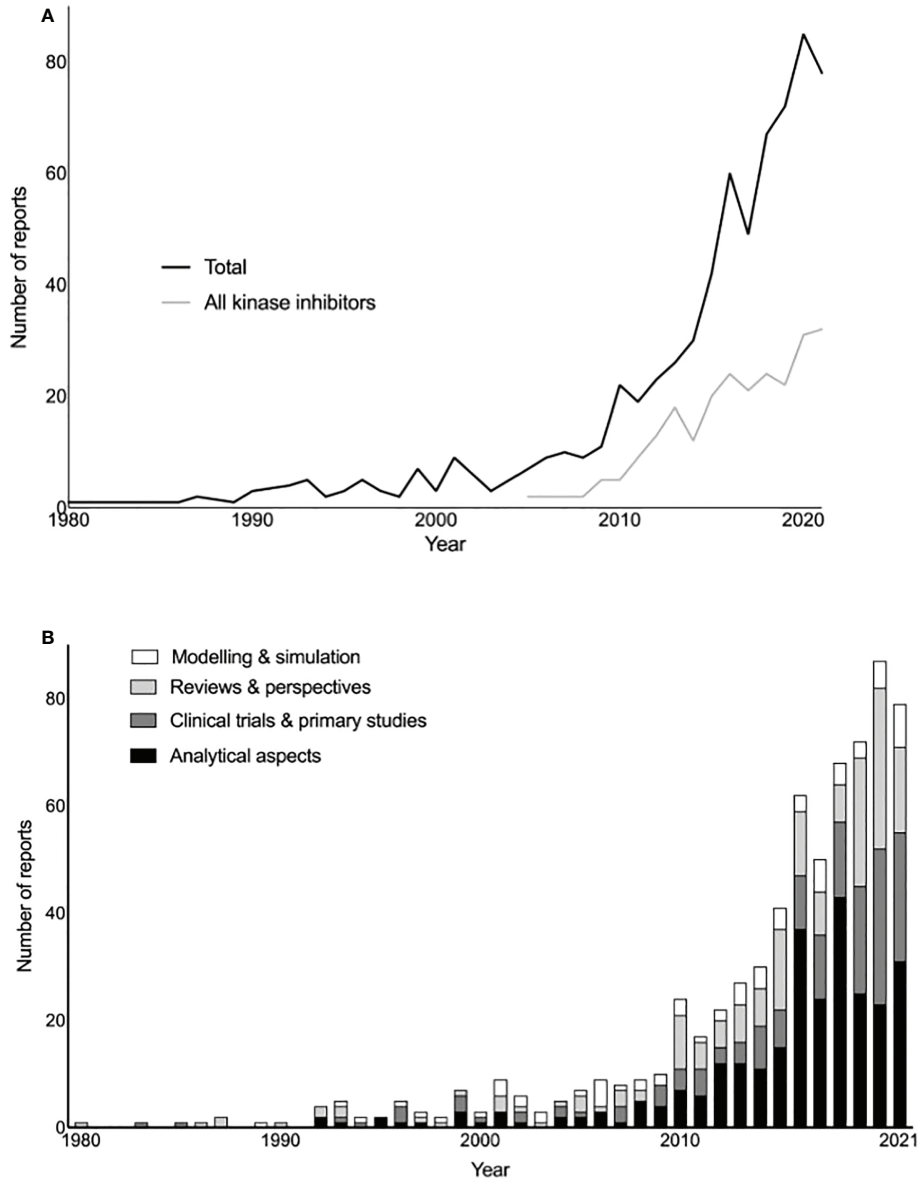

FIGURE 2
(A) Total reports and reports focusing on kinase inhibitors over time. **(B)** Total reports based on publication type over time.

year) was observed from 1980 until 2008 when the rate increased, aligning with the appearance of reports on kinase inhibitors, which were the object of 35.3% of all identified reports (n=242) (Figure 2A). Between 1980 and 1990 most publications identified were reviews and perspectives, while publications focusing on analytical aspects or clinical/other primary studies gradually increased in frequency from 1990 (Figure 2B).

Most cytotoxic antineoplastic drug classes had agents with first reports identified in the 1980s or 1990s; first reports for agents from the taxane and vinca alkaloid classes were identified in 2000 (paclitaxel) and 2001 (vincristine), respectively (Figure 3). The first report of agents from the hormonal antineoplastic class was identified in 2004 (tamoxifen), although reports for most other agents in this class were first identified in 2014 (mitotane) and later. The first report for a kinase inhibitor was identified in 2005 (imatinib), with multiple reports covering a variety of agents identified from 2009 onwards. The first report covering antineoplastic antibodies was identified in 2009 (cetuximab) (Figure 3).

FIGURE 3
Timeline of the year of first report identified for individual antineoplastic agents and selected concept terms (blue). HPLC: high-performance liquid chromatography; MS: mass spectrometry; MS/MS: tandem mass spectrometry; UHPLC: ultra-high-performance liquid chromatography.

When focusing on the most frequently reported antineoplastics, the proportion of the different publication types varied by agent (Table 1). For example, asparaginase was the object of a higher number of clinical studies (48%) and reviews (36%), relative to reports on analytical aspects (12%). In contrast, most publications relating to kinase inhibitors focused on analytical aspects, for example, 76% of the 33 publications identified for nilotinib. Similarly, reports about analytical aspects accounted for at least 40% of reports for methotrexate and taxanes. The proportion of reports about modelling and simulation was typically 10% or less, with the exception of platinum agents (26%).

Relatively few reports referred to 'immunoassay' (n=29) compared to 'chromatography' (n=157), both terms first appearing in 1992 (Supplemental Table S2). The first report involving HPLC was published in 1993 (n=66). The first report referring to 'mass spectrometry/MS' was published in 1999 (n=126), and for 'tandem mass spectrometry/MS/MS' in 2004 (n=115); most reports referring to mass spectrometry concerned tandem mass spectrometry (91%). More recent techniques identified include Raman spectroscopy (first identified in 2015, n=14), 'surface plasmon resonance/SPR' (first identified in 2012, n= 5), 'sensor' or 'biosensor' (first identified in 2015, n=13 and 5, respectively), and 'aptamer' for this type of sensor (first identified in 2021, n=2).

Blood or plasma were the principal sampling matrices across reports. Alternative sampling matrices were referred to in few reports: 'urine', 'saliva' and 'hair' in 5, 4 and 2 reports, respectively (Figure 3; Supplemental Table S2). The term 'intracellular' first appeared in 2006 (n=10) and 'peripheral blood mononuclear cell/PBMC' in 2021 (n=2). Terms referring to alternative sampling methods included 'dried blood spots/DBS' (n=26) and 'volumetric absorptive microsampling/VAMS' (n=2), first reported in 2011 and 2019, respectively.

We selected terms referring to special populations, including extremes of age and obesity (Supplemental Table S2). The terms child (n=44 reports), pae/ediatric (n=33 reports), neonate (n=6 reports), and infant (n=4 reports) were first identified in reports from 1983, 2007, 2015 and 2016, respectively. The term 'elderly' first appeared in 1994 (10 reports), and 'obese' in 2002 (n=3 reports). The primary comorbidity evaluated was renal disease and its consequences. The terms 'renal function', 'acute kidney injury/AKI', 'hae/emodialysis' and 'end stage renal disease' first appeared in reports from 1980, 2009, 2009 and 2018, and in 11, 2, 8 and 2 reports, respectively.

Terms relating to pharmacometrics, modelling and simulation appeared throughout the sample and those relating to dose adaptation and decision support ('Bayesian', 'forecast', 'decision support') first appeared in the 2000s (Supplemental Table S2). Concepts such as 'target concentration intervention' and 'PK/PD', first appeared in 2012 and 2014, in 5 and 7 reports, respectively (Supplemental Table S2). Regarding terms with greater than 25 reports, 'population pharmacokinetic', 'Bayesian' and 'simulation' primarily featured in reports about modelling rather than other study categories. 'Trough' and 'AUC', however, appeared more frequently in clinical or other primary studies (Supplemental Table S3). Terms related to metabolism and pharmacogenetics/genomics appeared throughout the sample, with terms referring to metabolic enzymes (CYP, P450) first appearing in 2005 (Supplemental Table S2). The stem 'pharmacogen-' predominantly appeared in reviews and perspectives.

Other unique concepts that appeared throughout the sample included 'toxic/toxicity', 'matrices/matrix' and 'targeted'. 'Cost' first appeared in 2010 (n=35). An emerging term of interest identified was 'circadian' (first report 2015, n=2). (Supplemental Table S2).

10.3389/fonc.2022.959741

TABLE 1 Publication type identified for the most commonly reported cytotoxic and non-cytotoxic antineoplastics (25 reports or more).

DRUG	Total	Analytical method development and validation	Clinical trials and primary studies	Modelling and simulation	Reviews and perspectives
Cytotoxic antineoplastics					
methotrexate	78	35 (44.9%)	14 (17.9%)	10 (12.8%)	19 (24.4%)
5-fu/fluorouracil	57	15 (26.3%)	13 (22.8%)	6 (10.5%)	23 (40.4%)
carboplatin	34	3 (8.8%)	11 (32.4%)	9 (26.5%)	11 (32.4%)
paclitaxel	25	10 (40%)	4 (16%)	3 (12%)	8 (32%)
Cytotoxic antineoplastic classes					
platinum agents	50	6 (12%)	18 (36%)	13 (26%)	13 (26%)
taxanes	32	12 (37.5%)	7 (21.9%)	3 (9.4%)	10 (31.2%)
Non-cytotoxic antineoplastics					
tamoxifen	30	7 (23.3%)	11 (36.7%)	3 (10%)	9 (30%)
asparaginase	25	3 (12%)	12 (48%)	1 (4%)	9 (36%)
Kinase inhibitors					
all kinase inhibitors	242*	116 (47.2%)	69 (28%)	23 (9.3%)	38 (15.4%)
imatinib	117	47 (40.2%)	26 (22.2%)	11 (9.4%)	33 (28.2%)
sunitinib	50	16 (32%)	16 (32%)	5 (10%)	13 (26%)
erlotinib	35	19 (54.3%)	6 (17.1%)	4 (11.4%)	6 (17.1%)
pazopanib	34	14 (41.2%)	11 (32.4%)	3 (8.8%)	6 (17.6%)
nilotinib	33	25 (75.8%)	3 (9.1%)	0 (0%)	5 (15.2%)
dasatinib	31	22 (71%)	4 (12.9%)	0 (0%)	5 (16.1%)
sorafenib	25	16 (64%)	2 (8%)	1 (4%)	6 (24%)
Antineoplastic monoclonal antibodies					
all monoclonal antibodies	39	16 (41%)	7 (17.9%)	2 (5.1%)	14 (35.9%)

*Four reports were in two of the categories indicated.

Discussion

Pharmacological therapy is the mainstay of treatment for cancer patients. Interest in the application of TDM for dosing antineoplastics is suggested by the rise in publications that included this term in titles and abstracts over the last 10 years. This coincides with the advent of kinase inhibitors, where numerous diverse agents enter global markets annually. Advances in analytical instrumentation and sampling methodologies likely also play a role in the rise of such publications, and this is reflected in our timeline.

Of 27 cytotoxic antineoplastic agents among reports, four had 25 or more publications identified (methotrexate, 5-fluorouracil, carboplatin, paclitaxel; Table 1). Though not universal, TDM is established practice for two of these agents, methotrexate and 5-fluorouracil, while for paclitaxel evidence is emerging and clinical application is at present not widespread (2, 11, 12). Although taxanes were discovered in the 1960s, paclitaxel, the first commercially available agent, obtained regulatory approval in 1992 due to challenges with synthesis and formulation (13). It is thus reasonable that the first report about paclitaxel therapeutic drug monitoring we identified was published in 2000.

Carboplatin deserves special mention. About a third of studies concerning this drug were clinical and other primary studies. Dosing is determined by the Calvert formula which relates renal function to a target AUC (14). This approach does not require measuring drug concentrations and is therefore not an example of the application of TDM. However, the example represents a departure from BSA dosing that came from the evaluation of drug concentrations through clinical use that ultimately resulted in reduced interindividual variability and improved outcomes. Among clinical studies within our sample, drug monitoring for carboplatin was used for high dose chemotherapy (15), neonates and infants (16, 17), amputees (18), obesity (19), and determining irreversible alopecia (20); several of these were case reports. This suggests interest in the application of concentration measurement of carboplatin to optimise dosing in special populations and unique scenarios. Similarly, that 5-fluorouracil concentrations achieved by BSA dosing differ in women compared to men was determined by clinical pharmacokinetic studies, and this is now accounted for in BSA based formulae (21); dosing based on concentration measurement for 5-fluorouracil is nonetheless superior in reducing inter-patient variability in systemic concentrations.

Central to performing TDM is ready access to relevant assays that are precise and sensitive. Commercial immunoassays are available for a limited number of antineoplastics; methotrexate (globally), 5-fluorouracil, paclitaxel and docetaxel (Europe only) (2). Of the 29 reports we identified with the term 'immunoassay', 25 related to analytical aspects and 16 concerned methotrexate. While chromatographic assays have been developed for many agents, few have attained regulatory approval for clinical use (2). At present, most laboratories employ LC-MS/MS as the principal analytic method applied to measure these drugs, reflected by the large number of reports since 2004 in our sample (n=115), relative to U/HPLC and traditional mass spectrometry.

The availability of suitable instrumentation and methodology has likely impacted which drugs are evaluated as TDM candidates over time. Vincristine provides an example of an agent, that despite a long history of clinical use (13), first appeared in our sample in 2001. While an analytical method was published in 1985 (22), improved separation procedures and novel detection sensors resulted in more sensitive assays (23–25). These reports did not refer to therapeutic drug monitoring and thus did not appear in our sample. The earlier assays required relatively large sample volumes, and further procedural and instrumental improvements enabled concentration measurement in paediatric populations, especially neonates and children, as illustrated by three publications we identified (16, 26, 27).

Kinase inhibitors were referred to in 17.5% of all reports identified in our sample; most publications referred to analytical aspects (47.2%). Of 25 kinase inhibitors, seven had 25 or more publications identified (28%), and reports about analytical aspects comprised 32-76% of publications for individual agents. Kinase inhibitors are typically marketed at a single dose but exhibit substantial interindividual variability (6), and the impact of interindividual variability on achievement of suggested trough targets varies by agent. For imatinib and sunitinib, an estimated 73% and 49% of individuals fail to meet targets for efficacy with standardised dosing, while for erlotinib a majority achieve suggested targets (89%) (28).

TDM involves a multidisciplinary team, including clinical and laboratory staff, and represents a complex, service level intervention that involves multiple steps. Adoption of TDM by clinicians requires a change in the way they make dosing decisions. One consideration when exploring TDM in oncology is the need for practice change. Implementation of evidence-based approaches into clinical practice can take an average of 17 years (29). Avoiding this time lag necessitates identifying and addressing barriers to uptake. For TDM in other fields of medicine, such as infectious diseases, studies have identified barriers including time constraints, as well as integration of TDM processes into clinical workflow (30).

Perhaps key for incorporation of TDM in oncology, are barriers aligned with knowledge (30). As evidence to support TDM in oncology is largely provided by academic initiatives, the body of literature is affected by factors such as limited funding and time, and may be the reason for a paucity of clinical studies. Lack of robust evidence for an exposure-response relationship is often cited as a primary reason why TDM is not widely adopted in oncology, and, in particular, lack of randomized controlled trials (31). In our sample we found 6 interventional controlled trials, all conducted relatively recently (2011–2021) (12, 32–36). Interventional trials involving TDM are difficult to undertake as TDM is a complex intervention; some specific challenges include inability to blind clinicians and lack of uptake of TDM-based dose advice by prescribers (37, 38).

We observed increasing interest in the application of TDM to guide antineoplastic dosing in special populations, for example, those that might not have been included in phase 3 clinical trials. Terms related to the very young (pae/ediatric, neonate, infant) were identified from 2007 onwards. Similarly, the term obese was first identified in 2002, albeit in relatively few reports. Availability of context-specific knowledge would help build clinician trust in the ability of TDM to guide dosing decisions, supporting sustained uptake.

Robust evidence for clinical implementation requires studies that are of a high quality. Quality evaluation of the studies in our sample was out of scope. While there is a reporting guide for clinical pharmacokinetic studies (39), this is not often used (published 2015; 70 citations in 2022). Risk of bias tools applied in evidence summaries, such as systematic reviews and clinical guidelines, are used to appraise quality. There are tools to cover a variety of study designs (40, 41), however those currently available do not reflect the particular challenges involved in clinical pharmacokinetic studies and studies that evaluate TDM as an intervention.

We limited our search to reports with the term 'therapeutic drug monitoring' in the title and abstract. This is not a limitation *per se*, but rather reflects our objective to perform a rapid scoping exercise, executed in a limited time frame. We selected this term as we consider it the most precise term to retrieve relevant reports. We excluded more general terms such as 'drug monitoring', 'trough concentrations' and 'pharmacokinetics' as these increased the retrieval of irrelevant reports many-fold. Our results must therefore be interpreted as reflecting the sample, rather than the complete body of work.

Work prior to 1990 might be underrepresented due to factors including increasing but not established adoption of the term, and relative lack of completeness of bibliographic databases prior to this date. The first report we captured is a review about methotrexate TDM and refers to previously published work that was not captured in our rapid scoping approach (42). Over time, reporting standards have developed, and it is possible that abstracts from earlier publications may have lacked detail compared to more recent work. Nevertheless, most antineoplastics currently in use were marketed after 1990, including some classic agents, such as paclitaxel, and all hormonal and targeted agents (13).

Concept based exploration was limited to concepts that could be defined by specific terms. For example, our approach did not permit determining changes in opinion about BSA based dosing over time, as it would be difficult to reduce this discourse to a set of key terms. Concept-based exploration was limited to the terms we proposed or identified through the tagging process. Topic modelling might be a helpful approach for future work (43), however might not capture important concepts of interest with low representation. Finally, the exploratory approach means that some agents not known to the authors with low representation in the data set may have been missed, however it is unlikely that highly represented agents were missed in the sample.

Conclusions

We undertook a bibliometric evaluation of the literature referring to the TDM of antineoplastic agents. Our sample primarily concerned reports about analytical methods, and relatively few reports relating to clinical outcomes of a design to support implementation. Gaps related to the agents evaluated might be explained by instrumental developments, for example, LC-MS/MS enabling measurement of vincristine. TDM offers an opportunity to improve the effectiveness and safety of antineoplastics, particularly with complex drug regimes, high risk populations and perhaps even in resistant disease. However, more robust evidence is needed to support implementation.

Data availability statement

The data that support the findings of this study are available on request from the corresponding author.

Author contributions

JSt, JC, BM, and VS performed screening and tagging. JSt, JC, and BM analyzed and interpreted data. JSi and FL provided clinical feedback and discussion. JSt, JC, BM, and FL wrote the manuscript draft. JSt conceived and supervised the project. All authors contributed to the article and approved the submitted version.

Funding

The article processing charge was supported by the Research Directorate of Universidad de Valparaíso (Grant CIDI8 Interdisciplinary Centre for Health Studies).

Acknowledgments

The authors would like to acknowledge Christian Valero Berretta for preparing data summaries in R.

Conflict of interest

The authors declare that the research was conducted in the absence of any commercial or financial relationships that could be construed as a potential conflict of interest.

Publisher's note

Supplementary material

The Supplementary Material for this article can be found online at: https://www.frontiersin.org/articles/10.3389/fonc.2022.959741/full#supplementary-material

References

1. Dasgupta A. Chapter 1 - introduction to therapeutic drug monitoring: Frequently and less frequently monitored drugs. In: Dasgupta A, editor. *Therapeutic drug monitoring*. Boston: Academic Press (2012). p. 1–29. Available at: https://www.sciencedirect.com/science/article/pii/B9780123854674000014.

2. Knezevic CE, Clarke W. Cancer chemotherapy: The case for therapeutic drug monitoring. *Ther Drug Monit* (2020) 42(1):6–19. doi: 10.1097/FTD.0000000000000701

3. Fleisher B, Ait-Oudhia S. A retrospective examination of the US food and drug administration's clinical pharmacology reviews of oncology biologics for potential use of therapeutic drug monitoring. *OncoTargets Ther* (2018) 11:113–21. doi: 10.2147/OTT.S153056

4. Bayer plc. Stivarga 40 mg film-coated tablets - summary of product characteristics (SmPC). In: *Electronic medicines compendium (emc)* (2022). Available at: https://www.medicines.org.uk/emc/product/1263.

5. Janssen-Cilag Ltd. Imbruvica 140 mg film-coated tablets - summary of product characteristics (SmPC). In: *Electronic medicines compendium (emc)* (2022). Available at: https://www.medicines.org.uk/emc/product/10025/smpc.

6. Lucas CJ, Martin JH. Pharmacokinetic-guided dosing of new oral cancer agents. *J Clin Pharmacol* (2017) 57(Suppl 10):S78–98. doi: 10.1002/jcph.937

7. Widmer N, Bardin C, Chatelut E, Paci A, Beijnen J, Levêque D, et al. Review of therapeutic drug monitoring of anticancer drugs part two–targeted therapies. *Eur J Cancer Oxf Engl 1990* (2014) 50(12):2020–36. doi: 10.1016/j.ejca.2014.04.015

8. Feng Y, Roy A, Masson E, Chen TT, Humphrey R, Weber JS. Exposure-response relationships of the efficacy and safety of ipilimumab in patients with advanced melanoma. *Clin Cancer Res Off J Am Assoc Cancer Res* (2013) 19 (14):3977–86. doi: 10.1158/1078-0432.CCR-12-3243

9. Ouzzani M, Hammady H, Fedorowicz Z, Elmagarmid A. Rayyan–a web and mobile app for systematic reviews. *Syst Rev* (2016) 5(1):1–10. doi: 10.1186/s13643-016-0384-4

10. R Core Team. R: A language and environment for statistical computing. In: *Vienna, Austria: R foundation for statistical computing* (2022). Available at: https://www.R-project.org/.

11. Muth M, Ojara FW, Kloft C, Joerger M. Role of TDM-based dose adjustments for taxane anticancer drugs. *Br J Clin Pharmacol* (2021) 87(2):306–16. doi: 10.1111/bcp.14678

12. Joerger M, von Pawel J, Kraff S, Fischer JR, Eberhardt W, Gauler TC, et al. Open-label, randomized study of individualized, pharmacokinetically (PK)-guided dosing of paclitaxel combined with carboplatin or cisplatin in patients with advanced non-small-cell lung cancer (NSCLC). *Ann Oncol Off J Eur Soc Med Oncol* (2016) 27(10):1895–902. doi: 10.1093/annonc/mdw290

13. Chabner BA, Roberts TG. Chemotherapy and the war on cancer. *Nat Rev Cancer* (2005) 5(1):65–72. doi: 10.1038/nrc1529

14. Calvert AH, Newell DR, Gumbrell LA, O'Reilly S, Burnell M, Boxall FE, et al. Carboplatin dosage: Prospective evaluation of a simple formula based on renal function. *J Clin Oncol Off J Am Soc Clin Oncol* (1989) 7(11):1748–56. doi: 10.1200/JCO.1989.7.11.1748

15. Chevreau C, Massard C, Flechon A, Delva R, Gravis G, Lotz JP, et al. Multicentric phase II trial of TI-CE high-dose chemotherapy with therapeutic drug monitoring of carboplatin in patients with relapsed advanced germ cell tumors. *Cancer Med* (2021) 10(7):2250–8. doi: 10.1002/cam4.3687

16. Veal GJ, Errington J, Sastry J, Chisholm J, Brock P, Morgenstern D, et al. Adaptive dosing of anticancer drugs in neonates: Facilitating evidence-based dosing regimens. *Cancer Chemother Pharmacol* (2016) 77(4):685–92. doi: 10.1007/s00280-016-2975-0

17. Nijstad AL, van Eijkelenburg NKA, Kraal KCJM, Meijs MJM, de Kanter CTMM, Lilien MR, et al. Cisplatin and carboplatin pharmacokinetics in a pediatric patient with hepatoblastoma receiving peritoneal dialysis. *Cancer Chemother Pharmacol* (2020) 86(3):445–9. doi: 10.1007/s00280-020-04130-z

18. van Gorp F, van Rens MTM, Kuck EM, Rozemeijer R, Huitema ADR, Brouwers EEM. Dosing of carboplatin in a patient with amputated legs: A case report. *J Oncol Pharm Pract Off Publ Int Soc Oncol Pharm Pract* (2014) 20(6):473–5. doi: 10.1177/1078155213514470

19. De Jonge ME, Mathôt RAA, Van Dam SM, Beijnen JH, Rodenhuis S. Extremely high exposures in an obese patient receiving high-dose cyclophosphamide, thiotepa and carboplatin. *Cancer Chemother Pharmacol* (2002) 50(3):251–5. doi: 10.1007/s00280-002-0494-7

20. de Jonge ME, Mathôt R a. A, Dalesio O, Huitema ADR, Rodenhuis S, Beijnen JH. Relationship between irreversible alopecia and exposure to cyclophosphamide, thiotepa and carboplatin (CTC) in high-dose chemotherapy. *Bone Marrow Transplant* (2002) 30(9):593–7. doi: 10.1038/sj.bmt.1703695

21. Mueller F, Büchel B, Köberle D, Schürch S, Pfister B, Krähenbühl S, et al. Gender-specific elimination of continuous-infusional 5-fluorouracil in patients with gastrointestinal malignancies: Results from a prospective population pharmacokinetic study. *Cancer Chemother Pharmacol* (2013) 71(2):361–70. doi: 10.1007/s00280-012-2018-4

22. De Smet M, Van Belle SJ, Storme GA, Massart DL. High-performance liquid chromatographic determination of vinca-alkaloids in plasma and urine. *J Chromatogr* (1985) 345(2):309–21. doi: 10.1016/0378-4347(85)80168-7

23. Bloemhof H, Van Dijk KN, De Graaf SS, Vendrig DE, Uges DR. Sensitive method for the determination of vincristine in human serum by high-performance liquid chromatography after on-line column-extraction. *J Chromatogr* (1991) 572 (1–2):171–9. doi: 10.1016/0378-4347(91)80481-Q

24. Crom WR, de Graaf SS, Synold T, Uges DR, Bloemhof H, Rivera G, et al. Pharmacokinetics of vincristine in children and adolescents with acute lymphocytic leukemia. *J Pediatr* (1994) 125(4):642–9. doi: 10.1016/S0022-3476(94)70027-3

25. de Graaf SS, Bloemhof H, Vendrig DE, Uges DR. Vincristine disposition in children with acute lymphoblastic leukemia. *Med Pediatr Oncol* (1995) 24(4):235–40. doi: 10.1002/mpo.2950240405

26. Koopmans P, Gidding CE, de Graaf SS, Uges DR. An automated method for the bioanalysis of vincristine suitable for therapeutic drug monitoring and pharmacokinetic studies in young children. *Ther Drug Monit* (2001) 23(4):406–9. doi: 10.1097/00007691-200108000-00014

27. Corona G, Casetta B, Sandron S, Vaccher E, Toffoli G. Rapid and sensitive analysis of vincristine in human plasma using on-line extraction combined with liquid chromatography/tandem mass spectrometry. *Rapid Commun Mass Spectrom RCM* (2008) 22(4):519–25. doi: 10.1002/rcm.3390

28. Lankheet NAG, Knapen LM, Schellens JHM, Beijnen JH, Steeghs N, Huitema ADR. Plasma concentrations of tyrosine kinase inhibitors imatinib, erlotinib, and sunitinib in routine clinical outpatient cancer care. *Ther Drug Monit* (2014) 36(3):326–34. doi: 10.1097/FTD.0000000000000004

29. Morris ZS, Wooding S, Grant J. The answer is 17 years, what is the question: understanding time lags in translational research. *J R Soc Med* (2011) 104(12):510–20. doi: 10.1258/jrsm.2011.110180

30. Chan JOS, Baysari MT, Carland JE, Sandaradura I, Moran M, Day RO. Barriers and facilitators of appropriate vancomycin use: Prescribing context is key. *Eur J Clin Pharmacol* (2018) 74(11):1523–9. doi: 10.1007/s00228-018-2525-2

31. Saleem M, Dimeski G, Kirkpatrick CM, Taylor PJ, Martin JH. Target concentration intervention in oncology: where are we at? *Ther Drug Monit* (2012) 34(3):257–65. doi: 10.1097/FTD.0b013e3182557342

32. Engels FK, Loos WJ, van der Bol JM, de Bruijn P, Mathijssen RHJ, Verweij J, et al. Therapeutic drug monitoring for the individualization of docetaxel dosing: a randomized pharmacokinetic study. *Clin Cancer Res Off J Am Assoc Cancer Res0* (2011) 17(2):353–62. doi: 10.1158/1078-0432.CCR-10-1636

33. Gotta V, Widmer N, Decosterd LA, Chalandon Y, Heim D, Gregor M, et al. Clinical usefulness of therapeutic concentration monitoring for imatinib dosage individualization: Results from a randomized controlled trial. *Cancer Chemother Pharmacol* (2014) 74(6):1307–19. doi: 10.1007/s00280-014-2599-1

34. de Wit D, van Erp NP, den Hartigh J, Wolterbeek R, den Hollander-van Deursen M, Labots M, et al. Therapeutic drug monitoring to individualize the dosing of pazopanib: A pharmacokinetic feasibility study. *Ther Drug Monit* (2015) 37(3):331–8. doi: 10.1097/FTD.0000000000000141

35. Zhang J, Zhou F, Qi H, Ni H, Hu Q, Zhou C, et al. Randomized study of individualized pharmacokinetically-guided dosing of paclitaxel compared with body-surface area dosing in Chinese patients with advanced non-small cell lung cancer. *Br J Clin Pharmacol* (2019) 85(10):2292–301. doi: 10.1111/bcp.13982

36. Rousselot P, Mollica L, Guilhot J, Guerci A, Nicolini FE, Etienne G, et al. Dasatinib dose optimisation based on therapeutic drug monitoring reduces pleural effusion rates in chronic myeloid leukaemia patients. *Br J Haematol* (2021) 194 (2):393–402. doi: 10.1111/bjh.17654

37. Kredo T, der WJSV, Siegfried N, Cohen K. Therapeutic drug monitoring of antiretrovirals for people with HIV. *Cochrane Database of Systematic Reviews* (2009) (3). doi: 10.1002/14651858.CD007268.pub2

38. Scheetz MH, Lodise TP, Downes KJ, Drusano G, Neely M. The case for precision dosing: medical conservatism does not justify inaction. *J Antimicrob Chemother* (2021) 76(7):1661–5. doi: 10.1093/jac/dkab086

39. Kanji S, Hayes M, Ling A, Shamseer L, Chant C, Edwards DJ, et al. Reporting guidelines for clinical pharmacokinetic studies: The ClinPK statement. *Clin Pharmacokinet* (2015) 54(7):783–95. doi: 10.1007/s40262-015-0236-8

40. Higgins JPT, Savović J, Page MJ, Elbers RG, Sterne JAC. Chapter 8: Assessing risk of bias in a randomized trial. In: Higgins JPT, Thomas J, Chandler J, Cumpston M, Li T, Page MJ, et al. (editors). *Cochrane Handbook for Systematic Reviews of Interventions version 6.3 (updated February 2022)*. Cochrane (2022). Available from: www.training.cochrane.org/handbook.

41. Sterne JA, Hernán MA, McAleenan A, Reeves BC, Higgins JP. Chapter 25: Assessing risk of bias in a non-randomized study. In: Higgins JPT, Thomas J, Chandler J, Cumpston M, Li T, Page MJ, et al. (editors). *Cochrane Handbook for Systematic Reviews of Interventions version 6.3 (updated February 2022)*. Cochrane (2022). Available from: https://training.cochrane.org/handbook/current/chapter-25.

42. Sadée W. Antineoplastic agents: high-dose methotrexate and citrovorum factor rescue. *Ther Drug Monit* (1980) 2(2):177–85. doi: 10.1097/00007691-198004000-00012

43. Asmussen CB, Møller C. Smart literature review: A practical topic modelling approach to exploratory literature review. *J Big Data* (2019) 6(1):93. doi: 10.1186/s40537-019-0255-7

frontiers | Frontiers in Oncology

TYPE Review
PUBLISHED 08 December 2022
DOI 10.3389/fonc.2022.1015200

OPEN ACCESS

EDITED BY
Robert Clarke,
University of Minnesota Twin Cities, United States

REVIEWED BY
Dominique Leveque,
Hôpital d'Hautepierre, France
Zhifeng Du,
Huazhong University of Science and Technology, China

*CORRESPONDENCE
Pattanaik Smita
pattanaik.smita@pgimer.edu.in

SPECIALTY SECTION
This article was submitted to Pharmacology of Anti-Cancer Drugs, a section of the journal Frontiers in Oncology

RECEIVED 09 August 2022
ACCEPTED 24 October 2022
PUBLISHED 08 December 2022

CITATION
Pattanaik S, Patil AN, Kumaravel J and Prakash G (2022) Therapeutic drug monitoring for cytotoxic anticancer drugs: Principles and evidence-based practices.
Front. Oncol. 12:1015200.
doi: 10.3389/fonc.2022.1015200

Therapeutic drug monitoring for cytotoxic anticancer drugs: Principles and evidence-based practices

Pattanaik Smita[1]*, Patil Amol Narayan[1], Kumaravel J[1] and Prakash Gaurav[2]

[1]Department of Pharmacology, Post Graduate Institute of Medical Education and Research, Chandigarh, India, [2]Department of Clinical Hematology and Medical Oncology, Post Graduate Institute of Medical Education and Research, Chandigarh, India

Cytotoxic drugs are highly efficacious and also have low therapeutic index. A great degree of caution needs to be exercised in their usage. To optimize the efficacy these drugs need to be given at maximum tolerated dose which leads to significant amount of toxicity to the patient. The fine balance between efficacy and safety is the key to the success of cytotoxic chemotherapeutics. However, it is possibly more rewarding to obtain that balance for this class drugs as the frequency of drug related toxicities are higher compared to the other therapeutic class and are potentially life threatening and may cause prolonged morbidity. Significant efforts have been invested in last three to four decades in therapeutic drug monitoring (TDM) research to understand the relationship between the drug concentration and the response achieved for therapeutic efficacy as well as drug toxicity for cytotoxic drugs. TDM evolved over this period and the evidence gathered favored its routine use for certain drugs. Since, TDM is an expensive endeavor both from economic and logistic point of view, to justify its use it is necessary to demonstrate that the implementation leads to perceivable improvement in the patient outcomes. It is indeed challenging to prove the utility of TDM in randomized controlled trials and at times may be nearly impossible to generate such data in view of the obvious findings and concern of compromising patient safety. Therefore, good quality data from well-designed observational study do add immense value to the scientific knowledge base, when they are examined in totality, despite the heterogeneity amongst them. This article compiles the summary of the evidence and the best practices for TDM for the three cytotoxic drug, busulfan, 5-FU and methotrexate. Traditional use of TDM or drug concentration data for dose modification has been witnessing a sea change and model informed precision dosing is the future of cytotoxic drug therapeutic management.

KEYWORDS

therapeutic drug monitoring, cytotoxic drugs reconstitution, busulfan, methotrexate, 5-FU, 5 fluorouracil, precision medicine

Introduction

Cytotoxic drugs are the oldest class of anticancer drugs. They are highly efficacious and also have low therapeutic index; therefore, a great degree of caution needs to be exercised in their usage. To optimize the efficacy, these drugs need to be given at the maximum tolerated dose. This dose leads to a significant amount of toxicity to the patient. The fine balance between efficacy and safety is the key to the success of cytotoxic chemotherapeutics. However, it is possibly more rewarding to obtain that balance for this class drugs as the frequency of drug-related toxicities is higher compared to the other therapeutic class and is potentially life-threatening and may cause prolonged morbidity. Significant efforts have been invested in the last three to four decades in therapeutic drug monitoring (1) research to understand the relationship between the drug concentration and the response achieved for therapeutic efficacy as well as drug toxicity for cytotoxic drugs. TDM evolved over this period and the evidence gathered favored its routine use for certain drugs. Since TDM is an expensive endeavor, both from an economic and a logistic point of view, to justify its use, it is necessary to demonstrate that the implementation leads to perceivable improvement in patient outcomes. It is indeed challenging to prove the utility of TDM in randomized controlled trials and at times may be nearly impossible to generate such data in view of the obvious findings and concern of compromising patient safety. Therefore, good quality data from a well-designed observational study add immense value to the scientific knowledge base, when they are examined in totality, despite the heterogeneity among them. This article compiles the summary of the evidence and the best practices for TDM for the three cytotoxic drug, busulfan, 5-FU, and methotrexate (Mtx) (Figure 1).

This article compiles the summary of the evidence for three cytotoxic drugs, busulfan, 5-FU, and Mtx, where the case for TDM is much established. Though there is evolving evidence for TDM in favor of the platinum group of drugs (paclitaxel, docetaxel, and carboplatin), tyrosine kinase inhibitors (1), and others like abiraterone and tamoxifen, they are beyond the scope of this review as we primarily intend to bring out the TDM best practices for the established cytotoxic drugs only (1–4).

Busulfan

Busulfan is a bifunctional DNA alkylating anticancer agent and acts in a cell cycle nonspecific manner. After systemic absorption, the carbonium ions are rapidly formed, which react with guanine molecules of the DNA through a nucleophilic substitution reaction (SN2) (5) forming intra- and interstrand crosslinks. This leads to breaks in the DNA molecule as well as crosslinking of the twin strands, resulting in interference of DNA replication and transcription of RNA and hence cell proliferation (6, 7).

Clinical use of busulfan

Oral busulfan had been used for the treatment of chronic myeloid leukemia (CML) (8, 9) and other myeloproliferative

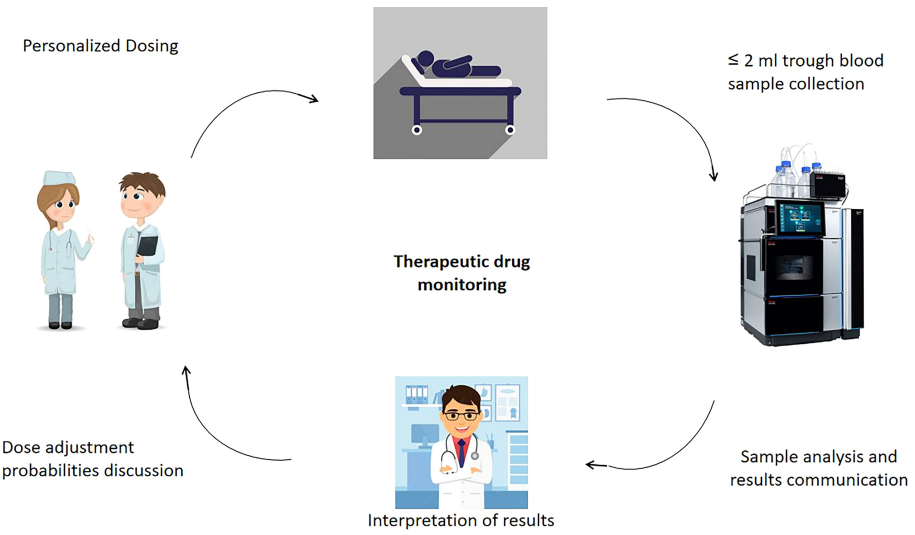

FIGURE 1
Overview of TDM applications in cytotoxic anticancer drug therapy.

disorders since the 1950s due to the inhibitory activity of the sulfonic derivatives of the drug on hematopoiesis (10, 11). In the last few decades, this use has become less popular due to the unsatisfactory curative potential despite initial good cytoreduction, thus reducing its use as a palliative therapy only. It was also found to have dismal efficacy in certain subsets of patients like those who have Philadelphia negative CML (12). In the present time, the use of oral busulfan is limited to palliative treatment of CML (myeloid, myelocytic, and granulocytic) and myeloproliferative neoplasms (13). In the late 1980s, oral busulfan was started to be used as a pretransplant myeloablative agent along with cyclophosphamide (8, 14). Oral administration of busulfan results in significant gastrointestinal irritability leading to nausea and vomiting that typically led to unpredictable systemic bioavailability (15, 16). Erratic absorption from the intestine coupled with GI complications substantially increased the systemic exposure variability to more than 10-fold (reported bioavailability ranged from 20% to 99%) (9). This unpredictability was responsible for poor efficacy and higher failure rate of the oral regimen and therefore paved the way for a major refinement in busulfan delivery. The i.v. formulations of busulfan were developed by Anderson and colleagues at the MD Anderson Cancer Center in the USA and was approved by the US FDA in 1999 (17, 18). Later on, intravenous busulfan replaced the oral route, as it provided better control over drug administration, bringing down the intradose exposure variation to 2- to 2.5-fold and maximizing the antitumor efficacy (19).

Though the use of oral busulfan was short-lived and it has now been replaced by intravenous use, it provided great insight to understand the pharmacokinetics (PK) of the drug and helped in the evolution of the TDM strategy. The PK profile of the drug is best described as a single compartment model, with rapid absorption and maximum plasma concentration achieved within 1 h. Majority of the drug is metabolized in the liver by the glutathione-S-transferase (20) enzyme and the metabolites are excreted *via* urine. A minimal amount of the drug (<2%) is excreted unchanged in the urine. The drug is eliminated by a log-linear fashion. We will discuss the PK of i.v. administered drug especially in the context of high-dose busulfan therapy as a part of myeloablative regimen before hematopoietic stem cell transplantation (HSCT). It is generally administered at a dose of 0.8 mg/kg in normal saline or 5% dextrose 6 hourly infusion over 2 h (or 3.2 mg/kg daily). Sixteen such doses (or four doses for once daily doses) are administered over 4 days (−7, −6, −5, and −4 days when day 0 is the day for infusion of the hematopoietic stem cell transfusion). The PK profile of the i.v. drug is similar to that of oral administration, which skips the fast-pass metabolism, providing 100% bioavailability.

High-dose intravenous busulfan has now been the preferred choice for myeloablation at most of the HSCT centers compared to total body irradiation (TBI) (12). It is currently the standard of care in the pretransplant myeloablative conditioning regimens along with other lymphotoxic chemotherapeutic agents (cyclophosphamide and fludarabine), for hematopoietic stem cell transplantation (HSCT). HSCT is a widely used potentially curative treatment strategy for several diseases, including hematological malignancies (e.g., leukemia and lymphoma), solid tumors, and nonmalignant disorders (e.g., thalassemia and sickle cell anemia).

Justification for TDM of busulfan

As described above, though busulfan is a highly efficacious cytotoxic drug, it poses several challenges in optimum dosing. Many factors qualify busulfan as an ideal candidate for TDM. The need for optimization of the dose was realized right at the beginning of the therapeutic failure of the oral regimen due to inadequate exposure. On the other hand, the serious adverse drug effects associated with higher exposure of busulfan lead to both hematological and nonhematological events. The onset of some of the ADRs are acute and some lead to chronic effects due to exposure over longer periods (21). The most common ADR include acute graft versus host disease (GVHD), mucositis, myelosuppression, seizures, hepatic veno-occulsive disease (HVOD, also known as sinusoidal occlusion syndrome), bronchopulmonary dysplasia, pulmonary fibrosis, and embryo–fetal toxicity. Robust evidence from several clinical studies support direct relationship between exposure–efficacy–toxicity. The introduction of the i.v. formulation led to better control over the concentration of the drug achieved in the systemic circulation circumventing the unpredictable intestinal absorption and hepatic fast-pass metabolism. However, the need for TDM was realized because of the bimodal distribution in the posttransplant mortality. Those who achieved inadequate concentration or those who achieved undesirably high concentration succumbed. With 6 hourly regimen, the threshold for therapeutic response is an exposure over one dosing interval, which is found to be 900–950 μM·min, whereas the threshold for toxic adverse effects is 1,200–1,500 μM·min. Hence, it can be concluded that busulfan has a narrow therapeutic window (900–1,200 mM·min) and consequently has a low therapeutic index (1,500/900 is <2).

With the use of i.v. formulation, the systemic concentration of busulfan had attained better predictability. Previously, interindividual variability of busulfan bioavailability with oral administration varied more than 10 fold, whereas it reduced to 2- to 2.5-fold with the use of i.v. formulation (19, 21). The reported coefficient of variation in busulfan maximal plasma concentration, clearance, and AUC was 18%, 25%, and 25% (13, 18) (Otsuka America Pharmaceutical Inc., Rockville,). Several subsequent clinical studies also confirmed the same (19, 22). The globally reported interindividual variability with i.v. use of busulfan is about 30%. Moreover, the intraindividual variability in exposure for the same dose may be as high as fivefold. Pharmacogenetic alterations in the metabolizing enzymes, drug transporters, and chronopharmacology have

been studied in this context. Single-nucleotide polymorphisms (SNPs) of the GST isoenzymes (GSTA1, GSTM1, and GSTP1) have been demonstrated to significantly affect the PK (clearance) of busulfan, thereby contributing to interindividual variability in small-sized studies and mostly in a pediatric population (23–25). However, their effect on the pharmacodynamics and incidence of therapeutic success vis-à-vis adverse events is not clear and hence their clinical relevance has not yet been demonstrated (26, 27). Similarly, polymorphic variants of CYP 2C9, 2B6, and membrane transporters like ABCB1 and SLC have also been studied for their association with busulfan disposition. Nevertheless, their role has not been found to be consequential (28). Chronopharmacologic variability in GST and CYP enzyme activity have also been studied in the context of variability in PK of busulfan. It has been postulated that this may contribute to intraindividual variability of AUC for the same dose of busulfan. However, these studies were conducted in the earlier period with oral busulfan and had several operational confounding factors, most importantly changes in intestinal motility. Moreover, the results from other studies have also yielded conflicting results (29, 30). To summarize, it was observed that the interindividual variability is significant enough with high-dose intravenous busulfan therapy to merit practice of TDM.

In addition to the above factors, potentially important drug–drug interactions may be kept in mind to optimize busulfan exposure and TDM could help in dose and exposure optimization. Several classes of drugs have been studied (Table 1). The most important class that needs a cautious approach is antifungal drugs, and the strategy of spacing the prescription is adopted at many centers to avoid the interaction. Another drug that merits mention is phenytoin, which had been the most common antiseizure prophylaxis prescribed during high-dose busulfan therapy, which potentially induces busulfan clearance. The newer antiepileptics like levetiracetam is used these days to avoid the interaction. Nevertheless, TDM can be a very useful tool in case of inadvertent drug interaction.

Other factors contributing to variability in busulfan exposure are age and body composition. Clearance of busulfan is 30% higher in children compared to adults, which has been postulated to be due to the higher physiological activity of the GST in young age groups. Patients with higher fat composition have a prolonged elimination half-life for busulfan as the fat tissue behaves as a temporary storage compartment for busulfan due to its high lipid solubility (31).

Evidence for exposure–adverse event relationship

At the advent of the oral conditioning regimen by Santos et al., a classical veno-occlusive disease of the liver was reported in the early 1980s, and by the end of the 1980s, it was suggested that TDM could have a potential role in reducing such adverse events (32–36). The oral dose regimen underwent several modifications; however, it was increasingly realized that several adverse events other than HVOD were associated with higher exposure to busulfan like acute GVHD (a cytokine storm that damages the normal organs in the body), seizures (typically of generalized type), and total incidence of treatment-related mortality. Though a multivariate analysis confirmed that oral administration is the single most important factor for HVOD, several other concomitant drugs like cyclophosphamide used in the preconditioning regimen, individual patient susceptibility, and disease type were also found to contribute to the event (12). Nevertheless, HVOD and hepato-renal failures are considered to be a classical trademark toxicity of high-dose busulfan therapy (12). Grochow and Dix demonstrated that the hepatic events are related to the drug concentration (34, 37). Both the studies indicated that an AUC of >1,500 μM·min and a steady-state plasma concentration (C_{ss}) above 1,025 ng/ml were significantly associated with HVOD after 6 hourly oral administration of busulfan. The evidence from these studies confirmed that the

TABLE 1 Potential drug interactions with busulfan.

Drug class and agents	Interaction with oral busulfan	Interaction with i.v. busulfan
Antifungals: Itraconazole	Likely	Likely
Fluconazole	Exercise caution	Exercise caution and avoid starting these drugs during preconditioning
Voriconazole		
Posaconazole		
Isavuconazole		
Antiepileptic: Phenytoin	Potential	Potential
Antimicrobials: Metronidazole	Inconsequential for both	Inconsequential for both
Ciprofloxacin		
Others: Deferasirox	Potential	Potential
Acetaminophen	Unlikely	Unlikely
N-acetylcystine	Unlikely	Unlikely
Oral contraceptive pills	Unlikely	Unlikely

threshold to HVOD is about 1,500 μM·min for a 6 hourly dosing (22, 38–40). Other studies, which used single daily dose administration, showed that the incidence of death due to HVOD was significantly increased above the exposure level of 6,000 μM·min (41, 42), hence confirming a full concordance between the findings. Similarly, the incidence seizure occurrence during treatment were significantly more during the higher exposures (30, 43). This is clearly explained by the PK profile of the drug, busulfan being lipophilic, and small molecules crossing the blood–brain barrier, and a higher concentration is achieved in the brain (1.3:1.0), hence causing acute neurotoxic effects. Apart from reducing toxicity, a pooled analysis of data of 674 patients who underwent stem cell transplant has shown that maintaining busulfan concentration within a therapeutic range led to better posttransplant survival. In the study, event-free survival at 2 years was 77.0% in patients with an optimum intravenous busulfan AUC of 78–101 mg·h/L compared with 66.1% in patients at the low historical target of 58–86 mg·h/L. Moreover, acute toxicity (p = 0.011) and transplant-related mortality (p < 0.0001) were significantly higher in high (>101 mg·h/L) busulfan AUC (44).

Evidence for exposure–efficacy relationship

A substantial number of studies in the early period during the oral busulfan use documented therapeutic failures. The patients with nonmalignant disease were especially prone to failed engraftment due to the intact immune system and faster clearance of busulfan. On the other hand, the patients with malignant disease failed engraftment, which led to the relapse and recurrence (45, 46) of the disease (47, 48). Slattery et al. suggested a concentration cutoff of 1,250 μM·min and a Css of 925 ng/ml for optimal therapeutic effect in bone marrow transplantation (39). Subsequently, they performed the study in patients with CML and showed that targeting an AUC of >1,350 μM·min led to treatment success (38). Radich et al. also showed similar findings; with AUC >1,350 μM·min, excellent outcome was observed (49). More recently, Anderson et al. showed that an AUC value <900 μM·min was associated with higher failure rates in the 6 hourly i.v. busulfan regimen (22). There was another interesting observation that confirmed the exposure–response relationship for busulfan. Children who clinically tolerated oral busulfan better than adults perhaps experienced more relapse after HSCT due to graft failure. As the understanding in busulfan PK was consolidated for its effect related to age, it was found that these children had faster clearance of busulfan and hence had reduced exposure to the drug, leading to better tolerance as well as therapeutic failure (48, 50, 51). Hence, the TDM-based dose adjustment to keep the AUC above 900 μM·min has been the consensus agreement for achieving desirable therapeutic effect. Several large retrospective studies established a therapeutic window for clinical response between 900 and 1,500 μM·min for AUC over 6 h in a 16-dose administration schedule. The corresponding cumulative AUC over 16 doses was set at 144,000 to 240,000 mM·min (32, 38, 39, 52, 53).

Evolution of the estimate of choice for TDM

In the 1980s, it was realized that single time point concentration would not be enough due to erratic absorption. Hence, exposure needs to be determined. With intravenous dosing, the concept of monitoring steady-state concentration was floated. Researchers came up with several formulas to calculate the Css and extrapolate a Css curve with first-dose AUC assuming that an ideal true steady state is reached. However, this was not a universal phenomenon, and a variation of 500% is noted between days 1 and 4 of infusion, as the volume of distribution (Vd) appeared to change with time. The hepatic enzyme activity decreases with progressive administration; hence, higher concentrations are observed in pretreated patients. Therefore, targeting the Css was found to be difficult and only 55% could achieve it even with best possible dose titration. Subsequent studies demonstrated that the exposure over a single dose is a better parameter to target. Hence, a limited sampling approach is adopted and the exposure is assessed by the calculation of area under the curve over the dosing interval (AUC0-τ), which is the parameter of interest for TDM (54). The current best practices for sample collection is described in the subsequent section.

Evidence for usefulness of TDM for busulfan

The published literature that constitutes the evidence base for deployment of TDM in routine patient care is very heterogeneous. Adequately powered controlled clinical studies are sparse. Despite this, the expert opinion fully favors practice of TDM for personalized busulfan therapy so as to optimize the exposure, maximize the therapeutic effect, and minimize the adverse events. This is applicable only in the setting of high-dose busulfan for preconditioning before HSCT but not reduced intensity preconditioning (55). The landmark randomized controlled study by Grochow et al. demonstrated a reduction of HVOD to reduce from 75% to 15% when the busulfan dose titration was done based on the TDM data to keep the AUC below 1,500 μM·min and only 5% of the patients were maintained within therapeutic range. Thereafter, it had been really difficult to refute this finding by conducting randomized controlled studies, as it involved concerns of patient safety. Several studies conducted in different settings (different age

groups like adult and children; several disease conditions like CML, AML, and multiple myeloma; and different co-conditioning agents like cyclophosphamide and melphalan) encountered similar findings (5, 38, 41, 49, 56–59). Traditionally, oral busulfan was administered in 6 hourly doses to minimize the GI adverse events. The same schedule continued for i.v. drug also due to the short half-life of the drug. The subsequent phase I/II PK studies did not demonstrate that there is a significant difference in the busulfan volume of distribution, half-life, and clearance between 6 hourly and 24 hourly dosing (60). As expected, the C_{max} values achieved with once daily doses were higher compared to the 6 hourly doses, but it was found that the clinical outcomes like rates of disease relapse (61), overall survival (61, 62), and HVOD (61–63) were not significantly different. Though definitive conclusions were impossible to arrive at, due to significant heterogeneity between the studies with regard to the disease population, concomitant medications, and inconstant use of TDM, QID dosing and OD dosing are in general considered to be equivalent.

Available assays for TDM of busulfan

A number of analytical techniques have been used for the quantification of busulfan (e.g., HPLC, LC/MS, and GC/MS) to measure circulating plasma concentrations. Liquid chromatography methods coupled with mass spectrometry have been the most commonly used technique for clinical care because of their sensitivity, specificity, and accuracy of results (64, 65). However, it is technically demanding and the sample processing and analysis may be time-consuming. Busulfan degrades quickly at room temperature; hence, the samples have to be analyzed quickly. It is also desirable to have a short turnaround time as the dose modification decisions have to be provided within a window of as less as 6 h. For delivering an efficient TDM service, these factors must be taken into consideration. Recently, several automated assays have been developed. Nanoparticle- and microparticle-based immunoassays are the two significant additions. These assays can be quickly performed without any sample processing steps. It has also been shown that they are in good conformity with the LC-MS/MS methods (20, 66) and are gaining acceptance.

Best practice for TDM of busulfan

The steady-state plasma concentration for busulfan is not achieved over 6–24 h even if the half-life is 2–3 h. Therefore, several samples are needed to determine the exposure to the drug over a dosing interval. A limited sampling approach is adopted, and the best schedule for sample collection as per the FDA monograph for the first dose is 2 h (end of infusion), 4 h, and 6 h (just before the start of next infusion) after the start of the infusion. For subsequent doses another sampling time point (baseline, before the start of the infusion) is added. The blood sample should be collected in heparinized vials and placed on wet ice till centrifugation. The plasma should be separated within 1 h and transferred to cryo vials. All plasma samples should be frozen at −20°C until analysis. The samples are stable for 3–4 days at 2–8°C and up to 6 months at −20°C. The AUC over the dosing interval is calculated by the simple trapezoidal rule. For once daily dosing, the terminal part of the elimination curve is calculated from a preinfusion "0" concentration for the first dose or the preinfusion concentration for the next dose. $AUC_{0–24\ h}$ is calculated by adding $AUC_{0\text{-}6\ h}$ and $AUC_{6–24\ h}$. The FDA-recommended AUC and Css values are similar to the consensus statement by the American Society for Bone Marrow Transplantation Practice Guideline Committee. The AUC and Css targets for high-dose busulfan therapy is enumerated in Table 2. The attempt to optimize the exposure is started as early as the first day dose modifications.

Clinical impact of busulfan precision therapy strategies

Model informed precision dosing (MPID) has been gaining popularity over the last decade. These methods are attractive as they use less number of samples to predict the AUC and suggest dose modification using Bayesian forecasting. The model-informed dosing also takes into account the body size, age, organ function, etc. for dose prediction unlike the traditional dosing, which is weight based. Examples of some of the available software are insightRX and NextDose. The web-based services are www.insight-rx.com and https://doseme-rx.com. It has been shown to have relatively less bias in AUC estimations of busulfan compared to the conventional trapezoidal method (78, 79) and may be less prone for error that may creep in due to inadequate documentation of sampling time (80). The MIPD strategy may be software or web-based platforms.

5 Fluorouracil

5-fluorouracil (5-FU) is a pyrimidine analogue used in the treatment of several solid tumors (breast, colorectal, stomach, head, and neck). It is typically administered intravenously as prolonged infusion due to its very short half-life (20 min) (81).

After administration, 5-FU penetrates cells by a facilitated transport route, where it is transformed into fluorodeoxyuridine monophosphate (FdUMP). FdUMP inhibits the synthesis of the deoxythymidine monophosphate (dTMP) by forming complexes with the enzyme thymidylate synthase (TS). dTMP is integral to DNA replication and repair, and its depletion causes an imbalance of intracellular nucleotides, which allows the enzyme endonuclease to cause double-stranded breaks in the DNA (82).

TABLE 2 Summary of dose and exposure–concentration targets for high-dose busulfan therapy.

Pediatric population	Adult population
EMEA: Weight-based dosing* 4 days <9 kg:1.0 mg/kg Q6H or 4 mg/kg OD >9–<16 kg: 1.2 mg/kg Q6H or 4.8 mg/kg OD 16–23 kg: 1.1 mg/kg Q6H or 4.4 mg/kg OD 23–34 kg: 1.0 mg/kg Q6H or 4 mg/kg OD >34 kg: 0.8 mg/kg Q6H or 3.2 mg/kg OD FDA: Weight-based dosing* 4 days <12 kg: 1.1 mg/kg Q6H or 4 mg/kg OD >12 kg: 0.8 mg/kg Q6H or 3.2 mg/kg OD	EMEA and FDA dose recommendations are the same for adults for dosing as well as targets in adults 1.0 mg/kg Q6H * 4 days 4 mg/kg OD * 4 days
EMEA Target for 6 h dosing AUC: 1,125 (900–1,500) µM·min Css: 770 (650–1,026) ng/ml Target for 24-h dosing AUC: 4,500 (5,262–6,000) µM·min Css: 770 (650–1,026) ng/ml FDA Target for Q6H dosing AUC: 1,125 (900–1350 ± 5%) µM·min Css target: 770 (650–924) ng/ml Target for 24-h dosing AUC: 5,262 µM·min Css target: 900 ng/ml	EMEA and FDA Target for 6-h dosing AUC: 1,125 (900–1,500) µM·min Css: 770 (800–1,000) ng/ml Target for 24-h dosing AUC: 4,500 (5,262–6,000) µM·min Css: 900 (800–1,000) ng/ml

Dosing should be according to the ideal body weight or lean body weight, whichever is lower.

When used orally, 5-FU shows poor absorption in the gastrointestinal tract. To maximize systemic absorption, parenteral administration of 5-FU is used when treating visceral cancers. 5-FU can be given intravenously as a bolus infusion over a period of days or as a "protracted" infusion using an ambulatory pump for 1 to 2 weeks. Fluorouracil is distributed throughout the body, including the liver, brain, bone marrow, CSF, and intestinal mucosa. About 80% of 5-FU is metabolized in the liver by dihydropyrimidine dehydrogenase (DPD) to the inactive metabolite dihydrofluorouracil (5-FUH_2) (83). Due to the fast catabolism in the liver, the terminal half-life of 5-FU when administered intravenously is about 8 to 20 min. This finding can be explained by the saturation of 5-FU metabolism by DPD as plasma concentrations approach the Km of DPD, which is known to be approximately 4.6 mg/L, which subsequently causes a more than proportionate increase in 5-FU plasma concentrations with dosage (73). 5-FU undergoes dose-dependent elimination and is excreted *via* urine as unchanged drug within 6 h of 5% to 20% and metabolites over 3 to 4 h.

Diarrhea was the most often reported side effect in patients undergoing systemic 5-FU treatment. Dehydration, nausea, and vomiting are typical side effects. Neutropenia, pyrexia, pulmonary embolism, thrombocytopenia, and leukopenia are more serious side effects that need to be monitored in individuals receiving systemic 5-FU chemotherapy (82).

Rationale for TDM of 5-FU

5-FU therapy meets the most important criteria for TDM, i.e., an established exposure–toxicity and exposure–clinical activity relationship. Currently, body surface area (BSA)-based calculation is used for dosing the fluoropyrimidine 5-FU (84). At typical doses, 5-FU's therapeutic effectiveness is moderate, as the dosing is often limited by the safety profile, with myelosuppression and gastrointestinal toxicity being the most common side effects. The conservative dose adjustment steps without TDM support result in delayed nonattainment of requisite exposure and, therefore, lead to suboptimal therapeutic success. The exposure–toxicity and exposure–clinical activity relationship has been reported in several clinical studies both prospective and retrospective (Table 3).

The second factor that adds to the justification for TDM is extremely high interindividual variability and intraindividual variability. While it was brainstormed in several professional meetings of physicians and laboratory scientists that there might be methodological variability in studies reporting 5-FU blood concentration, it would be important to evaluate more closely the technical and pharmacological issues while interpreting the results. The technical and pharmacological issues include the use of elastomeric pump balloons, which are sensitive to pressure, temperature, season, and patient activity, causing variability in infusion pump speed and resulting in variability in steady-state

TABLE 3 Evidence base in support of exposure–response–toxicity for 5-FU.

Study details	Disease	Pk parameter	Exposure–toxicity	Exposure–clinical response
Hillcoat (1978) (67) (original study)	GI malignancies	AUC	Not reported	RR with TDM: 40% RR without TDM: 5%
Thyss (1986) (68) (original study)	Head and neck cancer	AUC	Strong relationship	Good response rate
van Groeningen (1988) (69) (original study)	Advanced malignancies	AUC	Strong relationship	Not Available
Fety (1998) (70) (original study)	Head and neck cancer	AUC	Reduced adverse events	Good response rate RR with TDM: 18% RR without TDM: 8%
Gamelin (2008) (71) (original study)	mCRC	AUC	Strong relationship	Not Available
Yoshida (2008) (72) (original study)	mCRC	AUC	Strong relationship	Not Available
Wilhelm (2016) (73) (original study)	mCRC	AUC	Decreased toxicities	RR with TDM: 20% RR without TDM: 12%
Yang (2016) (74) (original study)	Colorectal cancer	AUC		Superior overall response rate
Fang (2016) (75) (original study)	Solid tumors	AUC	Lower the probability of grade 3/4 adverse drug events	Superior overall response rate
Salamone (2017) (76) (original study)	mCRC	AUC	Less rates of grade 3/4 adverse events	Good response rate
Deng (2020) (77) (original study)	mCRC	AUC	Incidence of adverse events reduced	Long-term efficacy improved

This is a nonexhaustive list, including only the important, landmark studies that led to the consensus for adoption of 5-FU TDM.

plasma concentrations of 5-FU (85, 86). Variability in infusion pump speed will also occur when using portable pumps, which essentially deliver a series of boluses. Due to the fact that even trace levels of DPD are present in blood, particularly the buffy coat, which makes 5-FU unstable after sample collection (87–90), it is crucial to properly separate the plasma and/or add DPD inhibitors. A sampling time of five half-lives following the start of the infusion does not yet equate to a sample at genuine steady state since, biologically, the elimination of 5-FU seems to fluctuate upon dosing. In fact, reaching steady-state 5-FU levels could take several hours (91–93). Furthermore, as DPD activity and maybe that of other 5-FU metabolizing enzymes exhibit some circadian rhythm (94, 95), variations in the timing of samples may further contribute to variability 84–88.

Nevertheless, it was unanimously agreed that by using the existing BSA-based dosing techniques and administering 5-FU by prolonged infusion, the interindividual variability in 5-FU plasma concentrations reached 40% and intraindividual variability reached 20%. Causes of interindividual variability include significant variation in DPD-mediated catabolism due to pharmacogenetic factors like SNPs in DPYD gene encoding DPD activity and environmental factors like nutritional status (68, 76).

Discounting technical and pharmacological issues, the intraindividual variability is considered to be modest and less than interindividual variability but significant enough for disproportionate systemic exposure (69) [22].

There are some important metrics of exposure that can correlate the clinical outcome, including AUC, time above threshold concentration, and C_{max} (73). The exposure to the drug (AUC) over the dosing interval is the most important PK correlate from a TDM perspective. The cumulative dosage and the exposure AUC are two metrics that have been shown to be substantially linked to clinical outcomes. Determining AUC for bolus 5-FU dosages is logistically challenging given the amount of samples that must be obtained in a short period of time. AUC measurements with 5-FU infusion schedules are relatively easier as only one sample is necessary with advanced modeling techniques, which is usually collected at steady state to predict the exposure (AUC) (84). The current consensus is a single sample at 18 h after the commencement of the infusion is the best parameter of evaluation, and the target therapeutic window is 20–30 mg/h/L (96).

Evolution of TDM of 5-FU

In 1989, a study done by Santini et al. is the first study of TDM for 5-FU (71). In that PK study, AUC was measured and considered as an important PK parameter for predicting toxicity. AUC was used as a significant parameter for dosing in the second half of the cycle. The monitoring of these individuals' PK has proven to be a reliable way to objectively improve the therapeutic index. AUC is reported as a measure of exposure

in the majority of studies while Css is only rarely reported in earlier studies.

Evidence for the exposure–response relationship

Using the existing BSA-based dosing techniques, there is about a 40% interindividual variability in 5-FU plasma concentrations *via* infusion. There is about 20% intraindividual variability in 5-FU plasma concentrations. Every drug has an exposure–response relationship that can be observed when comparing proximal biochemical effects brought on by target modification to drug concentration at the target site. Therefore, before attempting to change dose based on measures of such exposure, it is crucial to assess the exposure–response relationship.

Hillcoat et al. found a strong relationship between 5-FU plasma concentrations and tumor response in patients with gastrointestinal malignancies. In this study, patients received a 5-day continuous infusion of 5-FU given every 6 weeks at a dose of 1,200 mg/m^2/day on days 1–5. The patients' plasma 5-FU concentrations were estimated and found to differ greatly. Furthermore, plasma 5-FU area under the plasma concentrations × time curve (AUC) was shown to be considerably larger in patients with either a partial response (PR) or stable disease (SD) compared to individuals who did not have a tumor response. This was the first evidence of clinical data correlating 5-FU plasma exposure to clinical activity (72).

Martin et al. demonstrated the efficacy of therapeutic drug management (TDM) in individualized 5-FU dose in patients with metastatic colorectal cancer in routine clinical practice. Study results suggested that there was a decreased incidence of 5-FU-related toxicities and a much improved 5-FU exposure if TDM is adopted in clinical practice (90).

Yang et al. (2016) performed a meta-analysis to assess the efficacy and possible side effects of 5-FU using PK-guided vs. BSA-based dose modification in advanced malignancies using data from two randomized control trials (RCTs) and three observational studies involving 654 patients. A significant improvement in overall response rate (odds ratio = 2.04) compared with the conventional BSA technique was found to be an outcome of PK-monitored 5-FU therapy. The study revealed that PK-monitored 5-FU dosage has the potential to be used in colorectal cancer personalized therapy. The researchers concluded that PK-based 5-FU dosage showed superior overall response rate when compared to BSA-based dosing and improved toxicities irrespective of significant difference (77).

Fang et al. (2016) conducted a meta-analysis to evaluate the PKG-based algorithm for 5-FU compared with BSA-based methodology (5-FU). There were four studies (n = 504) included. The objective response rate to 5-FU treatment was "substantially" higher with the PKG algorithm than with the BSA-based method. Additionally, PKG was shown to "significantly" lower the probability of grade 3/4 potential adverse drug events (70). Salamone et al. (2017) conducted a study to validate the use of TDM to adjust 5-FU dose in mCRC patients under regular clinical settings. A total of 75 patients with metastatic colorectal cancer (mCRC) from eight German medical facilities participated in this trial. They were given up to six administrations of 5-FU infusions using the AIO (n = 16), FOLFOX6 (n = 26), or FUFOX (n = 33) regimens based on BSA. The subsequent 5-FU infusion dosages were modified in accordance with the 5-FU AUC of the preceding cycle in order to reach the desired AUC of 20 to 30 mg·h/L. The main goal was to demonstrate that TDM of 5-FU enhanced the proportion of patients in the desired AUC range at the fourth treatment compared to the first dose. Average 5-FU AUC at the time of the first administration was 18 + 6 mg·h/L, with 64%, 33%, and 3% of the patients having AUCs that were below, within, or beyond the target range, respectively. By the fourth dosage, 54% of patients were within the desired 5-FU AUC range (p = 0.0294), and the average 5-FU AUC was 25 + 7 mg·h/L (p < 0.001). Even though 55% of patients had their doses raised, the rates of grade 3–4 diarrhea (4.6%), nausea (3.4%), fatigue (0.0%), and mucositis (0.2%) associated with 5-FU were less compared to the historical data (97).

Evidence for the exposure–adverse event relationship

A PK/PD study by Thyss determined the plasma concentration of 5-FU in 29 patients with head and neck cancer who were receiving a combination chemotherapy regimen that included cisplatin at a dose of 100 mg/m^2 on day 1 and a continuous 5-day infusion of 5-FU at a dose of 1,000 mg/m^2/24 h on days 2–6. In this study, a strong relationship was found between the incidence of toxicities such myelosuppression, mucositis, and diarrhea and greater systemic exposure to 5-FU (5-FU AUC > 30 mg·h/L) (98).

Twenty-one patients with advanced malignancies underwent 5-FU PK analysis by van Groeningen et al. from the Free University in Amsterdam, the Netherlands (99). 5-FU was given as an i.v. bolus once a week at a starting dose of 500 mg/m^2, increasing the dose by 20% every 4 weeks until dose-limiting toxicity was noticed. The prevalence of toxicities was found to be strongly linked to 5-FU versus AUC using the logistic regression approach (96).

The first significant, prospective, multicenter, phase III randomized trial was carried out by Gamelin and colleagues in patients with mCRC receiving a weekly, 8-h infusion of 5-FU at a dose of 1,500 mg/m^2. These patients would have been more likely to experience toxicity if the 5-FU dose had not been altered (100). This work is significant because it established for the first time that PK-guided 5-FU dose adjustment for the treatment of

mCRC patients is practicable in clinical practice on an individual basis. The best way to ensure the right dose intensity for better results while limiting toxicity appears to be to evaluate plasma 5-FU AUC values. This method is more efficient and safe than dose adjustment based solely on clinical evaluation (100).

Yoshida and colleagues evaluated if there might be a relationship between the amount of 5-FU administered and the level of toxicity in 19 patients with mCRC. Patients in this study received a continuous i.v. infusion of 5-FU for 7 days straight at a dosage of 190–600 mg/m^2/day. Nine patients (toxic group) out of the total study participants experienced toxic dermatitis, anorexia, nausea/vomiting, and >grade 2 stomatitis. AUC from 0 to 72 h after the start of 5-FU infusion ($AUC_{0-72\ h}$) and steady-state concentrations (CSS) of 5-FU were calculated. Between the individuals who experienced toxicity (n = 9) and those who did not (n = 10), there was a roughly twofold difference in the serum 5-FU CSS, $AUC_{72\ h}$, and total body clearance (101).

Deng et al. (2020) studied the efficacy of PK-based 5-FU dosing. A total of 153 patients with advanced colorectal cancer were randomly assigned to undergo either 5-FU chemotherapy with BSA-guided dose or a double-week chemotherapy regimen with 5-FU using PK dosing. When using AUC-based dosage, oral mucositis incidence dropped and the frequency of diarrhea was dramatically reduced. The researchers found that for patients with advanced CRC, PK-based dose control of 5-FU lowers the toxicity of chemotherapy and increases its long-term efficacy when compared to BSA-based dosing (102).

A randomized multicentric trial was conducted by Fety et al. (1998) to assess the clinical value of 5-FU dose adaptation guided by PK. A total of 122 patients with head and neck cancer were randomized to receive either the normal dose of cisplatin (100 mg/m^2, day 1) and 5-FU (96-h continuous infusion) or a dose adjusted for the 5-FU level ($AUC_{0-48\ h}$; PKarm). A total of 106 patients were evaluated for toxicity and response. In comparison to the St-arm (n = 57), the 5-FU dosages and AUC were considerably lower in the PK-arm (n = 49) during cycles 2 and 3. Grade 3–4 neutropenia and thrombopenia were substantially more common in the St-arm compared to the PK-arm. In both treatment arms, the objective response rate was similar: 77.2% in the St-arm and 81.7% in the PK-arm. The authors concluded that therapeutic index can be improved by PK-based individual dose adaptation for 5-FU (103).

Evidence for usefulness of TDM for 5-FU

Pharmacoeconomic considerations of cancer therapy become crucial while choosing a chemotherapeutic regimen. When patients frequently cannot receive therapy because of considerable financial burden labeled as “financial toxicity,” cost-effectiveness has now become an even more crucial factor to take into account. There are two studies [conducted by Goldstein (2014) and Soh (2015)] that evaluated the cost-effectiveness of TDM, and it has been observed that 5-FU TDM is economical in the management of both mCRC and SCCHN (104, 105). Associated toxicities with 5-FU, such as febrile neutropenia, nausea/vomiting, and diarrhea, can have serious negative clinical and cost effects on patients and the healthcare system. It is possible to modify the dosage of 5-FU depending on the quantity of 5-FU in the plasma, and it is obvious that PK-based dosing can greatly enhance clinical outcomes by lowering toxicities and boosting efficacy (104). In the UK, patients with mCRC treated with various 5-FU combination regimens had the potential cost benefit of PK-based versus BSA dosing of 5-FU examined (106). The cost-effectiveness of administering 5-FU by PK versus BSA in various standard chemotherapy regimens in the UK population was counterfactually simulated using a decision tree model, and all patients were presumptively treated with first-line therapy for 6 or 12 cycles or until disease progression. From the viewpoint of the national health system, the model’s costs were calculated, and it was found to be effective (106).

The use of 5-FU TDM in patients with mCRC resulted in significant cost savings and a gain in quality-adjusted life-years (QALYs), according to emerging data. 5-FU TDM should be regarded as a clinically significant and essential component of individualized therapy in the routine care of cancer patients in this era of precision medicine (73).

Analytical methods employed for TDM of 5-FU

Compared to the majority of other anticancer medicines, 5-FU TDM faces obstacles that start much earlier in the preanalytical stage. Due to the widespread presence of the catabolic enzyme (DPD), which quickly converts 5-FU to its metabolite dihydro-5-FU, 5-FU is incredibly unstable in whole blood and plasma at ambient temperature. In order to separate plasma from cells, blood samples should typically be promptly put on ice and plasma extracted (73).

The last 40 years have seen huge breakthroughs in 5-FU TDM, and today, there is a validated algorithm of 5-FU dose adjustment based on plasma 5-FU levels to decrease toxicity and improve 5-FU efficacy. The levels of 5-FU in peripheral blood can be measured directly using a number of techniques, such as HPLC, GC-MS, and LC-MS/MS. Recently, a sensitive and accurate immunoassay for measuring 5-FU has become available. Comparing this test to conventional HPLC and LC-MS/MS procedures reveals significant logistical benefits. The immunoassay has a number of potential advantages over conventional HPLC and/or LCMS assays, including (1) a quicker turnaround time for clinical samples, (2) a smaller sample size requirement, and (3) automated quantitation using a reputable, validated clinical chemistry analyzer that can test a large number of samples at once. Conventional chromatographic

techniques need sophisticated equipment and a higher level of staff training to operate the equipment. Given the necessity of more sample preparation stages and the lengthier time required to analyze samples and all calibrators before the sample result can be completed than immunoassay, the turnaround time for HPLC and/or LC-MS/MS procedures is often longer than immunoassay. Cross-reactivity of the antibody to analytes structurally related to the target analyte has historically been one of the possible drawbacks of immunoassays (107).

Best practices for TDM of 5-FU

There are a number of crucial factors that must be taken into account while performing TDM 5 FU. Since 5-FU has a short half-life of only 10–15 min, steady-state conditions are expected 1 h after 5-FU infusion begins. Clinical studies actually suggest getting TDM samples at least 18 h following the onset of a 5-FU infusion (73, 91–93, 108). In view of this, the majority of the current protocols for 5-FU TDM suggest sampling be done on day 2 of a 48-h 5-FU infusion. Regarding the latter, blood sample is not advised if the infusion pump is empty or if it is thought to be within 30 min of emptying. Patients should be called back to the facility around 4 h before the expected completion of the drug infusion if blood collection for TDM is planned in order to prevent a significant fraction of TDM failures due to empty drug pumps. For patients undergoing 5-FU TDM, electric pumps are preferred over elastomeric pumps because they provide better timing accuracy, as the balloons of elastomeric pumps are sensitive to pressure, temperature, season, and patient activity (73, 85, 86). The blood sampled should be collected from a peripheral vein at a distance from the central port being used for 5-FU infusion. 5-FU is unstable in whole blood at room temperature due to *ex vivo* catabolism by DPD in the RBC; therefore, the collected blood sample should be placed on ice and plasma should be separated as soon as possible. Alternatively, a DPD inhibitor (gimeracil) may be added to the sample that allows centrifugation up to 24 h. However, a minimal turnaround time is important to continue the dose modification by modifying the infusion rate.

Clinical impact of 5-FU TDM for precision dosing strategy

The conventional 5-FU dose based on BSA produces a wide range of 5-FU systemic exposure that correlates with a wide range of effectiveness measurements. BSA-based dosing allows for more customized 5-FU administration, although in adults, BSA does not correspond well with any PK measures (67). Many US centers use PK-based dosing to achieve a target concentration, and there are solid comparative data about the mortality benefit of TDM-guided 5-FU dose [32]. By lowering toxicities and boosting efficacy, dose modification of 5-FU is doable and can greatly enhance therapeutic outcomes (90). Two prominent dose modification algorithms have been proposed. Gamerlin et al. recommended dose adjustment over a 5-FU concentration range on <4 to >31 mg·h/L (91) while the Kaldate algorithm is proposed for a wider range of concentration; 8–10 to >40 mg·h/L (108). The proposed dose modification algorithm by Kaldate has been prospectively validated in a single cohort of patients in a clinical trial setting (90) and hence also the algorithm of choice as recommended by the IATDMCT consensus statement for TDM of 5-FU in oncological practices (73). Bayesian forecasting based on PB-PK modeling and simulation is an upcoming strategy proposed for MPID of 5-FU. The greatest advantage it may offer is to do away with the DPD genotyping or phenotyping for dose optimization of 5-FU. The MPID has been proposed to overcome genotype or phenotypic misclassification, by predicting the clearance of the drug accurately (109).

Methotrexate

Mtx is an antifolate drug used in low doses (7.5–25 mg/week) as a disease-modifying antirheumatic drug (DMRD) whereas it is used at large doses (i.e., >500 mg/m^2 intravenously) to treat a variety of malignancies [(acute lymphoblastic leukemia (ALL), non-Hodgkin lymphoma (NHL), osteosarcoma, and medulloblastoma]. The majority (90%) of Mtx is cleared unchanged *via* the kidneys, with the hepatic metabolism producing only a minor amount of metabolite 7-hydroxy methotrexate. The systemic clearance is roughly 50–135 ml/min/m^2, and the terminal half-life ranges from 8 to 15 h. The PK, pharmacodynamic, and toxicity profiles depend on the dose (110). Upon entering the cells, Mtx is converted into a series of Mtx-polyglutamates (Mtx-PGs). High-dose Mtx (HDMtx) acts through inhibition of the dihydrofolate reductase (DHFR) enzyme with very high potency and hence blocks the purine synthesis in the s-phase of the cell cycle, thereby preventing cell proliferation in both tumor and normal cells. At low doses, Mtx-PGs prevent the inflammatory processes in the white blood cells and hence prevent the immune-mediated damage. Both low-dose and high-dose Mtx may cause life-threatening events such as hepatotoxicity, myelosuppression, and pulmonary toxicity, but the high-dose therapy may cause potentially life-threatening nephrotoxicity due to crystallization of the drug in the nephrons, which is rarely seen with low-dose therapy (111). Therefore, dose reduction is recommended when the creatinine clearance is decreased (112). The guiding principle is maintaining hydration, urinary alkalinization, monitoring serum creatinine, and a pharmacokinetically guided leucovorin rescue with TDM.

Rationale for TDM of methotrexate

HDMtx therapy meets the most important criteria for TDM, a large inter- and intraindividual variability in the systemic concentration achieved (113–115). The extent of interpatient variability is 52% and intrapatient variability is as high as 48% (116). This is reflected in the wide range of incidence of nephrotoxicity from 1.8% to 10.7% (110, 117). Pharmacogenetic factors like SNPs of MRP2 and OATP1B1 affecting the expression of these transport proteins partly contribute to the interindividual variability of disposition of Mtx. Several drug–drug interactions (NSAIDs, ciprofloxacin, probenecid, sulfamethoxazole, trimethoprim, amiodarone, tyrosine kinase inhibitors, and proton pump inhibitors) and known disease conditions like Down's syndrome. Coupled with all these known factors that affect Mtx elimination, there is an unexplained and variable delay in the renal clearance of Mtx despite all preventive measures taken. Maintaining the concentration in a nontoxic and efficient target range is made possible by using TDM and optimizing the doses of MTX and leucovorin. HDMtx is one of the prototype oncologic scenarios for which TDM had been employed (118).

Evidence for the concentration–toxicity relationship

Classically, the purpose of Mtx TDM has been to monitor the plasma concentration of the drug to avoid toxicity. Most lines of evidence come from observational studies and not from the randomized controlled clinical trials for obvious reasons. The plasma levels that define toxic exposure evolved over time. In one of the earliest studies by Stoller et al., it was suggested that a concentration >0.9 μM/ml at 48-h increases the risk of myelotoxicity (119, 120). These levels are important to guide the dose of folinic rescue therapy. Pediatric ALL consensus statement recommends a standard 50 mg/m^2 infusion of leucovorin every 6 h, if the Mtx concentration is >20 μM/ml at 36 h, >10 μM/ml at 42 h, and >5 μM/ml at 48 h. Supplemental leucovorin must be administered until the Mtx level falls to 0.1 to 0.05 μM/ml. A delay in measurement of plasma Mtx concentration by 24–36 h equates to having an uncompromised therapeutic action of the drug. It would be interesting to note that while Mtx nephrotoxicity has been most consistently associated with plasma concentration across studies, it has been found to be a poor predictor of other toxicities like myelotoxicity and hepatotoxicity with variable results reported from studies (118). If acute kidney injury occurs with high-dose Mtx therapy, or an extremely high concentration of Mtx is found in the blood, glucapidase (carboxypeptidase G2) is the drug of choice, and not leucovorin, as it is extremely efficient and has removed 98% of the Mtx in first 30 min.

Evidence for the concentration–response relationship

Mtx has long been used as a disease-modifying agent in low doses (<50 mg/m^2) in many rheumatic and autoimmune diseases. Due to its low cost, it is still the drug of choice in such chronic diseases (121, 122). However, 40% of the patients do not show clinical response to Mtx. Some of them have early nonresponse and some cease to respond after an initial period of nonresponse. Apart from the reasons like noncompliance and inadequate dosing, the variation in Mtx uptake and metabolism has been postulated to play a role. The cellular uptake of Mtx and their polyglutamation rate may be important contributors for such variable response. The activity of the folypolyglutamase synthase enzyme, which is responsible for polyglutamation, and the levels of Mtx-PGs have been proposed to be the biomarkers for detecting patients who are at the risk of nonresponse (123). Sensitive LC-MS/MS-based methods have been developed to detect them with precision. Studies have shown that there is a great variation in the levels of polyglutamates in the blood cells for patients receiving the same dose of Mtx (123). De Rotte et al. have proposed a multivariate model including age, gender, folate status, and genotype to correlate the disease activity with the polyglutamate levels (124). Recently, a randomized controlled study showed that daily therapy is as effective as weekly therapy when the polyglutamate-3 levels are similar. This study also showed that obese patients achieve a lower concentration of Mtx-PG3 (125). Clinical response in several other diseases like juvenile rheumatoid arthritis, juvenile dermatomyositis, and inflammatory bowel disease was also reported to be affected by the Mtx-PG concentrations. However, this is still investigated and not yet ready for clinical use; more concrete evidence is needed.

Best practices for TDM of Mtx

For the 24-h infusion schedule, it is advised to use TDM at least 24 h (the end of the infusion), 48 h, and 72 h following the start of high-dose MTX infusion, until the concentration is below 0.1–0.2 mol/L. The TDM protocols can be divided into two modes: The steady-state concentration for the 24-h infusion regimen is thought to be C24h (the end of infusion), which is correlated to efficacy and safety, whereas C48h and C72h are mostly related to safety. C3-6h (the end of the infusion), for the rapid infusion (less than 6 h) regimen, is thought to represent the peak concentration in terms of efficacy and safety, while C24h, C48h, and C72h are primarily connected to safety. In most circumstances, the safe MTX concentration range is below 0.1–0.2 mol/L, and TDM can be discontinued once it is attained. It is important to note that MTX levels less than 0.05 mol/L can be

regarded as a stricter safe range for patients with delayed MTX elimination and/or indications of acute renal dysfunction.

Analytical methods employed for TDM

Both MTX and its metabolites can be distinguished and detected using the HPLC and HPLC-MS/MS procedures, although they are expensive and require sophisticated sample processing. Automated immunoassay platforms are also available for Mtx concentration measurement. Both liquid chromatography and immunoassay could be used in a TDM laboratory. It must be kept in mind that the immunoassays have the disadvantage of slightly overestimating the concentrations due to nonspecific interactions with the Mtx metabolites. Another instance where immunoassay can falter is during treatment with glucarpidase, as Mtx degradation products interfere with the analysis and true estimates may not be found. Therefore, chromatographic methods must be employed during this situation.

Clinical impact of TDM in Mtx dose optimization

Apart from the pharmacokinetically dosing leucovorin, Mtx TDM data have also been utilized to build dose prediction models taking into account covariates like creatinine clearance and alanine transaminase levels to forecast the dose. This is to facilitate a personalized dose for the patients, which attempts to attain the desired fall in the concentration of Mtx in a desired time frame and minimizing hospital stay (126, 127). These studies reported the lower incidence of nephrotoxicity, the therapeutic concentration of Mtx was within the therapeutic range, and the clearance of Mtx was as anticipated (94, 95).

The main purpose of using HDMtx administration in patients with ALL and NHL is to address the CNS disease and to reduce risk of CNS relapse. Most studies with Mtx TDM have been performed on serum samples. A study on 138 CSF samples from children with ALL and NHL was conducted to evaluate the Mtx concentration in the cerebrospinal fluid (CSF). Serum Mtx concentrations at the end of infusion were assessed by routine TDM. Cytotoxic Mtx concentrations of 1 μM or greater were detected in 81.2% of CSF samples before administering intrathecal Mtx. One micromolar concentration is proposed to provide the desired antileukemic effect to prevent CNS relapse. This important study made a case for reducing the need for intrathecal injection of Mtx and, hence, reducing the risk of multiple lumbar puncture in children suffering from ALL and NHL (128).

Future directions

Bayesian modeling and simulation-based MIPD are some of the noteworthy precision medicine tools likely to be implemented in routine patient care in the near future. Busulfan has made a significant progress in terms of clinical testing for MIPD, though widespread application of Bayesian adaptive dosing is yet to be achieved. For 5-FU, it is still in the evolution phase and a through work in this direction is needed. For Mtx, two extremes of doses are practiced; thus, this calls for an Mtx TDM separately for autoimmune diseases apart from the well-established practice for HDMtx. Utilizing the chronic toxicity data of Mtx TDM could be tuned in for understanding the Mtx nonresponder profile in patients with rheumatic diseases. Though a few model informed dosing are in practice, it is time to refine these strategies and the development of user-friendly clinical decision support tools and their wider application. The reduction in the turnaround time in TDM reporting along with the implementation of MIPD should be aimed for in the future to make quicker as well as smarter therapeutic decisions in patient care. In addition, pharmacometabolomic approaches are gaining momentum and their association with different clinical end-points have also been demonstrated (129, 130).

Author contributions

PS accepted the invitation and built the team. She conceived the idea, compiled the first draft with PA and JK. PG provided the clinical inputs and practice oriented points. All authors contributed to the article and approved the submitted version.

Conflict of interest

The authors declare that the research was conducted in the absence of any commercial or financial relationships that could be construed as a potential conflict of interest.

Publisher's note

References

1. Groenland SL, Mathijssen RHJ, Beijnen JH, Huitema ADR, Steeghs N. Individualized dosing of oral targeted therapies in oncology is crucial in the era of precision medicine. *Eur J Clin Pharmacol* (2019) 75(9):1309–18. doi: 10.1007/s00228-019-02704-2

2. Knezevic CE, Clarke W. Cancer chemotherapy: The case for therapeutic drug monitoring. *Ther Drug Monit* (2020) 42(1):6–19. doi: 10.1097/FTD.0000000000000701

3. Mueller-Schoell A, Groenland SL, Scherf-Clavel O, van Dyk M, Huisinga W, Michelet R, et al. Therapeutic drug monitoring of oral targeted antineoplastic drugs. *Eur J Clin Pharmacol* (2021) 77(4):441–64. doi: 10.1007/s00228-020-03014-8

4. Westerdijk K, Desar IME, Steeghs N, van der Graaf WTA, van Erp NP. Imatinib, sunitinib and pazopanib: From flat-fixed dosing towards a pharmacokinetically guided personalized dose. *Br J Clin Pharmacol* (2020) 86 (2):258–73. doi: 10.1111/bcp.14185

5. Bleyzac N, Souillet G, Magron P, Janoly A, Martin P, Bertrand Y, et al. Improved clinical outcome of paediatric bone marrow recipients using a test dose and Bayesian pharmacokinetic individualization of busulfan dosage regimens. *Bone Marrow Transplant* (2001) 28(8):743–51. doi: 10.1038/sj.bmt.1703207

6. Aspen Pharmacare Canada Inc. *MYLERAN® product monograph*. Toronto OJ. 8-1155 North Service Road West Oakville, Ontario, L6M 3E3.

7. Otsuka Pharmaceutical Inc. *BUSULFEX® product monograph*. Saint Laurent QM. Otsuka Pharmaceutical Co., Ltd. Tokyo, 101-8535 Japan.

8. Tutschka PJ, Copelan EA, Klein JP. Bone marrow transplantation for leukemia following a new busulfan and cyclophosphamide regimen. *Blood* (1987) 70(5):1382–8. doi: 10.1182/blood.V70.5.1382.1382

9. *Myeleran (Busulfan) prescribing information*. Greenville N, USA: GlaxoSmith Kline (2002).

10. Haddow A, Timmis GM. Myleran in chronic myeloid leukaemia; chemical constitution and biological action. *Lancet* (1953) 264(6753):207–8. doi: 10.1016/S0140-6736(53)90884-8

11. Galton DA. Myleran in chronic myeloid leukaemia; results of treatment. *Lancet* (1953) 264(6753):208–13. doi: 10.1016/S0140-6736(53)90885-X

12. Ciurea SO, Andersson BS. Busulfan in hematopoietic stem cell transplantation. *Biol Blood Marrow Transplant* (2009) 15(5):523–36. doi: 10.1016/j.bbmt.2008.12.489

13. MYLERAN®. (Busulfan, 2-mg Scored tablets) US-FDA prescribing information. Available at: https://www.accessdata.fda.gov/drugsatfda_docs/label/2003/09386slr023_myleran_lb%20l.pdf.

14. Santos GW, Tutschka PJ, Brookmeyer R, Saral R, Beschorner WE, Bias WB, et al. Marrow transplantation for acute nonlymphocytic leukemia after treatment with busulfan and cyclophosphamide. *N Engl J Med* (1983) 309(22):1347–53. doi: 10.1056/NEJM198312013092202

15. Krivoy N, Hoffer E, Lurie Y, Bentur Y, Rowe JM. Busulfan use in hematopoietic stem cell transplantation: Pharmacology, dose adjustment, safety and efficacy in adults and children. *Curr Drug Saf* (2008) 3(1):60–6. doi: 10.2174/157488608783333899

16. Buggia I, Locatelli F, Regazzi MB, Zecca M. Busulfan. *Ann Pharmacother* (1994) 28(9):1055–62. doi: 10.1177/106002809402800911

17. Bhagwatwar HP, Phadungpojna S, Chow DS, Andersson BS. Formulation and stability of busulfan for intravenous administration in high-dose chemotherapy. *Cancer Chemother Pharmacol* (1996) 37(5):401–8. doi: 10.1007/s002800050404

18. *IV busulfex (busulfan injection)*. Rockville M, USA: Otsuka America Pharmaceutical Inc (2011).

19. Madden T, de Lima M, Thapar N, Nguyen J, Roberson S, Couriel D, et al. Pharmacokinetics of once-daily IV busulfan as part of pretransplantation preparative regimens: a comparison with an every 6-hour dosing schedule. *Biol Blood Marrow Transplant* (2007) 13(1):56–64. doi: 10.1016/j.bbmt.2006.08.037

20. Verougstraete N, Stove V, Verstraete AG, Oyaert M. Automation in busulfan therapeutic drug monitoring: Evaluation of an immunoassay on two routine chemistry analyzers. *Ther Drug Monit* (2022) 44(2):335–9. doi: 10.1097/FTD.0000000000000933

21. Geddes M, Kangarloo SB, Naveed F, Quinlan D, Chaudhry MA, Stewart D, et al. High busulfan exposure is associated with worse outcomes in a daily i.v. busulfan and fludarabine allogeneic transplant regimen. *Biol Blood Marrow Transplant* (2008) 14(2):220–8. doi: 10.1016/j.bbmt.2007.10.028

22. Andersson BS, Thall PF, Madden T, Couriel D, Wang X, Tran HT. , 477–85. toxicity eaBsertr-r, window aag-v-hddat, Blood fivBicmlBMT.

23. Ansari M, Lauzon-Joset JF, Vachon MF, Duval M, Théoret Y, Champagne MA, et al. Influence of GST gene polymorphisms on busulfan pharmacokinetics in children. *Bone Marrow Transplant* (2010) 45(2):261–7. doi: 10.1038/bmt.2009.143

24. Ansari M, Rezgui MA, Théoret Y, Uppugunduri CR, Mezziani S, Vachon MF, et al. Glutathione s-transferase gene variations influence BU pharmacokinetics and outcome of hematopoietic SCT in pediatric patients. *Bone Marrow Transplant* (2013) 48(7):939–46. doi: 10.1038/bmt.2012.265

25. Andersson BS, Thall PF, Madden T, Couriel D, Wang X, Tran HT, et al. Busulfan systemic exposure relative to regimen-related toxicity and acute graft-versus-host disease: defining a therapeutic window for i.v. BuCy2 in chronic myelogenous leukemia. *Biol Blood Marrow Transplant* (2002) 8(9):477–85. doi: 10.1053/bbmt.2002.v8.pm12374452

26. Kim MG, Kwak A, Choi B, Ji E, Oh JM, Kim K. Effect of glutathione s-transferase genetic polymorphisms on busulfan pharmacokinetics and veno-occlusive disease in hematopoietic stem cell transplantation: A meta-analysis. *Basic Clin Pharmacol Toxicol* (2019) 124(6):691–703. doi: 10.1111/bcpt.13185

27. Nishikawa T, Yamaguchi H, Ikawa K, Nakayama K, Higashi E, Miyahara E, et al. Influence of GST polymorphisms on busulfan pharmacokinetics in Japanese children. *Pediatr Int* (2019) 61(6):558–65. doi: 10.1111/ped.13859

28. Myers AL, Kawedia JD, Champlin RE, Kramer MA, Nieto Y, Ghose R, et al. Clarifying busulfan metabolism and drug interactions to support new therapeutic drug monitoring strategies: A comprehensive review. *Expert Opin Drug Metab Toxicol* (2017) 13(9):901–23. doi: 10.1080/17425255.2017.1360277

29. Hassan M, Oberg G, Bekassy AN, Aschan J, Ehrsson H, Ljungman P, et al. Pharmacokinetics of high-dose busulphan in relation to age and chronopharmacology. *Cancer Chemother Pharmacol* (1991) 28(2):130–4. doi: 10.1007/BF00689702

30. Vassal G, Deroussent A, Hartmann O, Challine D, Benhamou E, Valteau-Couanet D. , 6203–7. eaD-dnoh, study. bicacapCR.

31. Matar KM, Alshemmari SH, Refaat S, Anwar A. UPLC-tandem mass spectrometry for quantification of busulfan in human plasma: Application to therapeutic drug monitoring. *Sci Rep* (2020) 10(1):8913. doi: 10.1038/s41598-020-65919-9

32. Grochow LB, Jones RJ, Brundrett RB, Braine HG, Chen TL, Saral R, et al. Pharmacokinetics of busulfan: correlation with veno-occlusive disease in patients undergoing bone marrow transplantation. *Cancer Chemother Pharmacol* (1989) 25 (1):55–61. doi: 10.1007/BF00694339

33. Shulman HM, Hinterberger W. Hepatic veno-occlusive disease–liver toxicity syndrome after bone marrow transplantation. *Bone Marrow Transplant* (1992) 10(3):197–214.

34. Dix SP, Wingard JR, Mullins RE, Jerkunica I, Davidson TG, Gilmore CE, et al. Association of busulfan area under the curve with veno-occlusive disease following BMT. *Bone Marrow Transplant* (1996) 17(2):225–30.

35. Jones RJ, Lee KS, Beschorner WE, Vogel VG, Grochow LB, Braine HG, et al. Venoocclusive disease of the liver following bone marrow transplantation. *Transplantation* (1987) 44(6):778–83. doi: 10.1097/00007890-198712000-00011

36. McDonald GB, Sharma P, Matthews DE, Shulman HM, Thomas ED. Venocclusive disease of the liver after bone marrow transplantation: diagnosis, incidence, and predisposing factors. *Hepatology* (1984) 4(1):116–22. doi: 10.1002/hep.1840040121

37. Grochow LB. Busulfan disposition: the role of therapeutic monitoring in bone marrow transplantation induction regimens. *Semin Oncol* (1993) 20(4 Suppl 4):18–25.

38. Slattery JT, Clift RA, Buckner CD, Radich J, Storer B, Bensinger WI. , 3055–60. eaMtfcml, transplantation. tiopblotooB.

39. Slattery JT, Sanders JE, Buckner CD, Schaffer RL, Lambert KW, Langer FP. , 31–42. eaG-ratfbm, Bone tirtbpMT.

40. Slattery JT, Sanders JE, Buckner CD, Schaffer RL, Lambert KW, Langer FP, et al. Graft-rejection and toxicity following bone marrow transplantation in relation to busulfan pharmacokinetics. *Bone Marrow Transplant* (1995) 16(1):31–42.

41. Williams CB, Day SD, Reed MD, Copelan EA, Bechtel T, Leather HL. (2004), 614–23. eaDmpuib, allogeneic Bacfbao, with pbsctiphmBBMT.

42. Geddes M, Kangarloo SD, Naveed F, Quinlan D, Chaudhry MA, Stewart D. , 220–8. eaHbeiaww, transplant oiadivbafarBBMT.

43. Hassan M, Ehrsson H, Smedmyr B, Totterman T, Wallin I, Oberg G. , 113–4. eaCfapcobdhdtBMT.

44. Bartelink IH, Lalmohamed A, van Reij EML, Dvorak CC, Savic RM, Zwaveling J, et al. Association of busulfan exposure with survival and toxicity after haemopoietic cell transplantation in children and young adults: A multicentre, retrospective cohort analysis. *Lancet Haematol* (2016) 3(11):e526–36. doi: 10.1016/S2352-3026(16)30114-4

45. Tran HT, Madden T, Petropoulos D, Worth LL, Felix EA, Sprigg-Saenz HA. 463–70. eaIh-dobp, allogeneic daiappu, malignancies. sctfahBMT.

46. McCune JS, Gibbs JP, Slattery JT. , 155–65. Plasma concentration monitoring, Pharmacokinet obdiicoC.

47. Hobbs JR, Hugh-Jones K, Shaw PJ, Downie CJ, Williamson S. , 201–8. dosages Errtbac, children. fdbmtifBMT.

48. Pawlowska AB, Blazar BR, Angelucci E, Baronciani D, Shu XO. (1997), 915–20. high-dose BBRoppo, transplantation obttooabmicwtBMT.

49. Radich JP, Gooley T, Bensinger W, Chauncey T, Clift R, Flowers M, et al. HLAmatched related hematopoietic cell transplantation for chronic-phase CML using a targeted busulfan and cyclophosphamide preparative regimen. *Blood* (2003) 102(1):31–5. doi: 10.1182/blood-2002-08-2619

50. Poonkuzhali B, Srivastava A, Quernin MH, Dennison D, Aigrain EJ, Kanagasabapathy AS, et al. (1999), 5–11. Pharmacokinetics of oral busulphan, allogeneic icwbtmubmtBMT.

51. Bolinger AM, Zangwill AB, Slattery JT, Glidden D, DeSantes K, Heyn L. 25:925–30. eaAeoe, toxicity and busulfan, for cicrbmtlogdBMT.

52. Grochow LB. Busulfan disposition: The role of therapeutic monitoring in bone marrow transplantation induction regimens. *Semin Oncol* (1993) 20(4 Suppl 4):18–25.

53. Ljungman P, Hassan M, Békássy AN, Ringdén O, Oberg G. High busulfan concentrations are associated with increased transplant-related mortality in allogeneic bone marrow transplant patients. *Bone Marrow Transplant* (1997) 20 (11):909–13. doi: 10.1038/sj.bmt.1700994

54. Russell JA, Kangarloo SB. Therapeutic drug monitoring of busulfan in transplantation. *Curr Pharm Des* (2008) 14(20):1936–49. doi: 10.2174/138161208785061382

55. Palmer J, McCune JS, Perales M-A, Marks D, Bubalo J, Mohty M, et al. Personalizing busulfan-based conditioning: Considerations from the American society for blood and marrow transplantation practice guidelines committee. *Biol Blood Marrow Transplant* (2016) 22(11):1915–25. doi: 10.1016/j.bbmt.2016.07.013

56. Slattery JT, Risler LJ. Therapeutic monitoring of busulfan in hematopoietic stem cell transplantation. *Ther Drug Monit* (1998) 20(5):543–9. doi: 10.1097/00007691-199810000-00017

57. Tran HT, Madden T, Petropoulos D, Worth LL, Felix EA, Sprigg-Saenz HA, et al. Individualizing high-dose oral busulfan: prospective dose adjustment in a pediatric population undergoing allogeneic stem cell transplantation for advanced hematologic malignancies. *Bone Marrow Transplant* (2000) 26(5):463–70. doi: 10.1038/sj.bmt.1702561

58. Deeg HJ, Storer B, Slattery JT, Anasetti C, Doney KC, Hansen JA, et al. Conditioning with targeted busulfan and cyclophosphamide for hemopoietic stem cell transplantation from related and unrelated donors in patients with myelodysplastic syndrome. *Blood* (2002) 100(4):1201–7. doi: 10.1182/blood-2002-02-0527

59. Clopés A, Sureda A, Sierra J, Queraltó JM, Broto A, Farré R, et al. Absence of venoocclussive disease in a cohort of multiple myeloma patients undergoing autologous stem cell transplantation with targeted busulfan dosage. *Eur J Haematol* (2006) 77(1):1–6. doi: 10.1111/j.0902-4441.2006.t01-1-EJH2478.x

60. Parmar S, Rondon G, de Lima M, Thall P, Bassett R, Anderlini P, et al. Dose intensification of busulfan in the preparative regimen is associated with improved survival: a phase I/II controlled, randomized study. *Biol Blood Marrow Transplant* (2013) 19(3):474–80. doi: 10.1016/j.bbmt.2012.12.001

61. Bartelink IH, Bredius RGM, Belitser SV, Suttorp MM, Bierings M, Knibbe CAJ, et al. Association between busulfan exposure and outcome in children receiving intravenous busulfan before hematologic stem cell transplantation. *Biol Blood Marrow Transplant* (2009) 15(2):231–41. doi: 10.1016/j.bbmt.2008.11.022

62. Mellgren K, Nilsson C, Fasth A, Abrahamsson J, Winiarski J, Ringdén O, et al. Safe administration of oral BU twice daily during conditioning for stem cell transplantation in a paediatric population: a comparative study between the standard 4-dose and a 2-dose regimen. *Bone Marrow Transplant* (2008) 41 (7):621–5. doi: 10.1038/sj.bmt.1705947

63. Ryu S-G, Lee J-H, Choi S-J, Lee J-H, Lee Y-S, Seol M, et al. Randomized comparison of four-Times-Daily versus once-daily intravenous busulfan in conditioning therapy for hematopoietic cell transplantation. *Biol Blood Marrow Transplant* (2007) 13(9):1095–105. doi: 10.1016/j.bbmt.2007.06.005

64. Andersen AM, Bergan S, Gedde-Dahl T, Buechner J, Vethe NT. Fast and reliable quantification of busulfan in blood plasma using two-channel liquid chromatography tandem mass spectrometry: Validation of assay performance in the presence of drug formulation excipients. *J Pharm Biomed Anal* (2021) 203:114216. doi: 10.1016/j.jpba.2021.114216

65. De Gregori S, Tinelli C, Manzoni F, Bartoli A. Comparison of two analytical methods for busulfan therapeutic drug monitoring. *Eur J Drug Metab Pharmacokinet* (2021) 46(1):155–9. doi: 10.1007/s13318-020-00660-2

66. Hilaire MR, Gill RV, Courtney JB, Baburina I, Gardiner J, Milone MC, et al. Evaluation of a nanoparticle-based busulfan immunoassay for rapid analysis on routine clinical analyzers. *Ther Drug Monit* (2021) 43(6):766–71. doi: 10.1097/FTD.0000000000000883

67. Jiang H, Lu J, Ji J. Circadian rhythm of dihydrouracil/uracil ratios in biological fluids: a potential biomarker for dihydropyrimidine dehydrogenase levels. *Br J Pharmacol* (2004) 141(4):616–23. doi: 10.1038/sj.bjp.0705651

68. Davis LE, Lenkinski RE, Shinkwin MA, Kressel HY, Daly JM. The effect of dietary protein depletion on hepatic 5-fluorouracil metabolism. *Cancer* (1993) 72 (12):3715–22. doi: 10.1002/1097-0142(19931215)72:12<3715::AID-CNCR2820721225>3.0.CO;2-W

69. Kline CL, Sheikh HS, Scicchitano A, Gingrich R, Beachler C, Finnberg NK, et al. Preliminary observations indicate variable patterns of plasma 5-fluorouracil (5-FU) levels during dose optimization of infusional 5-FU in colorectal cancer patients. *Cancer Biol Ther* (2011) 12(7):557–68. doi: 10.4161/cbt.12.7.18059

70. Fang L, Xin W, Ding H, Zhang Y, Zhong L, Luo H, et al. Pharmacokinetically guided algorithm of 5-fluorouracil dosing, a reliable strategy of precision chemotherapy for solid tumors: a meta-analysis. *Sci Rep* (2016) 6:25913. doi: 10.1038/srep25913

71. Santini J, Milano G, Thyss A, Renee N, Viens P, Ayela P, et al. 5-FU therapeutic monitoring with dose adjustment leads to an improved therapeutic index in head and neck cancer. *Br J Cancer* (1989) 59(2):287–90. doi: 10.1038/bjc.1989.59

72. Hillcoat BL, McCulloch PB, Figueredo AT, Ehsan MH, Rosenfeld JM. Clinical response and plasma levels of 5-fluorouracil in patients with colonic cancer treated by drug infusion. *Br J Cancer* (1978) 38(6):719–24. doi: 10.1038/bjc.1978.278

73. Beumer JH, Chu E, Allegra C, Tanigawara Y, Milano G, Diasio R, et al. Therapeutic drug monitoring in oncology: International association of therapeutic drug monitoring and clinical toxicology recommendations for 5-fluorouracil therapy. *Clin Pharmacol Ther* (2019) 105(3):598–613. doi: 10.1002/cpt.1124

74. Milano G, Etienne MC. Individualizing therapy with 5-fluorouracil related to dihydropyrimidine dehydrogenase: theory and limits. *Ther Drug Monit* (1996) 18(4):335–40. doi: 10.1097/00007691-199608000-00004

75. Milano G, Chamorey AL. Clinical pharmacokinetics of 5-fluorouracil with consideration of chronopharmacokinetics. *Chronobiol Int* (2002) 19(1):177–89. doi: 10.1081/CBI-120002597

76. Fleming RA, Milano G, Thyss A, Etienne MC, Renée N, Schneider M, et al. Correlation between dihydropyrimidine dehydrogenase activity in peripheral mononuclear cells and systemic clearance of fluorouracil in cancer patients. *Cancer Res* (1992) 52(10):2899–902.

77. Yang R, Zhang Y, Zhou H, Zhang P, Yang P, Tong Q, et al. Individual 5-fluorouracil dose adjustment *via* pharmacokinetic monitoring versus conventional body-Area-Surface method: A meta-analysis. *Ther Drug Monit* (2016) 38(1):79–86. doi: 10.1097/FTD.0000000000000238

78. Shukla P, Goswami S, Keizer RJ, Winger BA, Kharbanda S, Dvorak CC, et al. Assessment of a model-informed precision dosing platform use in routine clinical care for personalized busulfan therapy in the pediatric hematopoietic cell transplantation (HCT) population. *Front Pharmacol* (2020) 11:888. doi: 10.3389/fphar.2020.00888

79. Lawson R, Paterson L, Fraser CJ, Hennig S. Evaluation of two software using Bayesian methods for monitoring exposure and dosing once-daily intravenous busulfan in paediatric patients receiving haematopoietic stem cell transplantation. *Cancer Chemother Pharmacol* (2021) 88(3):379–91. doi: 10.1007/s00280-021-04288-0

80. Dadkhah A, Alihodzic D, Broeker A, Kröger N, Langebrake C, Wicha SG. Evaluation of the robustness of therapeutic drug monitoring coupled with Bayesian forecasting of busulfan with regard to inaccurate documentation. *Pharm Res* (2021) 38(10):1721–9. doi: 10.1007/s11095-021-03115-8

81. Paci A, Veal G, Bardin C, Levêque D, Widmer N, Beijnen J, et al. Review of therapeutic drug monitoring of anticancer drugs part 1–cytotoxics. *Eur J Cancer* (2014) 50(12):2010–9. doi: 10.1016/j.ejca.2014.04.014

82. Zhang N, Yin Y, Xu SJ, Chen WS. 5-fluorouracil: mechanisms of resistance and reversal strategies. *Molecules* (2008) 13(8):1551–69. doi: 10.3390/molecules13081551

83. Diasio RB, Harris BE. Clinical pharmacology of 5-fluorouracil. *Clin Pharmacokinet* (1989) 16(4):215–37. doi: 10.2165/00003088-198916040-00002

84. Salman B, Al-Khabori M. Applications and challenges in therapeutic drug monitoring of cancer treatment: A review. *J Oncol Pharm Pract* (2021) 27(3):693–701. doi: 10.1177/1078155220979048

85. Blaschke M, Cameron S, Emami K, Blumberg J, Wegner U, Nischwitz M, et al. Measurement of 5-FU plasma levels in patients with advanced cancer: correct approach to practical procedures is essential. *Int J Clin Pharmacol Ther* (2011) 49 (1):83–5.

86. Salman D, Barton S, Nabhani-Gebara S. Effect of environmental conditions on performance of elastomeric pumps. *Am J Health Syst Pharm* (2013) 70 (13):1100. doi: 10.2146/ajhp130150

87. Lu Z, Zhang R, Diasio RB. Dihydropyrimidine dehydrogenase activity in human peripheral blood mononuclear cells and liver: population characteristics, newly identified deficient patients, and clinical implication in 5-fluorouracil chemotherapy. *Cancer Res* (1993) 53(22):5433–8.

88. Wattanatorn W, McLeod HL, Macklon F, Reid M, Kendle KE, Cassidy J. Comparison of 5-fluorouracil pharmacokinetics in whole blood, plasma, and red blood cells in patients with colorectal cancer. *Pharmacotherapy* (1997) 17(5):881–6.

89. Highlights from: 5-fluorouracil drug management pharmacokinetics and pharmacogenomics workshop; Orlando, florida; January 2007. *Clin Colorectal Cancer* (2007) 6(6):407–22. doi: 10.1016/s1533-0028(11)70480-7

90. Wilhelm M, Mueller L, Miller MC, Link K, Holdenrieder S, Bertsch T, et al. Prospective, multicenter study of 5-fluorouracil therapeutic drug monitoring in metastatic colorectal cancer treated in routine clinical practice. *Clin Colorectal Cancer* (2016) 15(4):381–8. doi: 10.1016/j.clcc.2016.04.001

91. Gamelin E, Boisdron-Celle M, Delva R, Regimbeau C, Cailleux PE, Alleaume C, et al. Long-term weekly treatment of colorectal metastatic cancer with fluorouracil and leucovorin: results of a multicentric prospective trial of fluorouracil dosage optimization by pharmacokinetic monitoring in 152 patients. *J Clin Oncol* (1998) 16(4):1470–8. doi: 10.1200/JCO.1998.16.4.1470

92. Mueller F, Büchel B, Köberle D, Schürch S, Pfister B, Krähenbühl S, et al. Genderspecific elimination of continuous-infusional 5-fluorouracil in patients with gastrointestinal malignancies: results from a prospective population pharmacokinetic study. *Cancer Chemother Pharmacol* (2013) 71(2):361–70. doi: 10.1007/s00280-012-2018-4

93. Terret C, Erdociain E, Guimbaud R, Boisdron-Celle M, McLeod HL, Féty-Deporte R, et al. Dose and time dependencies of 5-fluorouracil pharmacokinetics. *Clin Pharmacol Ther* (2000) 68(3):270–9. doi: 10.1067/mcp.2000.109352

94. Harris BE, Song R, Soong SJ, Diasio RB. Relationship between dihydropyrimidine dehydrogenase activity and plasma 5-fluorouracil levels with evidence for circadian variation of enzyme activity and plasma drug levels in cancer patients receiving 5-fluorouracil by protracted continuous infusion. *Cancer Res* (1990) 50(1):197–201.

95. Kuwahara A, Yamamori M, Nishiguchi K, Okuno T, Chayahara N, Miki I, et al. Effect of dose-escalation of 5-fluorouracil on circadian variability of its pharmacokinetics in Japanese patients with stage III/IVa esophageal squamous cell carcinoma. *Int J Med Sci* (2010) 7(1):48–54. doi: 10.7150/ijms.7.48

96. Lee JJ, Beumer JH, Chu E. Therapeutic drug monitoring of 5-fluorouracil. *Cancer Chemother Pharmacol* (2016) 78(3):447–64. doi: 10.1007/s00280-016-3054-2

97. Salamone SJ, Jaehde U, Mueller L, Link K, Holdenrieder S, Bertsch T, et al. Prospective, multi-center study of 5-fluorouracil (5-FU) therapeutic drug management (TDM) in metastatic colorectal cancer (mCRC) patients treated in routine clinical practice. *J Clin Oncol* (2017) 35(4_suppl):650–. doi: 10.1200/JCO.2017.35.4_suppl.650

98. Thyss A, Milano G, Renée N, Vallicioni J, Schneider M, Demard F. Clinical pharmacokinetic study of 5-FU in continuous 5-day infusions for head and neck cancer. *Cancer Chemother Pharmacol* (1986) 16(1):64–6. doi: 10.1007/BF00255288

99. van Groeningen CJ, Pinedo HM, Heddes J, Kok RM, de Jong AP, Wattel E, et al. Pharmacokinetics of 5-fluorouracil assessed with a sensitive mass spectrometric method in patients on a dose escalation schedule. *Cancer Res* (1988) 48(23):6956–61.

100. Gamelin E, Delva R, Jacob J, Merrouche Y, Raoul JL, Pezet D, et al. Individual fluorouracil dose adjustment based on pharmacokinetic follow-up compared with conventional dosage: results of a multicenter randomized trial of patients with metastatic colorectal cancer. *J Clin Oncol* (2008) 26(13):2099–105. doi: 10.1200/JCO.2007.13.3934

101. Yoshida T, Araki E, Iigo M, Fujii T, Yoshino M, Shimada Y, et al. Clinical significance of monitoring serum levels of 5-fluorouracil by continuous infusion in patients with advanced colonic cancer. *Cancer Chemother Pharmacol* (1990) 26 (5):352–4. doi: 10.1007/BF02897292

102. Deng R, Shi L, Zhu W, Wang M, Guan X, Yang D, et al. Pharmacokinetics-based dose management of 5-fluorouracil clinical research in advanced colorectal cancer treatment. *Mini Rev Med Chem* (2020) 20(2):161–7. doi: 10.2174/1389557519666191011154923

103. Fety R, Rolland F, Barberi-Heyob M, Hardouin A, Campion L, Conroy T, et al. Clinical impact of pharmacokinetically-guided dose adaptation of 5-fluorouracil: results from a multicentric randomized trial in patients with locally advanced head and neck carcinomas. *Clin Cancer Res* (1998) 4(9):2039–45.

104. Goldstein DA, Chen Q, Ayer T, Howard DH, Lipscomb J, Harvey RD, et al. Cost effectiveness analysis of pharmacokinetically-guided 5-fluorouracil in FOLFOX chemotherapy for metastatic colorectal cancer. *Clin Colorectal Cancer* (2014) 13(4):219–25. doi: 10.1016/j.clcc.2014.09.007

105. Soh IPT, Mogro MJ, Soo RA, Pang A, Tan CS, Chuah B, et al. The optimization of 5fluorouracil (5FU) dose by pharmacokinetic (PK) monitoring in Asian patients with advanced-stage gastrointestinal (GI) cancer. *J Clin Oncol* (2015) 33(3_suppl):770. doi: 10.1200/jco.2015.33.3_suppl.770

106. Becker R, Hollenbeak CS, Choma A, Kenny P, Salamone SJ. Cost-effectiveness of pharmacokinetic dosing of 5Fluorouracil in metastatic colorectal cancer in the united kingdom. *Vale Health* (2013) 16:A139. doi: 10.1016/j.jval.2013.03.680

107. Beumer JH, Boisdron-Celle M, Clarke W, Courtney JB, Egorin MJ, Gamelin E, et al. Multicenter evaluation of a novel nanoparticle immunoassay for 5-fluorouracil on the Olympus AU400 analyzer. *Ther Drug Monit* (2009) 31 (6):688–94. doi: 10.1097/FTD.0b013e3181b9b8c0

108. Kaldate RR, Haregewoin A, Grier CE, Hamilton SA, McLeod HL. Modeling the 5fluorouracil area under the curve versus dose relationship to develop a pharmacokinetic dosing algorithm for colorectal cancer patients receiving FOLFOX6. *Oncologist* (2012) 17(3):296–302. doi: 10.1634/theoncologist.2011-0357

109. Darwich AS, Ogungbenro K, Hatley OJ, Rostami-Hodjegan A. Role of pharmacokinetic modeling and simulation in precision dosing of anticancer drugs. *Trans Cancer Res* (2017) 6(Suppl 10):S1512–S29. doi: 10.21037/tcr.2017.09.14

110. Widemann BC, Adamson PC. Understanding and managing methotrexate nephrotoxicity. *Oncologist* (2006) 11(6):694–703. doi: 10.1634/theoncologist.11-6-694

111. Comandone A, Passera R, Boglione A, Tagini V, Ferrari S, Cattel L. High dose methotrexate in adult patients with osteosarcoma: Clinical and pharmacokinetic results. *Acta Oncol* (2005) 44(4):406–11. doi: 10.1080/02841860510029770

112. Kintzel PE, Dorr RT. Anticancer drug renal toxicity and elimination: dosing guidelines for altered renal function. *Cancer Treat Rev* (1995) 21(1):33–64. doi: 10.1016/0305-7372(95)90010-1

113. Fukuhara K, Ikawa K, Morikawa N, Kumagai K. Population pharmacokinetics of high-dose methotrexate in Japanese adult patients with malignancies: a concurrent analysis of the serum and urine concentration data. *J Clin Pharm Ther* (2008) 33(6):677–84. doi: 10.1111/j.1365-2710.2008.00966.x

114. Graf N, Winkler K, Betlemovic M, Fuchs N, Bode U. Methotrexate pharmacokinetics and prognosis in osteosarcoma. *J Clin Oncol* (1994) 12 (7):1443–51. doi: 10.1200/JCO.1994.12.7.1443

115. Joerger M, Ferreri AJ, Krähenbühl S, Schellens JH, Cerny T, Zucca E, et al. Dosing algorithm to target a predefined AUC in patients with primary central nervous system lymphoma receiving high dose methotrexate. *Br J Clin Pharmacol* (2012) 73(2):240–7. doi: 10.1111/j.1365-2125.2011.04084.x

116. Levêque D, Becker G, Toussaint E, Fornecker L-M, Paillard C. Clinical pharmacokinetics of methotrexate in oncology. *Int J Pharmacokinet* (2017) 2 (2):137–47. doi: 10.4155/ipk-2016-0022

117. Wiczer T, Dotson E, Tuten A, Phillips G, Maddocks K. Evaluation of incidence and risk factors for high-dose methotrexate-induced nephrotoxicity. *J Oncol Pharm Pract* (2016) 22(3):430–6. doi: 10.1177/1078155215594417

118. Howard SC, McCormick J, Pui CH, Buddington RK, Harvey RD. Preventing and managing toxicities of high-dose methotrexate. *Oncologist* (2016) 21(12):1471–82. doi: 10.1634/theoncologist.2015-0164

119. Stoller RG, Hande KR, Jacobs SA, Rosenberg SA, Chabner BA. Use of plasma pharmacokinetics to predict and prevent methotrexate toxicity. *N Engl J Med* (1977) 297(12):630–4. doi: 10.1056/NEJM197709222971203

120. Schmiegelow K, Attarbaschi A, Barzilai S, Escherich G, Frandsen TL, Halsey C, et al. Consensus definitions of 14 severe acute toxic effects for childhood lymphoblastic leukaemia treatment: a Delphi consensus. *Lancet Oncol* (2016) 17 (6):e231–e9. doi: 10.1016/S1470-2045(16)30035-3

121. Saag KG, Teng GG, Patkar NM, Anuntiyo J, Finney C, Curtis JR, et al. American College of rheumatology 2008 recommendations for the use of nonbiologic and biologic disease-modifying antirheumatic drugs in rheumatoid arthritis. *Arthritis Care Res* (2008) 59(6):762–84. doi: 10.1002/art.23721

122. Ramanan A, Whitworth P, Baildam E. Use of methotrexate in juvenile idiopathic arthritis. *Arch Dis Child* (2003) 88(3):197–200. doi: 10.1136/adc.88.3.197

123. Muller IB, Hebing RF, Jansen G, Nurmohamed MT, Lems WF, Peters GJ, et al. Personalized medicine in rheumatoid arthritis: methotrexate polyglutamylation revisited. *Expert Rev Precis Med Drug Dev* (2018) 3(6):331–4. doi: 10.1080/23808993.2018.1517025

124. de Rotte MCFJ, Pluijm SMF, de Jong PHP, Bulatovic Calasan M, Wulffraat NM, Weel AEAM, et al. Development and validation of a prognostic multivariable model to predict insufficient clinical response to methotrexate in rheumatoid arthritis. *PloS One* (2018) 13(12):e0208534. doi: 10.1371/journal.pone.0208534

125. Rodríguez-Báez AS, Huerta-García AP, Medellín-Garibay SE, Rodríguez-Pinal CJ, Martínez-Martínez MU, Herrera-Van Oostdam D, et al. Disease activity and therapeutic drug monitoring of polyglutamates of methotrexate after daily or weekly administration of lowdose methotrexate in patients recently diagnosed with rheumatoid arthritis. *Basic Clin Pharmacol Toxicol* (2022) 130(6):644–54. doi: 10.1111/bcpt.13728

126. Dupuis C, Mercier C, Yang C, Monjanel-Mouterde S, Ciccolini J, Fanciullino R, et al. High-dose methotrexate in adults with osteosarcoma: a population pharmacokinetics study and validation of a new limited sampling strategy. *Anticancer Drugs* (2008) 19(3):267–73. doi: 10.1097/CAD.0b013e3282f21376

127. Foster JH, Thompson PA, Bernhardt MB, Margolin JF, Hilsenbeck SG, Jo E, et al. A prospective study of a simple algorithm to individually dose high-dose methotrexate for children with leukemia at risk for methotrexate toxicities. *Cancer Chemother Pharmacol* (2019) 83(2):349–60. doi: 10.1007/s00280-018-3733-2

128. Niemann A, Mühlisch J, Frühwald MC, Gerss J, Hempel G, Boos J. Therapeutic drug monitoring of methotrexate in cerebrospinal fluid after

systemic high-dose infusion in children: can the burden of intrathecal methotrexate be reduced? *Ther Drug Monit* (2010) 32(4):467–75. doi: 10.1097/FTD.0b013e3181e5c6b3

129. Shanker Kasudhan K, Patial A, Mehra N, Verma Attri S, Malhotra P, Pattanaik S, et al. Cyclophosphamide, hydroxycyclophosphamide and carboxyethyl phosphoramide mustard quantification with liquid chromatography mass spectrometry in a single run human plasma samples: A rapid and sensitive method development. *Journal of Chromatography B* (2022) 1198:123228.

130. Grover S, Kasudhan KS, Murali N, Patil AN, Pattanaik S, Chakrabarti S, et al. Pharmacometabolomics-guided clozapine therapy in treatment resistant schizophrenia: Preliminary exploration of future too near. *Asian Journal of Psychiatry* (2022) 67:102939.

frontiers | Frontiers in Oncology

TYPE Case Report
PUBLISHED 11 January 2023
DOI 10.3389/fonc.2022.960116

OPEN ACCESS

EDITED BY
Jennifer Martin,
The University of Newcastle, Australia

REVIEWED BY
Jennifer June Schneider,
The University of Newcastle, Australia
Miao Yan,
Second Xiangya Hospital, Central South University, China

*CORRESPONDENCE
Fenna de Vries
f.devries@olvg.nl

SPECIALTY SECTION
This article was submitted to Pharmacology of Anti-Cancer Drugs, a section of the journal Frontiers in Oncology

RECEIVED 02 June 2022
ACCEPTED 16 December 2022
PUBLISHED 11 January 2023

CITATION
de Vries F, Smit AAJ, Wolbink G, de Vries A, Loeff FC and Franssen EJF (2023) Case report: Pharmacokinetics of pembrolizumab in a patient with stage IV non–small cell lung cancer after a single 200 mg administration. *Front. Oncol.* 12:960116. doi: 10.3389/fonc.2022.960116

Case report: Pharmacokinetics of pembrolizumab in a patient with stage IV non–small cell lung cancer after a single 200 mg administration

Fenna de Vries[1]*, Adrianus A. J. Smit[2], Gertjan Wolbink[3], Annick de Vries[4], Floris C. Loeff[4] and Eric J. F. Franssen[1]

[1]Department of Pharmacy, OLVG Hospital, Amsterdam, Netherlands, [2]Department of Pulmonary Medicine, OLVG Hospital, Amsterdam, Netherlands, [3]Department of Rheumatology, Amsterdam Rheumatology and Immunology Centre, Amsterdam, Netherlands, [4]Diagnostic Services, Sanquin Health Solutions, Amsterdam, Netherlands

Background: Pembrolizumab is a well-tolerated biologic agent with a potentially stable and durable anti-tumor response. Unfortunately, discontinuation of therapy can occur as a consequence of immune-related adverse effects (irAEs). These irAEs appear independent of dose and exposure. However, such irAEs might also result from pembrolizumab's highly specific mechanism of action and current dosing regimens. However, the currently available pharmacokinetic (PK) and pharmacodynamic (PD) data to reassess dosing strategies are insufficient. To highlight the importance of additional PK/PD studies, we present a case describing the complexity of pembrolizumab's PK/PD after a single 200 mg pembrolizumab dose in a treatment-naive patient with non–small cell lung cancer (NSCLC).

Case description: A 72-year-old man with stage IV NSCLC presented hepatotoxic symptoms 19 days after receiving the first 200 mg pembrolizumab dose. Hence, pembrolizumab therapy was paused, and prednisolone therapy was initiated, which successfully inhibited the toxic effect of pembrolizumab. However, repeated flare-ups due to prednisolone tapering suggest that the toxic effect of pembrolizumab outlasts the presence of pembrolizumab in the bloodstream. This further suggests that the T-cell–mediated immune response outlasts the programmed cell death protein 1 (PD-1) receptor occupancy by pembrolizumab, which challenges the need for the current fixed-interval strategies and their stop criteria. Furthermore, a validated ELISA quantified pembrolizumab levels in 15 samples within 123 days after administration. A shift in the pembrolizumab clearance rate was evident ensuing day 77 (0.6 µg/mL) after administration. Pembrolizumab levels up to day 77 (9.1–0.6 µg/mL) strongly exhibited a linear, first-order clearance (R^2 = 0.991), whereas after day 77, an accelerated non-linear clearance was observed. This transition from a linear to non-linear clearance was most

10.3389/fonc.2022.960116

likely a result of full target receptor saturation to non-full target receptor saturation, in which the added effect of target-mediated drug disposition occurs. This suggests that pembrolizumab's targets were fully saturated at levels above 0.6 µg/mL, which is 43 to 61 times lower than the steady-state trough levels ($C_{trough,ss}$) of the currently registered fixed-dosing regimens (3–5).

KEYWORDS

pembrolizumab, immunotherapy, immune-related adverse events, programmed cell death protein 1 (PD-1), pharmacodynamic (PD), pharmacokinetic (PK)

Introduction

Pembrolizumab is a humanized immunoglobulin G4 monoclonal antibody, highly selective for programmed cell death protein 1 (PD-1). PD-1 expressed on activated T cells and this biologic agent aim to remove the immunosuppressive effect resulting from the engagement of PD-1 by programmed cell death ligands 1 or 2 (PD-L1/PD-L2) expressed on tumor cells, resulting in a stable and durable anti-tumor response in a subset of patients (1, 2). However, as an undesired effect, the blockage of PD-1 may result in unrestrained T-cell–mediated immune activation, manifesting as severe immune-related adverse effects (irAEs). According to the literature, approximately 10% of the occurring irAEs lead to (temporary) discontinuation of therapy (3–5).

However, the incidence and severity of irAEs appear unrelated to the pembrolizumab exposure at doses of 2 to 10 mg/kg per 3 weeks. The absence of an exposure–toxicity relation may be partly the consequence of pembrolizumab's highly selective PD-1 inhibition, thereby limiting off-target toxicity. In addition, the toxic effect from on-target but undesired immune activation may not have been evident in clinical trials executed with pembrolizumab doses equal to or higher than the currently registered dose due to the full target receptor saturation throughout the study, resulting in a maximum toxic effect at all dose levels (6, 7). This full target receptor saturation throughout the dosing interval implicates the possibility of excess pembrolizumab in the bloodstream, which raises the question of whether pembrolizumab is being overdosed.

Considering the vastly increasing treatment cost using pembrolizumab and the financial burden among patients (in the Netherlands: € 29 million per year in 2016 versus €210 million per year in 2020), overdosing becomes even more highly undesirable (8–11). Alternative dosing strategies such as concentration-based dosing, dose banding, and weight-based dosing are suggested to be more cost-efficient than the current fixed-dose strategy (12–14). Therefore, it is vital to assess these alternative dosing strategies to lower the financial toxicity among patients being treated with pembrolizumab and warrant the accessibility of worldwide healthcare system.

A precondition for successfully assessing pembrolizumab's dosing strategies is to obtain robust and relevant pharmacokinetic (PK)/pharmacodynamic (PD) data. Data from the registration trials are insufficient because these data come with some difficulties. For example, traditionally, the maximum tolerated dose is used to define a new drug's start dose, but pembrolizumab's highly selective mechanism of action made it impossible to identify a maximum tolerated dose. Consequently, the optimal dosing regimen was determined on the basis of a combination of animal–human transposition studies, *ex vivo* and *in vitro* assays, and PK/PD translational models, which resulted in the registration of a body weight–based dose of 2 mg/kg. A few years later, a fixed dosing regimen was considered more practical because body weight weakly influences the pembrolizumab clearance, side effects are not dose-related, and tolerable range is wide. Thus, the currently used fixed-dose regimens of 200 mg per 3 weeks (200 mg Q3W) and 400 mg per 6 weeks (400 mg Q6W) were registered (7, 15–20).

The PK/PD data in these registration trials lack real-life patient data concerning the minimal effective pembrolizumab level. Therefore, we present a case describing the PK/PD in a treatment-naive patient with non–small cell lung cancer (NSCLC) who developed hepatocellular and cholestatic toxicity after a single 200 mg pembrolizumab administration. This case provides a unique, real-life insight into pembrolizumab's complex PK/PD and highlights the importance of additional real-life PK/PD studies in patients receiving pembrolizumab therapy.

Case description

Diagnosis, treatment, and complications

A 72-year-old white man with a body surface area (BSA) of 2.03 m^2, Chronic obstructive pulmonary disease (COPD) Gold IIIC, and 45 pack years was diagnosed with a not otherwise specified stage IV NSCLC (cTxN1M1c) originating from the right lower lobe of the lung (21). Non-symptomatic metastases were observed in the right lung hilum, the fourth thoracic

10.3389/fonc.2022.960116

vertebrae (Th4), the fifth right rib (costae 5), and the ilium. A biopsy from the ilium evinced a carcinoma positive for cytokeratin 7 and negative for cytokeratin 20, prostate-specific antigen, P40, and thyroid transcriptase factor 1. The tumor was not likely related to the squamous cell lung carcinoma (pT1aN0M0 PL0 R0), removed by lobectomy from the right upper lobe of the lung in 2009 (22). Next-generation sequencing did not reveal mutations in the B-rapidly accelerated fibrosacroma (BRAF), Kirsten rat sarcoma virus (KRAS), erythroblastic leukemia viral oncogene-2 (ERBB2), and mesenchymal–epithelial transition (MET) genes. Immunohistochemistry analysis on Anaplastic lymphoma kinase (ALK) and neurotrophic tyrosine receptor kinase (NTRK) was negative, and immunohistochemistry analysis on PD-L1 (using clone 22C3) was positive in over 90% of the tumor cells. Systemic treatment with 200 mg pembrolizumab Q3W was initiated on the basis of these carcinomas' characteristics.

The first 200 mg pembrolizumab dose was administered 3 weeks after diagnosis (Figure 1). Nineteen days after administration, the patient presented with elevated levels of alanine aminotransferase (ALT), aspartate transaminase (AST), alkaline phosphatase (ALP), and γ-glutamyl (γ-GT) transferase (Figure 2). Additional diagnostics on day 77 after pembrolizumab administration excluded the presence of liver metastasis or any toxic or viral origin but indicated multiple liver cysts, steatosis hepatitis, and gallstone debris in the common bile duct (CBD) for which 300 mg of ursodeoxycholic acid (UDCA) three times a day was started. Furthermore, additional laboratory results indicated elevated levels of lactate dehydrogenase (LDH) from day 77 to day 95 after pembrolizumab administration (ranging from 261 to 298 IU/L, with an upper boundary of normal levels of 248 IU/L) and elevated albumin levels from day 84 to day 89 after pembrolizumab administration (ranging from 29 to 30 g/L, with reference values of 35 to 52 g/L). Meanwhile, physical controls indicated a 9% decrease in BSA to 1.86 m^2 between the diagnosis and 95 days after pembrolizumab administration. Nevertheless, none of these observations were the apparent cause of hepatotoxicity.

Because it could not be ruled out that the patient had a grade 2 immune-related hepatitis (ir-hepatitis) (AST/ALT = 2.5 − 5.0 × Upper limit normal value (ULN), pembrolizumab therapy was paused. Prednisolone therapy was considered but not initiated directly as developing ir-hepatitis after the first administration is uncommon (0.1%), and a spontaneous and inexplicable improvement of the levels of transaminases was observed. Nonetheless, 4 weeks after pembrolizumab administration, prednisolone therapy (1 mg/kg; 90 mg daily) was initiated when the levels abnormalized again (23). In the following 6 weeks, repeated attempts to reduce the daily prednisolone dose resulted in an immediate increase in liver enzyme levels, strengthening the idea that the patient suffered from pembrolizumab-induced ir-hepatitis. Therefore, pembrolizumab therapy was not restarted, and the patient proceeded with prednisolone therapy for over 14 weeks. Even after the discontinuation of prednisolone therapy and the start of UDCA, the cholestatic liver function never fully normalized (ALP, 454 IU/L; γ-GT, 459 IU/L).

Ten weeks after pembrolizumab administration, tumor imaging revealed no nodular abnormalities in the lower right lung; a stable costae 5 metastasis; and no axillary, hilar, or mediastinal lymphadenopathy. Similar observations were made 4 and 16 weeks later (13 and 25 weeks after pembrolizumab administration). However, the latter tumor imaging revealed a new osteoporotic compression fracture at thoracic vertebrae 8 (Th8) without specific signs of metastasis. Nearly 10 months after pembrolizumab administration, tumor imaging revealed a new lesion (either malignant or infectious) in the right lower lobe of the lung, extensive axillary and mediastinal lymphadenopathy, and extensive progression of the skeletal metastasis. Almost 4 weeks later (10 months after the 200 mg pembrolizumab administration), the patient died without apparent cause (most likely cardiac arrest during his sleep).

Pharmacokinetics of pembrolizumab

Before administering pembrolizumab, the patient gave informed consent for an observational study in which pembrolizumab levels were quantified in residual plasma obtained for routine laboratory tests. In total, 15 samples were

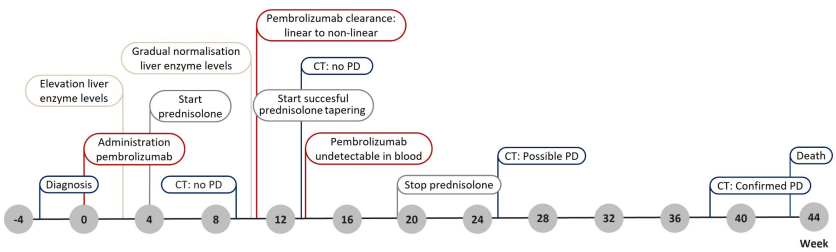

FIGURE 1
Timeline presenting the main events throughout the patient's treatment. CT, computer tomography; PD, progression of disease.

10.3389/fonc.2022.960116

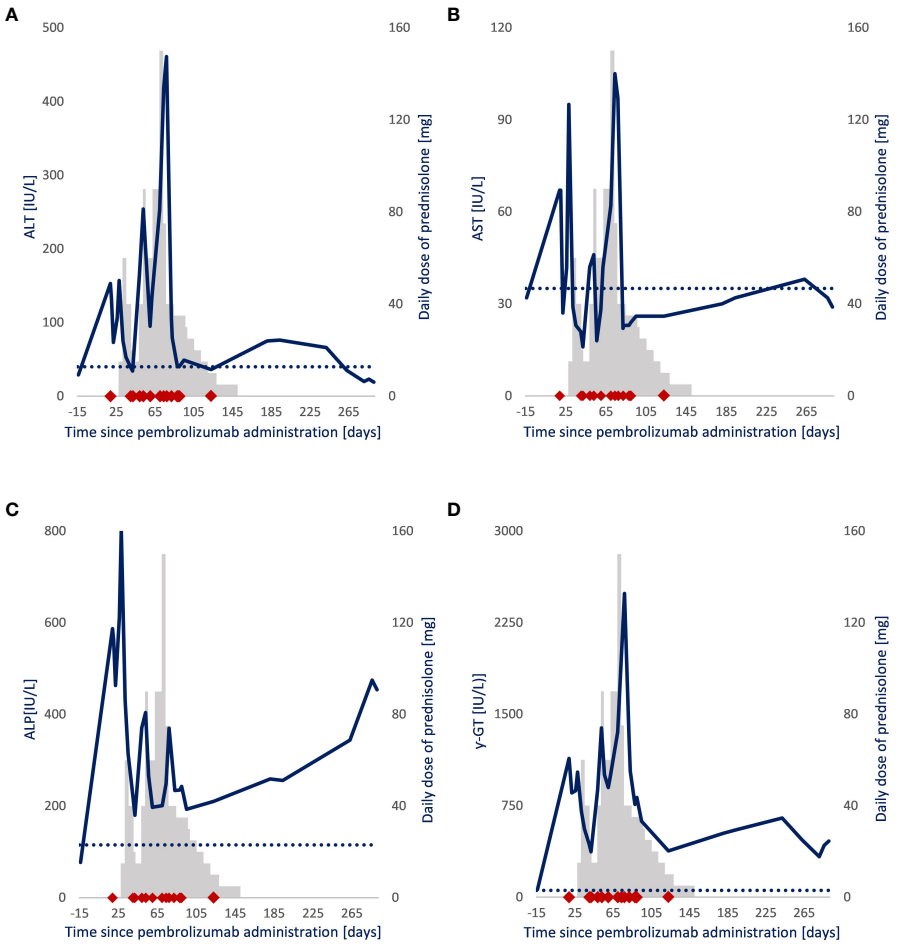

FIGURE 2
Follow-up of liver enzyme levels and daily prednisolone dose in a patient with NSCLC. Blue line: **(A)** Alanine aminotransferase (IU/L), **(B)** aspartate transaminase (IU/L), **(C)** alkaline phosphatase (IU/L), **(D)** γ-glutamyl (IU/L) transferase. Gray bars: Daily prednisolone dose (mg). ◆: Sample drawn for pembrolizumab quantification after pembrolizumab administration. ···: Upper boundary of the liver enzymes' normal range.

gathered in the days after pembrolizumab administration (respectively, on days 19, 40, 42, 49, 53, 60, 70, 74, 77, 82, 88, 89, 90, 91, and 123).

The pembrolizumab levels of these samples were quantified using an ELISA method developed by Sanquin Diagnostics Services and validated following the U.S. Food and Drug Administration (FDA) guidelines. This method is an assay with a mean accuracy of 97% to 105% from 0.1 µg/mL (lower limit of quantification) to 200 µg/mL (upper limit of quantification) and coefficients of variation between 3.0% and 9.9%. The highest pembrolizumab level of 9.1 µg/mL, as seen in Figure 3, was observed in the earliest sample collected (19 days after the 200 mg pembrolizumab administration). The pembrolizumab level decreased below the assay's lower detection limit 90 days after administration. A clear shift in clearance rate was evident from day 77 (0.6 µg/mL) after administration. Pembrolizumab levels up to and including day 77 (9.1–0.6 µg/mL) strongly exhibit a linear (first-order) clearance (R^2 = 0.991) with a 14.6-day half-life ($t_{1/2}$), whereas an accelerated non-linear clearance was observed after day 77.

Discussion

The patient experienced hepatocellular and cholestatic toxicity 3 weeks after a single 200 mg pembrolizumab administration. Despite its low incidence, this toxicity was most likely related to a grade 2 ir-hepatitis (2). However, a hepatic irAE, such as ir-hepatitis, typically resolves within 6 to 9 weeks. However, in this patient, the elevated cholestatic liver enzymes (γ-GT and ALP) persisted until death (24–26). Therefore, the attribution of the patient's comorbidities to elevated liver enzymes should be considered. An attribution to liver cysts is improbable because liver cysts rarely affect liver enzymes. Hypothetically, hepatic steatosis could cause a slight chronic elevation of ALT (approximately 100 IU/L) and γ-GT

10.3389/fonc.2022.960116

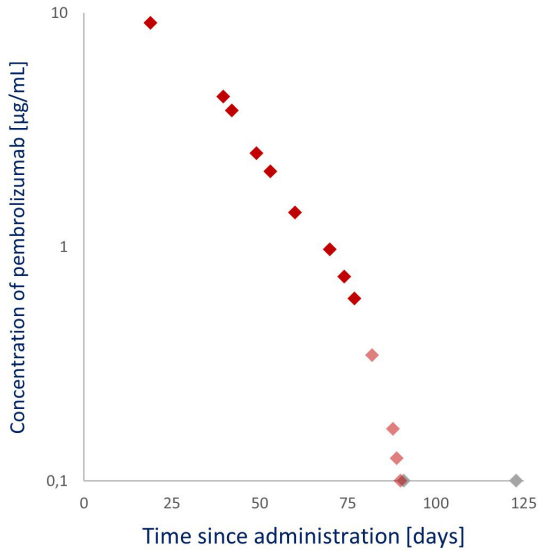

FIGURE 3
Observed pembrolizumab levels after a 200 mg per 3 weeks (Q3W) administration. ◆: Linear pembrolizumab clearance (samples from 19, 40, 42, 49, 53, 60, 70, 74, and 77 days after administration). ◆: Non-linear pembrolizumab clearance (samples from 82, 88, 89, and 90 days after administration). ◆: Below the lower limit of detection (samples from 91 and 123 days after administration).

(approximately 300 IU/L). Still, on the basis of the persisting normalization of the ALT, the attribution of steatosis hepatitis is unlikely.

On the other hand, gallstone debris in the CBD can indicate an (intermittent) obstruction. Such an obstruction could contribute to the abnormality in the cholestatic liver enzymes (27–29). Although the start of UDCA therapy and the improvement in enzyme levels coincide, the extent of this attribution is inconclusive because no endoscopic retrograde cholangitis and pancreatography were performed. Nonetheless, prednisolone therapy was started because ir-hepatitis due to pembrolizumab toxicity was most likely.

The normalization of transaminases (ALT and AST) and declining cholestatic enzymes, as seen in Figure 2, are a consequence of the successful inhibitory effect of prednisolone on the toxic effect of pembrolizumab. Flare-ups when reducing the daily prednisolone dose suggest that the toxic effect of pembrolizumab is ongoing at that time. Moreover, this toxic effect outlasts the detectable presence of circulating pembrolizumab, suggesting that the T-cell–mediated immune response outlasts the PD-1 receptor occupancy by pembrolizumab. The occurrence of delayed immune-related events supports this hypothesis. There are published case reports of patients developing life-threatening irAEs, up to 12 months after their final pembrolizumab dose, which challenges the need for a 3- or 6-week dosing interval (23, 30–32). Nevertheless, a successful prednisolone tapering was initiated 77 days after pembrolizumab administration.

Notably, as seen in Figure 3, after the 77th day, pembrolizumab clearance transitioned from linear to non-linear. The pembrolizumab $t_{1/2}$ up to that day was 14.6 days, and the quantified pembrolizumab level on that day was 0.6 µg/mL, corresponding to previously published levels where the clearance ($t_{1/2}$, 14.1 days) transitions from linear to accelerated non-linear (0.68 µg/mL) (16–19). This linear and non-linear clearance phenomenon occurs *via* numerous physiological pathways. The predominant linear clearance occurs when the target receptor (PD-L1) is saturated, and the elimination rate is driven by proteolytic catabolism in plasma and peripheral tissues.

On the other hand, target-mediated drug disposition, a combination of linear and non-linear clearance, occurs when the target receptor is no longer saturated. Then, the elimination rate is driven by proteolytic catabolism and receptor-mediated endocytosis from the plasma or interstitium to the target cells (23, 33). Because the patient was not in a cachexic state and UDCA therapy is not expected to impact pembrolizumab's PK, this knowledge makes it reasonable to suggest that the transition from linear clearance to a combination of linear and non-linear clearance, and thus from full receptor saturation to non-full receptor saturation, occurs close to a pembrolizumab level of 0.6 to 0.68 µg/mL, which poses the question of what concentrations far above these plasma levels add to the effectiveness of pembrolizumab.

Early *in vitro* studies described that 50% inhibition (IC_{50}) of T cells reached a level of 0.535 µg/mL and maximum inhibition (I_{max}) at 0.961 µg/mL (8, 11). Steady-state simulations of a post-registration study revealed a 90% probability of at least 99.31% target achievement for a 70-kg patient with a regimen of 200 mg Q3W, whereas a regimen of 1 mg/kg Q3W had a 90% probability of 96.8% target achievement. Thus, a regimen of 1 mg/kg Q3W ($C_{trough,ss}$, 12.8 µg/mL) versus a 2 mg/kg Q3W ($C_{trough,ss}$, 25.5 µg/mL) is predicted to only result in a modest reduction in efficacy (16, 34). Remarkably, marketing-authorization holder Merck & Co. already observed this modest reduction in efficacy 2 years earlier. They noted that no difference in the exposure–response relationship was seen across doses of 1 to 10 mg/kg and even suggested that a regimen of 1 mg/kg Q3W may be sufficient to achieve clinical efficacy. Nevertheless, the dosing strategies at 200 mg Q3W ($C_{trough,ss}$, 36.4 µg/mL) and 400 mg Q6W ($C_{trough,ss}$, 25.6 µg/mL) are the currently registered dosages (1, 2, 15, 34).

Unfortunately, the pharmacokinetic data from these early dose-finding studies have some difficulties. For example, defining the minimal anticipated biologic effect level is not bound to universal guidelines; wherefore, the transposition of non-human data to predict a human effect differs per study. Even so, real-world studies frequently demonstrate that clinical

trial data differ from clinical practice data. Clinical trial cohorts often comprise a selective patient group that is relatively well-performing and has little to no comorbidities, whereas a real-life population is often more complex (4, 7, 35, 36). As a result, interpatient variability in pharmacokinetics was similar in trial populations but varied highly in real-life populations (16, 17, 35, 37). In conclusion, the full potential of pembrolizumab in real-life patient population is yet to be identified.

Thus, although this case report describes the PK/PD of a single patient, and an impact on the PK of pembrolizumab by covariates such as BSA, LDH, and albumin cannot be ruled out, these real-life data slightly fill existing real-life PK/PD data gap and demonstrate the complexity of pembrolizumab's PK/PD (35). Furthermore, this case report emphasizes the need to gather additional real-life PK/PD data and explore possible alternative dosing strategies, such as concentration-guided personalized dosing strategies, to prevent overdosing on this expensive drug without compromising patient safety and drug efficacy.

Data availability statement

The raw data supporting the conclusions of this article will be made available by the authors, without undue reservation.

Ethics statement

The studies involving human participants were reviewed and approved by MEC-U, Nieuwegein, the Netherlands. The patients/participants provided their written informed consent to participate in this study. Written informed consent was obtained from the individual for the publication of any potentially identifiable data included in this article.

Author contributions

FV was responsible for the database's organization, performed the data analysis, and wrote the manuscript. FV and AS were responsible for processing the patient information. AV and FL were responsible for the sample analysis. FV, GW, and EF were responsible for the pharmacokinetic analysis. All authors contributed to the manuscript's revision and read and approved the submitted version.

Funding

This study was supported by OLVG, Subsidie Stichting Wetenschappelijk Onderzoek 2021.

Conflict of interest

The authors declare that the research was conducted in the absence of any commercial or financial relationships that could be construed as a potential conflict of interest.

Publisher's note

References

1. Merck & Co. Inc. *Higlights of prescribing information: Keytruda (Pembrolizumab)* (2014). Available at: www.fda.gov/medwatch (Accessed April 28, 2020).

2. Merck & Co. Inc. *Summary of product characteristics - KEYTRUDA (Pembrolizumab)*. (2022). Available at: https://www.ema.europa.eu/documents/product-information/keytruda-epar-product-information_en.pdf [Accessed November 20, 2022].

3. Kumar V, Chaudhary N, Garg M, Floudas CS, Soni P, Chandra AB. Current diagnosis and management of immune related adverse events (irAEs) induced by immune checkpoint inhibitor therapy. *Front Pharmacol* (2017) 8:49/FULL. doi: 10.3389/FPHAR.2017.00049/FULL

4. Bastacky ML, Wang H, Fortman D, Rahman Z, Mascara GP, Brenner T, et al. Immune-related adverse events in PD-1 treated melanoma and impact upon anti-tumor efficacy: A real world analysis. *Front Oncol* (2021) 11:749064/FULL. doi: 10.3389/FONC.2021.749064/FULL

5. Wang PF, Chen Y, Song SY, Wang TJ, Ji WJ, Li SW, et al. Immune-related adverse events associated with anti-PD-1/PD-L1 treatment for malignancies: A meta-analysis. *Front Pharmacol* (2017) 8:730/FULL. doi: 10.3389/FPHAR.2017.00730/FULL

6. Shulgin B, Kosinsky Y, Omelchenko A, Chu L, Mugundu G, Aksenov S, et al. Dose dependence of treatment-related adverse events for immune checkpoint inhibitor therapies: A model-based meta-analysis. *Oncoimmunology* (2020) 9:1748982. doi: 10.1080/2162402X.2020.1748982/SUPPL_FILE/KONI_A_1748982_SM6611.DOCX

7. le Louedec F, Leenhardt F, Marin C, Chatelut É, Evrard A, Ciccolini J. Cancer immunotherapy dosing: A Pharmacokinetic/Pharmacodynamic perspective. *Vaccines (Basel)* (2020) 8:1–23. doi: 10.3390/VACCINES8040632

8. Zorginstituut Nederland. *Horizonscan geneesmiddelen, pembrolizumab* . Available at: https://www.horizonscangeneesmiddelen.nl/geneesmiddelen/pembrolizumab-oncologie-en-hematologie-blaaskanker/versie1 (Accessed April 19, 2020).

9. Tax S, van der Hoeven J, van Reijsen J, Karssen H. Signaleringscommissie kanker van KWF kankerbestrijding. In: *Toegankelijkheid van dure kankergeneesmiddelen: Nu en in de toekomst* (2014). Available at: https://www.kwf.nl/toegang-tot-geneesmiddelen/rapporten-dure-geneesmiddelen [Accessed April 17, 2020].

10. Nederlandse Zorgautoriteit (NZA). *Zorgmonitor: Geneesmiddelen in de medisch-specialistische zorg.* (2019). Available at: https://puc.overheid.nl/nza/doc/PUC_264248_22/1/ [Accessed April 17, 2020].

11. Nederlandse Zorgautoriteit (NZA). *Uitgaven intramurale geneesmiddelen en overige medisch specialistische zorg*, 1. (2022). Available at: https://puc.overheid.nl/nza/doc/PUC_715091_22/ [Accessed September 28, 2022].

12. Ogungbenro K, Patel A, Duncombe R, Nuttall R, Clark J, Lorigan P. Dose rationalization of pembrolizumab and nivolumab using pharmacokinetic modeling and simulation and cost analysis. *Clin Pharmacol Ther* (2018) 103:582–90. doi: 10.1002/cpt.875

13. Goldstein DA, Gordon N, Davidescu M, Leshno M, Steuer CE, Patel N, et al. Phamacoeconomic analysis of personalized dosing vs fixed dosing of pembrolizumab in firstline PD-L1-Positive non-small cell lung cancer. *JNCI J Natl Cancer Insy* (2017) 109(11). doi: 10.1093/jnci/djx063

14. Peer CJ, Heiss BL, Goldstein DA, Goodell JC, Figg WD, Ratain MJ. Pharmacokinetic simulation analysis of less frequent nivolumab and pembrolizumab dosing: Pharmacoeconomic rationale for dose deescalation. *J Clin Pharmacol* (2021). doi: 10.1002/jcph.1984

15. CHMP. *Committee for medicinal products for human use assessment report pembrolizumab* (2015). Available at: www.ema.europa.eu/contact (Accessed October 30, 2020).

16. Elassaiss-Schaap J, Rossenu S, Lindauer A, Kang S, de Greef R, Sachs J, et al. Using model-based "Learn and confirm" to reveal the pharmacokinetics-pharmacodynamics relationship of pembrolizumab in the KEYNOTE-001 trial. *CPT Pharmacometrics Syst Pharmacol* (2017) 6:21–8. doi: 10.1002/psp4.12132

17. Ahamadi M, Freshwater T, Prohn M, Li C, de Alwis D, de Greef R, et al. Model-based characterization of the pharmacokinetics of pembrolizumab: A humanized anti-PD-1 monoclonal antibody in advanced solid tumors. *CPT Pharmacometrics Syst Pharmacol* (2017) 6:49–57. doi: 10.1002/psp4.12139

18. Chatterjee M, Elassaiss-Schaap J, Lindauer A, Turner D, Sostelly A, Freshwater T, et al. Population Pharmacokinetic/Pharmacodynamic modeling of tumor size dynamics in pembrolizumab-treated advanced melanoma. *CPT Pharmacometrics Syst Pharmacol* (2017) 6:29–39. doi: 10.1002/psp4.12140

19. Patnaik A, Kang SP, Rasco D, Papadopoulos KP, Elassaiss-Schaap J, Beeram M, et al. Phase I study of pembrolizumab (MK-3475; anti-PD-1 monoclonal antibody) in patients with advanced solid tumors. *Clin Cancer Res* (2015) 21:4286–93. doi: 10.1158/1078-0432.CCR-14-2607

20. CHMP. *Committee for medicinal products for human use (CHMP) assessment report* (2017). Available at: www.ema.europa.eu/contact (Accessed December 7, 2022).

21. Brierly JD, Gospodarowicz MK, Wittekind C. International union against cancer (UICC). In: *TNM classification of malignant tumours, 8th edition*. Oxford, UK: Wiley-Blackwell (2016).

22. Sobin L, Gospadarowicz M, Wittekind C. International union against cancer (UICC). In: *TNM classification of malignant tumors, 7th ed*. Oxford, UK: Wiley-Blackwell (2009).

23. Centanni M, Moes DJAR, Trocóniz IF, Ciccolini J, van Hasselt JGC. Clinical pharmacokinetics and pharmacodynamics of immune checkpoint inhibitors. *Clin Pharmacokinet* (2019) 58:835–57. doi: 10.1007/S40262-019-00748-2/TABLES/6

24. Gauci M-L, Baroudjian B, Zeboulon C, Pages C, Poté N, Roux O, et al. Letters to the Editor: Immune-related hepatitis with immunotherapy: Arecorticosteroids always needed? *J Hepatol* (2018) 69:548–50. doi: 10.1016/j.jhep.2018.03

25. Doherty GJ, Duckworth AM, Davies SE, Mells GF, Brais R, Harden S v., et al. Severe steroid-resistant anti-PD1 T-cell checkpoint inhibitor-induced hepatotoxicity driven by biliary injury. *ESMO Open* (2017) 2(4):e000268. doi: 10.1136/ESMOOPEN-2017-000268

26. Imoto K, Kohjima M, Hioki T, Kurashige T, Kurokawa M, Tashiro S, et al. Clinical study clinical features of liver injury induced by immune checkpoint inhibitors in Japanese patients. *Can J Gastroenterol Hepatol.* (2019) 2019:6391712. doi: 10.1155/2019/6391712

27. Gowda S, Desai PB, Hull VV, Math AAK, Vernekar SN, Kulkarni SS. A review on laboratory liver function tests. *PanAfrican Med J* (2009), 3(11):1–11.

28. Green RM, Flamm S. AGA technical review on the evaluation of liver chemistry tests. *Am Gastroenterol Assoc* (2002) 123:1367–84. doi: 10.1053/gast.2002.36061

29. Kim K-N, Joo J, Sung HK, Kim CH, Kim H, Kwon YJ. Associations of serum liver enzyme levels and their changes over time with all-cause and cause-specific mortality in the general population: A large-scale national health screening cohort study. *BMJ Open* (2019) 9:26965. doi: 10.1136/bmjopen-2018-026965

30. Phan T, Patwala K, Lipton L, Knight V, Aga A, Pianko S. Very delayed acute hepatitis after pembrolizumab therapy for advanced malignancy: How long should we watch? *Curr Oncol* (2021) 28:898. doi: 10.3390/CURRONCOL28010088

31. Nakako S, Nakashima Y, Okamura H, Tani Y, Ueda T, Makuuchi Y, et al. Delayed immune-related neutropenia with hepatitis by pembrolizumab. *Immunotherapy* (2021) 14(2):101–105. doi: 10.2217/IMT-2021-0131

32. Couey MA, Bell RB, Patel AA, Romba MC, Crittenden MR, Curti BD, et al. Delayed immune-related events (DIRE) after discontinuation of immunotherapy: Diagnostic hazard of autoimmunity at a distance. *J Immunother Cancer* (2019) 7:1–11. doi: 10.1186/S40425-019-0645-6/TABLES/1

33. Stein AM, Peletier LA. Predicting the onset of nonlinear pharmacokinetics. *CPT Pharmacometrics Syst Pharmacol* (2018) 7:670. doi: 10.1002/PSP4.12316

34. CADTH. Dosing and timing of Immuno-oncology drugs. In: *Technology review: Optimal use 360 report* (2019).

35. Hurkmans DP, Sassen SDT, de Joode K, Putter L, Basak EA, Wijkhuijs AJM, et al. Prospective real-world study on the pharmacokinetics of pembrolizumab in patients with solid tumors. *J Immunother Cancer* (2021) 9:e002344. doi: 10.1136/JITC-2021-002344

36. Waterhouse D, Lam J, Betts KA, Yin L, Gao S, Yuan Y, et al. Real-world outcomes of immunotherapy–based regimens in first-line advanced non-small cell lung cancer. *Lung Cancer* (2021) 156:41–9. doi: 10.1016/j.lungcan.2021.04.007

37. Bajaj G, Suryawanshi S, Roy A, Gupta M, Address Gaurav Bajaj P. Evaluation of covariate effects on pharmacokinetics of monoclonal antibodies in oncology. *Br J Clin Pharmacol Pharmacol Soc* (2019) 85:2045–58. doi: 10.1111/bcp.13996

Frontiers in Oncology

Advances knowledge of carcinogenesis and tumor progression for better treatment and management

The third most-cited oncology journal, which highlights research in carcinogenesis and tumor progression, bridging the gap between basic research and applications to imrpove diagnosis, therapeutics and management strategies.

Discover the latest Research Topics

See more →

Frontiers

Avenue du Tribunal-Fédéral 34
1005 Lausanne, Switzerland
frontiersin.org

Contact us

+41 (0)21 510 17 00
frontiersin.org/about/contact